

# Non Contact Surface Metrology in a Hazardous Environment

A thesis submitted to University College London (UCL) for the  
degree of Doctor of Philosophy (Ph.D.)

Andrew Brownhill

Department of Civil, Environmental and Geomatic Engineering

London, 2012

## **Declaration of Ownership**

I, Andrew Brownhill, confirm that the work presented in this thesis is my own. Where information has been derived from other sources, I confirm that this has been indicated in the thesis.

Signed:.....

Date:.....

## **Acknowledgements**

Undertaking this research has been a great privilege but also a challenge, I would like to take this opportunity to thank certain individuals and groups for their support.

The support of Professor Stuart Robson of University College London has been essential in reaching the successful completion of the project. As academic supervisor, he has helped to guide me and the project in the right direction and I would like to thank him for his calm, considered advice and unwavering support.

As industrial supervisor, Bob Brade has provided hands-on engineering and metrology advice based on many years of experience. His knowledge of metrology and EFDA-JET has been essential in understanding the engineering challenge and tackling real world dimensional metrology. His guidance on metrology matters and beyond has been gratefully received.

The staff of EFDA-JET and specifically the inspection team is owed great thanks for assisting me in all my work whilst at Culham. Always willing to answer my questions and show me how things work in the real world, their support enabled the successful completion of the equipment trial and improved many engineering drawings.

Thanks to staff at W7X in Greifswald, Germany for making me welcome during my secondment and providing the opportunity to experience the complete lifecycle of metrology data. Thanks also to UK National Physical Laboratory, specifically staff of the dimensional metrology department for their support in validating the manufactured artefacts and providing a superb environment for dimensional measurement.

Manufacturers' equipment used in this work has remained anonymous, however, thank you to all those companies and individuals who took part in the trial, without your data we would have nothing to report. InnovMETRIC software and 3D Scanners UK for providing a longer than planned evaluation license of software package PolyWorks and essential training.

Finally a special thanks to my wife, family and friends who have been incredibly supportive and offered nothing but encouragement throughout the process. Thank you.

This work has been funded by the UK Atomic Energy Authority and the Engineering and Physical Sciences Research Council (EPSRC).

## **Abstract**

The EFDA-JET tokamak is an experimental fusion device researching fusion as a means of energy production. Inside the toroidal vessel, plasma with temperature in excess of 100 million degrees Celsius is generated and constrained by high power magnetic fields. Additional protection is provided by tiles which clad the inside of the machine. As part of a major upgrade existing heat protective tiles are to be replaced with an advanced design, and renewed interest has been shown in dimensional measurement of the surface.

Measurement must occur during shutdown periods where temperature and pressure are at ambient levels. Manned entry is not permissible and all work should be performed remotely. To avoid contamination which could affect the fusion reaction and experimental results, contact with the measurement surface is not permitted.

This work assesses non-contact surface measurement technologies, along with standards and guidelines for dimensional surface measurement. Existing measurement test artefacts do not offer the required surface finish and features, so specific test artefacts have been designed and produced. These artefacts are traceable to the national length standard, as traceability is a pre-requisite to evaluate accuracy.

Exploratory tests highlighted two technologies for further investigation, laser triangulation and white light fringe projection. Two commercially available, state-of-the-art examples of each technology have been evaluated using a processing method developed to highlight performance in key areas relevant to EFDA-JET. These areas include quantitative assessments of the effect of surface angle on measurement quality, the effect of depth of field for fringe projection systems and the ability of technologies to record gap and flush from tens of micrometres to millimetres.

Tests enable a user to begin to assess the impact the measurement system has on the measurement result, how different technologies and systems used alone or in combination may resolve or compound erroneous results, clarifying or disrupting the meaning of results.

# Contents

List of Figures .....	9
List of Tables .....	18
1. Introduction .....	20
1.1. Context .....	20
1.2. Motivation for Research .....	22
1.3. Problem Statement .....	23
1.4. Research Objectives .....	23
1.5. Research Process .....	25
1.6. Research Tools .....	26
1.7. Structure Summary .....	26
2. The Engineering Problem .....	28
2.1. The Fusion Process & EFDA-JET .....	28
2.2. Measurement Environment and Constraints .....	31
2.2.1. Remote Handling .....	33
2.3. Tile Design .....	34
2.3.1. Design of Plasma Facing Components .....	35
2.3.2. Manufacture & Effect on Measurement .....	39
2.4. Data Required .....	41
2.4.1. Measurement of the complete machine volume .....	41
2.4.2. Measurement data of the intersection between two or more tiles .....	42
2.4.3. Measurement of a single tile assembly or part thereof .....	43
2.4.4. Collection speed .....	43
2.4.5. Data format .....	44
2.5. Current Measurement Technology and Process .....	45
2.6. Metrology in the Fusion Industry .....	50
2.7. Summary of Requirements .....	53
3. Metrology .....	55
3.1. Reference Terms .....	55
3.2. Technology .....	56
3.2.1. Measurement of Targets and Surfaces .....	57
3.2.1.1. Target measurement .....	57

3.2.1.2.	Surface measurement.....	60
3.2.2.	Equipment Classification.....	66
3.2.3.	Passive Measurement Techniques.....	67
3.2.4.	Active Measurement Techniques.....	75
3.2.4.1.	Polar Measurement Systems.....	75
3.2.4.2.	Laser Triangulation.....	82
3.2.4.3.	Light Projection: Bundle of Rays.....	91
3.2.5.	Hybrid Techniques.....	97
3.3.	Data Handling.....	104
3.3.1.	Representation.....	104
3.3.2.	Registration.....	106
3.3.2.1.	Surface Based Registration.....	107
3.3.2.2.	Multi-View Registration.....	109
3.4.	Standards, Guidelines & Artefacts.....	110
3.5.	Summary.....	119
4.	Preliminary Experimental Work.....	122
4.1.	Test Artefact.....	123
4.1.1.	Material Selected.....	123
4.1.2.	Features.....	125
4.2.	Measurement Systems Tested.....	126
4.3.	Execution of Tests.....	128
4.4.	Results.....	130
4.4.1.	Length error.....	130
4.4.2.	Sphere Fitting.....	132
4.4.3.	Plane Fitting.....	133
4.4.4.	Surface Discontinuities.....	134
4.4.5.	Effect of Surface Roughness on Measurement Data.....	137
4.5.	Summary.....	138
5.	Primary Equipment Trial.....	140
5.1.	Experiment Rationale.....	140
5.2.	Experiment Design.....	142
5.2.1.	Artefacts.....	142
5.2.1.1.	Angle Artefact A.....	143
5.2.1.2.	Angle Artefact B.....	144

5.2.1.3.	Gap & Step.....	144
5.2.1.4.	Material Selection & Manufacture.....	145
5.2.1.5.	Test Frames.....	146
5.2.1.6.	Artefact Verification.....	149
5.2.2.	Equipment Tested.....	152
5.2.3.	Tests Performed.....	154
5.2.3.1.	Approach Angle.....	154
5.2.3.2.	Depth of Field.....	155
5.2.3.3.	Edge Measurement.....	156
5.2.3.4.	Gap Detection.....	157
5.2.3.5.	Registration.....	158
5.2.3.6.	Large Volume.....	159
5.3.	Experiment Execution.....	161
5.3.1.	Operator.....	161
5.3.2.	Environment.....	161
5.3.3.	Test Operation.....	162
5.3.3.1.	Common Setup/Processing Steps.....	163
5.3.3.2.	Approach Angle.....	165
5.3.3.3.	Depth of Field.....	174
5.3.3.4.	Edge Measurement.....	178
5.3.3.5.	Gap Detection.....	185
5.3.3.6.	Registration.....	190
5.3.3.7.	Large Volume.....	191
5.4.	Results.....	195
5.4.1.	Approach Angle Test.....	195
5.4.1.1.	Verification of as-built CAD.....	195
5.4.1.2.	Data Coverage and Quality.....	197
5.4.1.3.	Measurement system angle to surface normal.....	202
5.4.1.4.	Angular error.....	211
5.4.2.	Depth of Field Test.....	218
5.4.2.1.	Point spacing.....	220
5.4.3.	Edge Measurement.....	224
5.4.3.1.	Random Error & Step Height Measurement.....	224
5.4.3.2.	Assessment of edge measurement.....	229
5.4.4.	Gap detection.....	245
5.4.4.1.	Minimum resolvable gap.....	249
5.4.5.	Registration.....	256

5.4.6.	Large Volume .....	258
5.4.6.1.	Probing Error .....	258
5.4.6.2.	Length/Sphere spacing error .....	260
5.4.6.3.	Number of tracking device positions .....	262
5.5.	Summary .....	265
6.	Conclusions and Further Work.....	267
6.1.	Summary & Critical Analysis of Work.....	267
6.1.1.	Development of A New Evaluation Method.....	268
6.1.1.1.	Development of New Test Artefacts.....	268
6.1.1.2.	Development of Experiments and Data processing techniques .....	270
6.1.1.3.	Equipment Trials.....	273
6.1.2.	Results.....	275
6.1.2.1.	Approach angle .....	275
6.1.2.2.	Depth of Field .....	276
6.1.2.3.	Edge Measurement.....	276
6.1.2.4.	Registration.....	277
6.1.3.	Summary of Contribution .....	277
6.2.	Conclusions for EFDA-JET .....	279
6.2.1.	Can optical, non-contact surface measurement tools verify installation of plasma facing components to sub-millimetre accuracy?.....	279
6.2.2.	Can optical, non-contact surface measurement tools quantify dimensions and surface change of protective tiles?.....	282
6.2.3.	What is the optimal approach to a surface to perform surface measurement in the EFDA-JET tokamak? .....	284
6.2.4.	What method can be used by EFDA-JET to assess the performance of measurement systems, now and in the future?.....	287
6.2.5.	Summary for EFDA-JET .....	287
6.3.	Further Work.....	289
6.3.1.	Testing.....	289
6.3.2.	Processing .....	291
7.	References and Bibliography .....	292
7.1.	Publications & Presentations.....	306

## List of Figures

Figure 2.1: Inside the EFDA-JET tokamak, with image of plasma during operation inset. (EFDA-JET, 2007) .....	30
Figure 2.2: Three ITER-Like wall limiter tile assemblies (middle assembly is incomplete). EFDA-JET.....	31
Figure 2.3: Inside the EFDA-JET machine (June 2005) with two of the limiter beams highlighted (EFDA-JET).....	36
Figure 2.4: Pre-Prototype ITER-Like Wall Limiter tile (EFDA-JET). Plasma facing surface area of an outer wall tile is ~330 x 110mm. ....	37
Figure 2.5: Poloidal limiter tile assembly tolerances (EFDA-JET).....	37
Figure 2.6: Peak temperature on exposed edge. 40 $\mu$ m defined for ITER-Like wall (EFDA-JET).....	38
Figure 2.7: Roughness and Waviness of a surface (Taylor-Hobson, n.d.).....	39
Figure 2.8: Calculating the Ra (Taylor-Hobson, n.d.) .....	39
Figure 2.9: Measurement probe construction (Taylor-Hobson, n.d.) .....	40
Figure 2.10: Dump-plate target installed in-vessel. Target is attached to a single tile; other targets visible in the background (EFDA-JET).....	46
Figure 3.1: Accuracy, Precision and Repeatability, Courtesy of NPL (C) Crown Copyright 2003.....	56
Figure 3.2: Retro-reflective photogrammetry target (Geodetic Systems Inc., 2010a)....	58
Figure 3.3: Effect of optical thickness of retro-reflective targets. After Luhmann et al.(2006, p.184) .....	58
Figure 3.4: SMR/corner cube reflector (Brunson, 2010).....	59
Figure 3.5: Position calculation affected by surface reflectance change (El-Hakim et al., 1995).....	61
Figure 3.6: Behaviour of reflected light (Forest et al., 2004) .....	62
Figure 3.7: Specular surface directs light directly to sensor where light source and sensor are equiangular of surface normal.....	63
Figure 3.8: Erroneous range measurement caused by specular surface for triangulation systems. (Nitzan, 1988). Note: the surface is diffusely reflecting, other than the area identified as specular. ....	64
Figure 3.9: Erroneous range measurement caused by specular surface for time of flight systems (Nitzan, 1988). Note: the surface is diffusely reflecting, other than the area identified as specular. ....	64
Figure 3.10: Effect of surface penetration (Blais et al., 2005).....	65

Figure 3.11: Classification of non-contact 3D surface measurement techniques based on light waves (Beraldin et al., 2000) .....	67
Figure 3.12: AutoBar used with Geodetic Systems V-Stars system .....	69
Figure 3.13: Retro-reflective targets (Geodetic Systems Inc., 2010a).....	70
Figure 3.14: Coded target (Geodetic Services Inc., 2006).....	71
Figure 3.15: Ideal retro-reflective targets (Shortis et al., 1994).....	71
Figure 3.16: Surface with projected points .....	73
Figure 3.17: INCA 2 camera (Dold, 1998) .....	74
Figure 3.18: Commercially available laser trackers.....	76
Figure 3.19: Time of flight thresholding. Fixed threshold (left), Return signal level dependent threshold (Right). After Thiel & Wehr (2004) .....	78
Figure 3.20: Comparison of time of flight measurement tools (Blais, 2004) .....	78
Figure 3.21: Phase shift ToF measurement system, carrier wave and two modulated wavelengths (Pfeifer & Briese, 2007) .....	79
Figure 3.22: Phase difference between transmitted and received signal (Thiel & Wehr, 2004).....	79
Figure 3.23: Mixed pixel effect for ToF laser scanner. Path of laser beam (left), Resulting spot coverage on surface (right).....	81
Figure 3.24: Triangulation principle (El-Hakim & Beraldin, 1994).....	83
Figure 3.25: Auto-synchronized laser scanner. Principle (left), single axis (centre), dual axis (right).(El-Hakim et al., 1997) .....	84
Figure 3.26: GapGun laser gauge. Measurement without standoff (left), with standoff (right). (Third Dimension, 2010).....	85
Figure 3.27: GapGun in use at EFDA-JET .....	86
Figure 3.28: Commercially available hand held laser triangulation scanners .....	87
Figure 3.29: Effect of surface reflectance change on collected data (Blais et al., 2005) .....	87
Figure 3.30: Range error caused by step discontinuity (Blais et al., 2005) .....	89
Figure 3.31: Triangulation range errors. After Curless & Levoy (1995).....	89
Figure 3.32: Effect of centroid shift (Edge Effects) dependent on sensor orientation. After Buzinski et al.(1992).....	89
Figure 3.33: Desktop laser scanner .....	90
Figure 3.34: Waves (undulations) in the collected data as a result of sensor/camera movement (Beraldin, 2004).....	91
Figure 3.35: Coded light, building up a code word (Trobina, 1995) .....	93

Figure 3.36: (top) Natural binary code. (bottom) Gray binary code. After (Akca et al., 2007).....	93
Figure 3.37: Active range measurement principle (Wahl, 1986).....	94
Figure 3.38: Commercially available white light projection systems.....	95
Figure 3.39: CMM arms.....	99
Figure 3.40: Metris RCA .....	99
Figure 3.41: Creaform EXAscan (Creaform, 2010).....	100
Figure 3.42: Hexagon metrology laser tracker with T-Cam .....	101
Figure 3.43: API IntelliScan/IntelliProbe 360 .....	102
Figure 3.44: NDI Optotrak optical tracker (Northern Digital Inc., 2008).....	103
Figure 3.45: Calculation of nominal and actual point from CMM touch probe (Savio et al., 2007).....	113
Figure 3.46: a) General purpose freeform artefact: the "Doppelsinusfläche". b) MFG (left) simulating turbine blade (right)(Savio et al., 2007) .....	114
Figure 3.47: NPL engineering orientated test artefact collection (Rodger et al., 2007). .....	114
Figure 3.48: NPL Phantom, anthropometric dimensional metrology (Rodger et al., 2007).....	115
Figure 3.49: NPL freeform reference (300 mm)(National Physical Laboratory, 2009).....	115
Figure 3.50: Left to right: NIST Step artefact, NIST slotted disc artefact & anodised spheres, NIST multi-reflectivity target.....	116
Figure 3.51: NRC flat artefact (Beraldin et al., 2007a).....	116
Figure 3.52: (left) NRC angled test artefact, (right) NRC pyramid with steps of different heights (Beraldin & Gaiani, 2005) .....	117
Figure 3.53: Test artefact for deformation measurement (Luhmann et al., 2008).....	117
Figure 3.54: Influence of in-plane and out-of-plane angle on the standard deviation of residuals to a best fit plane (Van Gestel et al., 2009).....	118
Figure 3.55: Height test artefact (Notni, 2010) .....	119
Figure 4.1: Components of a large scale measurement (University College London, National Physical Laboratory, Leica UK, 1999).....	122
Figure 4.2: Spherical 1.5" Retro-Target for Photogrammetry (left). 1.5" CCR-Reflector for Laser tracker or Total station (right).....	125
Figure 4.3: Preliminary test artefact.....	126
Figure 4.4: 'Roof tile' feature for gap measurement, nominal gap: 0.35mm (left). Step feature, nominal step height: 0.20mm (right).....	126

Figure 4.5: Example point data of a sphere. Top to bottom: Arius3D, Breuckmann (single scan), Breuckmann (multiple scans), Metris.....	132
Figure 4.6: Arius3D single Scan (top), Breuckmann multiple scans (middle), Metris multiple scans (bottom).....	134
Figure 4.7: Scan data plan view. Arius3D (left), Breuckmann (centre), Metris (right). .....	134
Figure 4.8: Partial reflectance at edge.....	135
Figure 4.9: Multi-path reflectance, profile of ‘roof tile’ feature (Figure 4.4) meeting artefact base. CAD data in red (straight lines), collected data in blue (curved lines).....	135
Figure 4.10: Effect of multi-path reflectance on the collected data (error scale in mm). .....	136
Figure 4.11: Data of inside of IVTF collected by Surphaser scanner, point brightness determined by light intensity returned to scanner. Photograph of same area ~ 2.5m x 3m (inset). ....	136
Figure 4.12: Measurement data of a pre-prototype tile assembly. Photograph (above) and computer visualisation of collected data (below).....	137
Figure 5.1: Angle Artefact A .....	143
Figure 5.2: Angle Artefact B.....	144
Figure 5.3: Step artefact (front) & Gap artefact (back) on a single (small) mounting plate. ....	145
Figure 5.4: Datum cluster featuring ø50mm sphere and EFDA-JET target holders (left), Side view of sphere and collar (right). ....	147
Figure 5.5: Portable test frame with Gap/Step artefact mounted (left), Angle Artefact A mounted (right).....	148
Figure 5.6: Large volume measurement test frame with datum clusters at the corners and artefacts attached, metre length included. ....	149
Figure 5.7: Touch probe & Vision CMMs measuring prototype tile blocks at manufacturer.....	150
Figure 5.8: Complete surface of block 8 cannot be measured as probe comes into contact with block 9. ....	151
Figure 5.9: One surface measurement device, collecting dimensional measurement from four positions/directions (a, b, c, d).....	165
Figure 5.10: With reference to Figure 5.9:.....	166

Figure 5.11: Approach Angle Test - Orientation 1 - For Area Based Measurement Technologies e.g. White Light Fringe Projection. ....	167
Figure 5.12: Approach Angle Test - Orientation 1 - For Laser Line Triangulation Technologies. ....	169
Figure 5.13: Approach Angle Test - Orientation 2 - For Area Based Measurement Technologies e.g. White Light Fringe Projection. ....	170
Figure 5.14: Approach Angle Test - Orientation 2 - For Laser Line Triangulation Technologies. ....	171
Figure 5.15: End view of Angle Artefact B, showing a plane intersecting each angled facet to enable calculation of facet angle along a single axis.....	173
Figure 5.16: Depth of Field Test - For Area Based Measurement Technologies e.g. White Light Fringe Projection.....	175
Figure 5.17: Depth of Field Test - For Laser Line Triangulation Technologies.....	176
Figure 5.18: Segmenting data for Depth of Field test.....	177
Figure 5.19: Edge Measurement Test - For Area Based Measurement Technologies e.g. White Light Fringe Projection. One set of data collected per Equipment Position.....	179
Figure 5.20: Edge Measurement Test - For Laser Line Triangulation Technologies. One set of data collected per Equipment Position. ....	181
Figure 5.21: Quantifying the immeasurable region .....	184
Figure 5.22: Gap Detection Test - For Area Based Measurement Technologies e.g. White Light Fringe Projection. One set of data collected per Equipment Position.....	186
Figure 5.23: Gap Detection Test - For Laser Line Triangulation Technologies. One set of data collected per Equipment Position.....	188
Figure 5.24: Large volume measurement test frame with datum clusters at the corners and artefacts attached, metre length included .....	191
Figure 5.25: Air temperature around large volume frame in °C for the period July-October 2009. ....	192
Figure 5.26: Air temperature change over one week .....	192
Figure 5.27: CAD model of a portion of the EFDA-JET machine with manned access floor installed.....	193
Figure 5.28: Comparison of CMM data to as-built model of artefact. Error scale in mm. ....	196

Figure 5.29: Deviation of data from best-fit to model using planar areas. In-Plane Approach Angle. ....	199
Figure 5.30: Deviation of data from best-fit to model using planar areas. Out-Of-Plane Approach Angle. ....	200
Figure 5.31: RMS error of plane fitting for each facet. ....	203
Figure 5.32: RMS error of plane fitting for each facet, plotted according to facet position on artefact. ....	203
Figure 5.33: Influence of in-plane angle on the standard deviation.....	204
Figure 5.34: Possible trend in laser line B showing reduced residuals when measuring a ‘rising’ surface.....	205
Figure 5.35: Histogram of residuals for two passes of laser line scanner over a planar surface ( $\pm 4$ standard deviations shown). ....	206
Figure 5.36: Histogram of residuals for two passes of laser line scanner over a surface - combined data set ( $\pm 4$ standard deviations shown). ....	206
Figure 5.37: RMS error of plane fitting for each facet. ....	207
Figure 5.38: RMS error of plane fitting for each facet, plotted according to facet position on artefact. ....	207
Figure 5.39: Influence of out-of-plane angle on the standard deviation .....	209
Figure 5.40: Error distribution highlighting systematic errors within the data.....	210
Figure 5.41: Discrepancy of computed angle between overall best fit registration and least squares best fit plane. ....	211
Figure 5.42: Angular error for Out-Of-Plane approach. Data sorted by nominal facet angle. ....	212
Figure 5.43 : Angular error for Out-Of-Plane approach. Data shown according to position on artefact. ....	212
Figure 5.44: Out-Of-Plane approach angle - facet angle to as-built CAD reference plane, showing the effect of registration error. These data use facet angle computed to the CMM reference plane and are therefore reliant on registration between data and as-built CAD. The angular errors seen on the central $0^\circ$ reference facet demonstrate the magnitude of mis-registration. ....	214
Figure 5.45: Orientation of projected pattern and laser line for in-plane approach test. ....	216
Figure 5.46: Angular error for in-plane approach. Data shown according to position on artefact.....	216
Figure 5.47: Angular error misalignment types (Vizvary, 2007, p.8).....	217

Figure 5.48: RMS residuals of best fit planes at three depth ranges.....	218
Figure 5.49: White light projection systems - RMS residuals of best fit planes at three depth ranges.....	219
Figure 5.50: White light projection systems B - RMS residuals of best fit planes at three depth ranges - Optimised scale.....	219
Figure 5.51: Data point spacing: Laser line A (left), Laser line B (right).....	221
Figure 5.52: Laser line system B data. 15mm x 15mm area highlighted, used for inter- line and intra-line point pitch calculation. Irregularity of the inter-line spacing is visible. ....	222
Figure 5.53: Step height (flush) deviations from touch probe data (mm).....	225
Figure 5.54: Step height deviation as percentage of as-built step height.....	226
Figure 5.55: Step height deviation as percentage of as-built step height - limited to 50% of actual height. ....	226
Figure 5.56: Plane 1&2 (0.015mm flush) of step artefact viewed from above. Top left- bottom right: Area Based A, Area Based B, Laser Line A, Laser Line B. Green points are $\pm 1$ standard deviation of a best fit plane. Red points are $\pm 1$ standard deviation of both planes. Grey points are greater than $\pm 1$ standard deviation. ....	228
Figure 5.57: Plane 5&6 (0.201mm flush) of step artefact viewed from above. Top left- bottom right: Area Based A, Area Based B, Laser Line A, Laser Line B. Green points are $\pm 1$ standard deviation of a best fit plane. Red points are $\pm 1$ standard deviation of both planes. Grey points are greater than $\pm 1$ standard deviation. ....	228
Figure 5.58: Edge profiles of a 1mm step edge with nominal edge radius of 0.05mm, generated by four measurement systems (Left to right: Fringe Projection B, Fringe Projection A, Laser A, Laser B). ....	230
Figure 5.59(a & b): Edge profiles. Fringe projection B (left), Laser line A (right). ....	231
Figure 5.60: Profiles of 1mm step coloured by number of standard deviations from best fit plane.....	234
Figure 5.61: Area A ( $\sim 45^\circ$ ) angled view showing plane 8 (coloured) between plane 7 and 9. Edge points seen enlarged, separated from main area of plane 8 by 'dip' in the surface.....	235
Figure 5.62: Profile image of Area system A ( $\sim 45^\circ$ ). Data on the lower plane (plane 8) drops 0.479mm below calculated plane, coinciding with the height of plane	

7. This would cause these ‘low’ points to be wrongly associated with plane 7 instead of plane 8.....	235
Figure 5.63: Qualitative assessment of link between step height and affected area of lower plane. ....	236
Figure 5.64: Profiles of 1mm step coloured by number of standard deviations from best fit plane.....	238
Figure 5.65: Effect of reflection on laser line/point intersection (After Nitzan (1988)) .....	239
Figure 5.66: Laser line A, 45° to edge .....	240
Figure 5.67: Profile of 1mm step taken by GapGun laser gauge. ....	241
Figure 5.68: Laser line A perpendicular to edge showing irregular downward curvature of lower surface. Plan view with step size increasing left to right (above), angled view of 1mm step (below).....	241
Figure 5.69: One JPEG image of the 3mm slot on the gap artefact. One of eight images collected and used by GapGun to calculate gap and flush (image cropped top and bottom). Given the calculated gap as 3.08mm (Table 5.11), the line thickness would be ~0.15mm.....	245
Figure 5.70: Nominal 3mm slot width imaged by two white light fringe projection systems in various orientations. Top left to bottom right: Fringe System B at ~45° to slots, Fringe System B perpendicular to slots, Fringe System B titled so as not looking along the surface normal (optimal), Fringe System A parallel to slots. ....	246
Figure 5.71: Fringe projection system A: Optimal measurement consisting of multiple orientations aligned using targets.....	246
Figure 5.72: Laser Line System A - Parallel to edge. Optimised incl. dynamic illumination intensity.....	247
Figure 5.73: Laser Line System A - Parallel to edge. Without optimisation. ....	247
Figure 5.74: Laser Line System B - Parallel to edge. Optimised incl. dynamic illumination intensity.....	248
Figure 5.75: Laser Line System B - Parallel to edge. Without optimisation. ....	248
Figure 5.76: Perspective view of gap artefact side showing left to right, 0.7mm, 1mm and 3mm slots. Data collected by Arius3D laser scanner. ....	249
Figure 5.77: Fringe Projection System B. Top left to bottom right, orientation of projected fringes WRT slots: Parallel, 45°, Perpendicular, Angled away from surface normal. ....	250

Figure 5.78: Fringe Projection System A.....	250
Figure 5.79: Fringe Projection System B imaging slot 1 & 2 in four configurations/orientations (parallel, 45°, perpendicular, optimised). Green data are within $\pm 1$ standard deviation of plane red data is within $\pm 4$ standard deviation and grey are greater than 4. ....	251
Figure 5.80: Profiles of Gap artefact slot 2, 0.34mm slot width (Table 5.11). ....	253
Figure 5.81: Histogram of residuals of point data unaffected by edge effects, following registration with (top) and without (bottom) edge data.....	256
Figure 5.82: Sphere diameter from best fit free radius sphere. ....	260
Figure 5.83: Length measurement discrepancy of laser line scanner compared to target-based photogrammetry. ....	261
Figure 5.84: Sphere centre offset away from collected data. After (Feng et al., 2001). ....	261
Figure 6.1: Side view of 2.5mm slot between tile assemblies – it is suggested that measurement into the slot to a depth of 1mm is required in order to exceed the random error of data on primary plasma facing surface. ....	282

## List of Tables

Table 2.1: Capabilities of measurement systems at EFDA-JET .....	49
Table 3.1: Accuracy values of laser trackers following ASME B89.4.19-2006 standard (FARO, n.d.a; Leica Geosystems, 2008) .....	77
Table 3.2: Technical specifications of one commercially available AM-CW laser scanner including laser spot diameter (Basis software Inc., 2009) .....	81
Table 3.3: Commercially available hand held laser triangulation systems, data from manufacturer technical specifications .....	88
Table 3.4: Hybrid Measurement systems, comparison between local measurement with component ‘i’ and total measurement using hybrid system comprised of components ‘i’ and ‘ii’. .....	104
Table 4.1: Co-efficient of thermal expansion (Temperature range: 20-100°C). <sup>1</sup> Courtesy of NPL at 19.85°C. <sup>2</sup> Mean value for products of single supplier (Thornel). <sup>3</sup> Sample mean of range of Inconel products.....	123
Table 4.2: Distance between sphere centres .....	131
Table 4.3: Distance between sphere centres compared to CMM generated data (Parts Per Million) .....	131
Table 4.4: Sphere fit statistics after sampling at 0.6mm, data in microns .....	133
Table 4.5: Sphere fit statistics following outlier detection in GSI V-STARS (microns) .....	133
Table 4.6: Plane fit statistics (microns).....	133
Table 4.7: Surface roughness (Ra) of pre-prototype tile. Data in µm.....	138
Table 5.1: Nominal and as-built step height between blocks. CMM data ±0.003mm. All data in MM.....	151
Table 5.2: Mean surface roughness (Ra) of artefacts following surface treatment. ....	152
Table 5.3: Equipment Specifications – Fringe Projection Measurement Systems .....	153
Table 5.4: Equipment Specifications – Laser Line Measurement Systems .....	153
Table 5.5: Point pitch on measurement surface. ....	221
Table 5.6: Inter-line and intra-line point pitch for laser line system B (data in mm). ...	222
Table 5.7: Standard deviation of residuals to least squares best fit planes (mm) at various orientations to the edge feature.....	224
Table 5.8: Nominal and as-built step height between blocks. CMM data ±0.003mm. All data in mm.....	225
Table 5.9: Standard deviation of residuals normal to least squares best fit planes. Plane 1 & 2. MM.....	228

Table 5.10: Calculated horizontal (gap) distance between Step 8 & 9 (mm). .....	232
Table 5.11: As-built slot width and standard deviation of gap artefact (mm). .....	245
Table 5.12: Residuals of data to nominal CAD model following removal of 'edge' data. .....	256
Table 5.13: Diameter of portable test frame datum spheres from CMM measurement. (±0.0035mm).....	259
Table 5.14: Sphere diameter from best fit free radius sphere. Numbers in parenthesis indicate number of points available for sphere fitting.....	259
Table 5.15: Length measurement discrepancy of laser line system A compared to target- based photogrammetry. ....	260

## **1. Introduction**

Optical non-contact surface measurement systems record the form and features of a surface without physical contact with the object. Such systems are used in a variety of industries where contact with a surface is undesirable e.g. the recording of cultural heritage objects and art, where high speed dimensional measurements are required or where very high data density is needed. Measurement systems are classified into: light-in-flight using the known optical properties of a wave to determine ranging, or triangulation systems where the known geometry of the measurement system determines an intersection point in space. This project investigates these technologies for surface measurement inside the EFDA-JET experimental fusion device.

This research has been performed in collaboration with the UK Atomic Energy Authority, operators of the EFDA-JET experimental fusion device in Oxfordshire, England. The focus of the work has been the investigation of optical non-contact dimensional measurement systems for use inside the EFDA-JET fusion device, to verify the correct installation of components and monitor surfaces for change. The inner walls of the machine are clad with tiles which protect the machine from the fusion reaction and must be installed to their as-designed positions to be effective.

### **1.1. Context**

Within the classification of optical non-contact measurement systems there are two significant divisions, equipment which can measure to a surface directly and those which record the position of a co-operative surface attached to the measurement object. The two types may be referred to as target measurement and surface measurement respectively, with target measurement currently employed at EFDA-JET in the form of target-based photogrammetry. Surface measurement technology records the surface directly without need for markers or targets although does require optically cooperative surfaces, with a lambertian surface ideal (Forest et al., 2004; Beraldin et al., 2007b).

For non-contact measurement systems performing surface measurement, a distinction has to be made between active and passive measurement systems (Beraldin et al., 2000). Passive measurement systems use ambient light energy received by a sensor whilst active systems utilise additional information such as the positions of the light source and sensor, the known speed of light, change in properties of a light wave and the change in form of a known pattern to determine positions in 3D space (El-Hakim et al., 1995).

Within the active measurement system grouping comes the distinction between time delay and triangulation systems, the first using the speed of light and laser coherence, with the second using the cosine law. Time delay systems are polar measurement devices with the measurement device in the centre of a near hemi-spherical measurement volume where range data are provided by the time taken for a pulse of light to be reflected from a surface back to the measurement device or the phase-shift between a transmitted and received continuous wave of light (Payne, 1973; Blais, 2004). The light source is directed outward from the unit with the horizontal and vertical angle recorded and combined with the range measurement for that position. These systems are commonly referred to as pulsed and continuous wave laser scanners.

Triangulation measurement systems project a spot, line or number of lines onto a measurement surface and record the position of the line on the surface with a sensor at fixed, known distance and orientation to the light source. The projection of a single spot or line are commonly achieved by collimated or laser light and referred to as triangulation laser scanners (El-Hakim & Beraldin, 1994), systems projecting multiple lines simultaneously may be referred to as a white light projection system or area based scanner. Triangulation measurement systems are limited by the 'base length' between light source and sensor(s), as base length is increased, uncertainty reduces however the chance of occlusions and the challenge of maintaining stability increase (El-Hakim & Beraldin, 1994). In light of the physically limited measurement volume, triangulation systems may be combined with stationary tracking units which record the six degrees of freedom (6DoF) of the triangulation sensor and allow a total measurement volume exceeding the sensor measurement volume.

The usage of data from optical non-contact measurement systems may be in the form of a 'point cloud' of individual positions in 3D space with no connectivity information to surrounding data or a polygon mesh format where adjacency information is provided. Use of these formats within commercial CAD packages is increasing although only in the last year or so has the handling of large numbers of point objects (tens - hundreds of millions) become available. Conversion of point and polygonal data to CAD representation is a labour intensive task but is often required for reverse engineering purposes.

Evaluation of measurement system performance is limited to best practice and guideline documents published within the last few years, the most complete being VDI/VDE 2634

(The Association of German Engineers (VDI), 2008). Existing guideline documents for CMM measurement do not account for the complexity of the often multiple components in a non-contact surface measurement system. Work is ongoing at academic and standards institutions to further develop tests to assess the performance of these measurement systems, including the development of test artefacts against which to evaluate measurement equipment. Test artefacts provide a set of features to be measured by a system and produce a data set allowing comparison to other measurement systems and against the performance standards defined by the measurement system manufacturer to confirm the system is within specification.

### **1.2. Motivation for Research**

Fusion is the process which powers the Sun and the stars, under great temperature and pressure light nuclei in a low power state will fuse to produce heavier atoms and a large release of energy. Fusion offers the potential for safe, clean and virtually limitless energy, but to create fusion on Earth involves great challenges. One of the most promising methods of developing fusion is magnetic confinement inside a Tokamak, a large toroidal device in which gas is heated to in excess of 100 million °C inside an ultra high vacuum. The gas forms electrically ionised gas known as plasma which is constrained by high power magnetic fields, it is inside this plasma that fusion can occur.

The fusion machine is protected from the effects of the plasma by a ‘first-wall’ which absorbs heat radiated by the plasma and protects the machine during an off-normal event. In support of the ITER project which is constructing a fusion machine ~3 times the size of EFDA-JET, a new first-wall will be installed. The new first-wall will use new materials and be comprised of thousands of ‘tiles’. These tiles will be have an exposed surface area of up to ~330 x 110mm and a complex surface form including features such as 0.35mm slots and 0.04mm steps.

To avoid contamination of the measurement surface with impurities, the plasma facing surface must remain untouched once installed to avoid those impurities being released into the plasma during operation and affecting the fusion reaction. The complex surface will only provide the intended protection if installed to the as-designed position and so must be checked once installed. The complex surface of the protective tiles is designed to withstand the harsh environment inside the machine but will require checking during maintenance and upgrade phases. Monitoring must be performed without contact with the surface and must be able to quantify change of the surface including the step and

gap features. The new first wall with complex features has created interest in non-contact surface measurement technologies for installation and maintenance checks.

### **1.3. Problem Statement**

This work relates specifically to the metrology needs of the EFDA-JET tokamak and seeks to answer the following questions:

- Can optical, non-contact surface measurement tools verify installation of plasma facing components to sub-millimetre accuracy?
- Can optical, non-contact surface measurement tools quantify dimensions and surface change of protective tiles?
- What is the optimal approach to a surface to perform surface measurement in the EFDA-JET tokamak?
- What method can be used by EFDA-JET to assess the performance of measurement systems, now and in the future?

### **1.4. Research Objectives**

The EFDA-JET requirements identified in Section 1.3 can be addressed in this thesis as a set of generic research objectives. Completion of these objectives will not only meet the EFDA-JET requirements but will also provide information applicable to other researchers and practitioners utilising optical, non-contact dimensional measurement equipment for a wide variety of engineering applications. Whilst the experiments carried out in this work are directed towards a particular surface finish, the experimental design has been presented in such a way that other workers can repeat it and gain information about their own particular surfaces. The objectives are as follows:

- Develop a process for evaluating the performance of optical, non-contact dimensional surface measurement equipment (guidance on data collection and processing). Unlike the VDI/VDE 2634 (Section 3.4) which is concerned with surfaces which do not influence the measurement surface, this work will develop and demonstrate a procedure tailored to a specific material and surface finish, but which is repeatable for any surface finish. Components of the process will include the following:

## Introduction

- Determine how the angle of measurement system to the measurement surface affects the quality of the collected data. To take into account: random, systematic and angular error. Section 5.2.3.1.
- Determine how the measurement system to surface distance affects the quality of collected data. Section 5.2.3.2.
- Assess the impact of ‘edge effects’ (Section 3.2.4) on collected data through the development of a method to identify data between planar regions affected by edge effects. Quantify the extent (from the theoretical ‘sharp edge’) of affected data. Section 5.2.3.3.
- Gap Detection - For the measurement of sub-millimetre step/gap features, recommend a workflow to minimise errors in the collected data. Section 5.2.3.4.
- Registration – develop a technique that can reliably register data from multiple scans by automatically rejecting data that is predicted to be of indeterminate quality due to physical limitations in the capture process. A key example are edge effects (Section 3.2.4) where data are degraded by increased noise and systematic error and must be removed for accurate and reliable ‘surface based’ registration methods. Section 5.2.3.5.
- Large Volume – practical artefacts contain highly detailed local surfaces and need to be portable to test equipment on and off site. This work designs and implements a method to support the accurate placement of individual artefacts within a larger volume in order to test system capabilities that require registration, tiling of views and use of 6DoF tracking for example. Section 5.2.3.6.

Inspection requires that the system carrying out the inspection and its interaction with the surfaces to be inspected is fully understood. The challenge addressed by this thesis is to firstly gain a practical understanding of the influence of a surface material and form on some of the key inspection technologies. Given this understanding, the second challenge is to develop and validate a methodology that makes best use of the available systems to reliably inspect the new tile surfaces under development at EFDA-JET.

To place these challenges in context, at the start of this research (2006) the use of non-contact surface measurement equipment was rapidly increasing but without a common method to evaluate system performance for optically challenging surfaces. There being no agreed method to evaluate the performance of non-contact surface measurement systems, no standard artefacts and no defined data processing methodology. It should be noted that this work is testing measurement systems at the limit of their capability.

### **1.5. Research Process**

To meet the objectives identified in Section 1.4 and requirements of EFDA-JET, this work will:

1. Perform a study of the engineering background and needs of the EFDA-JET project relating to metrology to understand previous work performed on dimensional metrology within the EFDA-JET project and that performed by other fusion institutions and devices.
  - a. Obtain practical experience of dimensional metrology at another experimental fusion device where non-contact dimensional metrology equipment is in use. Experience the complete data lifecycle from requirement through to output.
2. Research commercially available metrology tools and the operating principles behind them, focussing on the technologies already available to EFDA-JET and expanding to include all dimensional measurement technologies which may meet the brief laid out in the problem statement. Work is limited to systems which are available or will be available within the course of this research, the development of a new dimensional metrology technology is outside the scope of this project.
3. Assess the currently available methods to evaluate the performance of non-contact dimensional metrology systems and work performed in this area, develop any additional processes to generate the required information.
  - a. Develop and document a procedure which the metrology department can use to evaluate current metrology equipment and allow future equipment to be compared without influence from external influences e.g. environmental influences.

- b. Obtain, through purchase or manufacture all necessary resources to enable the evaluation of dimensional metrology equipment at EFDA-JET.
4. Using the developed methodology, assess the performance of current state-of-the-art dimensional metrology systems and determine whether these technologies satisfy the EFDA-JET requirements (Section 1.3). Report the conclusions of testing to EFDA-JET.

### **1.6. Research Tools**

To process the data collected a number of tools have been written in Microsoft Visual Basic for Applications to run within the Microsoft Excel software package. The tools use a least squares shape fitting package developed at University College London (UCL) to generate equations for plane and sphere fitting, which the tool uses to calculate residuals to those geometric primitives and perform statistical processing. Other processing includes calculating angular error, identifying edge points and calculating gap dimensions between adjacent planar surfaces. Because of the large quantities of data to process, tools have been developed to automate the interaction between the tools and software used. A number of the tools developed have been utilised on a joint research project between UCL and company Airbus. Some use of commercial software was necessary and for this scripts were written in a proprietary language to automate functions within the software, speeding up data extraction, ensuring a consistent processing methodology and minimising the possibility of human error.

### **1.7. Structure Summary**

This thesis consists of five main chapters, a discussion of the engineering problem (Section 2), a review of relevant metrology (Section 3), two chapters of experimental work (Section 4 & 5) and the conclusions of the project and opportunities for further work (Section 6).

The Engineering Problem outlines the opportunities for fusion as a means of energy production, describing the hazardous environment required to recreate the Sun on Earth and the need for remote handling equipment to operate within this environment. The design of the protective tiles used inside the machine is discussed and dictates the

measurement requirements for the project, which are detailed. Current metrology work at EFDA-JET and other similar fusion devices concludes the chapter.

The metrology chapter defines the terms which will be used throughout the thesis and discusses the metrology technologies investigated in this work. Active measurement technologies including light in flight, laser line triangulation and white light fringe projection are researched in detail and relate to the equipment trials performed in this work. Methods of handling and representing the collected data are followed by discussion of methods of registering data from multiple device positions. Relevant work from other institutions and a review of measurement test artefacts are covered and guide the work performed in the following chapters.

Based on the review of metrology technologies and practices described in the metrology chapter, experimental work was performed in the first year of research (2006/2007) using a new test artefact produced for the project to investigate the performance of measurement systems available to EFDA-JET and University College London. This work is detailed in the preliminary equipment trial chapter (Section 4). Measurement systems tested include white light fringe projection, optically tracked laser line triangulation and a phase-shift polar measurement system. Quantitative results are produced for length, sphere spacing and plane fitting, along with qualitative results of surface discontinuities and the relationship between surface roughness and measurement ability of a laser line triangulation system.

The primary equipment trial chapter details the design and preparation of a set of tests and test artefacts to evaluate the performance of four state of the art non-contact dimensional surface measurement systems. The tests build on work performed during the preliminary equipment trial and the four new test artefacts created have been designed and manufactured to provide answers to the EFDA-JET requirements. The testing process, data processing method and results for the tests performed are described in depth.

The thesis concludes with a review of the work performed and conclusions reached, for EFDA-JET and other users of non-contact dimensional surface metrology equipment. The requirements of EFDA-JET laid out in the introduction are addressed, followed by a discussion of opportunities for further work.

## **2. The Engineering Problem**

Tiles fitted to the inside of the EFDA-JET experimental fusion device protect the machine from the high temperatures generated during fusion experiments and to be effective must be installed to their as-designed positions and subsequently inspected for damage such as melting, erosion and deposition. In this section the environment inside EFDA-JET in which measurements will be made is discussed along with the limitations the environment and materials impose on the project. Detailed information regarding the components to be measured is given, followed by the requirements to be met and alternative approaches to in-vessel inspection both at EFDA-JET and other experimental fusion machines.

### **2.1.The Fusion Process & EFDA-JET**

Fusion occurs in a high temperature ionised electrically conducting gas known as plasma which is generated inside an ultra-high vacuum created within a sealed area known as a vacuum vessel. Inside the vacuum vessel plasma is contained by high power magnetic fields which compress the plasma and separate it from the vessel walls. The magnetic fields are required to contain the plasma and prevent contact with the vessel as the plasma will be heated to more than 100 million degrees C. If the plasma were to come into contact with any solid object thermal loss from the plasma would occur, quenching the fusion reaction and damaging the material contacted.

Current research has shown the optimal design for the vacuum vessel to be toroidal (doughnut shaped), the device being known as a Tokamak, the name is derived from the Russian words 'toroidalnaya kamera' and 'magitnaya katushka' meaning 'toroidal chamber' and 'magnetic coil' (Wesson, 2000). It is inside this toroidal chamber that immense pressure and heat are combined with fuel to produce fusion. The fuel that has shown most promise is a combination of the hydrogen isotopes deuterium and tritium, available from water and lithium respectively, both abundant on Earth. To generate the equivalent energy output from a large coal power station which would use 2.7 million tons of coal in a year would require just 250Kg of fusion fuel; the lithium from a standard laptop battery and the deuterium in 100 litres of water could provide all the power required by an average European person for 30 years (EFDA-JET, 2007). The Earth has supplies of these fuels to provide many thousands of years of fusion power with minimal impact compared to current large scale energy production and without generating carbon dioxide.

## The Engineering Problem

As temperatures in excess of 100 million degrees C are created inside a tokamak, the machine must be protected from the high temperature plasma and energy released, this protection is provided by the 'first wall', the plasma-facing surfaces. These plasma facing surfaces must be able to handle high heat loading as although the plasma is created inside a vacuum, some heat will radiate to the wall during normal operation and if an off-normal event occurs, the plasma may become unstable and magnetic confinement lost. In this event plasma may touch the vessel wall and although the fusion process is very quickly quenched, a large amount of energy may be deposited onto the first wall. It is important that damage to the plasma facing components is kept to a minimum to maximise operational time before replacement is required.

During the fusion process various forms of radiation are released, two of note being alpha particles which are mostly retained within the plasma and help self-heating while neutrons are able to leave the magnetic confinement, passing through the vessel until they are physically stopped or lose their energy. As neutrons leave the plasma they will 'see' the first wall and activate the materials they pass through, to minimise the long term effects of fusion research, materials should be selected which are least affected by radiation released from the reaction.

Selection criteria for materials used inside the tokamak include heat handling capability, resistance to radiation and effect of impurities released following damage e.g. erosion and deposition, either visible or at the atomic level. Impurities reduce the efficiency of the plasma and the effectiveness of the fusion reaction (Section 2.3).

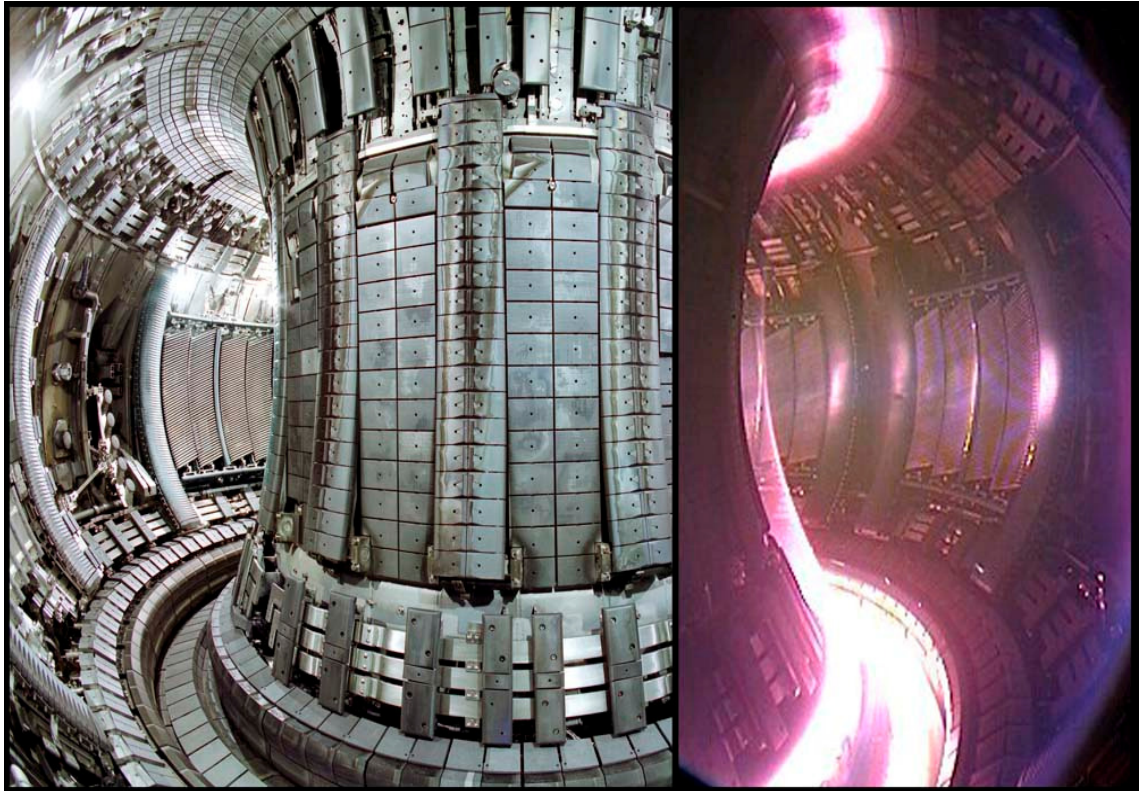


**Figure 2.1: Inside the EFDA-JET tokamak, with image of plasma during operation inset. (EFDA-JET, 2007). Figure courtesy of EFDA-JET**

Over 2000 ‘tiles’ are required to protect the inside of the EFDA-JET machine covering an area of more than  $200\text{m}^2$ . Various tile designs are required to protect all areas of the machine with special attention paid to those areas where the plasma will have the closest interaction with the first wall. The machine has tiles constructed of beryllium, tungsten and carbon fibre composite (CFC) with the latter capable of handling temperatures of  $\sim 3500^\circ\text{C}$ .

EFDA-JET has been operating with CFC as a plasma facing component for many years but now the first wall will be replaced to support research for ITER. The international ITER project will produce a new fusion device to demonstrate the scientific and technical feasibility of fusion power. Building on the research of EFDA-JET and other fusion institutions around the world, ITER has the scientific goal to achieve a fusion reaction where energy output exceeds energy input, specifically 10 times more energy output than input. ITER is the first fusion machine designed to exceed break-even and will be the largest fusion machine constructed, twice the size and ten times the plasma volume of EFDA-JET. The dimensions and increased plasma volume will result in slower cooling times and with the addition of technologies such as superconducting magnets allow for a longer fusion reaction (ITER, 2010).

## The Engineering Problem

EFDA-JET will support research for ITER by designing and installing a new ‘ITER-Like’ first wall that removes CFC as a plasma facing component. Tungsten and beryllium will be the primary plasma facing materials of the new wall as they have desirable properties and introduces fewer impurities into the plasma than CFC (Wesson, 2000, pp.135-36). Tungsten will be used in areas of extreme temperature with beryllium covering the majority of the protective tiles. Beryllium has a melting temperature of  $\sim 1270^{\circ}\text{C}$  compared to sublimation of CFC at  $\sim 3500^{\circ}\text{C}$ . To handle the heat, tile components have been re-designed incorporating complex features to allow them to operate within the demanding environment of the fusion machine. These new components will need to be installed to their as-designed positions to ensure they operate as calculated; further information on the protective tiles is given in section 2.3.

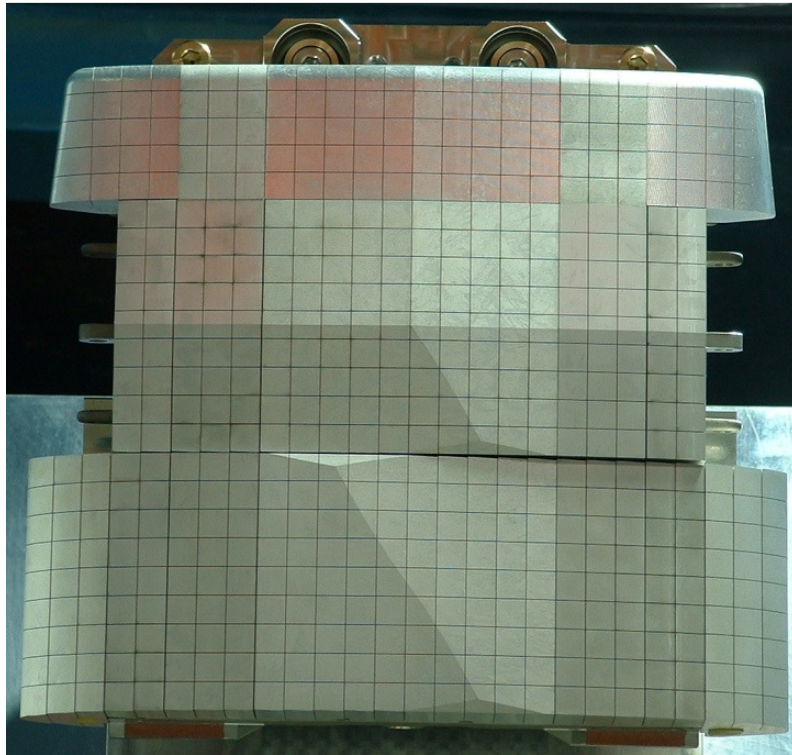


**Figure 2.2: Three ITER-Like wall limiter tile assemblies (middle assembly is incomplete). Figure courtesy of EFDA-JET**

### 2.2. Measurement Environment and Constraints

During an experimental campaign the fusion machine is in an ‘operational’ state, access to the machine and the ‘torus hall’ which surrounds it is closely controlled and the machine kept at vacuum. Two other machine states are possible, ‘maintenance’ and ‘shutdown’; a maintenance state allows limited access to the torus hall for certain tasks and the shutdown state requires the machine to be completely depressurised and isolated

## The Engineering Problem

from electrical supplies. It is during the shutdown state that any in-vessel inspection work will be completed. The vessel will be at ambient temperature and pressure and access ports opened to allow entry for remote handling equipment. Inspection of the inside of the machine during a state other than 'shutdown' has previously been investigated for EFDA-JET (Section 2.6) along with inspection approaches for other fusion machines.

The fusion process releases neutrons which are able to exit the magnetic confinement and react with materials in the closed fusion vessel causing them to become activated. In addition to activation, CFC used in the current first wall retains tritium used to fuel the reaction. The half-life of tritium is ~12 years and therefore its use is highly favourable compared to materials used in fission reactions whose half-lives are counted in hundreds of thousands of years. The activated materials and any tritium retained within them are hazardous to human health, in order to keep exposure to personnel As Low As Reasonably Practicable (ALARP), work within the EFDA-JET vessel is carried out remotely. Inspection work is currently carried out in vessel with a GSI V-Stars calibrated digital camera (Geodetic Systems Inc., 2010a) mounted to the end of the remote handling equipment performing photogrammetry (Section 2.5).

Equipment entering the vessel including during a shutdown period will receive a radiation dose; that dose being dependent on the experiments previously performed and the time period between the cessation of experiments and equipment entry. All equipment may be susceptible to the effects of radiation; in the metrology field CCD sensors used in digital cameras are an example of such equipment. Research suggests that exposure of a CCD sensor to low-level gamma radiation does not have any significant effect on the accuracy of measurements, but does affect other factors such as noise (Marbs & Boochs, 2006). Other optical components such as lenses, mirrors and prisms should be assessed prior to usage in-vessel, ensuring they can withstand the environment for the required length of service. Lenses and digital imaging metrology equipment used at EFDA-JET during shutdown periods have shown no damage by radiation (Brade, 2007).

During shutdown despite being isolated from electrical supply the fusion machine will continue to produce a residual magnetic field, an accurate measurement of the field has never been required but experience has shown the field to be weak. Camera equipment used for diagnostics has been rated to 0.002 Tesla, with the residual field likely to be

much less. If equipment were considered susceptible to the effects of low-level magnetism, methods would need to be developed to protect the equipment. Previous experience of in-vessel photogrammetric measurement by the Metrology team at EFDA-JET demonstrated the level of magnetism to be negligible in relation to metrology equipment (Brade, 2007).

### ***2.2.1. Remote Handling***

To keep exposure to personnel 'As Low As Reasonably Practicable' and demonstrate it is possible to operate a fusion device with minimal manned entry, remote handling technologies are used and manned entry strictly controlled. During the shutdown period the remote handling department operate two 10m long booms with 18 main articulations which can each reach 50% of the vessel from a single entry point. One boom is used to carry equipment and components for the use of the primary boom and enters the vessel through a port on the opposite side of the machine to the primary boom. Mounted to the end of a boom is 'Mascot', a unit with two force reflecting servo-manipulator 'arms' capable of performing complex operations in the vessel whilst providing a human operator adjustable force multiplier and feedback. Other custom units are available for specialised tasks or where higher load handling is required. The Mascot manipulator is capable of carrying 5kg in each of its two grippers for prolonged periods with a maximum load for short periods of 20Kg using both manipulators (EFDA-JET, 2010).

Human control is an essential part of the remote handling group and as such is different from robotic handling. Considerable planning occurs before remote handling operations begin as the route of the boom is designed and computer coded. During an operation the pre-determined route programmed into the computer is executed ensuring the boom travels at optimum speed whilst avoiding any possible collisions, minimises unnecessary movement and provides a clear work-flow for the operators. The planning process identifies the order of events and therefore the order of any equipment required by the boom, this process ensures components are presented in the correct order and in a suitable position for manipulation by the Mascot. Components required during an operation are placed by human operators into trays which are presented to the Mascot by the second boom which is withdrawn from the vessel when not in use. These components can be anything to be added or removed from the vessel; an example are retro-reflective photogrammetry targets which must be positioned by the Mascot in pre-

determined positions to allow a spread of targets necessary for a successful photogrammetric network calculation.

The inspection team work with the remote handling team to collect spatial data in the vessel during shutdown periods, the assistance and knowledge of the remote handling team will be essential for this project. As-built data generated from in-vessel surveys could be used by the remote handling team to augment their existing three-dimensional model of the inside of the vessel, indeed they are performing investigations into augmented reality to integrate the real-world data with that of their computer-aided design (CAD) model.

### **2.3. Tile Design**

Tile design is preceded by material choice for plasma-facing components which involves several primary factors: the introduction of impurities into the plasma, the amount of tritium retained within the material and the heat handling capabilities.

During fusion experiments ions released from the fusion reaction will come into contact with the first wall and impart energy which may dislodge atoms from the first wall and enter the plasma in a process known as sputtering. The impurities released reduce the efficiency of the plasma by allowing energy to escape in the form of electrons which cannot be stripped from their ions at the plasma temperature in use. In the early operation of EFDA-JET 70% of the energy lost was the result of radiation from impurities. Materials with a small number of electrons per atom (low atomic mass) are desirable for the plasma facing surface because their electrons can be stripped from the bulk of the plasma resulting in little radiation. Sputtering can also occur during plasma disruptions when plasma containment is lost and the plasma may come into contact with the first wall depositing huge energy on a small area. Introduction of impurities into the plasma is accelerated by the vessel being at vacuum which draws loose particles away from the wall into the main vessel area (Wesson, 2000, pp.37-38,47). The need to minimise impurities in the vessel creates a need to perform surface measurement without making contact with the surface, measurement equipment contacting the surface could contaminate the tile surface and off gas impurities when the machine is pumped down to vacuum.

Radiation released from the reaction will activate materials inside the fusion vessel, to minimise the long term effects of fusion research materials are studied to determine how

long it is before their level of radioactivity is such that they are usable again. Radiation levels are linked to the accumulation of tritium in the ITER vessel. ITER operations are expected to be suspended when 350g of tritium has accumulated in the vessel and as each pulse will introduce approximately 100g of tritium into the vessel the tritium retention in the plasma facing materials needs to be kept to a low percentage to allow several hundred pulses before tritium clean-up is required (Pamela, 2006). Materials which have a porous surface structure will retain more of these substances and release them back into the plasma at a later time with the potential to quench the reaction, additional tritium in the plasma will alter the balance of fuel required for fusion (EFDA-JET, 2007).

Along with the above considerations, materials must protect the vacuum vessel from the immense heat of the plasma. Reaching temperatures of 100-150 million degrees C, the plasma will radiate heat to the plasma facing surface through the vacuum equal to tens of megawatts of energy in EFDA-JET (Wesson, 2000). The internal surface area of EFDA-JET is  $>200\text{m}^2$  but power is not radiated evenly over this area but is placed on the first solid surface it comes into contact with. The effect of this is largely handled by the divertor region at the bottom of the device which is designed to handle the heat load and extract impurities from the plasma. During a disruption the plasma becomes unstable and contact with the first wall is possible, the plasma will immediately be quenched by the removal of the current but heat will be deposited at the strike point. Current first wall protection tiles made of Carbon Fibre Composite sublime at  $3500^\circ\text{C}$  whereas their replacements made of beryllium will melt at  $1270^\circ\text{C}$  (Wesson, 2000). Because of the different material properties the existing design for protective tiles will not be suitable for beryllium, new designs have been produced and a common tile design discussed below. Beryllium components have been used in the vessel since 1989 as protective tiles and as evaporator heads to coat other tiles in thin layers of beryllium (Patel & Parsons, 2002). Experience with beryllium as a plasma facing material in EFDA-JET has demonstrated damage even after significant pre-installation testing (Deksnis et al., 1997)

### ***2.3.1. Design of Plasma Facing Components***

In the early years of fusion research it was discovered that plasma was more stable if there was a solid structure near the plasma surface, this structure is implemented by the limiter tiles (Wesson, 2000). Limiter tiles form beams which run vertically around the

## The Engineering Problem

inner and outer walls of the Tokamak, 10 poloidal limiter beams on the outer wall and 16 inner wall guard limiters. During a disruption the limiter tiles have an increased risk of receiving a plasma strike than recessed tiles.

Areas subject to the highest heat loading are those where the plasma is closest to the vessel wall such as the divertor region at the bottom of the machine or where there is an outside influence, such as tiles opposite a neutral beam injection point. These tiles have a simpler design than limiter tiles but have to absorb large power levels over longer periods.

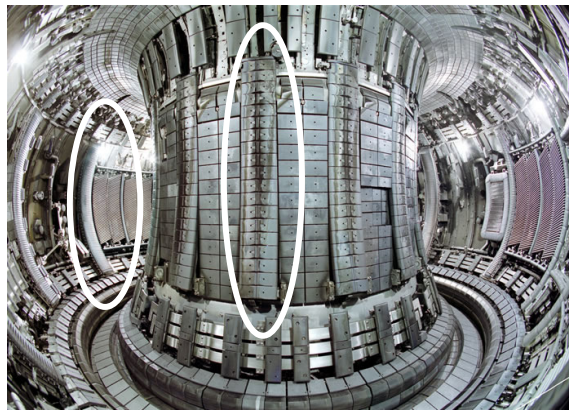


**Figure 2.3: Inside the EFDA-JET machine (June 2005) with two of the limiter beams highlighted**  
Figure courtesy of EFDA-JET

The plasma facing surface of limiter tiles for the ITER-Like wall are up to  $\sim 330 \times 110$ mm and is castellated to allow for rapid thermal expansion and contraction during operation, Figure 2.4. This design introduces a larger number of edges to the overall tile design than a single structure and as edges are more prone to damage than planar sections it is necessary to provide protection for these exposed edges. This is achieved by each castellation shadowing the next (Wesson, 2000, p.137). For the central section of a tile assembly a design tolerance of  $40\mu\text{m}$  step between castellations has been calculated to avoid material melting. The individual elements of tiles with this castellation design are not planar surfaces but are curved. This design increases the complexity of the manufacture and also inspection.



**Figure 2.4: Pre-Prototype ITER-Like Wall Limiter tile. Figure courtesy of EFDA-JET. Plasma facing surface area of an outer wall tile is ~330 x 110mm.**

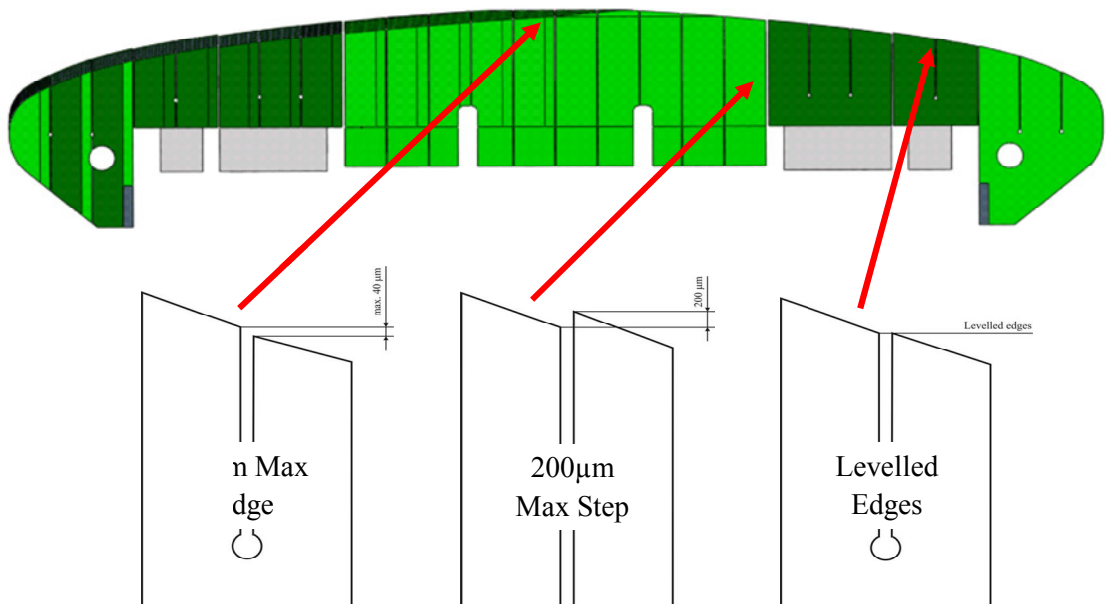


**Figure 2.5: Poloidal limiter tile assembly tolerances. Figure courtesy of EFDA-JET**

Based on calculations of material melting points (Figure 2.6) the optimum angle to position the tiles has been determined and introduces a constraint which must be met when installing the components. Melting of the protective tiles will remove the carefully designed profile and cause high points which will be more susceptible to plasma strike (Wesson, 2000).

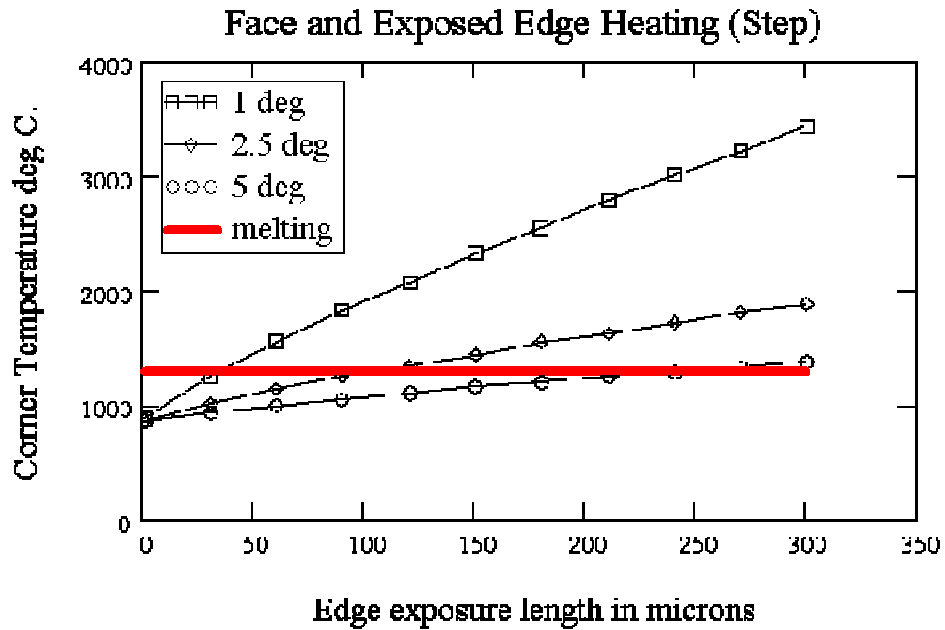


Figure 2.6: Peak temperature on exposed edge. 40 $\mu$ m defined for ITER-Like wall. Figure courtesy EFDA-JET

Along with angle of installation, the radial position of components must be considered. In the limiter regions where there is a higher risk of plasma strike than in recessed areas, each ITER-Like wall tile provides protection for its adjacent tile. This protection is afforded by machining the tiles such that they ‘shadow’ the subsequent tile, in the direction of the plasma flow. A tile misplaced in the radial direction may offer a lower level of protection for adjacent tiles if the misalignment is too great and therefore an installation tolerance for all components in the radial direction exists which has been calculated at 0.68mm (Vizvary, 2007). The EFDA-JET machine is an experimental device and as such there is no definitive value at which plasma will be affected by a radial misalignment, some physicists suggest a radial misalignment from design of 1mm would have little effect on the plasma operation. Early operation at EFDA-JET did not have such a high installation tolerance and there were several instances of components being melted by interaction with the plasma (Deksnis et al., 1997), to avoid similar occurrences in the future it would seem prudent to maintain or improve upon the current accuracy of installation in an attempt to avoid damage to plasma facing surfaces.

The complex design and importance of positioning within the vessel make the limiter tile the most challenging all the tile types installed in the vessel to be measured, because of the challenge the limiter tile was therefore selected as the focus of this research. If

non-contact measurement of the limiter tile assemblies can be achieved, measurement of other, simpler tile types should be achievable.

### ***2.3.2. Manufacture & Effect on Measurement***

When light is reflected by a surface, its intensity and dispersion is determined by the material and its finish, a dark material will reflect a smaller percentage of received light than a light coloured surface and a polished surface reflects more light in a single direction than an unpolished surface. Understanding these physical constraints is important to understand how certain materials may perform with non-contact measurement techniques.

Both material and surface finish for the EFDA-JET ITER-Like wall have already been chosen because of their suitability for use in the fusion device and therefore cannot be changed to aid non-contact measurement. It is necessary to understand the surface which will be measured and so the surface finish will be assessed by determining the Roughness Average (Ra). The Ra needs to be determined as however carefully a surface is made and finished it will be imperfect; to qualify this finish we need to assess the waviness of the surface and the roughness. Waviness will be exhibited as undulations in the surface which may be detected when performing a mathematical plane fit to the surface, whilst roughness will be smaller and can affect the reflectance of light from the piece.

**Figure 2.7: Roughness and Waviness of a surface (Taylor-Hobson, n.d.)**

To calculate the Ra of a surface we have used a Taylor-Hobson Surtronic3, the Ra is the average deviation from a centre line over a given distance where the centre line is positioned so that the area below the peaks and above the troughs is equal (Figure 2.8).

**Figure 2.8: Calculating the Ra (Taylor-Hobson, n.d.)**

The Surtronic3 measures the surface by drawing a diamond tipped stylus and skid over the surface and recording the deviation of the stylus from that of the skid. As the skid has a larger surface area than the stylus it ‘rides’ across the top of the roughness and leaves the stylus to record the relative movement over the sample length (Figure 2.9).

**Figure 2.9: Measurement probe construction (Taylor-Hobson, n.d.)**

A surface with a low Ra value will be locally smoother than one with a larger Ra and when smooth at the microscopic level will be more likely to produce specular reflection than the same material with a greater Ra (Pilkington, 2010). When light is reflected from a perfectly diffusing surface it will appear to be of equal luminance wherever it is viewed from, such materials are known to follow Lambert's Law and may be known as Lambertian surfaces (Trucco & Verri, 1998). Surfaces which are good as diffuse reflectors are matt white paper which reflects 70 to 80 percent of visible light and magnesium oxide, magnesium carbonate with 97 or 98 percent reflectance (Smith, 1966). A commercial product with high Lambertian reflectance known to be used for calibration checks of optical metrology systems is Spectralon (Labsphere, 2006)

The prototype beryllium ITER-Like wall tile components finished by acid etching have a Ra of  $1.6\mu\text{m}$  for the plasma-facing surfaces, but the magnitude of waviness is not given (Inspection & Metrology Team, 2006). Experience from this project has demonstrated that machining marks can remain even after an acid etch surface treatment has been applied and will be recorded as the 'waviness' of the surface. The waviness will affect any measurement of surface flatness, but not the interaction of light with that surface. The Ra will indicate how light interacts with the surface (i.e. producing Lambertian or diffuse reflectance) and therefore how challenging that surface is for optical measurement (too much light returned and the sensor may become saturated, too little and the signal to noise ratio results in noisy data - Section 3.2.1.2).

The material and surface finish of protective tiles has been chosen based on their suitability for use in the vessel and cannot be altered by this project. The material selected is Beryllium (Be), however it is controlled under United Kingdom Control of Substances Hazardous to Health (COSHH) legislation (United Kingdom Health and Safety Executive, 1995) because inhalation of the particles can cause Berylliosis, a disease affecting the lungs. Special precautions are to be taken when working with beryllium and therefore its use in this project will be avoided. However, by not using Beryllium within this research there is a risk that the results generated will not be representative of the performance of the systems on a Beryllium surface. This risk is mitigated by using materials with a surface finished engineered to simulate the optical properties of the Beryllium surface (Section 4.1).

## **2.4.Data Required**

This project will investigate surface measurement at three volumes inside the EFDA-JET vessel: the complete torus volume, the intersection of two or more tile assemblies and a single tile assembly. The surface measurement data at the three volumes described will supplement data from photogrammetry surveys and contact surface inspection of damaged tiles after removal from the machine. The three measurement volumes selected have been chosen to satisfy the needs of various users within EFDA-JET and confirm correct installation of the ITER-Like wall and allow long term monitoring of its physical performance.

### ***2.4.1. Measurement of the complete machine volume***

Monitoring the form and dimensions of the machine, at this level surface measurement can go beyond current single point measurements from photogrammetry and record dimensional data with greater number of samples with possibility of earlier detection of change. Surface data also provides a means to record and assess large scale damage to the first wall where imagery may be inconclusive because of shadows and inconsistent lighting. Measurement data of the whole volume could be used to validate installation of complete structures and for selection of areas in the machine requiring more detailed measurements.

Prior to resumption of operation, video cameras inside the EFDA-JET vessel are used to visually inspect the volume for any potential risks to the machine e.g. tools or equipment left behind. The use of dimensional measurement data collected on surfaces inside the vessel could supplement 2D images of the inside of the machine. Through the use of dimensional surface data it may be possible to detect large items which are present but should not be, but smaller items may be indistinguishable from noise in the measurement data. Data from full volume measurement of the vessel surface could augment existing CAD data of the machine and be used by the remote handling team for more precise simulation and clash detection of operations in vessel.

Data are required to be registered to the machine datum system, for this a number of fixed locations on the vessel wall are known and can be fitted with various target types. The installation of geometric feature targets into these locations would be possible. In discussion with the EFDA-JET Chief Engineer and Head of Metrology, it was determined that point resolution need not be better than 1mm with point pitch on the

measurement surface of 5-10mm acceptable. These values would enable the creation of a digital model for comparison to future metrology surveys with suitable resolution for detecting change in form of the vessel significant for EFDA-JET. Data collection should be completed as quickly as possible and in a single entry to the vessel unless otherwise planned (Brade, 2007).

#### ***2.4.2. Measurement data of the intersection between two or more tiles***

Each tile assembly protects adjacent assemblies by shadowing, it is therefore essential that each assembly and component of that assembly are installed within tolerance as incorrect installation will reduce or remove the desired shadowing effect increasing the likelihood of damage to adjacent assemblies. In the poloidal direction, distance between limiter tile assemblies (dimensions ~330mm x 110mm) is nominally 2.5mm, allowing for curvature of the limiter beam (Vizvary, 2007). To confirm the correct installation of an assembly the 6 degrees of freedom of the tile assembly are required, necessitating the collection of data which constrains the position and orientation of the assembly within 3D space. As each assembly is comprised of 5-7 tile blocks with independent movement, each block must be individually constrained. A challenge is to calculate the distance between tile assemblies when the assembly is not a solid unit but a collection of blocks capable of independent movement. Calculation of the build up of tolerance between components has been performed for the new ITER-Like wall but installation checks are still necessary. An example of the tolerance build up calculations used can be found in earlier work for the installation of the MKII divertor (Salavy, 2002).

The maximum relative toroidal misalignment between assemblies varies between 0.92mm and 1.037mm dependent on tile type (Vizvary, 2007). Assuming that measurements should have an uncertainty an order of magnitude smaller than the given installation tolerance, in line with determination of measurement accuracy (Section 3.1), measurements with an uncertainty of 0.10mm are required. The installation requirements are more complex than toroidal distance alone but this level of measurement precision will satisfy the requirements of assembly-assembly measurement.

If possible measurements should be collected in the machine datum system to allow the form of a complete limiter beam to be calculated, if this is not possible a suitable means of registering data collected of a single beam should be in place. A system capable of collection within the machine datum system would allow flexibility to perform a wide

range of inspection tasks and may be used for additional tasks such as external monitoring of the position and orientation of remote handling equipment.

#### ***2.4.3. Measurement of a single tile assembly or part thereof***

A single limiter tile assembly has plasma facing surface area of  $\sim 330 \times 110$ mm; it is this plasma facing area which is of interest as the remainder of the surface area will be inaccessible for inspection. At this measurement volume the gap and flush between individual tile blocks is required, nominally 0.6mm and 0.2mm respectively (Vizvary, 2007). Based on a requirement that measurement uncertainty should be an order of magnitude better than the measurement, measurement uncertainty of  $\leq 0.06$ mm and 0.02mm respectively are required.

This work will ascertain if non-contact metrology equipment can produce data with lower uncertainty than is required for inter tile block measurement and provide reliable data on the castellations of a single tile block. At this level each castellation in a tile block produces a slot of 0.35mm width around it with flush between two castellations in the centre block of an assembly being 0.04mm. A measurement system with uncertainty of  $\leq 0.004$ mm would be required if following the same method as for larger volumes, it is recognised that measurements with this uncertainty are usually performed in temperature and humidity controlled conditions using contact measurement technology such as coordinate measurement machines, it is therefore understood that such an uncertainty may be impossible to achieve with non contact equipment in the given environment.

Data with an uncertainty of  $< 0.010$ mm are currently collected using contact methods on components removed from the machine but it is a slow process and measurement is only of a small number of tiles. Non contact measurement at this volume inside the vessel is not intended to replace contact measurement currently performed, but instead to assist in identifying when removal and contact measurement of tiles is required.

#### ***2.4.4. Collection speed***

The financial value of time spent inside the vessel time during a shutdown can be considered by taking the total operating budget of EFDA-JET and dividing this by the number of operational days (those producing results). An approximate value for a day of lost operation is  $\sim \pounds 250,000$  where there are 16 hours of work possible. Therefore one hour when the machine is not in an operational state performing experiments has an

approximate financial cost of £15.5k. Knowing the financial cost of time in-vessel highlights the need to collect the maximum amount of data at the optimal resolution with a defined accuracy (Section 3.1) in the minimum time. The total time to complete a current photogrammetric survey is difficult to define as it is dependent on the number of retro-reflective targets required and the speed at which these can be installed by the remote handling team. The process of capturing the images is quick but relies on remote handling equipment to position the camera and then wait for vibration to settle and equipment become stable. Planning movement within the vessel is time consuming but can be performed in advance of the shutdown period, it is the movement of equipment and the delay required for stability which is time consuming. Research has been undertaken by several international agencies considering a variety of technologies to image the inside of the ITER device currently under construction, and several times larger than EFDA-JET. One such report suggests a total survey time of only 6 minutes (Heikkinen et al., 2002) for a system using 10 sensors while the vessel is at vacuum. Time taken to survey the EFDA-JET device is very likely to be longer than this as initial research shows the system will need to be mounted to the boom whose movement speed will increase the survey time, but other mounting options have not been discounted. Experience suggests the quoted time would be difficult to replicate in the EFDA-JET device but any system which met the requirements could have the equipment cost weighed against the time it would take to complete the task. An expensive system capable of completing a survey in a shorter time than a cheaper alternative which takes longer may provide better long term value.

### ***2.4.5. Data format***

Inspection is a service provided to the engineering department of EFDA-JET, the purpose of this work is to enhance the operation of the department and other groups i.e. Remote Handling department and the Design Office. To assist other departments and groups it is necessary to provide information in a usable form and therefore data must be presented in a format that does not require a change by the user.

The primary software used by the Design Office at EFDA-JET was Catia V5 by Dassault Systems with the Remote Handling group using a variety of 3D modelling software, the variety of software packages in use means data must be provided in a file format readable by all the required packages, or multiple file formats should be made available. Both approaches open the possibility that discrepancies could occur during

file conversion and so checks will need to be made. Once processed, data should be made available to all at EFDA-JET on the corporate intranet by a document management system and users made aware of its presence.

Following discussions with the design office and remote handling groups the preferred data format would be geometric primitives found in CAD packages but production of this data would be very time and labour intensive for the amount of data to be collected. Outputting 'raw' data in the form of individual points, each with Cartesian coordinate would require CATIA to process approximately 200million points assuming point pitch on the surface of 0.5mm for limiter tile assemblies (based on measurement of tile assemblies). Literature indicates point cloud processing within CATIA V5 has improved greatly in recent years with ~1 million points limit to maintain application performance and ~10 million points maximum in 2004 (Dobers et al., 2004), by 2005 IBM claim CATIA V5 able to handle 20 million points (IBM, 2005). For visualisation a splatting technique could be used to display the data, an example is the QSplat system developed at Stanford University capable of displaying hundreds of millions to billions of points (Rusinkiewicz & Levoy, 2000). Raw point cloud data could be processed into a polygon mesh but is likely to lose fine surface detail unless the maximum triangle edge length is very small which would produce very large and difficult to handle data files.

Information on data formats and representation can be found in Section 3.3.1.

### **2.5.Current Measurement Technology and Process**

In this section we discuss metrology equipment currently in use at EFDA-JET for large volume measurements and for non-contact measurement of components to be installed in the machine. The primary large volume measurement tools in use at EFDA-JET are GSI V-Stars photogrammetry cameras and a number of theodolites; stereo photogrammetry, white light fringe projection and laser line scanning technologies are also available. A brief overview of systems is given here with detailed information about the measurement technologies available in the chapter 3.

The EFDA-JET machine was assembled using large jigs and theodolites, these were the primary installation measurement tools for a decade until a comparative study between theodolites and photogrammetry in 1995 found photogrammetry fit for purpose (van Lente, 1995). Photogrammetry uses the principles of triangulation to determine the

## The Engineering Problem

position of points in 3D space following calculations to determine the position and orientation of the camera used to collect the images. Retro-reflective targets placed on features to be measured reflect light to a camera, their highly reflective surface providing excellent contrast with the image background. The contrast allows the centre of the target to be precisely calculated with respect to other targets in the image network. Further information regarding the principles of photogrammetry and all technologies discussed in this section can be found in section 3.2.3. EFDA-JET uses INCA2 cameras from Geodetic Systems Inc. (Geodetic Systems Inc., 2010a)

Inside the vessel, target based photogrammetry is used with calibrated template targets to provide high accuracy measurements of important features (Figure 2.10). Template targets are purpose designed objects which locate in or onto specific positions inside the vessel allowing measurement of the feature they physically attach to. Before use template targets are calibrated through the use of a calibration frame and photogrammetry. The survey defines the relationship between the photogrammetry targets attached to the template target and the feature to which the target is attached. Once calibrated, when the template target is used in a photogrammetry survey the targets are detected in software and the position of the feature calculated as an offset from the measured targets (Wilson et al., 1999).



**Figure 2.10: Dump-plate target installed in-vessel. Target is attached to a single tile; other targets visible in the background. Figure courtesy EFDA-JET.**

## The Engineering Problem

As part of an in-vessel photogrammetric survey it is necessary to measure known positions in order to relate the collected data to a known datum system. Without known positions the relative positions of the measured features will be known but not their position in the vessel. The primary datum for the machine is defined by the magnetic centre of the machine, datum positions installed during machine construction were related to datum positions outside the machine in the pit under the machine by measurement made with twin theodolites and plumb linear scale through an open port (Brade, 1992; Woodley, 1992; 2010).

Target based photogrammetry using retro reflective targets alone is not a feasible method for measuring surfaces inside the EFDA-JET vessel as contact with the measurement surface is not permitted. Surface measurement using photogrammetry is possible using point projection in association with retro-reflective targets, such a system is the GSI PRO-SPOT (Geodetic Systems Inc., 2010b) one of which is owned by EFDA-JET. From a static position the PRO-SPOT system projects up to 23 thousand points of light onto a surface which are captured by one or more cameras from multiple positions and the point positions calculated as if they were retro-reflective targets. Point projection photogrammetry is used at the EFDA-JET site and component manufacturer sites for pre-installation checks on the form of protective tiles once constructed into tile beams.

In addition to theodolites and photogrammetric systems, a non-contact surface measurement system based on white light fringe projection technology (Section 3.2.4.3), produced by Breuckmann GmbH (Breuckmann GmbH, 2010) is available at EFDA-JET. The system uses a white-light projector and single analogue camera with frame grabber to perform non-contact surface measurement through the projection of a series of fringes with increasing spatial frequency onto the measurement surface. The system relies on the geometric relationship between the camera and projector being known and must be calibrated if the relative orientation between the two devices is altered. The system was purchased in 2001 to enable non-contact measurement of carbon and Carbon Fibre Composite (CFC) tiles however, since its purchase the unit has been superseded several times by the manufacturer as digital imaging technologies have developed. The hardware is based on an analogue 1.3 megapixel CCD camera to give a measurement volume of 160 x 125 x 100mm. The hardware requires stability for a minimum of one second to complete a measurement and then can be moved as a rigid assembly. If the part to be measured is too large to fit within the measurement volume

## The Engineering Problem

or is too complex to be captured from a single viewpoint it is necessary to move the part or the measurement equipment in order to obtain additional view. Moving the system or part requires data collected from different positions to be registered together, into a common coordinate system (Section 3.3.2).

In 2009 a requirement for a measurement system to measure CFC tiles removed from the EFDA-JET machine was introduced in preparation for the installation of the ITER-Like first wall. When the CFC tiles were originally installed some modifications to the back of a subset of tiles were made where an obstruction was found during installation. Modifications were not fully documented so as CFC tiles are removed from the machine they are visually inspected for modifications to the back surface, tiles found to have been modified are to be inspected and recorded so that the ITER-Like tile for that location can be modified in a similar way. CFC tiles removed from the machine must be handled in a controlled manner as they will be contaminated by radiation and tritium. A measurement system was required which could be used in a controlled environment and exposed to the contaminated tiles. Surface information with uncertainty of ~1mm and a measurement volume of ~25 x 10 x 10cm was required. Existing equipment was considered: the Breuckmann fringe projection system was considered too valuable to be used for the task as once it had entered the controlled area it could not be used outside of this area in the future. A trial of point projection photogrammetry through a piece of acrylic was performed so that the camera and projector could remain outside the controlled area. The results were found to be acceptable even with a vibration to the acrylic but the setup required an operator inside the controlled area to position the part and an inspector with projector and photogrammetry camera to be positioned outside. Photogrammetry hardware and skilled operators were already in high demand so alternative technologies were investigated and tested, leading to the purchase of two NextEngine 3D laser line scanners (NextEngine Inc., 2010). The NextEngine scanners were installed in 2009 in a fixed location ready for measurement of tiles removed from the vessel (page. 90).

<u>Measurement Technology / System</u>	<u>Single Setup Measurement Area / Volume</u>	<u>Target (T) or Surface (S) Measurement</u>	<u>Measurement Accuracy</u>
Theodolite	Polar with range >100m	T	<sup>a</sup>
Target Based	Metres to Tens of	T	From 0.00X

<sup>a</sup> The measurement error of a theodolite is based on the angular error, commonly given in arc seconds.

The Engineering Problem

Photogrammetry	Metres <sup>b</sup>		mm
Point Projection Photogrammetry	1.2 x 1.2m – 6 x 6m	S	From 0.0X mm
Breuckmann White Light Fringe Projection	0.16 x 0.13 x 0.10m	S	0.0X mm
NextEngine Desktop Laser Scanner	0.34m x 0.26m <sup>c</sup>	S	0.X mm <sup>d</sup>

**Table 2.1: Capabilities of measurement systems at EFDA-JET**

Of the equipment owned by EFDA-JET preliminary investigation suggests none is immediately suited to non-contact surface measurement inside the vessel. Theodolites and total stations primarily function with a target or reflector touching the point to be measured and for accurate single point measurement, not non-contact surface measurement. PRO-SPOT has so far not been used in vessel because of stability issues, the projector must remain stationary throughout the remote collection of all photographs or the position of the points will be incorrectly estimated. The projector and two cameras could be mounted within a single unit which would require stability only for the time taken to collect an image however the dimensions of such system would be difficult to manipulate inside the vessel. In addition to stability problems a large number of coded targets well distributed throughout the volume would be required to form the photogrammetric network required. The white light fringe projection system requires stability for a period of several seconds but will require a large number of geometric features in the measurement volume to perform registration between different measurement ‘patches’ as the surface lacks unique features for surface registration. The NextEngine 3D scanner requires a stationary position for measurement and has a measurement volume of a single tile assembly, with approximately 2000 tile assemblies for measurement, a large number of scanner units connected or a long measurement time would be required.

Measurement equipment owned by EFDA-JET was not purchased with the requirement to perform in vessel non-contact surface measurement and the rapid growth of commercially available measurement tools in the last 10 years has created interest in re-assessing surface measurement inside the EFDA-JET tokamak.

<sup>b</sup> At EFDA-JET, the imaging distance is roughly equivalent to the height/width of the imaged area, i.e. metres to tens of metres. The classification of ‘Close-Range’ photogrammetry is distances up to ~300m(Luhmann et al., 2006, p.5).

<sup>c</sup> Manufacturer specification quote: 13.5 inches x 10.1 inches for the ‘Wide’ field measurement.

<sup>d</sup> Manufacturer specification quote: 0.015 inch accuracy in ‘wide mode’.

## **2.6. Metrology in the Fusion Industry**

Much metrology work has taken place at EFDA-JET with publications focussing on the use of photogrammetry (Macklin et al., 1994; 1995; 1998; Wilson et al., 1999) but in-vessel inspection of surface geometry has not been performed. In this section surface inspection at other fusion machines and with a different environment is discussed.

This research is focussed on inspection during a shutdown period (Section 2.2) but research has been performed into in-vessel surface inspection when the machine is not in a shutdown state and is still at vacuum. Investigation in 2001 focussed on providing a system capable of performing a survey while the vessel was at vacuum but the research yielded a demonstration system which failed to meet the criteria laid out by the EFDA-JET team due to excessive movement of the measurement head and the system was not commissioned (Talarico et al., 2001; Bartolini et al., 2001; n.d.; AEESF, 1998b; 1998a; 1999; Colleti, 2001).

Measurement while the machine is at vacuum is more technically challenging than during shutdown and requires alterations to engineering solutions e.g. to prevent out-gassing liquid lubricants cannot be used, instead dry lubricants must be used. During maintenance phases, certain components are to be capable of withstanding 350°C. This research investigates systems to enter the vessel during a complete shutdown where all systems required during the 'operational' phase are isolated before work is performed. But during a maintenance phase vacuum is maintained and diagnostic equipment accesses the inside of the machine by ports around the vessel.

The requirement for a metrology system where components are placed outside of the vessel in a protected area came from the need to operate in the vessel under vacuum and with higher radiation levels than considered for this research. This environment necessitated a move away from systems using a CCD sensor in vessel. The metrology technology proposed by the Associazione EURATOM ENEA sulla Fusione in Italy was an Amplitude Modulated laser with sensor detecting both intensity and phase shift. The intensity produces a target image while the phase shifting determines range. The sensor and other sensitive equipment were to be placed outside the Bioshield, where the laser beam was to travel from the source along the optical fibre down a vertical probe from the top of the machine and into the vessel. At the end of the probe a prism is mounted which tilts to move the laser spot vertically around the vessel wall whilst the probe rotated around a vertical axis. Tilt and pan motions were controlled by stepper motors

## The Engineering Problem

with a requirement to control backlash, eliminating the error associated with reversal of direction of the motor. The tilt and rotation angles are recorded by optical encoders with a reported precision in rotation and revolution respectively of  $0.036^\circ$  and  $0.005^\circ$  with a stated accuracy of 1mm at 10m (Talarico et al., 2001).

Materials entering the vessel have additional limitations because of the need to minimise outgassing which involves the evaporation or vaporisation of lubricants and insulation. At the vacuum used in the EFDA-JET device most natural materials are unsuitable and dry lubricants must be used, fortunately these limitations are not present for current research as we will be considering an environment at normal atmospheric pressure.

A fault analysis report by Associazione EURATOM ENEA sulla Fusione in 2001 detailed problems with the tilt and pan gears and unacceptable displacement orthogonal to the probe vertical axis, up to  $\pm 1\text{mm}$  in 'x' and  $\pm 2\text{mm}$  in 'y' at the end of the vertical probe (Colleti, 2001). The horizontal displacement was attributed to the port through which the system entered and was attached, the diameter was found to be too small to maintain stability of the probe during rotation of the probe tip, causing the lateral movement. A larger diameter port would have allowed for a larger diameter probe to be used, with increased stability. The system was never commissioned for use in-vessel and the development team moved focus to the ITER project.

In vessel has received much attention, the continuation of work by Neri et al. (2005b; 2007; 2009; 2005a) is the most significant and ongoing. Other groups have also performed research into imaging the ITER first wall: VTT Electronics in Finland (Ahola et al., 2001; 1998; TEKES FFUSION, 2003) performed similar work to the LIVVS investigation by Associazione EURATOM ENEA sulla Fusione as did a group from the United States of America with the interesting difference of using frequency modulation as opposed to amplitude modulation (Spampinato et al., 1996; 1998b; 1998a; 1999; Menon et al., 2001).

The technologies investigated by the above groups followed a similar format, a probe inserted into the vessel with sensitive equipment outside of the Bioshield. Research has taken place into alternative methods including a tracked vehicle for viewing of the RFX fusion device in Italy (Dal Bello et al., 1998), but this was not a metrology device and was only equipped with a video camera. EFDA-JET is larger than RFX (linear dimensions  $\sim 50\%$ ) and the device would have been unable to closely study features on

the roof of the vessel as the distance is likely to have been too great. Until 1991 viewing in RFX was performed using the Remote Handling System but unlike EFDA-JET, the length of RFX boom required its repositioning in 12 different toroidal locations whereas EFDA-JET has two 10m long booms each capable of reaching 50% of the vessel.

The systems and research mentioned above are related to in-vessel inspection but largely for the monitoring of large scale damage to the machine. This project is interested in quantification of damage, the checking of erosion and deposition and the validation that components have been correctly installed. For some fusion devices such information is not required, alternative designs are being developed in parallel with the tokamak which do not require a solid wall close to the plasma edge as the plasma is maintained at a greater distance from the vessel wall and therefore the positioning of the first wall is less important than in a tokamak such as EFDA-JET. EFDA-JET also faces problems because of its size, in a smaller tokamak it would be possible to use a portable Co-ordinate Measuring Machine (CMM) arm to measure components as is done in the Mega Ampere Spherical Tokamak (MAST) at Culham Science Centre; in EFDA-JET the  $>200\text{m}^2$  surface area and remote handling would make this a difficult task.

Construction of a new fusion machine by the Max-Planck-Institut für Plasmaphysik (IPP) in Greifswald, Germany is using non contact metrology equipment to perform full surface measurement and reverse engineering of major components prior to installation (Eeten et al., 2009). The W7X device will have smaller internal volume and considerably different design than EFDA-JET but their work on data collection and processing is very interesting as it uses surface data (rather than feature data) and encompasses the complete collection and processing lifecycle, from planning through to fully reverse engineered models which could be a model for EFDA-JET operation. Laser trackers, photogrammetry and laser line scanning with articulated arms are in use (Herd, 2005).

Each experimental fusion machine has its own set of measurement challenges e.g. not every machine is clad with heat protective tiles, some machines operate with the plasma a greater distance from the machine wall and some with only partial tile coverage. Experimental machines also differ greatly in size, from those where no human entry is possible to the larger machines such as JT-60 in Japan and EFDA-JET where manned access is possible. Not every machine uses the same fuel combination either, EFDA-

## The Engineering Problem

JET is one of the only fusion machines to have used a deuterium tritium fuel mix, which results in the need for remote operation inside the machine. Until the operation of ITER, EFDA-JET holds a unique set of metrology challenges for fusion machines.

A similar problem to that at EFDA-JET can be found on the NASA space shuttle which during re-entry must be protected from temperatures of  $\sim 1650^{\circ}\text{C}$  caused by friction with Earth's atmosphere (NASA, 2006). Heat protective tiles must be inspected to ensure they are not damaged or missing prior to take-off and re-entry. Prior to take-off, hand-held laser scanners developed at the NASA Ames Research Centre are used and in orbit before re-entry using a Laser Camera System (LCS) from Canadian company Neptec using technology licensed from the National Research Council of Canada (NASA, 2007; Neptec, 2007a).

Although the environment in which the NASA measurements will be made is similar to EFDA-JET in that no-manned access will be possible, NASA has additional hazards imposed by working in a vacuum and having to transport all required equipment into orbit. The High Temperature Re-usable Surface Tiles used on the shuttle are primarily 6" x 6" ( $\sim 15.2\text{cm} \times \sim 15.2\text{cm}$ ) whilst smaller tiles exist for certain areas (NASA, 2000). The shuttle tiles are solid pieces with spacing between tiles for thermal expansion, this surface although in a harsher environment presents a less complex structure than the surface of protective tiles at EFDA-JET for measurement.

### **2.7. Summary of Requirements**

The requirements for this project can be summarised as follows:

- The measurement system must be capable of being mounted and operated remotely as human access within the machine is not permitted.
- Non-contact measurement must be used as contact with the plasma facing surface is not permitted because of the possibility of contaminating the surface and the material is controlled under the COSHH legislation.
- The environment is un-evenly illuminated and subject to low-level residual magnetic fields and low-level radiation.
- The time available for capture has not been defined but it should be as short as possible whilst obtaining the required level of information.

## The Engineering Problem

- The choice of solution will be made by the engineering team at EFDA-JET and it will be their responsibility to assess the cost of equipment versus the cost of time in vessel.
- Measurements must be traceable to a national standard but other than first calibration should not require return to the manufacturer or an off-site laboratory for calibration as once equipment enters the vessel it will be handled and stored in-line with site procedures and all future work should be possible on site.
- In line with the previous requirement the reliability of the equipment is a high priority, if it fails to function when required, the in-vessel plan would need to be changed which would be likely to cause a delay. Time in vessel is valued at ~£15.5k per hour, calculated as the loss of time possible for experiments, all work is completed as quickly as possible and changes to the plan minimised.

Both the collection of local and machine level data has been discussed and data must be collected in the correct coordinate system for its use. For data in the machine coordinate system, locking into this system prior to data collection will ensure it is collected in the correct datum system without the need for transformation and capable of capturing data at the required data density and accuracy. In the local system a relative accuracy of better than 40µm would be required to capture the erosion and deposition on tile surfaces, but in the machine coordinate system an (absolute) accuracy of tile to tile measurement of better than 0.1mm would be required across a surface area of >200m<sup>2</sup> (when stripped of all protective cladding the vessel has a cross-section of approximately 4.27m by 2.7m with outer circumference of ~13.75m).

### **3. Metrology**

In Chapter 2 the measurement problem was defined. This chapter investigates technologies which may be capable of providing the data required, beginning by defining metrology terms used in this work, then discussing non-contact metrology technology suitable for measurement of the volume required, highlighting the current state of the art. Once data collection has been discussed, the processing of the collected data is covered including registration and filtering of those data. Best practice for non-contact surface metrology and methods for assessment of the collected data conclude this chapter.

#### **3.1.Reference Terms**

In this chapter and beyond the specifications and performance of measurement equipment will be described, in order to maintain clarity and consistency it is necessary to define the terms to be used. The basis for these descriptions is ‘Part 1, the Basic and general terms (VIM) of General Metrology’ published by British Standards Institution (1995) which reproduces verbatim the International Vocabulary of Basic and General Terms in Metrology (VIM) published by ISO.

No measurement is perfect, “the doubt that exists about the result of any measurement” is the measurement uncertainty (Bell, 1999). Uncertainty is a quantitative descriptor which defines a range about the measured value, within this range the ‘true’ but immeasurable value is expected to exist. Measurement uncertainty is affected by a range of factors, including but not limited to: the measurement tool, the object and measurement being made, the method, the environment and the operator. Each factor introduces an element of error which may be systematic or random, systematic errors may occur due to bias in equipment and can be modelled and compensated for, random error cannot be modelled but the collection of multiple measurements with a suitable sample size may allow its effect be minimised by statistical means.

Two processes to evaluate the uncertainty of a dimensional measurement can be performed: Type A and Type B evaluations; the former is based on statistical methods and the latter based on information from any other source e.g. calibration certificates or manufacturer specification. For a simple point to point measurement the use of such methods is relatively straightforward but for non-contact surface measurement, validating system performance requires different methods (Section 3.4).

The uncertainty in a measurement is inversely proportional to the precision of the measurement system; a low uncertainty indicates a high precision. Both measures indicate the agreement between multiple measurements of the same part (Figure 3.1).

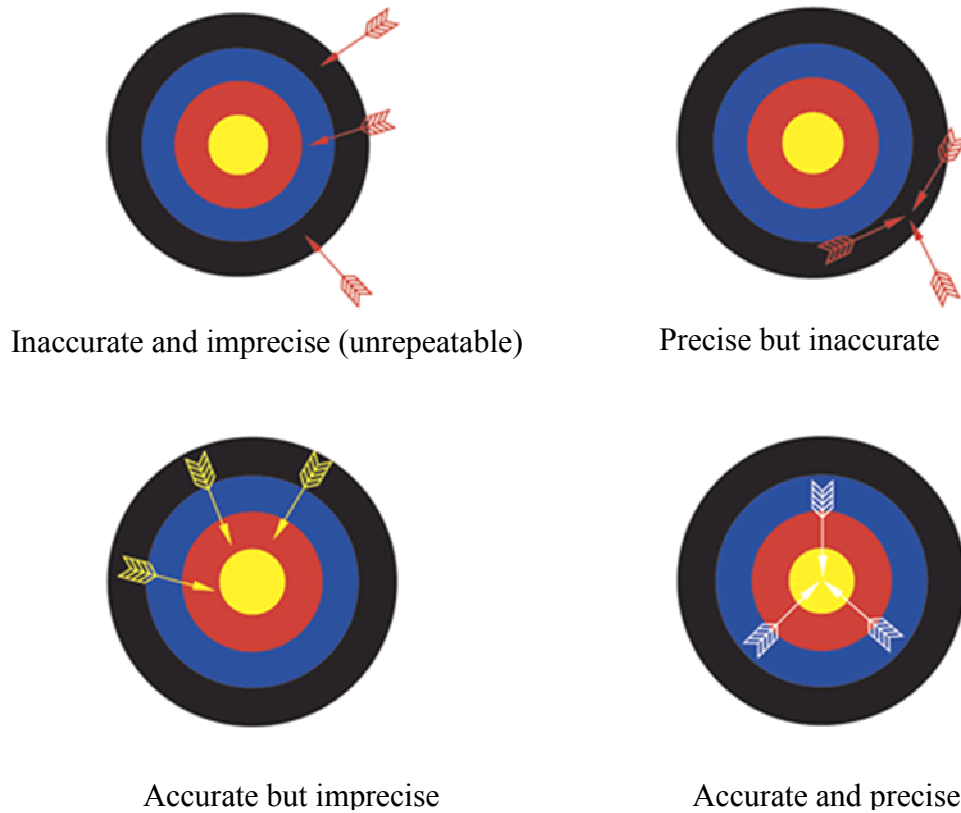


**Figure 3.1: Accuracy, Precision and Repeatability, Courtesy of NPL (C) Crown Copyright 2003**

Accuracy is the ‘closeness of the agreement between the result of a measurement and a true value’ (BSI, 1995). To ascertain if a measurement is accurate or not requires the measurement to be traceable to a known standard which is treated as the true value, or compared against a measurement system with calibrated accuracy an order of magnitude better than the measurement to be made. For dimensional measurement the known standard used is the metre, defined as ‘the length of the path travelled by light in vacuum during a time interval of  $1/299,792,458$  of a second.’ (Bureau International des Poids et Mesures, 1984).

### 3.2. Technology

This section considers measurement technologies which may be capable of meeting the requirements laid out in Section 2. All measurement systems considered in this work are capable of measuring a surface without contact, the systems may however be comprised of several technologies, some of which may not be able to measure to a

surface but instead to a cooperative surface. To distinguish between the two forms of measurement technology they shall be described as ‘surface’ and ‘target’ measurement systems respectively (Section 3.2.1).

### ***3.2.1. Measurement of Targets and Surfaces***

Surface measurement is the direct measurement of surface form and dimensions without the need for signalised markers, targets or known objects. Surface measurement technologies record the surface form and dimensions without surface contact, ideal for fast data collection of a given area or where the surface may be affected by contact measurement methods e.g. deformation of flexible materials, risk of cross-contamination in engineering and medical fields. Measurement systems capable of surface measurement may consist of multiple measurement technologies to produce a measurement system (Section 3.2.5), not all of the technologies used may be capable of direct surface measurement and may require measurement to a ‘target’.

#### **3.2.1.1. Target measurement**

Target measurement systems do not measure a surface directly, instead the position of a ‘target’ or ‘marker’ is measured and an offset applied to the measured position to derive a surface measurement. Target measurement is required where a position must be identifiable from a number of viewing positions e.g. photogrammetry (Section 3.2.3), or where the measurement method requires a transmitted wave to be returned directly to a measurement device e.g. laser tracker (Section 3.2.4.1). To differentiate the two types of measurement system the terms ‘multi-point measurement’ and ‘single point measurement’ shall be used to describe the two variants.

Multi-point measurement systems require targets which are easily identifiable within the measurement volume, each target position must be determined from more than one viewing position. Targets are affixed to features and surfaces for which measurements are to be made, making contact with the measurement surface. Measurements are only possible where targets have been placed and the form of the surface will determine the required target density, complex surfaces requiring a higher density of targets to correctly record the surface form. Ease of identification is achieved by target material having high contrast to the surrounding area e.g. white geometric shape on black background, retro-reflective targets (Figure 3.2). Retro-reflective targets commonly used in photogrammetry comprise a layer of retro-reflective glass beads or microprisms

(Luhmann et al., 2006, p.184) which reflects a high proportion of received light. The material typically reflects 100 to 1000 times more efficiently than a non reflective target material (Geodetic Services Inc., 2006) allowing high contrast with the background. Targets have a physical thickness defined by the method of construction and so the measured position must be offset normal to the target vector to calculate a position on the surface underneath. In addition to physical thickness, optical targets have an optical thickness, separate to the physical thickness but also defined by the manufacturing method. Retro-reflective targets may be stamped directly from the reflective material to produce the required shape or may have a ‘mask’ placed over the surface leaving only the desired shape visible, each design has a different optical thickness.

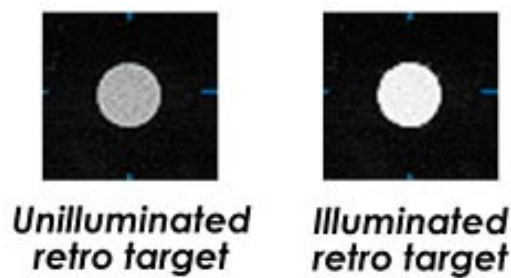


Figure 3.2: Retro-reflective photogrammetry target (Geodetic Systems Inc., 2010a) © Geodetic Systems Inc

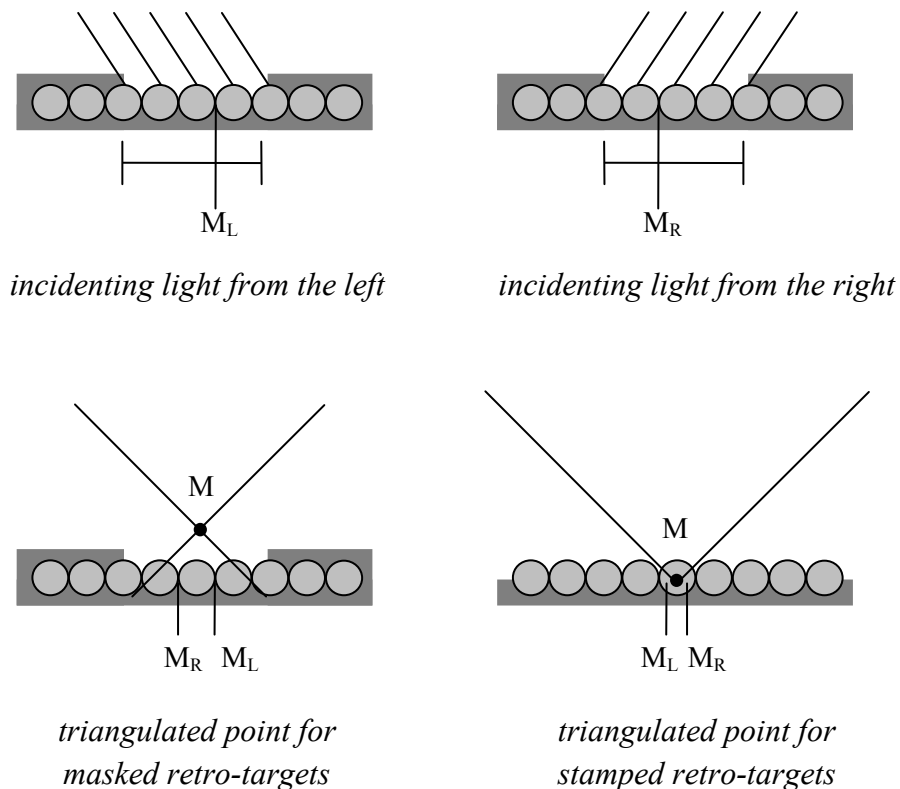


Figure 3.3: Effect of optical thickness of retro-reflective targets. After Luhmann et al. (2006, p.184), Figure with kind permission of Whittles Publishing.

Light emitting diodes (LED) may be used for optical measurement systems where the unique identification of positions is required. LEDs can pulse at set frequencies allowing each LED to be identified even when all use the same wavelength. In addition the optical sensor(s) capturing the LED positions can be fitted with a filter to allow only the wavelength of light used by the LED to pass through in order to provide resilience to ambient illumination. LEDs are used in measurement systems in the Hybrid Techniques group (Section 3.2.5) where a ‘constellation’ of LEDs can be used to track and determine the orientation of a portable device. The portable device with constellation of LEDs may be used as a surface measurement tool where the constellation of LEDs is known with respect to a probe tip through calibration.

Single point measurement systems collect positional data for a single point, the target is moved to a new position and another data point collected. An example of a single point measurement system is the laser tracker (Section 3.2.4.1) which measures the position of a cooperative target referred to as a ‘corner cube’ or ‘spherically mounted reflector’(SMR). Light entering a SMR is reflected back out along a path parallel to path of the input light. Measurement equipment such as the laser tracker use the lateral displacement of the returned light to adjust pointing direction until the transmitted and received light travel along the same path and therefore reflected from the centre of the SMR (FARO, 2006). The recorded position is not the point of contact on the surface but the centre of the SMR, so the measurement must be offset by the radius of the SMR. The SMR is required by this technology as the transmitted and received light must travel along the same optical path for a range measurement to be calculated.



**Figure 3.4: SMR/corner cube reflector (Brunson, 2010). Figure © Brunson.**

Targets allow high accuracy measurement of discrete points and the ability to perform repeatable measurements of the same feature. The disadvantages are the need to physically place a target at the position to be measured, making contact with the surface, and the need to offset measurements to account for the optical and physical thickness of the target. Multiple targets may be positioned before measurement (e.g. photogrammetry) or a single target moved to each measurement point (e.g. laser tracker). The duration of data collection will be determined by the measurement volume and the number of discrete positions requiring measurement, complexity of measurement will be determined by the accessibility of the measurement positions.

### **3.2.1.2. Surface measurement**

Target-less surface measurement allows dimensional measurement of a surface without contact or targets. Technologies capable of target-less measurement include: photogrammetry (Section 3.2.3), pulsed and continuous wave time of flight (Section 3.2.4.1), laser line triangulation (Section 3.2.4.2) and white light projection including phase-shifting (Section 3.2.4.3). Each technology highlighted uses light waves as part of the measurement process and therefore the interaction of the light wave with the measurement surface will impact the measurement.

Light hitting a surface will be partially absorbed or reflected dependent on the surface and the wavelength(s) of light used. An object illuminated by white light which appears red when viewed is absorbing all wavelengths of light other than red, objects which appear black are absorbing all wavelengths in the visible spectrum. Optical measurement systems utilising the visible light spectrum (Section 3.2.4.2 & 3.2.4.3) will be affected by surfaces which absorb light as the proportion of reflected light will be lower resulting in a reduced signal to noise (SNR) ratio. A low SNR will result in the sensing system having greater difficulty differentiating between the signal (reflected light) and noise (electrical noise in the sensing system or ambient illumination). Optical measurement systems using a reduced range of the light spectrum e.g. laser illumination, can filter the received light to reduce the effect of ambient illumination. Variation in the surface reflectance can cause range errors in triangulation technologies, specifically laser triangulation (Section 3.2.4.2) as calculation of the laser spot/line centre is affected (Figure 3.5) (El-Hakim & Beraldin, 1994; El-Hakim et al., 1995). Detailed information of how this affects laser triangulation measurement systems is covered in Section 3.2.4.2.

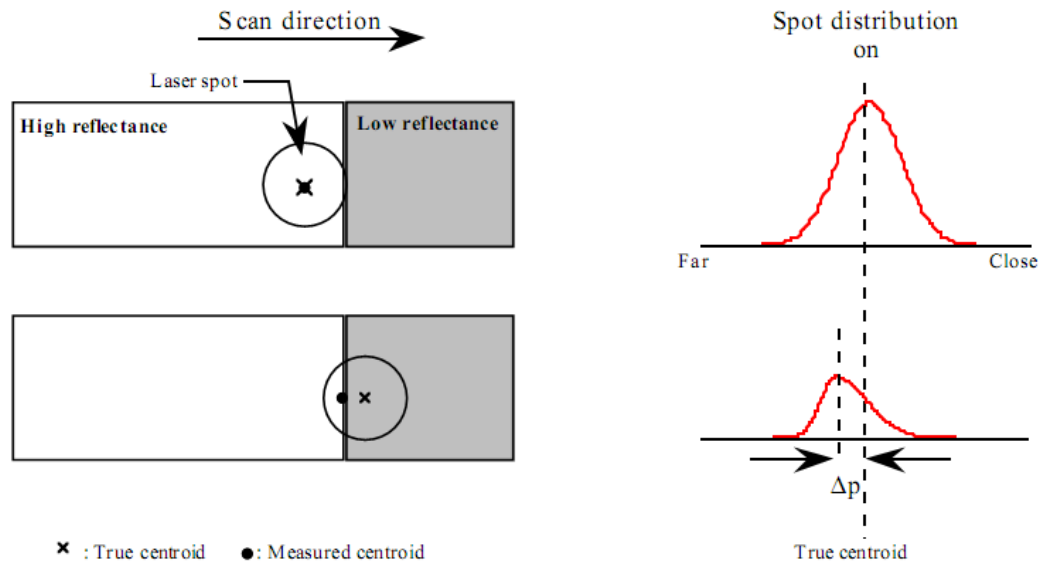


**Figure 3.5: Position calculation affected by surface reflectance change. Figure courtesy of NRC Canada**

The quantity of light a surface reflects will also affect pulsed time of flight laser scanners (Section 3.2.4.1) the darker the surface, the more the maximum achievable range is reduced (Wehr & Lohr, 1999). Darker surfaces may also affect the range calculation for pulsed time of flight laser scanners as a threshold is used to determine when the transmitted wave has been received and is therefore very dependent on the reflectivity of the measurement surface. A weaker return signal (from a low reflectivity surface) will result in a measured distance greater than the actual unless compensation is applied based on the intensity of received signal, Figure 3.19 (Thiel & Wehr, 2004).

Along with the quantity of light reflected by a surface the way in which that incident light is reflected must be considered, relevant to this work are specular and diffuse reflection (Figure 3.6). The ideal diffusely reflecting surface is one which follows the Lambertian surface reflectance model, adhering to Lambert's cosine law. A point on such a surface appears equally bright from all viewing directions, the luminance is equal regardless of viewing angle (Trucco & Verri, 1998; Ryer, 1997). Examples of diffuse reflectors are matt white paper which reflects 70 to 80 percent of visible light and magnesium oxide, magnesium carbonate with 97 or 98 percent reflectance (Smith, 1966), a commercial product with high Lambertian reflectance is Spectralon (Labsphere, 2006). A specular surface is one which follows the law of reflection, the angle of incidence at which light strikes a surface will equal the angle of reflection. A diffuse, completely Lambertian surface with high reflection index is optimal for optical triangulation measurement systems and is in fact assumed for active geometric

measurement systems (Forest et al., 2004; Beraldin et al., 2007b). Where the surface is not diffusely reflecting but instead a specular reflector, erroneous results may be produced. Figure 3.6 (a) demonstrates that for a specular surface and measurement system with given geometry and orientation to the surface, very little light will be recorded by the camera as the specular surface has directed the majority away. In contrast, a measurement system directed towards a specular surface with light source and sensor at equal angle either side of the surface normal will reflect light directly into the system sensor (Figure 3.7), possibly causing areas of the sensor to become saturated and record a maximum intensity value. Where the sensor is saturated sub-pixel determination of a laser spot/line for laser triangulation systems and lack of intensity values between phase intensity values in white light projection systems may occur, adversely affecting data. The proposed EFDA-JET first wall has a strong specular property necessitating the development of artefacts whose optical surface properties match those of the first wall materials.

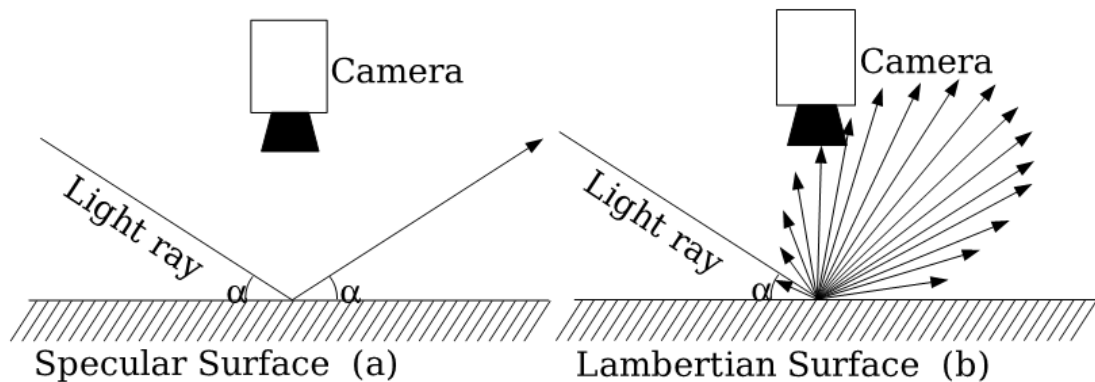
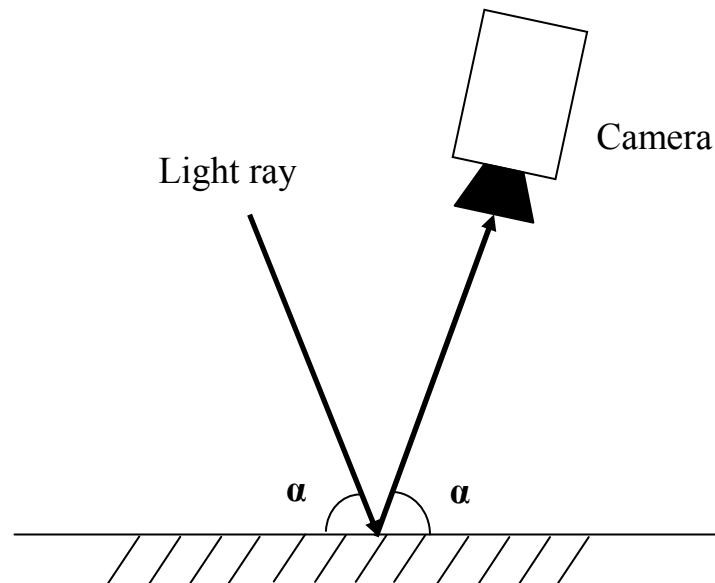
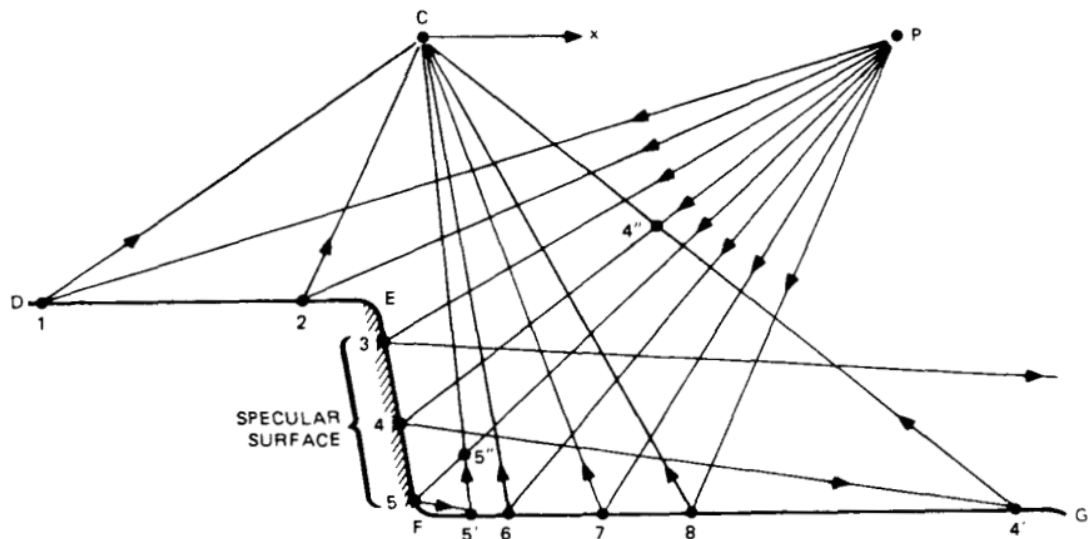


Figure 3.6: Behaviour of reflected light (Forest et al., 2004) © 2004 IEEE.



**Figure 3.7: Specular surface directs light directly to sensor where light source and sensor are equiangular of surface normal**

Measurement of a specular surface may also create erroneous measurements through multiple reflectance affecting triangulation (Section 3.2.4.2 & 3.2.4.3) and time of flight measurement systems (Section 3.2.4.1). Nitzan (1988) demonstrates that for triangulation measurement systems, light striking a specular surface will be largely reflected resulting in no range measurement (Figure 3.8, point 3). Where the reflected light strikes a non-specular surface visible to the imaging sensor erroneous data will be recorded (Figure 3.8, points 4 & 5). For laser triangulation measurement systems data may be missing, or if present be recorded with incorrect range, either reduced or increased dependent on the surfaces. For white light projection technology utilising phase from intensity, incorrect phase calculation may occur.



**Figure 3.8: Erroneous range measurement caused by specular surface for triangulation systems. (Nitzan, 1988) © 1988 IEEE. Note: the surface is diffusely reflecting, other than the area identified as specular.**

Time of flight measurement systems may also be affected by specular surfaces (Figure 3.9) where light is directed completely away and no signal is received by the sensor (Figure 3.9, point 3) or where the round trip time is increased because of reflection to and back from another surface (Figure 3.9, point 4).

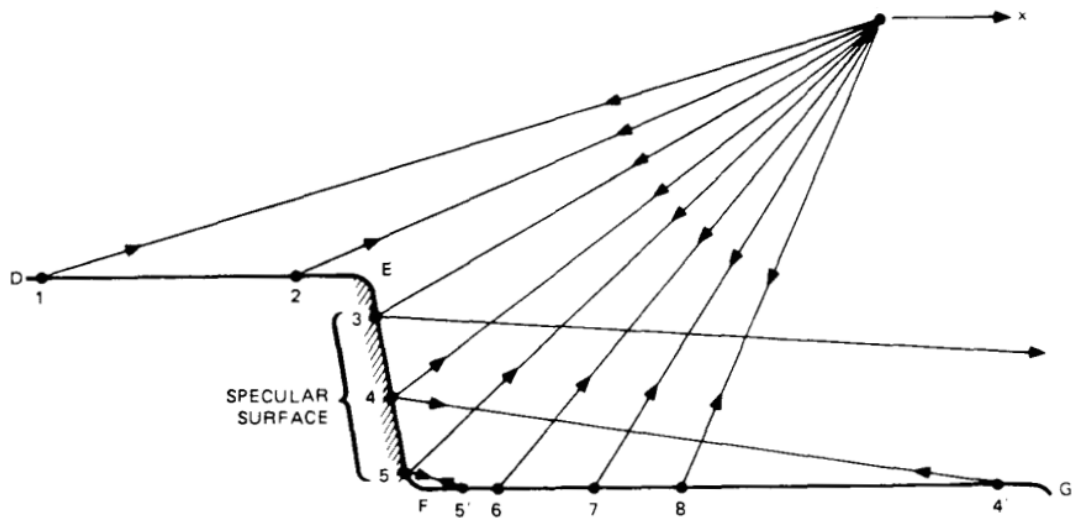


**Figure 3.9: Erroneous range measurement caused by specular surface for time of flight systems (Nitzan, 1988) © 1988 IEEE. Note: the surface is diffusely reflecting, other than the area identified as specular.**

Where the measurement surface material is translucent light will penetrate and produce range errors (Forest et al., 2004; Blais et al., 2005). Increasing light intensity increases the penetration depth whilst decreasing intensity increases the effect of noise as the signal to noise ratio decreases. Light penetration into the measurement surface will affect time of flight measurement systems (Section 3.2.4.1) as light has travelled a

greater distance and therefore greater range. Triangulation measurement systems may calculate an incorrect range and position and also have difficulty calculating the centroid of the projected light pattern as a result of light penetration (Figure 3.10). A material known to suffer from light penetration with a subsequent effect on surface measurement is marble (Godin et al., 2001). Recognising the effect light penetration into materials may have on range measurement, the National Institute of Standards and Technology performed a study into the laser penetration of the commercial material Spectralon (Cheok et al., 2009). Of interest to this project is the use of sand blasted aluminium as the reference material as testing showed “vapor-blasted aluminium to be as good as most commonly used diffusers” with minimal penetration.

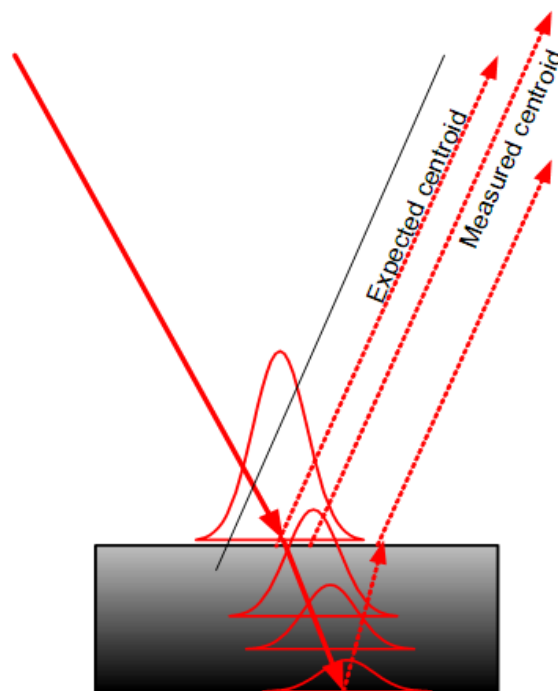


**Figure 3.10: Effect of surface penetration (Blais et al., 2005). Figure courtesy of NRC Canada.**

The use of a laser as the illumination source introduces certain problems, namely the inability to focus the laser to infinity and laser speckle. The laser spot/line has a physical width (diameter) when directed to a surface, and may therefore be reflected from more than one surface. Where this is the case a mean value between the measured points may be created and can affect time of flight and triangulation measurement systems (Section 3.2.4.1 & 3.2.4.2).

Speckle was first identified in the precursor to optical lasers, the microwave amplitude maser (Ridgen & Gordon, 1962; Oliver, 1963). Speckle is a result of coherent light being reflected by a surface whose roughness (Section 2.3.2) is comparable to the

wavelength of the light. The light reflected randomly from the surface may be constructive or destructive and result in bright speckles or dark speckles respectively, the appearance of the speckle altering with viewing angle. The influence of speckle on range finders is discussed by Goodman (1976), Baribeau and Rioux (1991) and Dorsch et al. (1994) summarising that speckle reduces the likelihood of target detection and introduces a physical limit to the power to resolve depth. The measurement surface affects the level of speckle, rough, uneven surfaces produce the most speckle with the optimal surface for minimum speckle being lambertian.

The errors which may occur when performing a measurement direct to a surface are greater than those for target based measurement and therefore a limited number of targets may be used inside the fusion vessel during measurement survey for data registration (Section 3.3.2). The use of targets is in-line with current procedures for photogrammetry (Section 3.2.3) surveys performed inside the EFDA-JET machine (Section 2.5), direct contact with the measurement surface is not permitted.

### ***3.2.2. Equipment Classification***

In this section vision technologies are divided using a taxonomy developed by researchers at the National Research Council Canada (NRC) (Beraldin et al., 2000; Beraldin & Gaiani, 2005). The taxonomy has been selected as it separates technologies based on their physical principles and is therefore particularly useful when investigating types of measurement technology, not individual implementations of that technology. An alternative approach considered would have categorised systems by the measurement volumes defined in Section 2.4, this approach was not selected as technologies could satisfy the requirements of more than one volume and their measurement volume could change greatly if combined with other technologies, in these cases the approach offered no advantage over the NRC taxonomy.

## Metrology

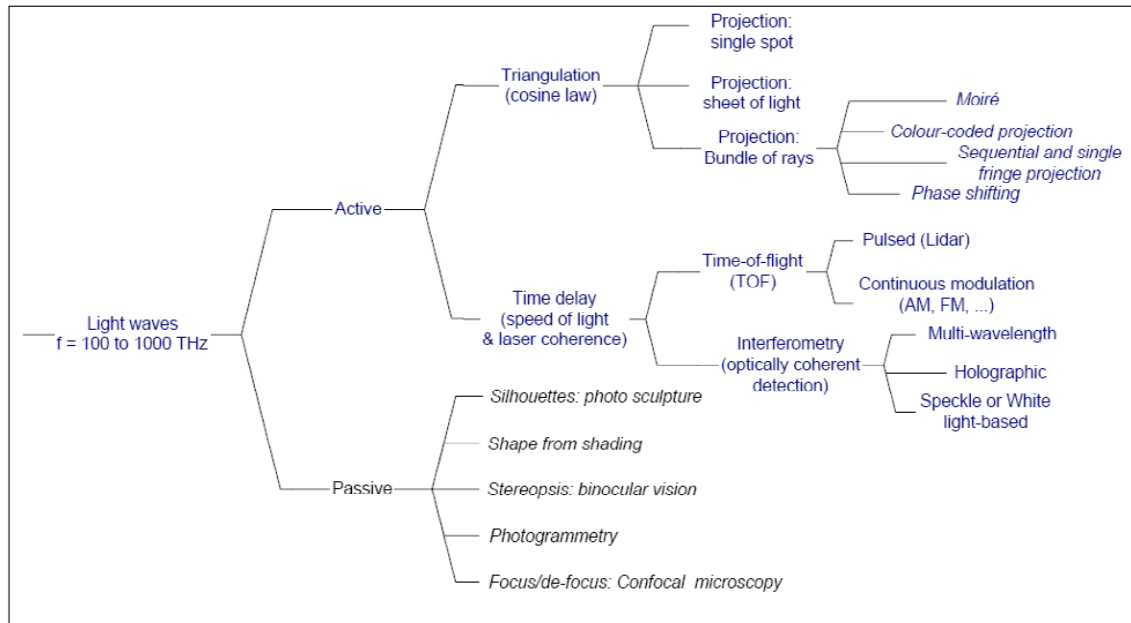


**Figure 3.11: Classification of non-contact 3D surface measurement techniques based on light waves (Beraldin et al., 2000) Figure courtesy of NRC Canada**

The NRC taxonomy begins by making the distinction between passive and active vision systems, the former uses ambient light energy received by the sensor and the latter utilises additional information such as the positions of the light source and sensor, the known speed of light, change in properties of a light wave and the change in form of a known pattern to determine positions in 3D space (El-Hakim et al., 1995).

### 3.2.3. *Passive Measurement Techniques*

Passive dimensional measurement systems use variation in light reflected from a surface to perform measurement, only surfaces visible to the sensor with clear changes in the intensity of light reflected can be measured. As seen in Figure 3.11, five passive measurement techniques are shown, photogrammetry is already in use at EFDA-JET for in vessel inspection and described in detail below. Of the other passive techniques, confocal microscopy is unsuitable because of its small measurement volume and the need for stability this introduces. Shape from shading requires that the surface be of a constant reflectance which cannot be guaranteed once the machine has been in operation as erosion, deposition and damage to surfaces will affect surface finish and therefore reflectance properties (Davies, 1997). Generating silhouettes of the components inside the EFDA-JET vessel would be impossible because of their attachment to the walls of the machine which removes photo sculpture as a measurement option. Binocular vision in the form of stereo photogrammetry is in use at EFDA-JET but suffers from the correspondence problem discussed below as part of the review of photogrammetry.

Photogrammetry is the measurement and reconstruction of 3D objects from one or more 2D images. Light reflected by an object is collected by one or more sensors to create an image, a 2D array of light intensity values. Measurement volumes range from the microscope level to satellite images, the volume required for this project being described as Close-Range Photogrammetry. Photogrammetry can be performed with a single image but commercially available photogrammetry systems for industrial and engineering measurement commonly use multiple images (multi-image photogrammetry) with one or more cameras. The use of a single camera to collect images, and processing of all images together to produce the measurement result is referred to as 'off-line' photogrammetry. Digital imaging technology has enabled the use of multiple cameras collecting synchronised images producing measurement results immediately and is referred to as 'on-line' photogrammetry.

Multi-image photogrammetry is based on the principle of triangulation, detecting position by the intersection of multiple lines of sight which are provided by multiple camera positions around the object to be measured. Multi-image photogrammetry requires that three sets of unknowns be solved: the triangulated positions of features of the object, the position and orientation of the camera and the internal geometry of the camera. The three sets of unknowns can be simultaneously solved by a 'bundle adjustment' and is described as the 'most powerful and accurate method of image orientation and point determination in photogrammetry' (Luhmann et al., 2006). Camera calibration is necessary to model the imperfections of the camera lens and other components and for digital cameras is included in the bundle adjustment (Fraser, 1997), detailed information of the development of calibration methods and models can be found in (Clarke & Fryer, 1998).

Multi-image photogrammetry requires the identification of a number of reference points in the collected images to define a relationship between those images, in the case of EFDA-JET this is performed using uniquely identifiable retro-reflective targets but could be performed by manual selection. Targets tie images together but to aid initial calculation of the position and orientation of the camera(s) a known object, a 'local reference tool' is included in the survey to establish a coordinate system (Luhmann et al., 2006, pp.255-57). In one commercial system the local reference tool is a cross shaped metal bar with retro-reflective targets attached known as an AutoBar (Figure 3.12), other manufacturers have similar devices. Images containing the local reference tool can undergo automatic resection in an iterative process, images not containing the

tool can then utilise targets for resection. The bundle adjustment is an iterative process and calculation of good approximate starting values through multi-image orientation will reduce the possibility that gross data errors will cause the adjustment to fail to converge to a solution.



**Figure 3.12: AutoBar used with Geodetic Systems V-Stars system**

The bundle adjustment uses two mathematical models to minimise the error of positioning camera and measured data; the functional model defines the relationship between the measured points in the image but does not contain information about the accuracy of the measured points, this is in the stochastic model, a covariance matrix containing the standard deviation of the unknowns along with a correlation coefficient for the relationship between points. Where measurements are independent and there is no correlation between measurements the matrix is reduced to a diagonal matrix of the variances of the observations.

The measurement of points or features of interest in a photogrammetric survey requires that those points/features are identifiable in multiple images. Points should be well distributed throughout the measurement volume and placed according to the measurement need. If dimensional information about a particular feature is required then that feature must be visible and measured in the images. If the feature is distinct and easily identifiable from other objects and the image background, it may be possible to use natural features in the images e.g. corner points, measuring the feature directly. Natural features can be selected manually by a user, or automatically by software, the precision of selecting the same point in each image will affect the final precision of the measurement. Object lighting must be carefully considered to present view independent lighting in order to minimise shadowing. In addition to ensuring the same point in each image is selected it is necessary to match points in one image to points in other images, this is referred to as the Correspondence Problem. Points selected in the images are used in the bundle adjustment as unknown values to be solved; incorrect identification

of points may adversely affect the bundle adjustment solution. Once the relative orientation of the images has been found, solving the correspondence problem becomes easier as it is then possible to search along the epipolar line with the image (Figure 3.37). The epipolar line in each image is the intersection of a plane defined by the camera base length and projected rays through the perspective centre of each camera to the object point (Figure 3.37). For a pair of images whose relative orientation is known, a point in one image will lie on, or close to the epipolar line in the second image (Luhmann et al., 2006, pp.217-18).

The use of natural features for photogrammetry can be improved upon by the introduction of engineered targets (Section 3.2.1.1) into the measurement volume which can provide an improvement in positioning precision over natural features by an order of magnitude (Robson & Shortis, 2007). The use of targets in the measurement volume simplifies identification of points for measurement and allows point determination for photogrammetry systems to sub-pixel accuracy. Retro-reflective targets may be directly stamped from a highly reflective material, or as used at EFDA-JET: reflective beads masked by a circular low reflectivity material (Figure 3.13), these targets reflect light 100 to 1000 times more efficiently than a non reflective target material (Figure 3.2) (Geodetic Services Inc., 2006) and can be combined with underexposed images to aid locating targets in collected images.



**Figure 3.13: Retro-reflective targets (Geodetic Systems Inc., 2010a) © Geodetic Systems Inc**

Targets are fixed to the measurement object surface but do not directly measure this surface, instead measuring a point displaced from the real position by the optical thickness of the target. The physical thickness of the target is defined by the materials used in the construction but the optical thickness is dependent on the design, either a stamped or masked design. Masked targets in use at EFDA-JET have an optical thickness of 0.11mm which must be removed following the bundle adjustment to obtain a point on the surface under the target. Removing the target thickness requires knowledge of the orientation of the target, at EFDA-JET this is usually performed for

planar surfaces by placing a minimum of three targets on a surface, creating a plane through those points in software and removing the target thickness along of the surface normal of the plane.

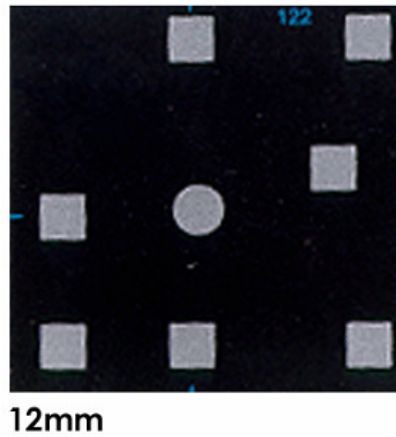


**Figure 3.14: Coded target (Geodetic Services Inc., 2006) © Geodetic Systems Inc**

The detection of retro-reflective target centres with sub-pixel precision is possible using a variety of techniques which are discussed in Shortis et al. (1994); in this work a simplified explanation is presented to demonstrate the principle. Retro-reflective targets reflect a much greater amount of light than the surrounding area and do so with a Gaussian intensity distribution (Figure 3.15). By setting a threshold and ignoring pixels which have an intensity below that threshold the image area to be searched becomes much less. For the remaining pixels, assuming a Gaussian intensity distribution calculate the centroid of the sample, with that point being the calculated target centre.

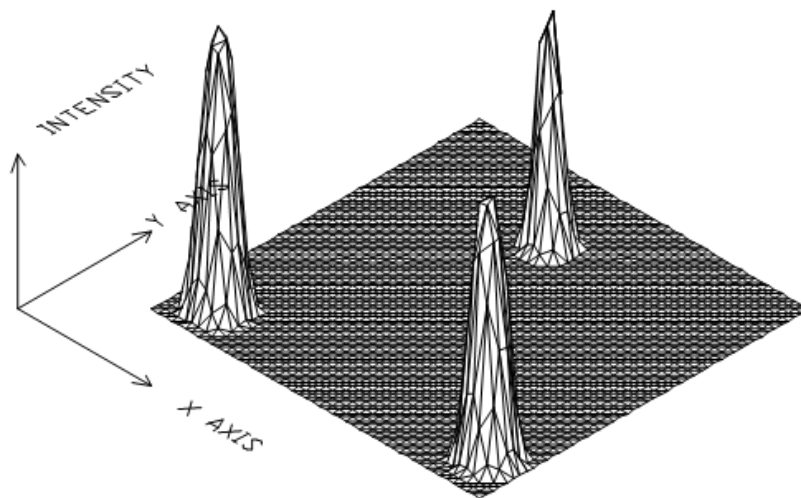


**Figure 3.15: Ideal retro-reflective targets (Shortis et al., 1994). Figure courtesy of SPIE.**

Coded targets are a special type of engineered target where each contains a pattern which can be uniquely identified by software; their use can automate the selection of tie points for image orientation. The coded targets in use at EFDA-JET are supplied by GSI and consist of a circular retro-reflective centre with a number of retro-reflective squares on a large back plastic square (Figure 3.14). Coded targets are re-usable and simplify the inspection process by removing the need for manual selection of points to tie images together. Where there is a feature to be measured which is complex or not directly visible, eccentric targets can be used and can provide single or multiple measured points e.g. a hole centre, or an edge. Eccentric targets are in use at EFDA-JET and referred to as 'feature targets' for the measurement of various features (Section 2.5).

Between the precision of non-contact natural feature measurement and engineered targets is point projection photogrammetry. Using a projector, points of light are projected onto the measurement surface and captured by the photogrammetry camera; while the projector and measurement part remain static the points in the collected image can be treated as engineered targets. Thousands of points can be simultaneous projected onto the measurement surface allowing dense non-contact surface measurement. The use of coded targets with point projection is advisable for resection of the collected images. Point projection is not without limitations, measurements are susceptible to ambient lighting and any movement of the projector will affect all projected points. The measurement area is limited by the point pitch and diameter on the surface, increasing the measurement area by increasing projector to surface distance will increase both. Unlike engineered targets it is possible that a projected point may not lay wholly on a single surface, also that the surface curvature may elongate the circle to become an ellipse, both will adversely affect the precision of locating the centre of that point.

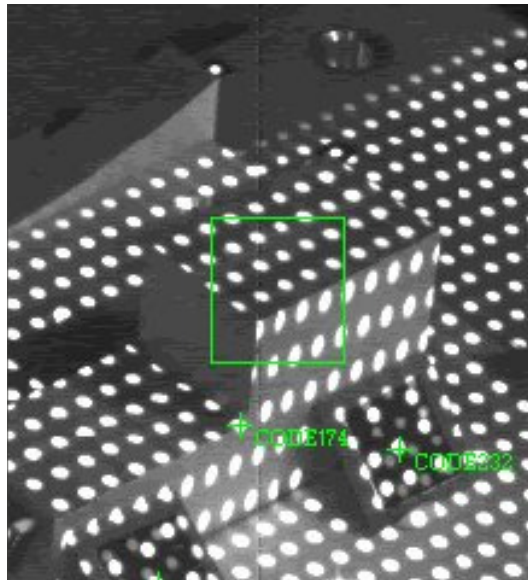


**Figure 3.16: Surface with projected points**

Where the object to be measured has a significant surface texture and/or colour variation, surface measurement is possible using a technique called dense surface modelling. Dense surface modelling uses areas of interest extracted from the collected images by feature detectors where there is variation in the collected image indicating high information content, recent techniques commonly use intensity variation between pixels to identify such areas (Jazayeri & Fraser, 2008). Selected areas are analysed to classify each interest point for the purpose of using in an image matching process. Commercially available measurement systems exist which can create a dense surface model from collected images e.g. Eos PhotoModeler Scanner (Eos Systems Inc., 2009). Where there is insufficient surface detail the projection of an irregular pattern onto the surface is required, a pseudo random pattern is used for the identification of individual regions in the image, a repeating pattern such as a grid of points provides no unique features and so do not meet the requirement that features should be scale and pose invariant.

The photogrammetric calculation can determine the precision of coordinates, but as “photogrammetric measurements are inherently dimensionless” (Geodetic Services Inc., 2006) it is not possible to determine accuracy in the object space, to do so requires external scale (Luhmann et al., 2006, pp.102,251). Scale is provided by at least one known distance and may be obtained through the measurement of a number of known points, the positions of which have been determined by a measurement system with an accuracy known to better than photogrammetry through calibration, or through the inclusion of an object with known dimensions in the collected images. At EFDA-JET

scale is provided through the inclusion of a number of calibrated INVAR scale bars within the measurement volume which are thermally stable with low coefficient of thermal expansion. The scale bars serve to provide traceability and accuracy to the survey as they have a calibrated length at a known temperature. By calculating the scale bar length at the measurement object temperature at the time of measurement they provide a known length by which to scale the survey results, without scale in the survey only relative distance measurement would be possible.

Commercially available photogrammetry systems vary greatly by intended use, some are designed to operate with off-the-shelf commercial cameras while other systems utilise metric cameras for greater precision. A metric camera is one which features stable optical-mechanical geometry and usually a fixed lens with fixed focus, interior geometry of this type of camera is calibrated by the manufacturer and is designed to maintain this geometry over a long period (Luhmann et al., 2006). The INCA 2 cameras from GSI owned by EFDA-JET are an example of a metric camera (Figure 3.17) which offer high performance for photogrammetry but are expensive (~£110k for the now current INCA 3 camera (Pace, 2010)), a less expensive option is to use non-metric amateur cameras, widely used for cultural heritage through to accident reconstruction.



**Figure 3.17: INCA 2 camera (Dold, 1998)**

Examples of commercially available photogrammetry systems for engineering include: GSI V-Stars, Aicon3D Systems DPAInspect, Photometrix Australis, GOM Tritop; alternative systems include: Eos Systems Photomodeler, Photometrix iWitness.

The information in this section shows that passive vision systems are dependent on the measurement surface featuring areas of interest e.g. varying surface texture or reflectance. The homogeneous surface finish and repeating design of protective tile components makes the use of a passive vision system for surface measurement inside EFDA-JET unsuitable.

### ***3.2.4. Active Measurement Techniques***

Active measurement techniques use information other than that available in the measurement scene to create measurements, the category is divided into systems using the principle of triangulation and those using the speed or coherence of light. In active triangulation systems a light source is directed onto a measurement object and is recorded by a sensor with known and fixed geometry from the source. Light may be a single spot, plane or number of planes. Where a single spot or plane of light is used it is typically collimated light from a laser, such systems are commercially referred to as triangulation laser scanners. Time delay systems where the properties of light are used to determine range measurements in a polar coordinate system are the first to be considered.

#### **3.2.4.1. Polar Measurement Systems**

Polar measurement systems may determine range based on time in flight, interference of waves or the phase shift of received light and may measure a cooperative target or the surface directly (Section 3.2.1). A target based measurement system for large scale metrology is the 'laser tracker' which is capable of collecting single point measurements in a near spherical measurement volume with a polar coordinate system. Their use is common for large-scale measurement such as aircraft manufacture because of relatively constant range accuracy values across their entire measurement volume (Blais, 2004) (Table 3.1). It is a target-based technology using a spherically mounted reflector (SMR) or other cooperative target which reflects light along a path parallel to the input direction (Section 3.2.1). A position measurement is the combination of 2 angle measurements, elevation and azimuth, and a range measurement commonly provided by an interferometer (IFM) or absolute distance meter (ADM).



**Figure 3.18: Commercially available laser trackers**

An interferometer is a relative distance measurement device capable of range measurement accuracy to a few microns (Kyle, 2005). A beam of coherent light from a laser is generated and directed outwards towards an object to be measured and reflected back by a cooperative surface, commonly a corner cube. The transmitted and reflected signals are combined within the tracker to produce a superposition wave which is affected by the distance the beam has travelled; each peak in the superposition wave indicates a change in distance equal to a portion of the wavelength of light in use. By counting the peaks of the superposition wave it is possible to accurately calculate distance from a known point in real time (Leica Geosystems, 2008). A known distance must be established prior to measurement and if the reflected beam of the IFM is broken, in these instances a distance can be obtained from placing the reflector in a target holder on the tracker commonly known as the ‘bird bath’, or in a previously measured position. The IFM is a highly accurate measurement tool but is now regularly combined with an absolute distance meter (ADM) or replaced entirely by so called ‘fast’ ADM systems.

The absolute distance meter is a ‘time of flight’ measurement device capable of absolute distance measurement by timing the return of a laser to a laser tracker from a cooperative target. The integration time of an ADM can be  $\sim 1000^{\text{th}}$ /second during which time the reflector must remain static. The uncertainty of range measurements

from an ADM is approximately 20µm (Kyle, 2005) so to combine the range accuracy of the IFM with the flexibility of an ADM, metrology suppliers have developed products such as the AIFM (Absolute Interferometer) and aADM (Agile Absolute Distance Meter). The AIFM negates the need for a target to remain static during measurement by measuring the relative movement of the target and factoring this into the ADM distance measurement, the aADM does not use an IFM but uses high speed electronics and three frequencies of light to calculate distance based on the phase of the received signal (FARO, n.d.a; Leica Geosystems, 2008).

	ADM Distance	IFM Distance	Angular
Faro Ion	8µm + 0.4µm/m	2µm + 0.4µm/m	10µm + 2.5µm/m
Leica Absolute	±5µm	±0.2µm + 0.15µm/m	±7.5µm + 3µm/m

**Table 3.1: Accuracy values of laser trackers following ASME B89.4.19-2006 standard (FARO, n.d.a; Leica Geosystems, 2008)**

To collect large numbers of surface measurements without the need for a cooperative target or surface contact (target-less) a time of flight (ToF) laser scanner can be used. A time of flight laser scanner operates similarly to a laser tracker in that two angle measurements and a range are recorded in a polar coordinate system, however the ToF scanner measures the surface directly without the need for a target i.e. corner cube, SMR. Commercial implementations collect data in a hemi-spherical volume centred on the unit by directing a laser by a moving mirror and rotating the unit itself. Range measurements are calculated by pulsed or continuous-wave time of flight.

Pulsed time of flight systems transmit a short intensive pulse of light which travels to a surface and is reflected back, covering twice the distance  $d$ . By measuring the time for the signal to be returned a distance can be calculated as:

$$2d = c\Delta t'$$

$$= c(t_R - t_E) \tag{Eq 3.1}$$

Where  $d$  = distance between instrument and surface,  
 $c$  = velocity of light (3.33 nanoseconds/metre)  
 $\Delta t'$  = flight time of pulse  
 $t_E$  = time of departure of pulse  
 $t_R$  = time of arrival of pulse

(Rüeger, 1990, p.11)

Determination of the flight time of the pulse ( $\Delta t'$ ) requires highly sensitive electronics, the need for which places a limitation on time of flight technologies (Beraldin et al.,

2000). An example of the sensitivity required is that to obtain a range resolution of 1mm it is necessary to accurately measure approximately 3.33 picoseconds. In order to calculate the flight time it is necessary to determine when the signal has been received, a method for doing so is thresholding, commonly performed on the leading edge the rising slope of the received laser signal is used to determine the arrival time of the pulse. As a surface measurement tool, the return will be affected by the reflectivity of the surface measured and where a fixed threshold is used will affect the time at which the signal is deemed to have been received. The level of the received signal is used to adjust the threshold value so the amplitude of the received signal does not affect the time measurement (Figure 3.19). An alternative method to determine the arrival of the returned wave is constant fraction discriminator (CFD) where the method is unaffected by the amplitude of the received signal (Kilpelä, 2004).

**Figure 3.19: Time of flight thresholding. Fixed threshold (left), Return signal level dependent threshold (Right). After Thiel & Wehr (2004)**

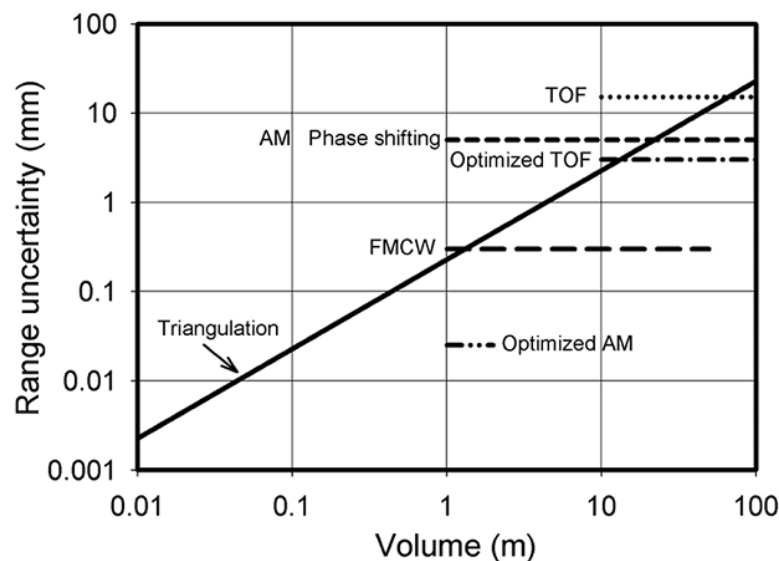


**Figure 3.20: Comparison of time of flight measurement tools (Blais, 2004) © 2004 IEEE**

The alternative to using a pulsed signal is to use a continuous wave to determine range by modulating characteristics of this ‘carrier’ i.e. amplitude or frequency, and comparing the transmitted and received waves (Payne, 1973). The carrier wave will be modulated with a signal with lower frequency than the carrier (Figure 3.21) with this signal carrying the ranging information. Such systems may be referred to as ‘phase-shift’ measurement devices as it is the difference in phase angle between the transmitted and received wave which determines a range.

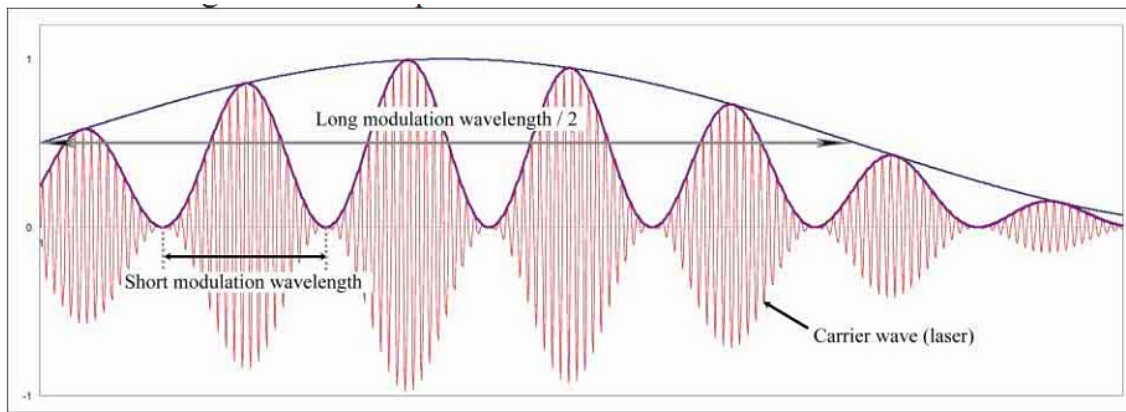


**Figure 3.21: Phase shift ToF measurement system, carrier wave and two modulated wavelengths (Pfeifer & Briese, 2007)**

**Figure 3.22: Phase difference between transmitted and received signal (Thiel & Wehr, 2004)**

A range measurement is calculated based on the wavelength of a transmitted wave and the phase angle between it and the wave received after reflection from a surface. The range is:  $R = \frac{1}{4\pi} \frac{c}{f} \Phi$  where  $c$  is the speed of light,  $f$  the frequency of the wave and  $\Phi$  the phase difference between the signals (Wehr & Lohr, 1999). The maximum unambiguous range is half the wavelength and therefore it is necessary to use multiple wavelengths, the largest wavelength determining the maximum range and the shortest wavelength determining the resolution of the range measurement. A detailed explanation of the technique can be found in Rüeeger (1990).

Commercially available implementations of the modulated technologies include the Leica-Geosystems HDS, FARO Photon and Surphaser 25-HSX, all operating on amplitude modulation whilst the Nikon Metrology Coherent Laser Radar uses frequency modulation, a list of other systems in this category now several years old is available in Blais (2004). Continuous-wave systems benefit from faster data collection than pulsed systems with hundreds of thousands of points per second common (Lichti et al., 2007). In addition to a range value, amplitude modulation techniques can record an intensity value relating to the quantity of light returned by the measured surface which may be used for visualisation. Accuracy values for the systems are difficult to obtain as no standard method is used to calculate results however uncertainty for single point measurement from manufacturer specifications is ~1-2mm with the FARO and Surphaser system quoting sub millimetre figures for shorter ranges. In light of accuracy values quoted by manufacturers not being comparable, independent assessment of laser scanner performance has been undertaken with notable work by Boehler et al. (2003).

Erroneous data may be caused by a number of factors, Hebert & Krotkov (1992) identify these as: fundamental, architectural and artefacts of particular hardware. One fundamental problem of continuous wave systems is that of ‘mixed pixels’ caused by the transmitted wave being returned by more than one surface, such a case may occur where the beam partially strikes an edge and another surface further along the line of sight. In such a case the range is a combination of both returned signals as it is integrated over the entire projected spot. Mixed pixels occur because the system emits a laser with a non-zero width, the ideal case is that all rays of light are parallel and can therefore be focussed to an infinitely small point, this is however unachievable. If no attempt is made to focus a beam of collimated light it will diverge with distance, in order to produce a smaller spot the beam can be focussed to a particular range. The effect of focussing the spot is that outside of the focal depth the divergence will increase more rapidly than for an un-focussed beam and that the tighter the focus the greater the rate of divergence (Jacobs, 2006; Beraldin & Gaiani, 2005).

Mixed pixels will commonly occur at surface edges (Figure 3.23) with the computed range point being somewhere between the edge surface and the second surface along the line of sight of the laser scanner or, because of ambiguity in the range measurement, the computed point may occur in front of, or even behind the measured scene (Hebert & Krotkov, 1992). The likelihood of mixed pixels occurring increases as the spot diameter does therefore the choice of measurement system range and focal depth become highly important (Table 3.2). Mixed pixels may be removed by filtering the collected image or once in a Cartesian coordinate system by identifying isolated points, early work suggested complete removal of mixed pixel outliers was impossible as only those significantly erroneous could be identified (Hebert & Krotkov, 1992) more recent work on full waveform detection for pulsed time of flight scanners has shown the ability to detect the multiple returns and therefore differentiate objects (Jutzi & Stilla, 2006; Rieger et al., 2006).

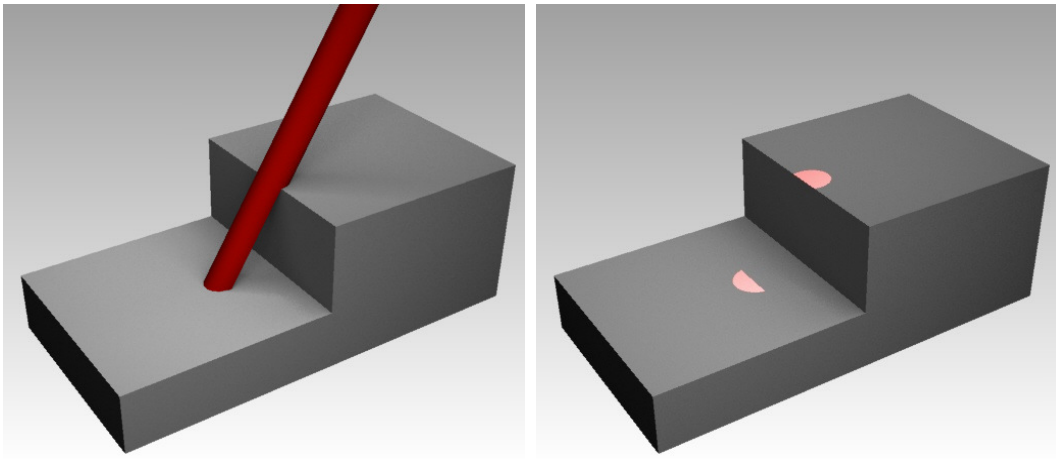


**Figure 3.23: Mixed pixel effect for ToF laser scanner. Path of laser beam (left), Resulting spot coverage on surface (right)**

	<b>Short Range</b>	<b>Intermediate Range</b>
Best Signal Distance (m)	1.3	2.7
Optimal Range, From: (m)	0.7	1.1
Optimal Range, To: (m)	3.6	8

<i>Single Pass Mode</i>		
Effective Range, From: (m)	0.45	1
Effective Range, To: (m)	5	16

<i>Laser Spot Data</i>		
Laser Spot Focal Distance (m)	1.8	5
Laser Spot Size at Focal Distance (mm)	0.5	2.3
Laser Spot Size at Aperture (mm)	2.8	2.8
Laser Spot Size at Far Effective Range (mm)	4.6	3.5

**Table 3.2: Technical specifications of one commercially available AM-CW laser scanner including laser spot diameter (Basis software Inc., 2009)**

A second error which may affect ToF systems is ‘multi-path reflection’ where the transmitted signal is reflected to a second surface before being returned to the sensor. The effect is most likely to occur where the beam strikes a specular surface (Section 3.2.1) at low incidence angle as a large proportion of the light will be reflected according to the law of reflection and not returned to the sensor. Where this reflected light strikes a second surface with diffuse reflection a proportion of the light energy will be returned to the original surface and be reflected back to the sensor (Figure 3.9) (Nitzan, 1988). Multi-path reflection can affect pulsed and continuous wave ToF systems as the beam travels a greater distance before being returned to the sensor, in pulsed systems this equates to a greater flight time and for continuous wave systems the increased distance will change the computed phase angle between the transmitted and received signals resulting in greater range.

ToF systems may see errors generated by ‘surface discontinuities’ caused by changes in the surface reflectance. Surfaces which are dark or specular reflectors will adversely affect the quantity of light returned to the sensor as opposed to diffusely reflecting surfaces which are ideal reflectors (Section 3.2.1). These changes in reflectance affected the strength of signal returned to the sensor which will decrease the signal to noise ratio and affect the range calculation for pulsed ToF systems using threshold detection and to a lesser degree may cause unpredictable results for amplitude modulated continuous wave systems because of range/intensity crosstalk (Nitzan, 1988).

The scanner to surface distance and angle of the measurement system with respect to the surface normal may need to be considered as the regular sampling of the scene is in the image space and not the object space. The result is that a surface close to the scanner will have a smaller point pitch (closer together) whilst for surfaces further away the point pitch is increased. The effect of surface angle was considered by Hebert & Krotkov (1992) and more recent research by Urban et al., (2009) noting the possible effect on signal to noise ratio.

Additional error sources may be created by the internal geometry of the measurement system, an example being where the transmitter and receiver are not co-axial occlusion may occur however such geometry may be predicted and is believed to only exist in terrestrial or aerial laser scanning systems (Liu et al., 2004). Other possible errors which were reported in early work include range drift due to insufficient temperature compensation in the measurement unit and errors in the synchronisation of the high speed moving mirrors (Hebert & Krotkov, 1992). These error sources are attributed to the hardware implementation of the particular scanner and therefore vary by manufacturer and model, the level to which these effects exist in current systems is unknown.

### **3.2.4.2. Laser Triangulation**

Given a collimated light source producing a single spot of light and a light sensor at a fixed known geometry, the position of a surface reflecting the light can be calculated using trigonometry. Knowing two angles of a triangle and the distance between those angles, the law of cosines allows the calculation of the position of the other corner of the triangle. Using a 2D example to explain the principle of operation (Figure 3.24), it

can be seen that the reflection from position  $(X,Z)$  has a direct impact on the area of the Position Detector activated by the reflected light.

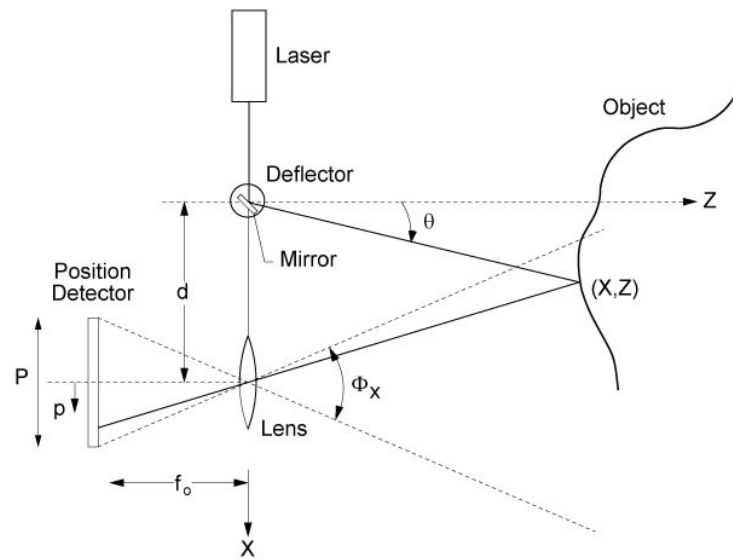


**Figure 3.24: Triangulation principle. Figure courtesy of NRC Canada**

In the measurement system described, a single profile would be recorded because the light is deflected by the mirror creating a moving point of light; to capture the complete object the measurement system or object must move and knowledge of the movement recorded. Without knowledge of the movement the newly collected data will have no relationship to the original. Methods for collecting data in a single coordinate system where the measurement object is greater than the measurement system volume are discussed in Section 3.2.5.

The light source for a triangulation system described above should be collimated as it can produce tightly focussed light; it is able to do so because its rays are nearly parallel and diverge minimally with distance. This low divergence allows a point of light to be projected onto a surface with a particular shape, often a spot (point) of light for laser triangulation, the smaller the point, the more precisely it can be recorded by the sensor. The laser is an example a collimated light source and for this work the term laser shall be used to describe the light source used in this measuring system. The light produced by a laser in addition to being collimated is coherent where all waves exhibit the same frequency and phase, the effect of which is the production of speckle on rough surfaces which is a fundamental limit to the performance of optical triangulation systems using laser light (Section 3.2.1).

Digital image sensors such as CCD and CMOS used in laser triangulation laser scanners are opto-electronic devices which collect photons emitted by the light source reflected from a surface and convert this analogue data to digital data proportional to the input energy of the photons. Sensors comprise a number of pixels to collect photons arranged in a matrix which is covered by a filter to remove frequencies of light other than those produced by the light source in order to allow relative insensitivity to ambient illumination.

Range uncertainty of triangulation laser scanners is inversely proportional to the base length ( $d$ ) between light source and sensor. Increasing length  $d$  will reduce range uncertainty but increase the likelihood of occlusions in the collected data for a non planar surface, occlusions will occur where the light source and sensor could not have line of sight to the same area of the measurement surface. In addition to occlusions, length  $d$  is constrained by the physical practicalities of maintaining stability as distance between source and sensor are increased (El-Hakim & Beraldin, 1994). Hand held laser scanners have source and sensor separated by  $\sim 100\text{-}200\text{mm}$  with a separation angle of  $\sim 30^\circ$ , a shorter base length with separation of  $\sim 10^\circ$  can be achieved, reducing unit dimensions without increasing range uncertainty with a synchronized laser scanner (Rioux, 1984). The synchronised laser scanner utilises a second moving unit which moves synchronously with the projection unit cancelling the angular movement of the projection unit (Figure 3.25). With a synchronised scanner the focal length of the lens can be increased providing increased range resolution and no reduction in the field of view (Rioux, 1984).

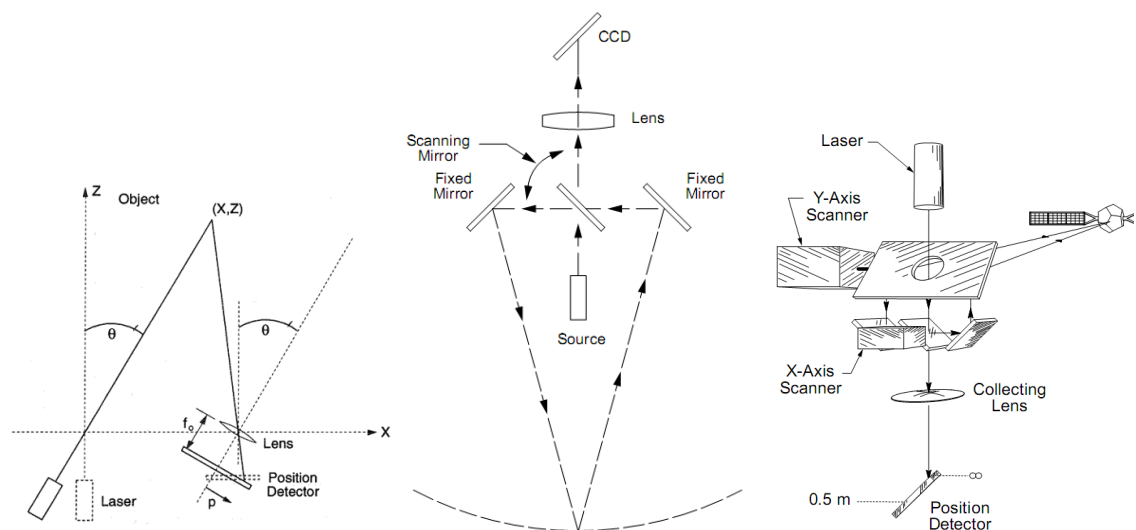


**Figure 3.25: Auto-synchronized laser scanner. Principle (left), single axis (centre), dual axis (right). Figure courtesy of NRC Canada**

The addition of a third deflecting mirror parallel to the sensor plane and moving at slower rate than the two primary mirrors introduces the ability to scan areas instead of single lines. The synchronised scanner has been implemented by the National Research Council Canada and licensed to the company Arius3D who have developed a coordinate measurement machine mounted colour laser scanner.

For non-synchronised scanners the data collection speed can be increased by projecting a laser line on the measurement surface instead of a single stationary point. A line projection system operates similarly to laser gauge systems which capture a profile of the projected laser line and use the form of the line to measure features such as flush and gap. Laser gauge systems are available from a variety of suppliers with the GapGun from Third Dimension (Third Dimension, 2010) in use at EFDA-JET for the measurement of flush and gap between tile blocks (Figure 3.27). The GapGun laser gauge projects a red line of collimated light onto a surface, perpendicular to the surface discontinuity and images the line in eight jpeg images. From the eight images, sixteen measurements are made in total and compute the final flush and gap result for that position. Some user adjustment of parameters is possible but the exact method used to calculate final values is proprietary. Measurement standoff between sensor and surface is 20mm for super high resolution sensor and 50mm for all other measurement heads. To increase collection speed and where small complex features exist, the use of ‘standoffs’ is advised which attach to the GapGun and make physical contact with the measurement surface. To achieve maximum accuracy and repeatability the unit should be used without ‘standoffs’, however for a human operator, practice and a steady hand are required.

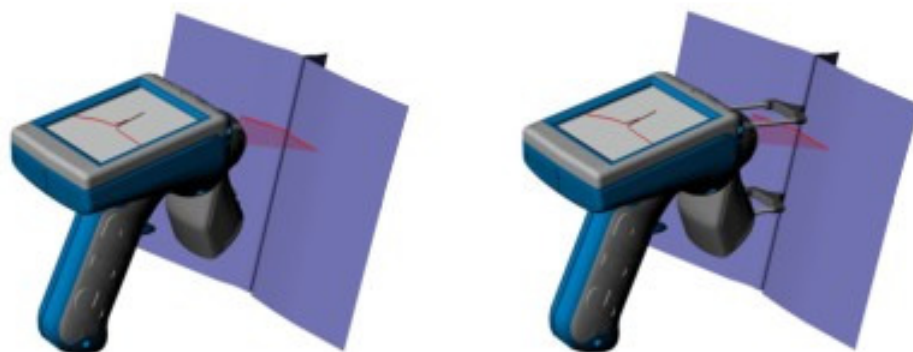


**Figure 3.26: GapGun laser gauge. Measurement without standoff (left), with standoff (right). (Third Dimension, 2010) © Third Dimension.**

## Metrology

The laser gauge is designed for single profile measurement whereas triangulation laser scanners are capable of capturing profiles at a rate in excess of 100Hz and are designed to collect data in a datum system other than of the hand held unit itself. The projected laser line is commonly generated in one of two ways, the laser line is projected onto a high speed moving mirror which reflects the laser to the surface creating the appearance of a line, referred to as a 'flying spot', or the laser can be directed through a cylindrical lens spreading the spot of light into a line. Both techniques are commercially available with manufacturer claims being that flying spot systems are larger and more fragile than the solid state alternatives because of the moving components and that the moving components generate electrical noise. However as flying spot systems are projecting single points of light onto the surface the intensity of each laser spot can be adjusted, a similar effect can be achieved for solid state systems but requires the intensity of the whole laser line to be altered.



**Figure 3.27: GapGun in use at EFDA-JET. Figure courtesy of EFDA-JET.**



**Figure 3.28: Commercially available hand held laser triangulation scanners**

The ability to alter the intensity of the projected light is beneficial when measuring surfaces with varying reflectivity because of the effect surface discontinuities caused by changes in surface reflectance may have on the calculation of laser spot position (Figure 3.5).

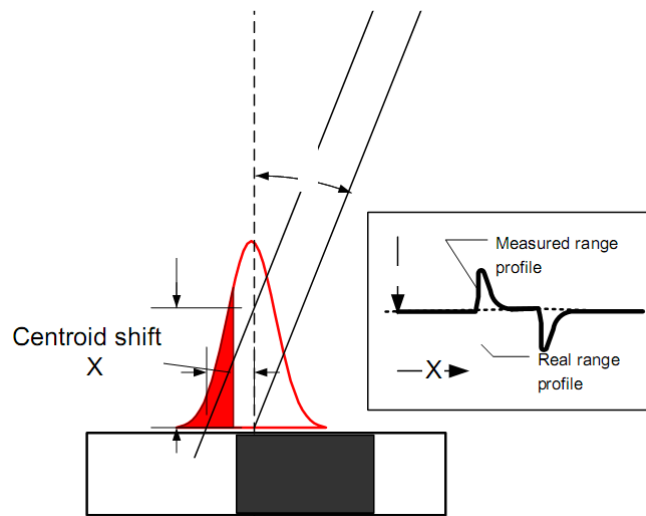


**Figure 3.29: Effect of surface reflectance change on collected data (Blais et al., 2005). Figure courtesy of NRC Canada**

The change in quantity of received light caused by a change in surface shade or reflectance (Section 3.2.1.2) affects the calculation of the centroid of the laser spot and therefore the position in 3D space (Figure 3.29). Early laser triangulation systems were not capable of dynamically adjusting laser intensity during scanning and would therefore measure an area of the object during on-site calibration and adjust laser intensity to be suitable for that surface. The need to model intensity change (Khali et al., 2003) or dynamically adjust the light intensity occurs when measuring a surface

with varying light absorption and reflectivity. Where the surface comprises light coloured or highly reflective surfaces which return a high proportion of projected light to the sensor and dark, light absorbing materials the sensor will receive differing quantities of light. Passing from an area of high reflectivity to low reflectivity the sensor will receive a lower proportion of reflected light and so it is necessary to increase laser intensity to avoid the skewed profile seen in Figure 3.5, in addition the increase in power increases the signal to noise ratio. The situation is reversed when moving from low reflectivity to high reflectivity where the sensor could become saturated by the reflected light. Sensor saturation or ‘blooming’ affects certain CCD sensors where the charge received by a pixel is too great that it overflows into adjacent pixels (Litwiller, 2001). Sensor saturation will affect certain sensors (CMOS generally having a natural immunity to blooming) and limit their ability to determine the centre of the imaged laser spot/line. Development of image sensors specifically for 3D imaging systems has occurred because sensors are traditionally not designed for this application (Beraldin et al., 2003).

	Stripe Width (mm)	Points per Stripe	Stripes per Second	Stand Off Distance (mm)	Depth of Field (mm)	Accuracy (mm)
FARO LLP	34-60	640	30	95	85	0.035
Metris MMD100	100	1024	80	100	100	0.023
Perceptron ScanWorks v5	93-140	7640	60	100	110	0.024
Steinbichler T-Scan3	90	92-12857*	10-140	83**	75	-
* Calculated from manufacturer data. Point density in scan direction= 0.007-0.98mm.						
** Value described as ‘Mean Measuring Distance’.						

**Table 3.3: Commercially available hand held laser triangulation systems, data from manufacturer technical specifications**

As surface reflectance discontinuities produce range errors so can actual discontinuities in the object surface (Figure 3.30). The edge shape will affect the calculated position dependent on the intersection of the calculated centroid and line of sight of the light source (Figure 3.31) (Curless & Levoy, 1995). For step edges the orientation of the sensor impacts the direction of ‘curl’ and although demonstrated by Curless & Levoy (1995), earlier work demonstrates the ‘upward’ or ‘downward’ curling effect more clearly (Figure 3.32) (Buzinski et al., 1992). Similar effects have been seen for wide baseline triangulation systems (Boehler et al., 2002) and will also occur where the projected light penetrates the surface material (Section 3.2.1.2) (Blais et al., 2005).

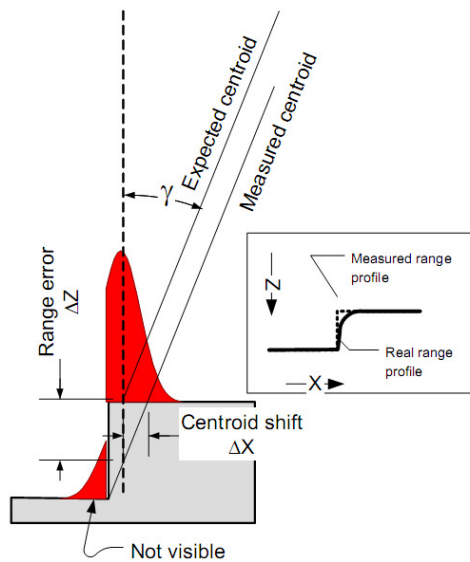


Figure 3.30: Range error caused by step discontinuity (Blais et al., 2005). Figure courtesy of NRC Canada

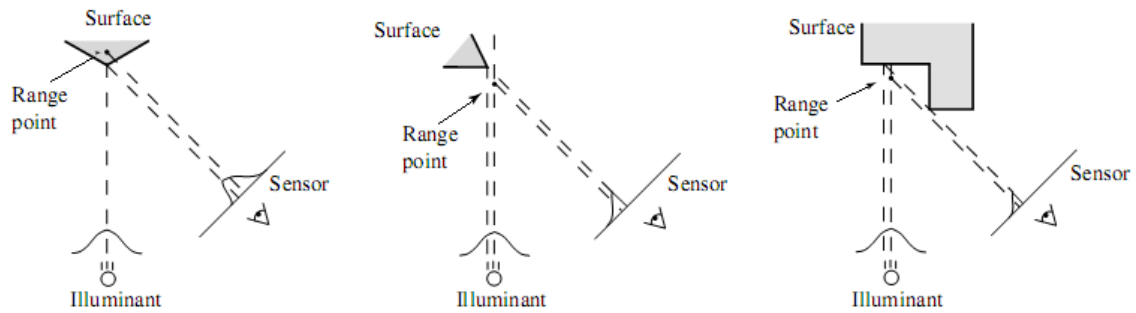


Figure 3.31: Triangulation range errors. After Curless & Levoy (1995) © 1995 IEEE.

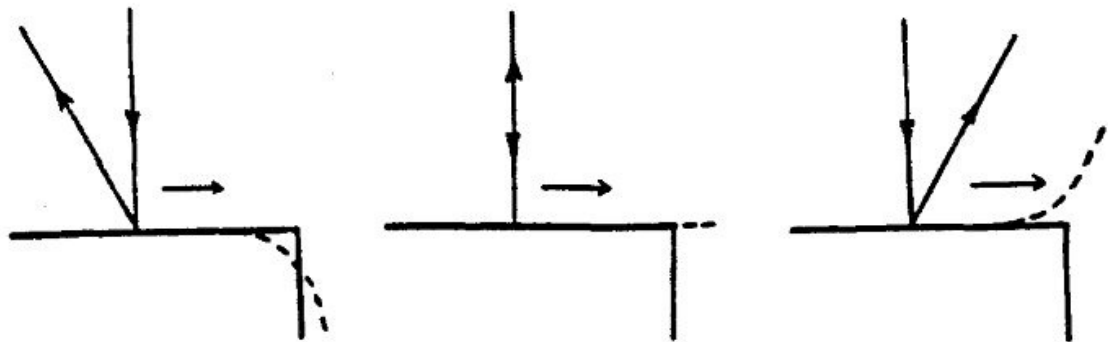
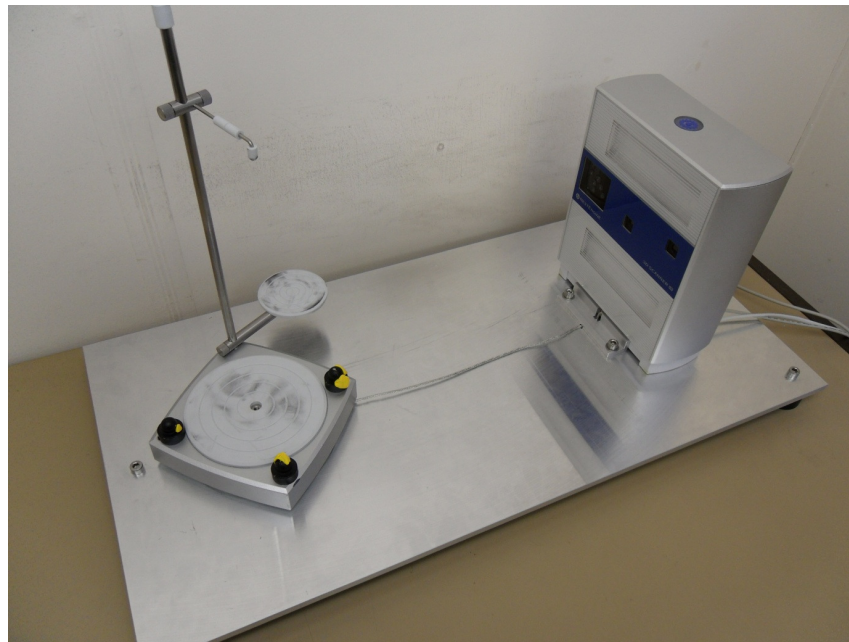


Figure 3.32: Effect of centroid shift (Edge Effects) dependent on sensor orientation. After Buzinski et al. (1992) © 1992 IEEE.

Surfaces with step edges and concave shape can lead to errors from specular highly reflecting surfaces where light is either reflected completely away from the sensor or reflected to another surface before being returned to the sensor (Figure 3.8) (Section 3.2.1.2). As with discontinuities the effect of multi-path reflectance is to create spurious data points and in some cases no data collection on certain surfaces.

In the laser triangulation systems discussed so far the light source and sensor have been a fixed known geometry from one another, an alternative is to move the light source but keep the sensor and measurement object fixed. Measurement systems operating on this principle are suitable for fixed measurement volumes where the geometry between sensor and object can be fixed such as for desktop use e.g. NextEngine scanner (NextEngine Inc, 2010) in use at EFDA-JET. The measurement object is positioned in front of the scanner and multiple moving laser lines projected onto the object and captured by the sensor, also a colour image registered to the data can be captured for visualisation, the part moved and more scans performed. Data are registered to form a single data set using surface matching techniques (Section 3.3.2) but where possible use starting values provided by a rotation stage connected to the scanner. Triangulation scanners using this technique require stability during the data collection and for the system mentioned data collection lasts approximately 2 minutes for a single scan, six scans or more may be required to fully capture the object.



**Figure 3.33: Desktop laser scanner**

Where movement in the measurement scene or of the sensor occurs erroneous data may be collected, with the result being waves in the collected data (Figure 3.34). This situation is most likely to occur when using a dual axis scanner or a flying spot/slit scanner with external tracking (Section 3.2.5) because as the number of components increases so does the chance of instability. The effect can be removed by filtering although this may alter the spatial resolution, through the use of a faster scanner or minimising movement/vibration (Beraldin, 2004).

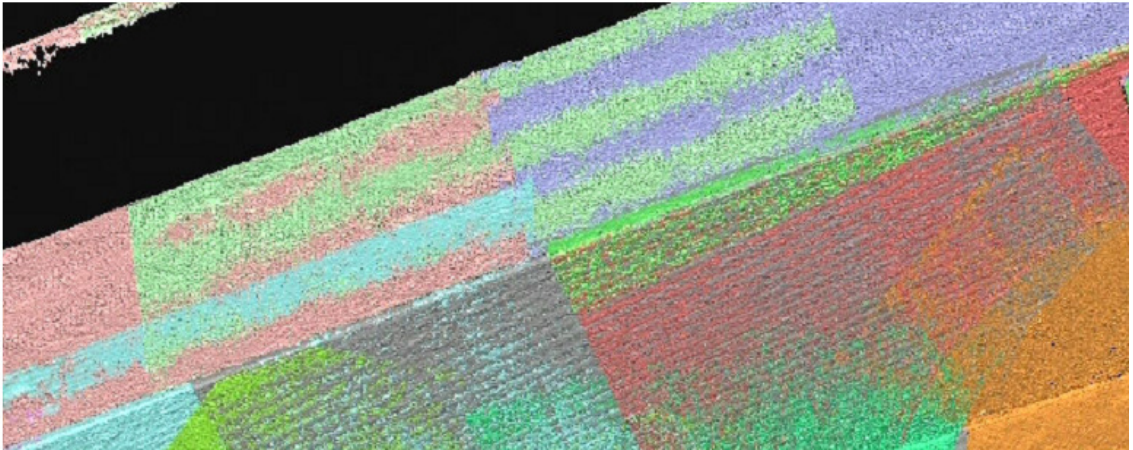


**Figure 3.34: Waves (undulations) in the collected data as a result of sensor/camera movement (Beraldin, 2004). Figure courtesy of NRC Canada**

The measurement volume of the triangulation systems discussed is insufficient to measure the complete volume inside the EFDA-JET machine and therefore the measurement system or surface must be moved with the new position related to previous positions through external tracking (Section 3.2.5) or the data sets must be registered post collection (Section 3.3.2).

#### **3.2.4.3. Light Projection: Bundle of Rays**

The projection of a bundle of light rays is an extension to the projection of a single point or plane of light. Following the principle of triangulation, the projection of multiple light planes simultaneously allows the coverage of a larger area in a short time. From a fixed position a single laser line triangulation system collects a single profile of ~200mm whereas a system projecting multiple light planes can cover an area several metres square; such systems may be referred to as ‘area based’ measurement systems. As with all triangulation technology, equipment requires careful calibration to ensure the projector and sensor are correctly positioned and careful handling to ensure equipment stays within calibration. This section discusses projection technologies encompassing terms such as pattern projection, coded light, structured light and moiré fringe.

Early projection systems operated by projecting light through a plane grating with equidistant spacing onto an object and viewing this object through an identical grating offset from the first, a series of fringes are produced from which depth data can be generated. This principle of measurement is referred to as Moiré Fringe. Work by Takasaki (1970) and Meadows et al. (1970) present a description, a background and

mathematical grounding for the technique. The work focuses on objects of medium size such as the human head and larger objects such as a motor car. Earlier work by Brooks & Heflinger (1969) is performed similarly but by the use of an interference pattern generated by laser. Contour data is collected by means of analysing the interference between the patterns at the source and receiver with an achievable resolution of up to  $25\mu\text{m}$  (Meadows et al., 1970).

Modern commercial measurement systems projecting bundles of rays now do so by linear projection, which is the projection of sequential and single fringes. Digital projectors are used as the illumination source with the received pattern being analysed directly, without need for linear gratings. These projection measurement systems are the focus of this section because of their commercial adoption. Early systems used a light source to project a series of light planes onto the measurement surface, sectioning the surface into profiles which were captured by a sensor with fixed known geometry from the light source. When viewed from the offset position of the sensor the projected line will be deformed where the surface is not flat, it is this deviation from the projected straight line which captures the form of the surface and is still used to determine shape in current laser triangulation systems (Section 3.2.4.2). By projecting a series of profiles simultaneously collection speed can be increased however the use of multiple planes of light introduces a correspondence problem similar to that seen in photogrammetry where identifying individual planes of light on a non-planar surface can be impossible. In order to simplify identification of individual light planes, coding strategies may be used to uniquely identify each plane in the collected image and gives rise to the technique being known as ‘coded light’.

An early coded light approach was the projection of a 2 bit binary pattern where the surface is illuminated or not by a projector. Using a matrix of laser beams Potsdamer & Altschuler (1982) projected a sequence of patterns onto a surface where rows of beams in each pattern were active or inactive and produced rows of light on the measurement surface furthering earlier work by Altschuler. Each projected pattern was recorded by the image sensor and for each pixel a binary code (0 or 1) generated dependent on whether the pixel was illuminated or not. By projecting a sequence of  $m$  patterns,  $2^m$  light planes could be encoded with each pixel in the image sensor having an  $m$  bit code related to a column in the projector matrix. All pixels with the same code word could now be identified as having been illuminated by the same row (Figure 3.35). Wahl (1984; 1986) expanded on the technique by utilising a transparent liquid crystal panel

instead of a laser matrix and Inokuchi et al. (1984) developed the coded light approach further by using ‘Gray Code’ instead of the existing binary which provides some resilience to noise (Figure 3.36).

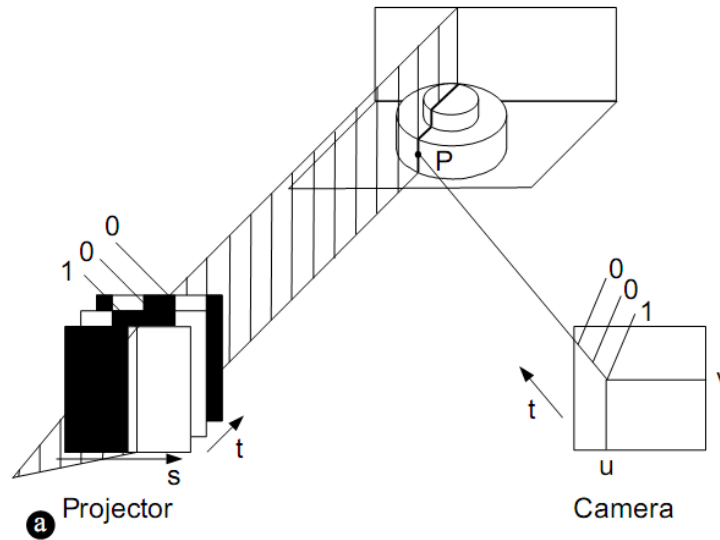


Figure 3.35: Coded light, building up a code word (Trobina, 1995)

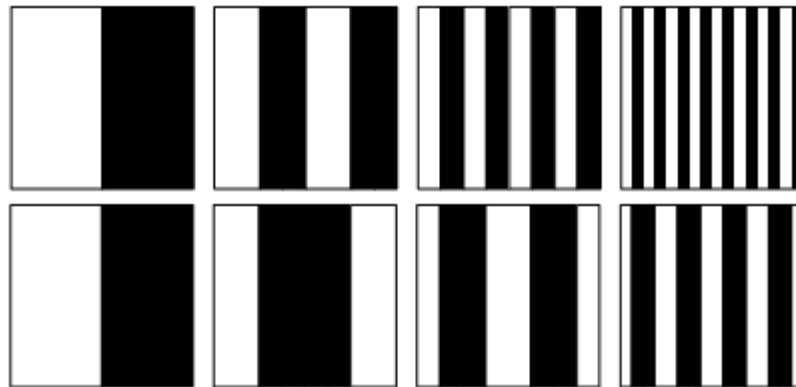
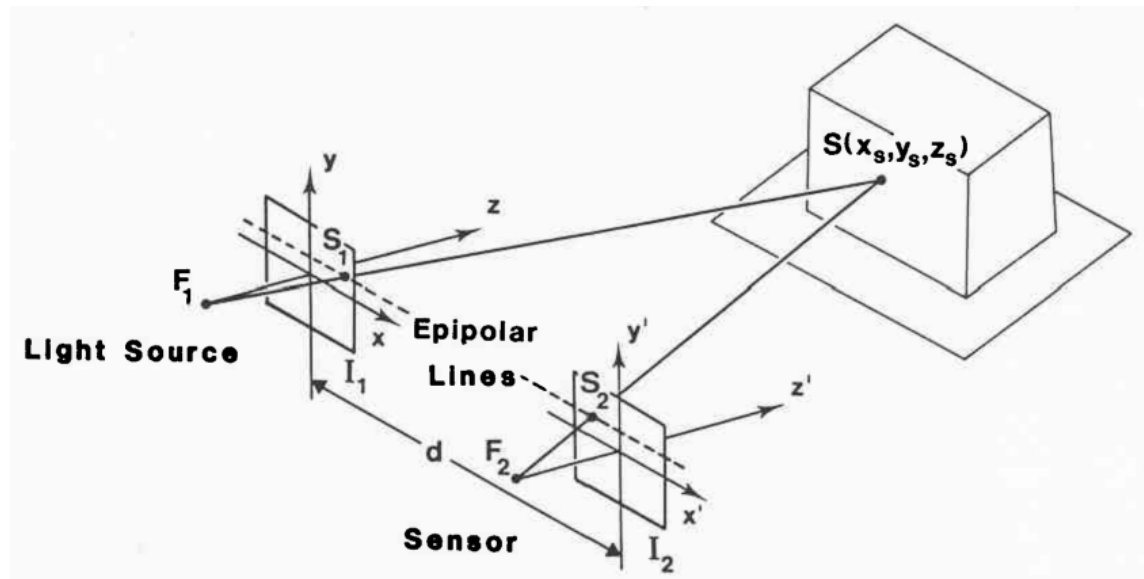


Figure 3.36: (top) Natural binary code. (bottom) Gray binary code. After (Akca et al., 2007)

The coding techniques allowed the correspondence problem between different light planes to be resolved as for each pixel in the projector an  $m$  bit binary code exists which will also exist in the collected image. By searching along the epipolar line (Section 3.2.3) in the image until the code word matching the projector pixel is found correspondence between projector and image can be established (Figure 3.37) (Sansoni et al., 1997). Binary code and Gray Code are two examples of coding strategies part of a larger group described by Salvi et al. (2004) as ‘Time Multiplexing’ where the codification is temporal as it is created over a period of time. These coding strategies are a means by which to implement the ‘sequential and single fringe projection’ technologies as identified in Figure 3.11. The temporal approach leads to a requirement

that the object and sensing system must remain stationary throughout data collection (Salvi et al., 2004).



**Figure 3.37: Active range measurement principle (Wahl, 1986).  
With kind permission of Springer Science+Business Media.**

The resolution of the coded light approach is limited to half the width of the highest frequency (finest pattern) projected onto the object surface and can suffer from edge effects where the line position is incorrectly calculated as the line passes over an edge resulting in a ‘lift-off effect’ (Harding & Qian, 2004). The coded light approach can achieve an accuracy of about 1:500 but can be improved by combining with the phase shift method where relative accuracies of 1:8000 are achievable (Luhmann et al., 2006; Akca et al., 2007).

The phase-shift method, more correctly referred to as ‘dynamic fringe projection’, projects onto the measurement object a series of fringes or sine wave with constant frequency but differing phase, when used as an extension to gray code the pattern may be the highest frequency used in the gray code. The intensity recorded by each pixel on the sensor is recorded for each projected pattern and the pattern moved laterally on the projector by a portion of the wavelength of the sine wave being projected. The translation of the pattern results in a change in the quantity of light projected onto the object surface at any given point and the quantity of light recorded by the image sensor for that point. The intensity recorded at each pixel can be related to a position on the known wave and through the shift of the wave a number of times, a map of the phase at each point on the surface can be calculated, with the phase map being directly proportional to the range.

The phase map is constructed using intensity values from the recorded images, each pixel having an intensity ( $I$ ) for each position of the projected fringes  $I_n(x,y)$  where  $n$  is the fringe position, there being 1 to  $m$  fringe positions and  $(x,y)$  being the pixel position. Each pattern is a shift of the phase by  $2\pi/m$ , where  $m \geq 3$  because there exist three unknowns to be solved. Where the fringes are shifted four times ( $m=4$ ), each pixel has a recorded phase:  $\delta(x,y)$ , which reduces to:

$$\delta = \arctan \frac{I_2 - I_4}{I_3 - I_1} \quad \delta = \delta(x,y) \quad I_n = I_n(x,y) \quad \text{Eq 3.2}$$

$I_n(x,y)$  intensity at pixel  $(x,y)$  for fringe position  $n$

$\delta(x,y)$  phase at pixel  $(x,y)$

$\lambda$  wavelength of the square or sine wave of the projected pattern

Once the phase map has been constructed, the unwrapping process converts this map into height values for the individual pixels with accuracy of about one hundredth of the wavelength ( $\lambda/100$ ). The height profile is given by:

$$Z(x,y) = \frac{\lambda}{2 \times 2\pi} \delta(x,y) \quad \text{Eq 3.3}$$

(Luhmann et al., 2006, p.426)



**Figure 3.38: Commercially available white light projection systems**

The process of converting the phase map into usable information requires that the map is ‘unwrapped’ however the process may fail where the surface is not continuous and discontinuities occur as ambiguity in the range cannot be resolved (Sansoni et al., 1997). In order to simplify the unwrapping process additional information in the form of a ‘coarse map’ may be used with gray code a possible solution to providing this information which allows the range value for each point in the visible scene to be calculated from the imaging camera (Harding & Qian, 2004). The phase shift and gray code projected light combination is used in commercially available systems including a

system owned by EFDA-JET from the company Breuckmann (Breuckmann GmbH, 2010).

Commercially available systems operating on the above principle for industrial measurement include: Breuckmann stereoSCAN 3D (Breuckmann, 2009), GOM ATOS (GOM, 2010), Steinbichler COMET 5 (Steinbichler Optotechnik, n.d.) (Figure 3.38). Systems vary by the number of cameras used with two of the listed systems using two cameras while the other uses only one. Pixel counts on the used sensors vary from 1.4 megapixels to 11 megapixels and affects the number of data points output after phase unwrapping. Pixel count also affects measurement time with less than a second for some systems to ~10 seconds for those utilising pixel counts over 10 megapixels. For the systems mentioned measurement volume varies from  $50\text{mm}^3$  to  $950\text{mm}^3$ , with larger volumes resulting in greater point pitch in the final data, varying from 0.025mm to 1.0mm. The measurement volume is closely tied to data density and range resolution (Sansoni et al., 1997) and therefore the volume covered would likely need to be altered dependent on the accuracy requirements of the part being measured, validation of gap and flush or the plasma facing surface would likely require the highest resolution and therefore a measurement volume large enough to contain a tile assembly or block only (Section 2.4). Where the measurement area is greater than the calibrated measurement volume such as is the case inside the EFDA-JET machine it is necessary to move the equipment or measurement object and perform multiple measurements. In such a situation data from different device positions may be combined by several methods, the first is to use engineered targets similar to those used with photogrammetry can be placed throughout the complete measurement volume and pre-surveyed using a photogrammetry system such as the GOM TRITOP system (GOM, 2010; Luhmann et al., 2006). Alternative approaches are mechanical or optical external tracking which are discussed in Hybrid Techniques (Section 3.2.5) or registration of data using the surface data itself (Section 3.3.2.1).

White light systems because they use an incoherent light source do not suffer from speckle (Section 3.2.1.2) which is a fundamental limitation to laser triangulation systems (Section 3.2.4.2) and therefore are capable of producing smoother data however the use of white light provides little resilience to ambient illumination and reduced contrast in comparison to laser illumination. The performance of white light systems is largely dependent on the surface to be measured with diffusely reflecting surfaces ideal, specular reflections must be avoided often through coating the surface in a thin layer of

white powder (Luhmann et al., 2006, pp.426-27; Chen et al., 2000). Areas of specular reflection may saturate the sensor with the affected area recording a maximum intensity value which will result in the incorrect calculation of the phase value. The incorrect calculation of the phase value may be affected by the multi-path reflectance effects highlighted by Nitzan (1988) for triangulation systems. In Figure 3.8, because of specular surface reflection a proportion of the light projected to point 5 is reflected to point 5' and imaged by the sensor, the intended intensity of light at point 5' is now increased by a proportion of light from point 5. Where point 5 is un-illuminated, point 5' is at the intended intensity, however when 5 is fully illuminated, point 5' is now imaged by the sensor as the intended intensity plus a proportion of light from point 5. The intensity of Point 5' and therefore the computed phase is now affected in a non-uniform manner and could conceivably result in an error in the computed phase map.

Recent developments in white light projection include viewpoint coded light where additional carefully placed cameras can reduce the number of projected patterns in a sequence (Young et al., 2007) and a measurement system developed by company Phase Vision (Phase Vision Ltd, 2008) using a network of inexpensive projectors and cameras instead of the traditional single unit solution with phase unwrapping algorithms developed at the University of Loughborough.

### ***3.2.5. Hybrid Techniques***

The combination of two or more measurement technologies to produce data can be termed a hybrid system or a 'bridge' design (Peggs et al., 2009). The combination of two or more separate measurement tools increases complexity and uncertainty calculations but can produce richer information than could be obtained from a single sensing system. An example of a hybrid system discussed by El-Hakim & Beraldin (1994) utilises range measurement for large scale surface measurement and intensity measurement for the accurate measurement of edges where range measurement are less reliable.

Hybrid systems offer the possibility to expand the working volume of active triangulation systems and allow the collection of data within a volume greater than that which is visible to the triangulation sensor. In this section, hybrid systems utilising active triangulation sensing systems and technologies to expand their operating volume will be investigated.

Hand-held laser triangulation systems employ a measurement head containing a coherent or collimated light source and receiving sensor, the data are collected with reference to the measurement head, with the same being true for white light projection systems. To collect data in a coordinate system other than that of the measurement device it is necessary to know the position and orientation of the measurement device in relation to another object, a tracking device. The tracking equipment must remain stationary during data collection if it is to be used as the datum or may be moved if tracking another datum system. Common methods of tracking a triangulation measurement head are: mechanically, by tracking of targets on the measurement device or by photogrammetry of targets fixed to the scene (Chen et al., 2000; Chen & Medioni, 1992). Commercial products which track white light projection systems do so using self-localisation or a laser tracker.

Mechanical tracking is the determination of position and pose of the measurement head through mechanical means, commercial measurement tools of this type are commonly referred to as: 'CMM arm', 'Articulated arm' or 'Measuring Arm' and are available under the brand names Romer (Hexagon Metrology, 2010), FARO (FARO, n.d.b), and Metris (Nikon Metrology NV, 2010) amongst others (Figure 3.39). Measuring arms use thermally stable bars connected by angle encoders to determine a position in 3D space. The length of the connecting bars determines the measurement volume and affects the uncertainty of the measurement, the impact of error in the angular encoders is increased as the bar length increases. Where the measurement volume is larger than the operating volume of the arm, a possible option is to re-position the arm and make further measurements, however data collected in each position will not be in a common datum system. To register data collected in different positions, previously measured points can be re-measured as part of a process known as 'leap-frogging' however each new location of the arm increases uncertainty of the combined data set. Measurement uncertainty can be affected by mishandling of the arm as joints in a CMM arm do not all feature unlimited rotation, the overextension of a joint may lead to equipment damage and poor quality of collected data. The automation of the CMM arm became a reality in 2008 with the announcement of the Metris Robot CMM Arm (RCA) (Figure 3.40), a traditional CMM arm surrounded by a motorised body capable of moving the 7 axis CMM arm inside (Nikon Metrology NV, 2010). The RCA is believed to have a spherical operating volume of 4.2m and a single point accuracy throughout the

measurement volume of 50-100 $\mu\text{m}$ , at time of writing the product is still being tested and is not commercially available (Morey, 2009).



**Figure 3.39: CMM arms**



**Figure 3.40: Metris RCA**

A form of self-localisation where the portable unit can determine its own position has been achieved for hand held triangulation laser scanners by the company Creaform (Creaform, 2010). The HandyScan range of 3D laser scanners (Figure 3.41) combine triangulation laser scanning with photogrammetry to enable the hand held unit to determine its position with relation to markers attached to the object surface. Markers must be attached with density so a minimum of three are visible at any time, in a random pattern and the relative distance between visible markers remaining constant during measurement. Where the measurement object is considerably larger than the measurement volume of the device e.g. a car or aircraft, the MAXscan unit can be

employed which surveys the markers using photogrammetry and then laser scans from the same unit.



**Figure 3.41: Creaform EXAscán (Creaform, 2010)**

Several commercial hybrid systems use a laser tracker (Section 3.2.4.1) as the tracking device allowing a large measurement volume and small equipment footprint. An example of the combination of hand held triangulation laser scanner and laser tracker is the Hexagon Metrology T-Scan system which allows tracking of an object with 6 degrees of freedom within a volume defined by the stationary laser tracker. Touch probe and hand held triangulation laser scan units can be tracked using corner cube reflectors integrated within the probe or scanner, the corner cube provides a range and position in the tracker coordinate system but cannot provide the complete 6 degrees of freedom (6DoF) of the hand held unit. To determine the orientation of the hand held unit a camera attached to the top of the laser tracker detects IR LEDs attached to the hand held unit, using the known positions of the LEDs through prior calibration, the orientation of the hand held unit can be determined (Figure 3.42). The laser tracker, camera and hand held unit must be synchronised so data is collected from all simultaneously for data from the hand held unit to be in the laser tracker coordinate system.



**Figure 3.42: Hexagon metrology laser tracker with T-Cam**

The use of a camera for determining orientation is not the only solution for 6DoF tracking with a laser tracker, tracker manufacturers API produce the IntelliProbe 360 and IntelliScan 360 (Figure 3.43) which use cooperative hand held units for touch probe and triangulation laser scanning respectively. The IntelliScan system works exclusively with API laser trackers and requires no additional parts attached to the laser tracker as the orientation of the hand held unit is determined by the unit itself. The hand held unit is composed of two parts connected by a joint rotating about a single axis, the top part rotates to maintain line of sight with the laser tracker while the angle between it and the lower section comprising the probe or triangulation scanner is directed towards the measurement surface. The addition of a gravity sensor completes the ability to determine the orientation of the sensor.



**Figure 3.43: API IntelliScan/IntelliProbe 360**

White light projection technologies can be tracked using the same techniques as hand held triangulation laser scanners; an API Laser Tracker 3 can be used with a Steinbichler COMET 5 white light scanner to collect dense surface information in a volume defined by the laser tracker. The COMET 5 is fitted with an API active target which tracks the position of the laser tracker, maintaining a constant line of sight between the two units and reflectors attached to ‘limbs’ at the extremities of the white light scanner. When data are collected by the COMET 5 the laser tracker records the position of the COMET 5 by recording the position of the active target with orientation information provided by the rotation of the active target. The approximate orientation allows the laser tracker to automatically position its laser beam to the approximate positions of the limb reflectors and records the position of each reflector for precise orientation. The COMET 5 unit is calibrated before use so the position and orientation of each limb target with respect to the active target on the COMET 5 is known.

Laser tracker based hybrid systems have a requirement that during measurement the laser tracker must remain static in order to define the coordinate system, a second class of hybrid measurement system using Optical Trackers can operate in unstable environments where the tracking system itself must move. The ‘Optical Tracker’ or ‘Optical CMM’ uses three linear arrays of photo-sensors mounted with fixed separation in a thermally stable unit directed outwards towards the measurement area. Two of the sensors are mounted with the same orientation whilst the third is rotated 90° (Figure 3.44). The photo sensors detect light from IR LEDs attached to the portable measurement tool which pulse with known frequency, uniquely identifying each LED.

The position of light from each LED on the three sensors allows the position of each LED to be triangulated. Through calibration of the portable device, the relative position of each LED with respect to the data collected by the portable unit is known, that unit may be a touch probe or triangulation laser scanner. At time of writing no white light projection systems are available for use with Optical Tracker/CMM systems. Commercial examples of this equipment for industrial metrology are the: NDI OPTOTRAK (Northern Digital Inc., 2008) and Nikon Metrology K-Series (Nikon Metrology NV, 2010).

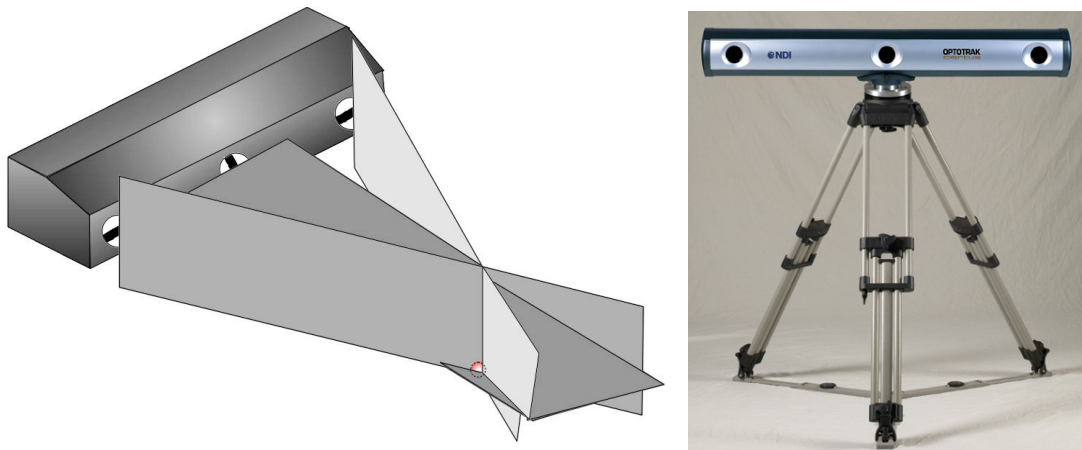


**Figure 3.44: NDI Optotrak optical tracker (Northern Digital Inc., 2008)**

The ability of optical trackers to track up to 512 targets (~40 attached to a hand held triangulation laser scanner) and capture 4500 measurements a second allows multiple units to be simultaneously tracked and allows for the optical tracker itself to move by fixing a number of targets to static locations in the measurement volume. By using the fixed targets to define the coordinate system and constantly monitor the tracker position with respect to those fixed targets the optical tracker can be used in an unstable environment.

Optical tracking systems also include the Breuckmann naviSCAN3D (Breuckmann GmbH, 2010) which is a stereoSCAN3D white light projection scanner enclosed in a carbon fibre frame with integrated pulsed LEDs which are tracked by a Metronor DUO portable CMM consisting of two synchronised CCD cameras operating on the triangulation principle (Metronor, 2009). Once the Metronor DUO has been setup and calibrated, data from the white light scanner is positioned with the coordinate system defined by the Metronor cameras.

Measurement Type (i)	Tracker Type (ii)	Local Measurement Volume	Total Measurement Volume (Approximate Equivalent Object)	Total Measurement Volume Shape
Laser Line	Laser	- <sup>5</sup>	Truck – Aeroplane	Hemi-Spherical
Laser Line	Mechanical	-	Motorcycle	Hemi-Spherical
Laser Line	Optical	-	Car – Truck	Pyramidal
White Light	Laser	Desktop	Truck – Aeroplane	Hemi-Spherical
White Light	Optical	Desktop	Car – Truck	Pyramidal

**Table 3.4: Hybrid Measurement systems, comparison between local measurement with component ‘i’ and total measurement using hybrid system comprised of components ‘i’ and ‘ii’.**

This section has reviewed commercially available state of the art measurement systems relevant to the volume and quality of data required. Its purpose is to provide the reader an explanation of how each technology operates such that they may understand any physical limitations imposed by the technology.

### 3.3.Data Handling

The method by which data are handled and processed can have a significant effect on the final result of a measurement. As there are a number of ways data can be collected and represented, in this section some common formats and representations are reviewed, highlighting those suitable for this project. Closely linked to data handling is the need to combine data from multiple device positions into a single datum system in a process known as registration, this is a common requirement for large volume measurements and is covered in this section.

#### 3.3.1. Representation

Dimensional data can be represented in numerous ways, from single points through to complex surface models constructed with mathematical equations. The ‘best’ representation is dependent on the purpose of the data e.g. engineering inspection, reverse engineering, visualisation. In this section different methods for representing data are studied with special consideration for those suitable for engineering inspection.

The measurement tools considered in Section 3.2 are all capable of outputting data in a three dimensional Cartesian coordinate system where a single point is represented by a triplet of values, each value denoting a distance from the origin along an axis. The single point can be considered the most basic representation and holds no additional information other than its position with respect to the origin, commonly seen as (X, Y,

<sup>5</sup> Hand-held Laser Line triangulation measurement devices collect a single profile and require external tracking to combine individual profiles into a common coordinate system; as such they do not have a measurement volume themselves, only a measurement area i.e. line length x depth of field.

Z). Points may additionally have orientation information in the form of a direction vector which adds an additional triplet, such data may be represented as  $(X, Y, Z, i, j, k)$ . Measurement equipment capable of capturing colour may add a red, green and blue value to a point. Data formats comprising point information in one of the discussed formats may be described as a 'point cloud', where there is no connectivity information to define a relationship between points in the cloud it is described as unorganised. A partially organised cloud is one where some connectivity information is known, such a case exists for line scans collected by triangulation laser scanners however this information is typically only saved within a proprietary file format.

The point cloud is not a representation of the surface but of discrete points in 3D space, to model the surface the first step is commonly to produce a polygon mesh from the collected data points. A mesh can be constructed using a variety of methods, one approach being Delaunay triangulation where three points lie within a circle which includes no other points are joined by three lines to create a closed surface. The accuracy of a triangulated model is highly dependent on the point pitch of the measured data, where the pitch is small the mesh will more accurately reflect the real object as the triangular planes will be smaller and better able to follow the form of the original surface.

Triangles in the mesh do not need to be of the same size, areas of low change may be modelled by larger triangles to reduce the quantity of data stored. Areas of high change such as edges and curves will continue to use smaller triangles to model the surface as accurately as possible. Remondino & El-Hakim (2006) discuss using random 3D points (unorganised point cloud) generated from 2D photography and state that it is "often quite difficult to correctly turn randomly generated point clouds into polygonal structures without losing important information and details." If the collected points are used as the vertices of a mesh then no data is lost but it is possible that data can be added, it is a relatively easy process to interpolate new points once a mesh has been formed, however these points may not correctly reflect the original surface and so should be avoided where possible if the data are to be used for inspection.

The polygon mesh as an explicit surface can be used as a starting point to create implicit surfaces where the surface is modelled using higher order functions such as quadrics. A quadric, or quadratic surface is a second order algebraic surface type which includes cones, cylinders, spheres, etc. The implicit surface is not as common for computer

aided design (CAD) as the de facto industry standard non-uniform rational b-spline surface (NURBS). NURBS allow the representation of virtually any surface including complex freeform surfaces, are transformation invariant and store data in an efficient way.

In addition to the data formats mentioned there are a variety of computer file formats, with each format having different internal storage methods. The conversion of one file format to another introduces an opportunity for data corruption to occur therefore wherever possible a single file format should be used. Based on the brief study of data representations the most suitable for this project is the use of discrete points in either an unorganised or line scan form as these most closely represent the collected data and allow simple manipulation. The collected discrete points can be stored within an ASCII (American Standard Code for Information Interchange) file i.e. a text file; vector and colour/intensity data can also be stored as extraction of position data is still possible.

### ***3.3.2. Registration***

Where an object to be measured is larger than the operating volume of the sensing system, or complete 3D coverage of an object is required, it is necessary to move the object or sensor to multiple positions to fully capture the object. Each sensor and object position will have its own local coordinate system, it is necessary to align these data sets to one another by performing a series of translations and rotations to solve the correspondence problem in a process referred to as registration (Gruen & Akca, 2005; Chen & Medioni, 1992). Only techniques utilising a rigid-body transform, where the same transformation will be performed on all data of a set, will be considered here in order that relative distance and orientation between data in a set remain constant.

The registration process for data sets consisting of point data, where a position in three dimensions is recorded i.e. (X,Y,Z) has been well researched and several options are available. Initial registration can use information provided by mechanical means i.e. rotation/motion stage or CMM arm, but the accuracy of this information is insufficient for accurate surface modelling and a refinement technique is required (Bergevin et al., 1996).

The two general approaches for registration are primitive based and surface based; the primitive based approach extracts geometric primitives from the data set and creates a representation of the data, possibly as a graph. The representations can be compared

and transformed to bring the data sets into alignment. This technique is suited to situations where there is large variance in the position of the two data sets (Zhang, 1994).

Surface based alignment uses large redundancy in the data sets to obtain a more precise result than primitive based approach (Zhang, 1994) without creating a new representation of the data. This is an iterative approach which requires a-priori knowledge of the approximate positions to converge to the correct minima and works best where small changes in the positions are required (Zhang, 1994). This method may be used as an extension to the primitive based approach, where a primitive based technique may be used to bring the data into good, but not optimal registration.

### **3.3.2.1. Surface Based Registration**

One of the most common methods and arguably the dominant of surface based registration is that of Iterative Closest Point (ICP) which is based on the principle of Least Squares Matching, minimising the mean-square distance between data sets (Besl & McKay, 1992). This method was independently developed by Besl & McKay (1992), Chen & Medioni (1992) and Zhang (1994).

To perform registration of two data sets it must be assumed that one set is a subset of the other or that there is suitable overlap between the two data sets, for correct operation the overlap is estimated to be around 25-30% (Rabbani et al., 2007). The work of Besl & McKay (1992) and Zhang (1994) assume that one data set is a subset of the other and therefore that each point has a corresponding point in the second data set (Eggert et al., 1998), this is also true of Chen & Medioni (1992).

When correspondences between the data sets are found, a transformation is performed on one set to minimise the distance between sets and the process performed again in an iterative manner until the data reaches a local minima. If it is assumed one set is a subset of the other and therefore each point has an exact match in the other and this assumption is not true, false pairs can be produced and may adversely affect the convergence of the data towards the optimal solution (Fusiello et al., 2002)

Rusinkiewicz & Levoy (2001) put forward six stages to an ICP algorithm: Selecting, Matching, Weighting, Rejecting, Error Metric, and Minimizing; when adjusted each can affect the performance of the algorithm, aspects of that being: speed, stability, tolerance of noise and/or outliers and maximum initial misalignment (Rusinkiewicz, 2005). The

following registration methods discussed are variants of the 'classic' ICP technique, each with certain performance enhancements.

The selecting stage of the ICP algorithm can use all of the data within a set, or only a subsection of the data, that data can be sampled in a variety of ways. Uniform sampling will reduce the number of data requiring matching but does not take into account the surface being sampled, with all surfaces sampled equally regardless of their influence on the registration process. Geometrically stable sampling (Gelfand et al., 2003) selects areas for registration which constrain a potentially unstable transformation, this approach will have similar effect to increasing the weighting of data where it better constrains the transformation in a traditional ICP implementation.

In addition to range data it is possible to use other collected data such as: surface normal, intensity and colour data as part of the registration process (Godin et al., 1994). These data can be used to 'rule out' correspondences between data where one or more of the data variables do not correspond e.g. when the difference between two surface normal of data are greater than a tolerance, or if the intensity or colour values are greatly different. This approach is referred to as the 'iterative closest compatible point' (ICCP), the technique varies from ICP at the matching stage of the process (Rusinkiewicz, 2005).

Chen & Medioni (1992) focus on matching point-to-plane as an alternative to point-to-point, utilising control points on planar surfaces and using their surface normal. The approach is based on the assumption that a-priori knowledge exists for the transformation between the data sets and that this method is therefore a fine alignment. This is generally true of all ICP based techniques as there may be multiple local minima and without good starting values the method may converge incorrectly. The point-plane method has been found to converge quicker than the point-point method but can fail to converge correctly where the overlapping data are planar or a uniform curve (Pulli, 1999).

Initial ICP techniques were only capable of reliably handling two data sets at a time, a process known as pair-wise registration, a comparison of such techniques can be found in Rusinkiewicz & Levoy (2001). Where more than two data sets required registration, the pair-wise registration technique led to an accumulation of errors necessitating 'global registration', or 'Multi-View Registration' techniques (Eggert et al., 1998).

### 3.3.2.2. Multi-View Registration

Early techniques to overcome the accumulation of errors from multiple pair-wise registrations include creation of a model from the data sets, registering new sets to this model and registration of data to an existing cylindrical data set. Work by Blais & Levine (1995) attempted to solve the global registration problem by utilising a calibrated sensor and reversing the calibration to find point correspondences directly. An alternative approach to multi-view registration is to calculate the transformations simultaneously; early work on multi-view registration was performed by Gagnon et al. (1994), later enhanced by the same authors (Bergevin et al., 1996) and was a generalisation of the earlier work on pair-wise registration using point-plane distances by Chen & Medioni (1992). The work improves on that of Chen & Medioni by detecting and discarding data in areas of discontinuity and using all remaining data as part of the algorithm rather than selecting areas known to be planar.

Stoddart & Hilton (1996) present a registration approach modelling the interaction between data sets based on them being connected by springs. This work makes a strong assumption that correspondences between data sets are already known according to Eggert et al. (1998) who present a similar, if enhanced version of the work.

Pulli (1999) uses pair-wise registration data as a starting point to register the complete data set. The data set with most connections is selected and other data sets introduced individually, based on a decreasing number of connections. Data from pair-wise registration is used to provide the starting position and as each new data set is added it can be used for new data sets to match against. The novel aspect of this work is the ability to work with very large data sets without performing the computationally expensive point matching technique for each iteration. Point matches generated during pair-wise registration are used throughout the matching process negating the need to keep the data sets in memory whilst the error in registration can be evenly spread between the data sets.

A comprehensive review of least squares surface matching can be found in Rusinkiewicz & Levoy (2001) and Gruen & Akca (2005) but since their publication new variants of the ICP algorithm have been developed. Chetverikov et al. (2005) propose Trimmed ICP (TrICP) based on a least trimmed squares (LTS) approach throughout the algorithm, the residuals (squared errors) between corresponding data are sorted in increasing order and the sum of a certain number of the smaller errors

minimised. Unlike traditional ICP, TrICP is robust in the presence of outliers and enhances the LTS variant by handling overlap between data of <50%, in addition the final least squares solution uses inliers only. Philips et al. (2007) propose a new distance metric which accounts for outliers in the data, fractional root mean square distance (FRMSD) and a variant of the ICP algorithm (FICP) to optimise this metric. The authors suggest the traditional RMS distance gives too great a weighting to outliers in the data set due to the squaring process and that TrICP is only suitable when the fraction of outliers in the data is known a-priori, of course as pointed out by Chetverikov et al. (2005), outliers in registration are not only incorrectly measured points but also correctly measured points which have no matching point in the other set, therefore the fraction of outliers is associated to the quantity of overlap in the data. In a comparison between ICP, TrICP and FICP performed by Philips et al. (2007) using a large sample of 2D data sets and a number of 3D sets, FICP was six to eleven times faster to converge than TrICP with similar difference to the total number of iterations. Both algorithms resulted in similar Root Mean Square Distance (RMSD) values, significantly outperforming the ICP implementation used.

In order to maintain consistency, a single registration method will be selected and applied to all collected data; the method will be selected for performance and availability using a currently available algorithm, creating a new algorithm is beyond the scope of this work and based on the review of currently available methods is unnecessary.

### **3.4. Standards, Guidelines & Artefacts**

This section discusses work by other researchers evaluating non-contact surface measurement equipment. Previous research into the performance and abilities of large volume and non-contact metrology equipment has been performed by the UK National Physical Laboratory (NPL), summarising the current capability, available standards and verification artefacts (Rodger et al., 2007). The report identifies that at the time of its publication the usage and complexity of non-contact measurement systems in industry is increasing yet no ISO specific guidelines exist and that verification tests and artefacts are required. Since publication NPL has continued working on measurement systems for free-form measurement and has setup the National Freeform Measurement Centre, the centre aims to support users along with providing evaluation and traceability, standards and best practice (National Physical Laboratory, 2009).

As identified by the NPL report (Rodger et al., 2007) and a paper from the National Research Council Canada (NRC) (Beraldin et al., 2007b) no standards currently exist for the evaluation of data collected using non-contact dimensional metrology equipment. The American Society for Testing and Materials (ASTM) formed committee E57 in 2006 to focus on issues related to 3D imaging systems although initial work is focussed on laser-based time-of-flight technologies (Cheok et al., 2007). Terminology and safety guidelines have been published with other work in progress, currently no guidance can be taken from this work (ASTM, 2010). The National Institute for Standards and Technology in the USA have held a number of 3D imaging systems workshops but similar to ASTM this work is focussed towards laser based time of flight and laser tracker systems (NIST, 2006).

The most applicable work is the VDI/VDE 2634 Part 3 guideline (The Association of German Engineers (VDI), 2008) dealing with multiple view measurement systems based on area-scanning. This work presents three quality parameters to be calculated for a measurement system: probing error, sphere spacing error and length measurement error, calculated by multiple measurements of a defined measurement artefact. The measurement artefact defines a measurement volume with a series of lengths defined by the distance between diffusely reflecting spheres in a variety of orientations. VDI/VDE 2634 Part 3 provides an opportunity for measurement systems to be compared using a standard set of tests with directly comparable results, these results are a great advantage to system users but the results should not be used as an indication of performance outside the given tests. The testing is highly dependent on the measurement of diffusely reflecting spheres and provides no information about the performance of the measurement system on other shapes and features. The use of a standard set of tests is a valid approach but the VDI/VDE 2634 guidelines could be expanded to encompass a larger set of tests, even then it is likely that a single set of tests will not provide suitable information for all projects. Project specific tests are likely to always be required in order to test the combination of features with surface material and finish. As with system calibration, artefacts with surfaces similar to the real object should be used in order to ensure the measurement accuracy (Chen et al., 2000, p.11). A selection of relevant projects dealing with non-contact metrology of free-form surfaces is now discussed.

The body of work relating to the assessment of non-contact free-form measurement equipment has increased in the last decade in-line with greater use of the technologies;

an early and large cultural heritage project was ‘The Digital Michelangelo project’ (Levoy, 2009). Led by Professor Levoy of Stanford University, Michelangelo’s David was scanned at night over a four week period beginning February 1999 using a custom designed laser scanner produced for the project by Cyberware Inc. (Cyberware, 1999) and a Faro arm with triangulation laser scanner from 3D Scanners (now part of Nikon Metrology) (Section 3.2.5). At the conclusion of the project in 2004 a digital model of Michelangelo’s David was produced with ~1mm resolution and incomplete models for other scanned statues. Remaining processing is described as a “monumental labor” including hard mesh alignment and completion problems (Levoy, 2009). The project demonstrates that although data collection can be time consuming, the time and effort required to process data can require even greater effort.

A group which has performed a large amount of work on the assessment of free-form measurement systems is the National Research Council of Canada (NRC). NRC work includes a cultural heritage project to image the Mona Lisa (Borgeat et al., 2007) and collaboration with Canadian company Neptec to produce a scanning system for the NASA Space Shuttle (National Research Council Canada, 2009; Neptec, 2007b). NRC has developed a metrology laboratory dedicated to traceable 3D imaging metrology in which a number of three dimensional objects, herein referred to as ‘test artefacts’ are used for calibration and evaluation of vision systems (Beraldin et al., 2007b).

Test artefacts are used to validate the performance of a measurement system and vary greatly in design, but all require calibration prior to use using a measurement system with accuracy an order of magnitude better than the measurement system to be tested (Beraldin et al., 2007b). The common system with which to calibrate a test artefact is the coordinate measurement machine (CMM) because of its high accuracy and well understood error model. However Tuominen & Niini (2008) do not agree with the use of a CMM for this purpose because measurements are based on discrete points and features inferred from these points, the authors identify the problem that in industrial measurement a hole is assumed to be an ideal circle and discrete points used to fit the circle to. Even where a large number of discrete points are collected e.g. using a scanning probe, an additional challenge exists which is the removal of the probe tip radius from the collected data. In most cases the removal of probe tip radius produces no error however this requires the orientation of the surface to be known. Errors in the calculated point position may occur where errors in the form of the surface exist,

misalignment between part and CAD is present, or no CAD exists (Figure 3.45) (Savio et al., 2007).

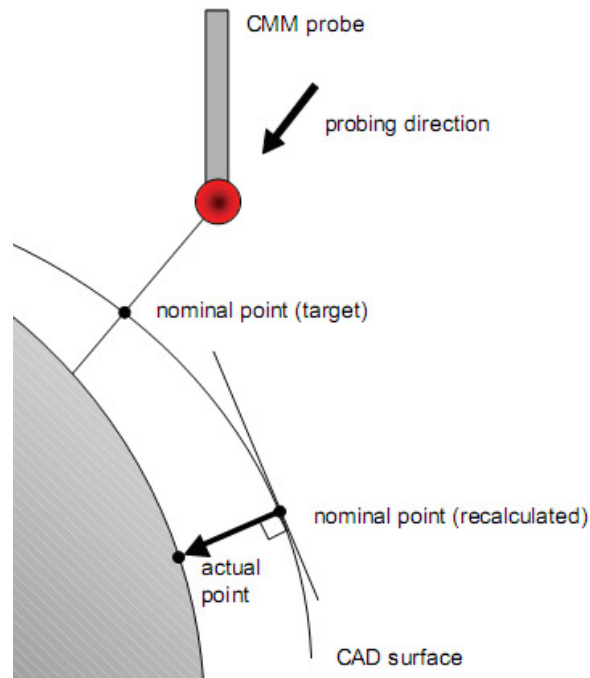


**Figure 3.45: Calculation of nominal and actual point from CMM touch probe (Savio et al., 2007).  
Figure courtesy of Elsevier**

A thorough review of metrology of freeform shaped parts with a focus on industrial measurement was performed by Savio et al. (2007). The paper covers a range of data collection technologies and presents freeform test artefacts from work published in Germany in 1998 (Figure 3.46a). A limiting factor to the use of artefacts is identified as “the relatively high calibration uncertainty and manufacturing costs”. The authors suggest that an alternative to complex artefacts is the use of computer simulation for uncertainty assessment and the use of the Modular Freeform Gauge (MFG). The MFG concept was proposed by earlier work from two of the authors and substitutes the surfaces of simpler objects in order to replicate the surface of interest as closely as possible (Figure 3.46b).

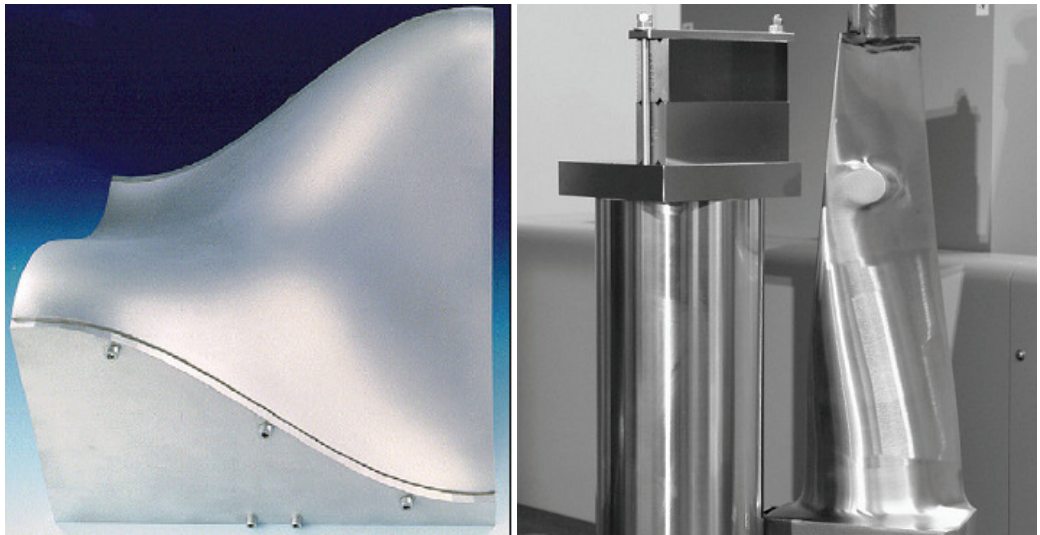


**Figure 3.46: a) General purpose freeform artefact: the "Doppelsinusfläche". b) MFG (left) simulating turbine blade (right) (Savio et al., 2007). Figures courtesy of Elsevier.**

The UK National Physical Laboratory produced a number of small artefacts for their 2007 project (Rodger et al., 2007) (Figure 3.47) and a much larger object (Figure 3.48). Later work from the group produced an artefact (Figure 3.49) which has been measured by a range of metrology equipment, results of this work have unfortunately not been published.

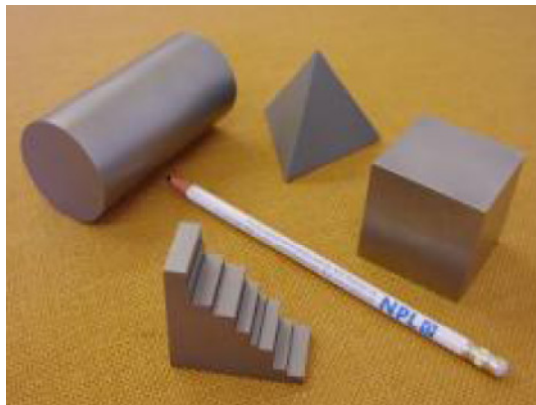


**Figure 3.47: NPL engineering orientated test artefact collection (Rodger et al., 2007). Courtesy of NPL (C) Crown Copyright**

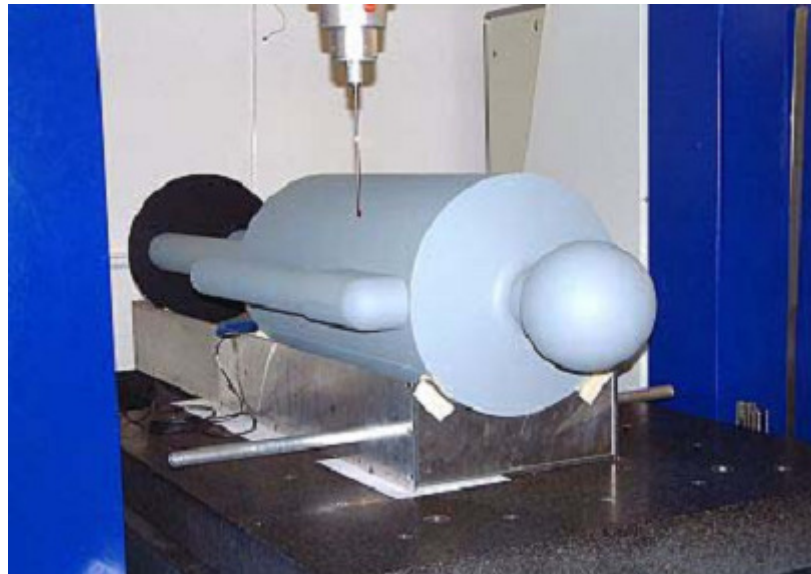


**Figure 3.48: NPL Phantom, anthropometric dimensional metrology (Rodger et al., 2007). Courtesy of NPL (C) Crown Copyright**

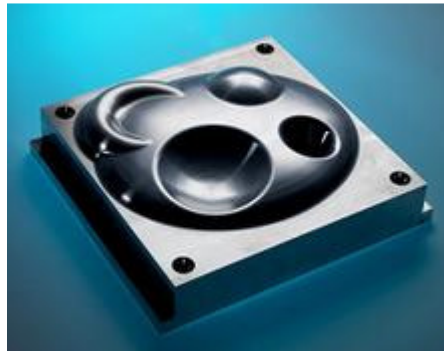


**Figure 3.49: NPL freeform reference (300 mm) (National Physical Laboratory, 2009). Courtesy of NPL (C) Crown Copyright**

The National Institute of Standards and Technology (NIST) in the USA have developed a facility for evaluating measurement systems based on the use of artefact including a step artefact with 30 steps of height varying from 1mm to 30mm and dimensions: 675mm x 465mm x 125mm, a slotted disc artefact, 2 anodised spheres and a multi-reflectivity target (Figure 3.50). It should be noted that project is currently evaluating time-of-flight laser scanners and so these artefacts are designed for use with this technology (Cheok et al., 2006).



**Figure 3.50: Left to right: NIST Step artefact, NIST slotted disc artefact & anodised spheres, NIST multi-reflectivity target. Figures courtesy of NRC Canada**

The National Research Council of Canada (NRC) has produced an artefact of interest to this project (Figure 3.51). The artefact is “made of a solid block of Amersil T08 fused quartz of dimensions 300 mm × 50 mm × 50 mm with all sides ground square and parallel to 0.005 mm with one face lapped flat to < 0.002 mm with a grit size of 0.005 mm. The lapped surface is coated with a vacuum deposited opaque layer of chromium.” (Beraldin et al., 2007a) The length, castellated features and finish of the artefact resemble that which will be required for the ITER-Like Wall project. Figure 3.52 is a test artefact manufactured from a stable material with a series of angled planes. The artefact was measured on a CMM with accuracy of 25µm over 1000mm before use and performance of a laser scanning system assessed using plane fits to the planar surfaces (El-Hakim et al., 1995).

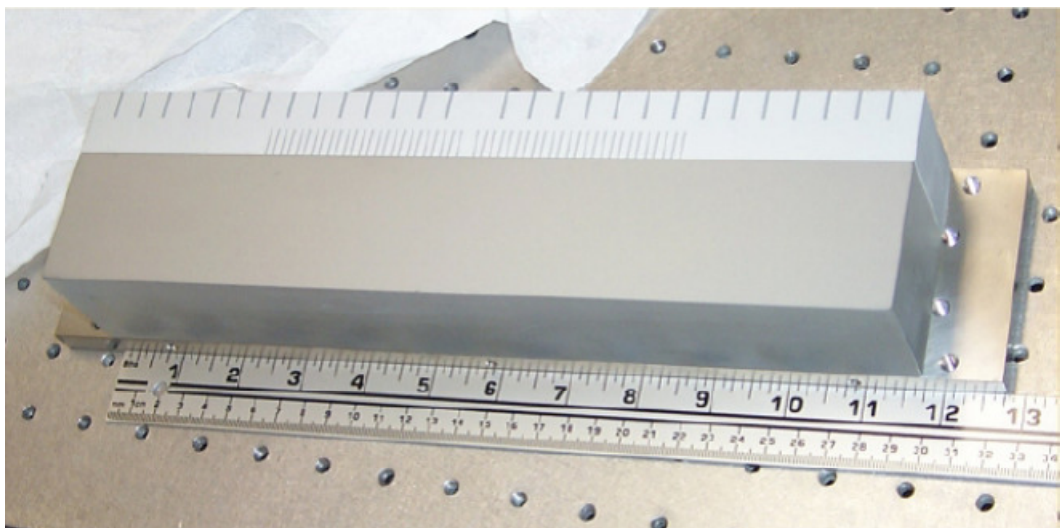


**Figure 3.51: NRC flat artefact (Beraldin et al., 2007a). Figure courtesy of NRC Canada**

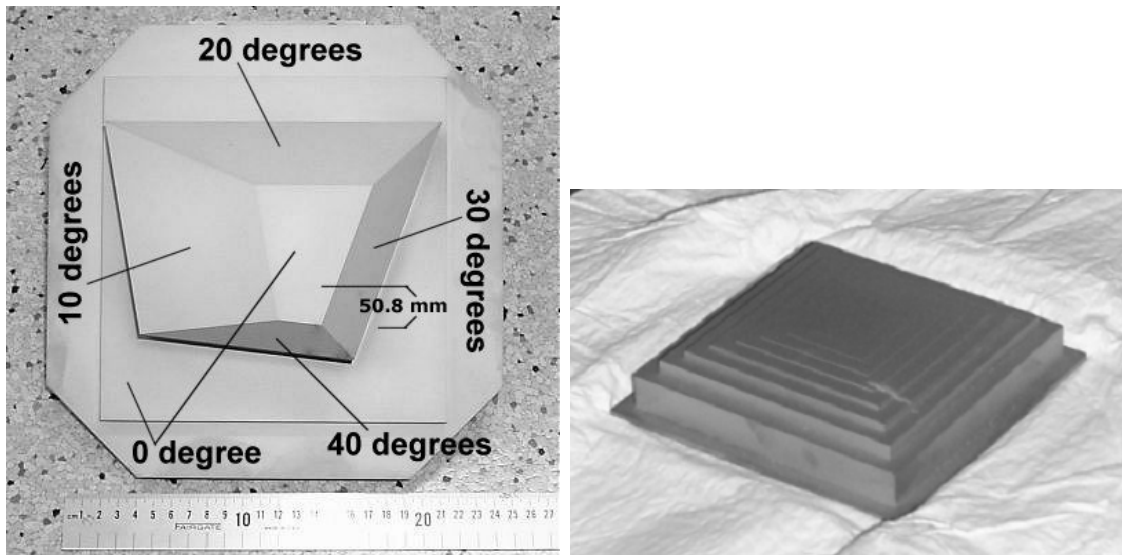


**Figure 3.52: (left) NRC angled test artefact, (right) NRC pyramid with steps of different heights. Figures courtesy of NRC Canada**

For the comparison and verification of deformation measurements Luhmann et al. (2008) created a freeform surface with double sine curve milled by a CNC machine from an industrial plastic, Ureol. The artefact is 400mm x 400mm x 100mm surrounded by a plane of 50mm width. On the plane are twelve retro-reflective targets and four reference holes, one in each corner used to locate spherical and cylindrical targets (Figure 3.53). The artefact itself is brown in colour and diffusely reflecting but a thin film can be applied to the surface with a random pattern necessary for image matching measurement methods.

**Figure 3.53: Test artefact for deformation measurement (Luhmann et al., 2008)**

Van Gestel et al. (2009) present possible designs for test artefacts for the evaluation of laser line scanners and perform tests using a CMM mounted laser line scanner and flat plate. The authors state a performance evaluation test should be “easy, fast and representative for the measurement task”, in light of this, tests based on a planar surface are used and a large amount of information created. Data of a planar surface were collected with different scan depth, in-plane angle and out-of-plane angles and least squares best fit planes fitted to the collected data.

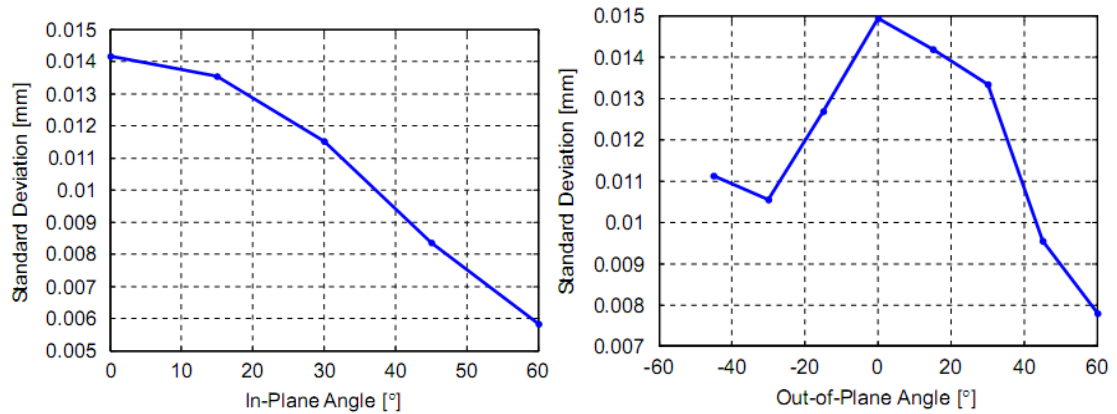


**Figure 3.54: Influence of in-plane and out-of-plane angle on the standard deviation of residuals to a best fit plane (Van Gestel et al., 2009)**

The standard deviation of each plane was used to assess the random error for the position in which the data were collected, and the overall change in position to a reference plane (commonly first or last data collected) used to quantify the systematic errors. This work follows that of Feng et al. (2001) who used planes and spheres to assess the effect of scan depth and projected angle on the accuracy of a CMM laser scanner, concluding the primary source of random error was speckle noise and that systematic error could be modelled with a resulting 50% improvement in accuracy. These papers demonstrate that a simple artefact can yield large amounts of usable information and simplify data processing in comparison to a complex surface artefact. The parameters used by Van Gestel et al. (2009) to evaluate point cloud quality are a subset of those defined by Lartigue et al. (2002), the four parameters they define are: noise, density, completeness and accuracy. Where errors of a data set compared to a model follow a Gaussian distribution the standard deviation can be taken as an indication of the digitising noise in the data. The density value can be obtained from division of the measurement volume into small cuboids related to the digitising step of the collection device; the method follows one defined by Hoppe et al. (1992). The completeness of a point set is linked to the noise and density values as the gap between two neighbouring points is not a gap unless it is greater than a given threshold, that threshold is defined as an area equal to the density e.g. if the density value is  $0.5\text{mm}^2$ , the completeness threshold would be  $0.5\text{mm}^2$ . The accuracy evaluation can be used to determine areas of a sensor which yield worse results than other areas, the authors note than for inspection purposes measurements collected from a certain area of the sensor could be excluded or a strategy adopted where measurement data are collected from the most accurate area of the sensor.

The Fraunhofer Institute for Applied Optics and Precision Engineering (IOF) have developed an optical measurement system for fixed volumes, a publication from the group shows measurement results of an object with a series of steps of varying heights believed to be a test artefact, dimensions of the artefact are not known (Figure 3.55). The same department have also performed tests to evaluate the effect of measurement system direction with respect to the surface angle of the measurement system (Kühmstedt et al., 2009a). The paper deals only with measurement systems operating using the phasogrammetry principle, a technique where a fringe pattern is projected onto the surface and imaged by two cameras, rotated by 90° and imaged again but the technique could be applied to other projection technologies.

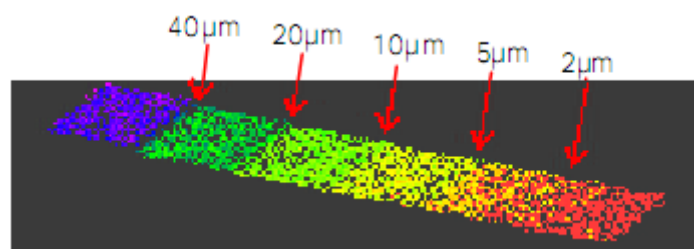


**Figure 3.55: Height test artefact (Notni, 2010)**

Although not using custom test artefacts, the work of Teutsch et al. (2005) has used a number of test objects in order to evaluate collected data from laser scanning. The authors developed a method for calculating a quality value for each point in a cloud by analysing the 2D image collected, assessing the thickness of the imaged laser line and contrast values. In 3D space, analysis of the surface normal at each point and comparison to the imaging geometry is performed. The process generates b-spline curves for each scanline where the distribution of points is determined by the previously calculated quality values. The approach removes high frequency noise caused by reflections and reduces the overall number of points in the final cloud by an average of 60%, the authors' claim this is achieved without appreciable loss of information.

### 3.5.Summary

In this chapter, commercially available dimensional measurement systems capable of surface measurement have been discussed. Their principles of operation have been described and their strengths and weaknesses highlighted. Polar measurement systems offer fast data collection over large areas from a static position, but with a high chance of occlusions for discontinuous surfaces and potential errors at those discontinuities.

Laser triangulation systems offer relative insensitivity to ambient illumination and high portability when combined with external tracking, giving great flexibility but are fundamentally limited by speckle from the laser illumination. White light projection technologies offer the potential for fast data collection with high resolution but reduced depth of field and a close link between resolution and measurement volume.

Of the technologies investigated all could be capable of measuring the complete volume inside the EFDA-JET machine but with greatly differing duration of data collection and quality of the collected data. For systems performing registration of data using surface features, the repeating, grid like structure of the tile surface will pose a challenge. Additionally, identification of an individual tile from data will be impossible and therefore a polar or hybrid measurement system is likely required. The measurement of a single tile assembly or tile block, for erosion and deposition checking would appear to be a challenge for all systems. At this small volume, polar systems are limited by laser spot diameter and speckle, laser triangulation systems suffer from similar problems and white light technologies may have difficulty with stability during data collection.

Errors associated with registering and processing the collected data in order to determine system accuracy and performance have been considered, concluding this stage can have a significant effect on the final data. Relevant work in the field of measurement test artefacts for assessment of surface measurement systems has been researched and other work on methods to assess measurement system performance. A variety of artefacts and processes exists but no complete process or guideline exists to evaluate surface measurement system performance.

*Three-dimensional imaging systems are now widely available, but standards, best practices and comparative data are limited. In order to take full advantage of 3D imaging systems, one must understand not only their advantages, but also their limitations. This process has to rely on a systematic method to assess the overall performance of a system, and metrology provides such a framework.*

(Beraldin, 2008)

In order to evaluate measurement technologies against the requirements of this project, the development of a test artefact and series of specific tests would be a suitable approach. Measurement technologies can then be assessed in a standard way against an

## Metrology

object with surface finish and features similar to that present inside the EFDA-JET machine.

#### 4. Preliminary Experimental Work

Evaluation of dimensional surface metrology equipment for a particular measurement cannot be performed solely by manufacturer specification. Quoted values are not calculated in a standard way by all manufacturers and may not reflect the real world performance for the measurement task required by the user. To evaluate metrology equipment performance and produce results which are comparable each measurement system should measure the same object in the same environment using a standard process. This procedure aims to minimise environmental impact on the measurement result, leaving the instrumentation error as the primary error source.

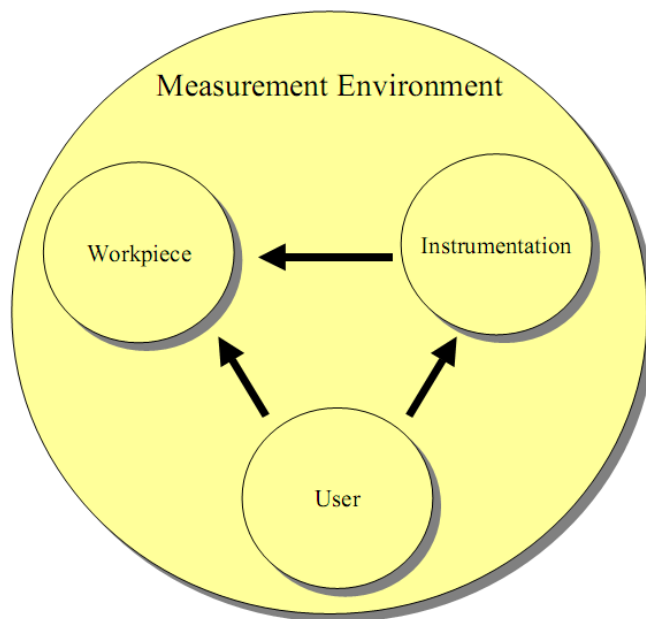


**Figure 4.1: Components of a large scale measurement (University College London, National Physical Laboratory, Leica UK, 1999).**

The measurement artefact (workpiece) should be an example of the measurement object or where this is not possible, should have similar surface features and finish to the real measurement surface. The use of a standard set of tests enables comparison of results and, where the measurement object has been previously calibrated, may provide an estimate of system accuracy in addition to the comparative analysis.

This chapter details exploratory experimental work performed in the first year of research (2006/2007), to assess equipment types (Section 3.2) and determine whether they should undergo further, more rigorous testing. A test artefact with surface finish and features similar to an ITER-Like Wall tile has been developed and measured by dimensional surface metrology equipment available to the project.

#### 4.1. Test Artefact

The use of an actual ITER-Like Wall tile as a measurement test artefact was not feasible because design was not finalised and the material used must be handled in a controlled manner. Pre-prototype tiles existed but although dimensionally correct their surface finish was significantly different than Beryllium, rapid prototyping models were also available but were translucent and therefore presented considerably different surface properties than the material to be measured e.g. light penetration. Because no piece currently existed which would be suitable for testing optical non-contact measurement equipment against, a new dedicated test piece was designed.

##### 4.1.1. Material Selected

Desirable properties for the test artefact were: thermal and dimensional stability, strength and resilience to damage, portability, size and weight. Other considerations were those of cost and availability of materials and the construction method. Stability of the artefact was of importance as the piece was to be transported to different locations in order to use different pieces of equipment. It was necessary that the material was: stable and strong, whilst light enough to be easily lifted by two people, ideally one. A case was required to protect the artefact in transit and storage, whilst being easily handled. The piece had to be large enough to represent an area of one large tile or greater whilst being small enough to be easily moved and fit onto a coordinate measurement machine (CMM).

Given that the artefact was to be used at various locations and there was need for dimensional stability, the Coefficient of Thermal Expansion (CTE) of materials was considered. The CTE of a material indicates how the material will expand or contract under temperature change, in parts per million per degree change in temperature (Table 4.1).

Material	$\alpha$ in 10 <sup>-6</sup> /K at 20 °C
Aluminium <sup>1</sup>	23
Beryllium	11.5
Carbon Fibre <sup>2</sup>	-0.96579
Inconel <sup>3</sup>	12.5
Invar (FeNi)	1.3
Stainless Steel <sup>1</sup>	11

**Table 4.1: Co-efficient of thermal expansion (Temperature range: 20-100°C).** <sup>1</sup>Courtesy of NPL at 19.85°C. <sup>2</sup>Mean value for products of single supplier (Thornel). <sup>3</sup>Sample mean of range of Inconel products.

## Preliminary Experimental Work

Although not exhaustive, Table 4.1 lists materials commonly found on the EFDA-JET site e.g. the vessel contains ~168 tonnes of Inconel. Carbon fibre is the most thermally stable of the materials closely followed by FeNi (commonly known by the brand name 'Invar'). The least stable material shown is aluminium with a change of  $23\mu\text{m}$  per metre per degree C. Based on a  $5^\circ$  increase in temperature a 500mm length of aluminium would increase by  $57.5\mu\text{m}$ . The thermal expansion of materials can be factored into measurement calculations if known and so does not pose an insurmountable problem. A scale bar made of a material with low CTE e.g. Invar, can also be used when performing non contact measurements to provide a trusted scale as is currently undertaken in photogrammetry surveys.

Budget constraints required the use of materials already on site at EFDA-JET, readily available materials were wrought and cast aluminium from Alcoa Mill Products (Alcoa, 2007a; 2007b) and the cast was selected. Although Aluminium has the largest CTE in Table 4.1, the surface temperature can be factored into calculations and an Invar scale bar used during measurement as a reference. The available material limited the size of the artefact to a maximum 500x400mm however, this was large enough for an adequate test piece and aided portability. Weight was calculated at ~22Kg.

As the artefact was constructed of aluminium plate, instead of being machined from solid, each part of the artefact was joined to produce a single stable object. In order to join the parts, they were bolted and doweled to a single piece of aluminium plate, which avoided welding and any dimensional change which could have resulted from the high temperatures. To produce a finish similar to that of Beryllium and the ITER-Like Wall tiles the aluminium was vapour blasted. The surface roughness (Ra) of the prototype Beryllium tiles was calculated as  $1.6\mu\text{m}$  using a Taylor-Hobson Talysurf Sertronic 3 (Section 2.3.2) on site at EFDA-JET. Using the same measurement equipment the initial Ra of the aluminium was calculated as  $3.53\mu\text{m}$  and following surface treatment a Ra of  $2.31\mu\text{m}$  was recorded. No further treatment of the aluminium surface was attempted as the  $0.71\mu\text{m}$  difference in desired and achieved Ra was less than the  $1.22\mu\text{m}$  change in Ra resulting from previous surface treatment. Further surface treatment could have produced a surface Ra of  $1.09\mu\text{m}$  ( $2.31\mu\text{m} - 1.22\mu\text{m}$ ) which would have been locally smoother than the prototype Beryllium tiles, a difference of  $-0.51\mu\text{m}$  to the desired Ra. Performing further surface treatment presented a risk of producing an inconsistent surface Ra with little improvement (in terms of closeness to the intended Ra of  $1.6\mu\text{m}$ ).

#### 4.1.2. Features

In order to allow registration of data collected from multiple viewpoints (Section 3.3.2) by a variety of measurement systems geometric primitives were included in the artefact. The artefact was constructed with eight removable spheres located in countersunk holes which allowed datum transformation of different measurement systems and the mountings simulated target nests suggested for use in ITER. Target nests planned for ITER detailed 1.5" spherical targets (Section 3.2.1.1) to be located in counter-sunk nests secured with magnets, this design would have been too costly to produce for this test piece as the targets were in the region of £1K upwards (Brade, 2007). In light of this financial limitation metallic spheres already on-site at EFDA-JET were used to replicate the ITER targets. The spheres already on-site were a different diameter than those specified for ITER, so the ITER nest was scaled-down to hold the smaller sphere.

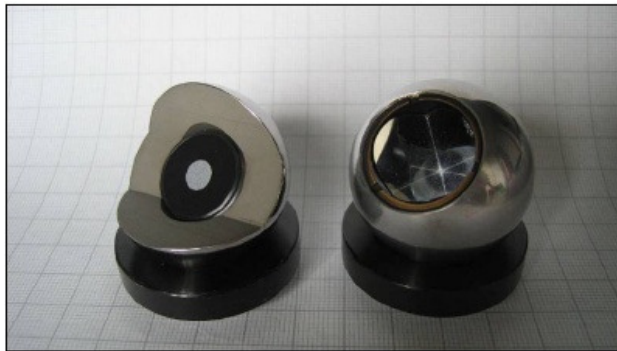


**Figure 4.2: Spherical 1.5" Retro-Target for Photogrammetry (left). 1.5" CCR-Reflector for Laser tracker or Total station (right)**

The artefact (Figure 4.3) was designed with features similar to those of an ITER-Like Wall tile, namely concave and convex curves, steps and gaps. The form was designed to resemble parts of a real tile but detail had been limited to constrain the price and allow data collection within a sensible time due to measurement off-site at vendor premises. The measurement of step and gap between tile units and the concave shape of tiles was replicated on the test artefact whilst leaving planar areas for the addition of further features in the future. The base dimensions were 350 x 500mm.

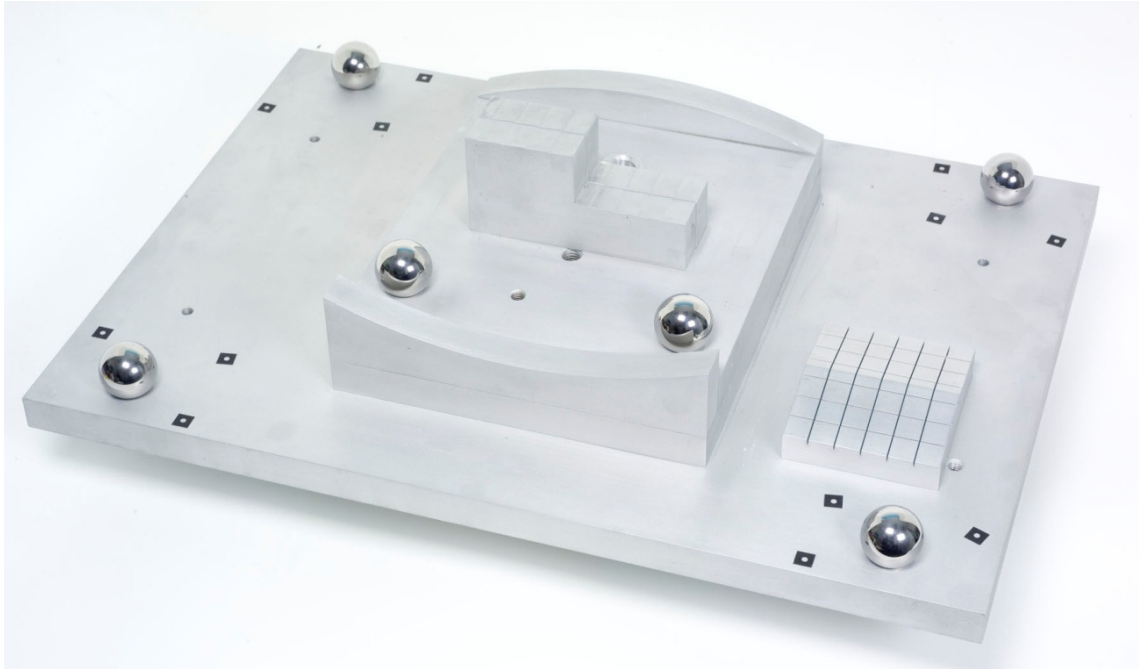


**Figure 4.3: Preliminary test artefact**

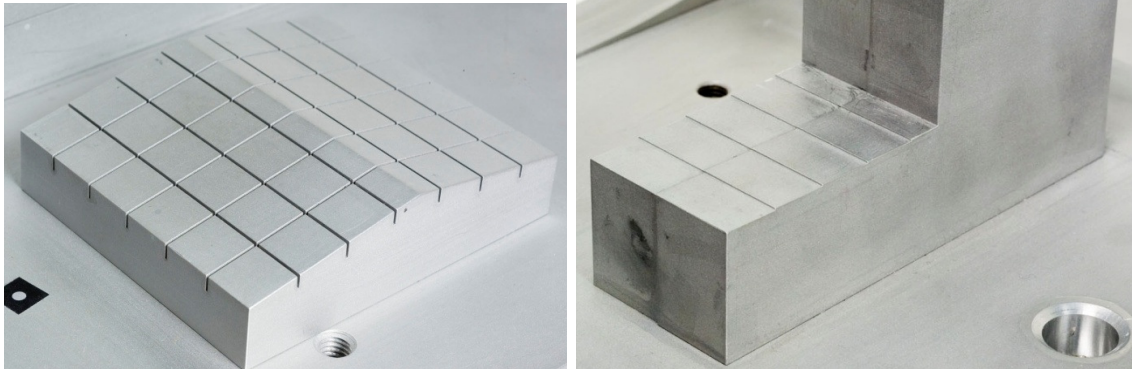


**Figure 4.4: 'Roof tile' feature for gap measurement, nominal gap: 0.35mm (left). Step feature, nominal step height: 0.20mm (right).**

#### **4.2.Measurement Systems Tested**

The measurement systems trialled were based on technologies discussed in Section 3.2 and represented the types of surface measurement technology commercially available. The individual systems were selected because of their availability to the project, all but one of the systems being owned by partners in the research, the UK Atomic Energy Authority and University College London. It is recognised that the systems tested were not all state of the art as several had been superseded by the manufacturer. Where this is the case, further details are provided along with the description of the system. Even where a system was not state of the art, it provided an indication of the abilities of the

measurement technologies and highlighted limitations caused by the fundamental principles e.g. illumination type.

Photogrammetry systems were represented by a GSI PRO-SPOT point projection photogrammetry system owned by the UK Atomic Energy Authority which was heavily used by the Inspection Team at EFDA-JET.

This system, an off-line photogrammetry system involves points of white (incoherent) light being projected onto the measurement surface and imaged by a single camera from multiple positions. The position of each light point on the measurement surface is recorded and a 3D coordinate calculated for each. In order for the photogrammetric bundle adjustment to be automatically calculated, retro-reflective targets are placed in the measurement volume and therefore this is not a fully non-contact measurement survey.

A Breuckmann OptoTop-HE white light projection system using gray-code and phase-shift owned by the UK Atomic Energy Authority was used. The system was purchased to construct 3D models of small parts and when purchased was a prototype unit.

The system is several years old and uses an analogue camera whilst newer systems are available with digital sensors with >10 million pixels. At time of testing, this system was not representative of the state of the art.

Two laser triangulation systems were used, both hybrid systems (Section 3.2.5), one attached to a Helmel coordinate measurement machine (CMM) and the other using an optical tracker, both at University College London.

The CMM mounted system was an Arius3D synchronised laser scanner (Section 3.2.4.2) capable of point pitch on the measurement surface of 0.1mm using a 0.1mm diameter laser spot. Although the use of a CMM mounted system inside the EFDA-JET vessel was impossible, the CMM provided a method for regularised data collection and an opportunity to assess the performance of the laser triangulation head with minimum error contributed by the tracking part of the hybrid solution. The second laser triangulation system was a Metris K-Scan, comprising a LC50 hand-held scanning head and K610 optical tracker. The laser triangulation scanner was not capable of dynamic laser intensity adjustment however at the time of the trials this feature was not present on all

commercially available systems. The two triangulation laser scanners differ in achievable measurement volume because of the different tracking solutions (CMM and optical tracker) and potential to capture complex objects. During the preliminary work, the optical tracker enabled the user to move around the object and capture the surface from more complex orientations whilst the CMM control provided a more linear motion, the synchronised architecture of the Arius3D scanner enabled the generation of data with fewer occlusions than the other system.

A Surphaser 25HSX amplitude modulated polar measurement system capable of direct surface measurement was used to collect data on the artefact and the EFDA-JET In-Vessel Test Facility (IVTF), a full size mock-up of a portion of the real machine. This measurement device was trialled for the potential to measure the overall shape of the vessel rather than the features of the artefact and as such only limited results from this system are presented.

Following measurement by the non-contact measurement systems the artefact underwent measurement by a Mitutoyo touch-probe CMM at the West Midlands Manufacturing Measurement Centre (WMMMC, 2007). The artefact surfaces were measured by the touch probe and used to reverse engineer a basic digital model of the artefact against which the results of the non-contact were compared. The CMM measurements provided traceability for these tests as the CMM was calibrated and checked against a length standard.

### **4.3.Execution of Tests**

Although a metrology laboratory with a temperature and humidity controlled environment would have offered the greatest chance of measurement without external influence, the use of such a laboratory was not possible. Tests had to be carried out in different locations due to the ownership of the equipment being used and although the environment was not optimal, it reflected the real measurements to be made. The environment inside the EFDA-JET machine and method by which equipment was to be handled were not ideal but combined with a test artefact with similar surface finish and features to the real measurement surface, the results are a good indication as to the real world use of such measurement systems.

## Preliminary Experimental Work

Before measurement the test artefact was left to acclimatise to ambient temperature and the artefact temperature monitored during measurement with a surface probe (Model: RS206-3722). No temperature compensation was applied to the measurements, but calculation of the effects of thermal expansion/contraction took place. Based on the temperature range  $20^{\circ}\pm 2^{\circ}\text{C}$  the variance of the longest length of the test artefact (500mm) could have been  $46\mu\text{m}$  (Brownhill et al., 2007).

Where time permitted the whole of the test artefact surface was recorded, however for some technologies this was not possible e.g. the Arius3D system, here only the geometric features of interest and an area of the planar surface were recorded. All systems were calibrated prior to use and where appropriate length standards included in the measurement process. Where possible data were collected by an experienced operator to minimise measurement uncertainty however, for several systems this was not possible.

For the trial of the amplitude modulated system, the test artefact was mounted inside the In-Vessel Tests Facility and data collected on the artefact and the surrounding area. As this was a 'line of sight' technology, multiple 'scans' were required to capture the measurement volume. 6 scans, each lasting 3 minutes were performed at various device positions. These data were registered into a single coordinate system using 14 spheres attached to the walls of the test facility in prominent positions to be visible from the different device positions. The positions of the spheres were determined by a photogrammetric survey performed by the EFDA-JET inspection team, natural feature detection was used to determine the positions of the spheres.

The calculated results take into account a particular environment, measurement surface and features and are therefore only of relevance to this project, the results may not be indicative of the potential of these measurement technologies.

Analysis of results took place using a variety of commercial software packages: GSI V-STARS, Delcam CopyCAD, Delcam PowerInspect, Polyworks IMAlign, Inition Pointstream and a non-commercial least squares shape fitting software package developed at UCL. A range of software was required as data collected varied in density greatly, this demonstrated the need to have a robust procedure for analysing point cloud data. Based on knowledge gained during these experimental tests data collected for the whole of the EFDA-JET vessel could quickly become prohibitively large and prevent

timely processing. Although processing of data can be an off-line event, data must be returned promptly as it is an input to other events in the shutdown schedule.

Data from each system were aligned to a single co-ordinate system in a process referred to as registration (Section 3.3.2) to present a single set of collected data, for most systems this was automatic but for some manual intervention was required. Where possible, other than visual detection and subsequent removal of gross errors, point clouds have not been edited so as to avoid additional error sources. Experience showed that certain packages interpolated points to produce a uniform point grid however, this method was not desired as this would have introduced an additional potential source of uncertainty and error.

#### **4.4. Results**

At the time of the trial no guidelines or standards were in place for non-contact measurement systems utilising multiple viewpoints to measure a surface. In light of this a series of basic tests on the collected data were performed to assess and compare systems. Some guidance was taken from the German guidelines: VDI/VDE 2634, Parts 1&2.

##### ***4.4.1. Length error***

Scale was particularly important to this project as it was unlikely there would be a single system which could generate all data required to the desired level of accuracy (Section 2.4). Consequently the combination of systems required registration and integration of data, necessitating a common scale.

To compare length measurements between the various measurement systems, the distance between the sphere centres on the test artefact were calculated (Table 4.2). The sphere centres were derived from sphere fits performed in GSI V-STARS (Table 4.5). These distances were therefore dependent on this sphere fit. The range of values between spheres 5 and 6 (on the longer artefact axis) was 0.427mm and on the shorter side, 0.192mm.

Preliminary Experimental Work

Data in mm	Spheres	
System	5 to 6	5 to 8
Arius3D	400.110	300.019
Breuckmann Original	400.420	300.103
Breuckmann Polyworks	400.435	300.122
Metris	400.104	299.930
GSI Pro-Spot	400.009	299.964
Crysta Apex C CMM	400.047	300.018

**Table 4.2: Distance between sphere centres**

Based on the co-efficient of thermal expansion for the aluminium used to produce the test artefact and a temperature range of  $20^{\circ} \pm 2^{\circ}\text{C}$  the maximum possible variation in length along 500mm could have been  $46\mu\text{m}$ . The range of length values between sphere 5 and 6 (along the 500mm length) was 0.427mm, so although temperature variation could have had an impact on the results seen, it was not the sole cause.

System	Sphere to sphere	
	5 to 6	5 to 8
Arius3D	158.3	1.9
Breuckmann Original	932.3	282.6
Breuckmann Polyworks	970.1	344.3
Metris	141.8	-294.9
GSI Pro-Spot	-96.4	-179.3

**Table 4.3: Distance between sphere centres compared to CMM generated data (Parts Per Million)**

Scale error was checked by comparing the data from the various systems to that provided by the CMM. Table 4.3 shows the difference in separation between spheres 5 to 6 and 5 to 8 compared to the Mitutoyo Crysta Apex C in parts per million. Nominally the distance from sphere 5 to sphere 8 was three quarters of the length between sphere 5 and sphere 6, therefore it would be expected that a constant scale error would lead to the distance of sphere 5 to 8 compared to the CMM to be 75% of the distance of sphere 5 to 6 compared to the CMM. The results did not support this expectation for any of the systems tested.

The Breuckmann white light system showed parts per million comparable with that from other technology between spheres 5 to 8 but much larger than others between spheres 5 to 6. During data collection spheres 5 and 8 were seen in the same scan sets but 5 and 6 were not seen in any combined scan from the Breuckmann system. It is postulated that insufficient features on the artefact and an abundance of data on planar surfaces has resulted in an incorrect fit of component scans during scan registration resulting in an extension along this axis.

To assess the uncertainty present in the different data sets, sphere and plane fits were performed to compare the error present in each data set.

#### 4.4.2. Sphere Fitting

The point data for a specified sphere was processed in least squares based software written at University College London which calculated the sphere centre, radius and RMS error for residuals normal to the surface. Input data for this process was sampled, using a nearest point algorithm, at a 0.6mm 3D point spacing in order to provide all systems with a similar sampling set (Table 4.4). Table 4.5 presents the original un-sampled data following mathematical filtering performed by the GSI V-Stars software which incorporated an outlier rejection process. Physical measurement of the spheres yielded a mean radius of  $15.0\text{mm} \pm 5\mu\text{m}$ . Data for the Surphaser system is not presented here as the test artefact spheres were not used inside the IVTF.

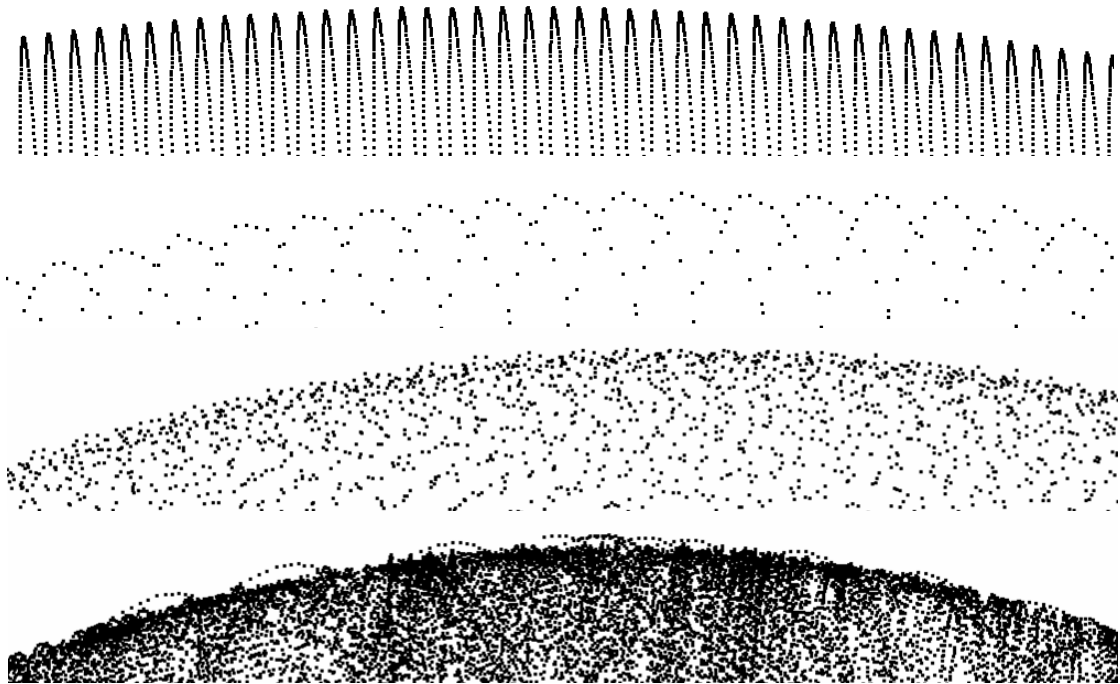


**Figure 4.5: Example point data of a sphere. Top to bottom: Arius3D, Breuckmann (single scan), Breuckmann (multiple scans), Metris.**

Data coverage on the sphere will have affect the calculated sphere centre where less than half the sphere is captured, resulting in an overestimation of the sphere radius. The resulting shift in the sphere centre could have been minimised by using knowledge of the position of the sensing system at the time of collection (Section 4.4.5) however, this approach would not have been applicable for measurement systems where multiple approach directions were used.

Preliminary Experimental Work

	Standard Deviation	Range	Minimum	Maximum	No Points	Radius (mm)
Arius3D	27.07	173.8	-51.6	122.2	2150	15.059
Breuckmann Original	46.09	464.1	-198.2	265.9	2089	15.112
Breuckmann Polyworks	37.95	365.0	-138.6	226.5	1825	15.108
Metris	46.07	282.6	-133.9	148.7	1518	14.949
GSI Pro-Spot	18.67	80.5	-38.5	42.1	67	14.957

**Table 4.4: Sphere fit statistics after sampling at 0.6mm, data in microns**

	Standard Deviation	Range	Minimum	Maximum	No. Points		Radius (mm)
					Used	Rej.	
Arius3D	12.34	71.7	-34.7	37.0	51819	5717	15.026
Breuckmann Original	36.77	214.0	-105.5	108.5	2020	69	15.077
Breuckmann Polyworks	34.25	203.1	-100.6	102.5	1827	32	15.081
Metris	45.18	270.5	-135.1	135.4	61836	367	14.940
GSI Pro-Spot	19.09	82.6	-36.6	46.0	70	0	14.945

**Table 4.5: Sphere fit statistics following outlier detection in GSI V-STARS (microns)**

**4.4.3. Plane Fitting**

A planar region of the test artefact was selected with good data coverage from all systems and extracted. As there was a large difference in the number of points collected by each system, each point cloud was re-sampled, by rejecting excess points over a 0.6mm spacing to produce a point cloud with similar number of points per system. For each system a plane was fitted through the points in the selected area using least squares plane fitting software written at UCL (Table 4.6).

	Standard Deviation	Range	Minimum	Maximum	No Points
Arius3D	14	84	-43	40.9	2786
Breuckmann Original	35	311	-179	131.4	2355
Breuckmann Polyworks	19	147	-88	59.2	2039
Breuckmann Single Scan	17	110	-54	55.9	2025
Metris	22	292	-145	147.0	2506
GSI Pro-Spot	17	108	-62	46.7	149
Surphaser	201	-	-	-	-

**Table 4.6: Plane fit statistics (microns)**

#### 4.4.4. *Surface Discontinuities*

Extraction of dimensional information in close proximity to an edge was of particular importance in the analysis of tile erosion and deposition due to complex design of the plasma facing components. Machined ‘steps’ in the tile design were created to shadow the next section of tile and prevent exposed edges which would be subject to higher heat loads in the EFDA-JET vessel. The Arius3D, Breuckmann and Metris systems had the highest point density and therefore more potential for capturing edge data.

The manufacture of the test artefact prevented accurate analysis of edge detection because insufficient knowledge of the edge profile existed. The CMM probing performed on the part provided planar and curved sections but could not provide accurate edge information, therefore the analysis performed was of a qualitative rather than quantitative nature. The artefact had edges were better identified by the Arius3D and Metris systems with noticeable smoothing in the Breuckmann data set. Such discrepancies were indicative of the different sampling sizes, imaging geometries and data filtering strategies of the systems.

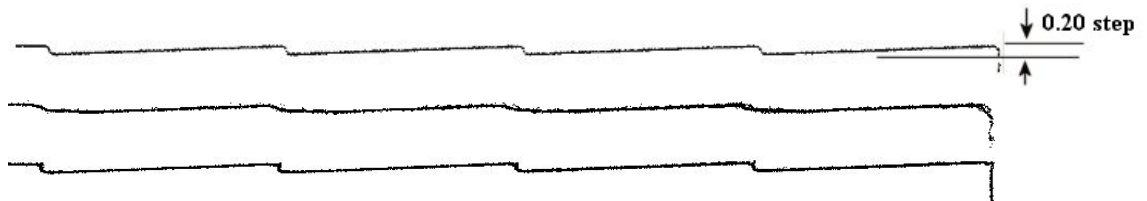


**Figure 4.6: Arius3D single Scan (top), Breuckmann multiple scans (middle), Metris multiple scans (bottom). Profile images visually aligned for presentation.**

The evidence inherent in the profile data was confirmed through visual analysis of plan views taken from a different area of the tile artefact (Figure 4.7) where it was clear that the 0.1mm laser spot diameter of the Arius3D system had delivered cleaner data. Data from the Metris K Scan system was more difficult to judge from this view since it highlighted the irregular nature of the hand held scanning process.

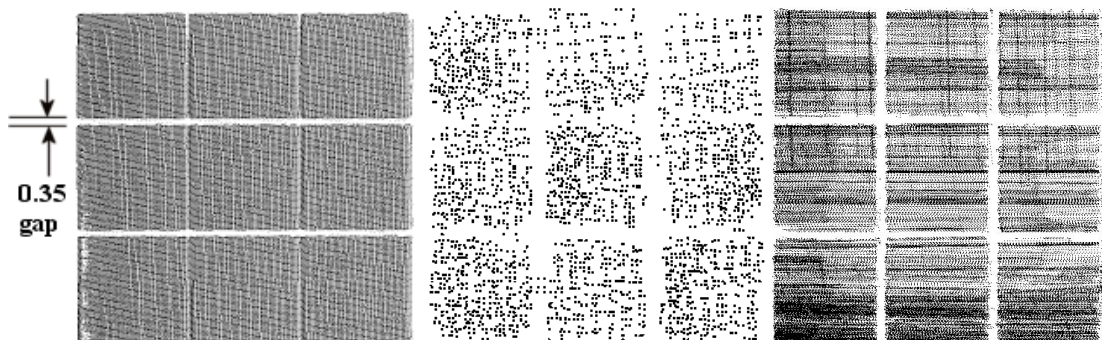


**Figure 4.7: Scan data plan view. Arius3D (left), Breuckmann (centre), Metris (right).**

The Surphaser polar measurement system demonstrated more errors at the mm level at edge discontinuities (Figure 4.8) attributable to the diameter of the laser spot on the measurement surface causing reflectance from multiple surfaces (Section 3.2.4.1). The spot diameter was in the range 2.3 – 5mm for the model used however a shorter range model with reduced spot diameter (0.5 – 1.8mm) was produced but unavailable at time of testing.

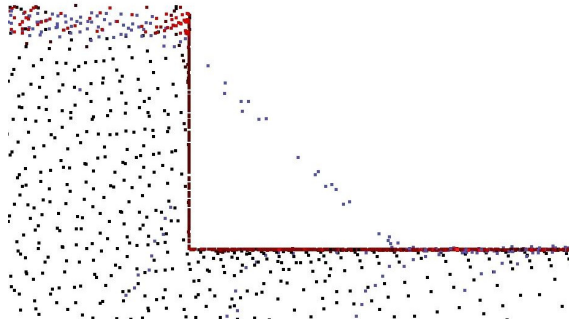


**Figure 4.8: Partial reflectance at edge.**

Multi-path reflectance (Figure 3.9) was also seen in the collected data (Figure 4.9) causing two planar surfaces to be recorded as curved. The magnitude of the error at its largest was ~2mm (Brownhill et al., 2009b) and affected surfaces which met to form angles  $\sim 90^\circ$  (Figure 4.10).

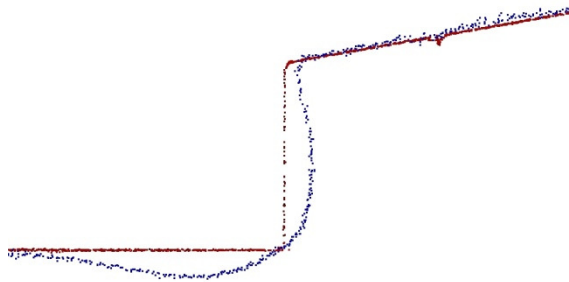


**Figure 4.9: Multi-path reflectance, profile of 'roof tile' feature (Figure 4.4) meeting artefact base. CAD data in red (straight lines), collected data in blue (curved lines).**

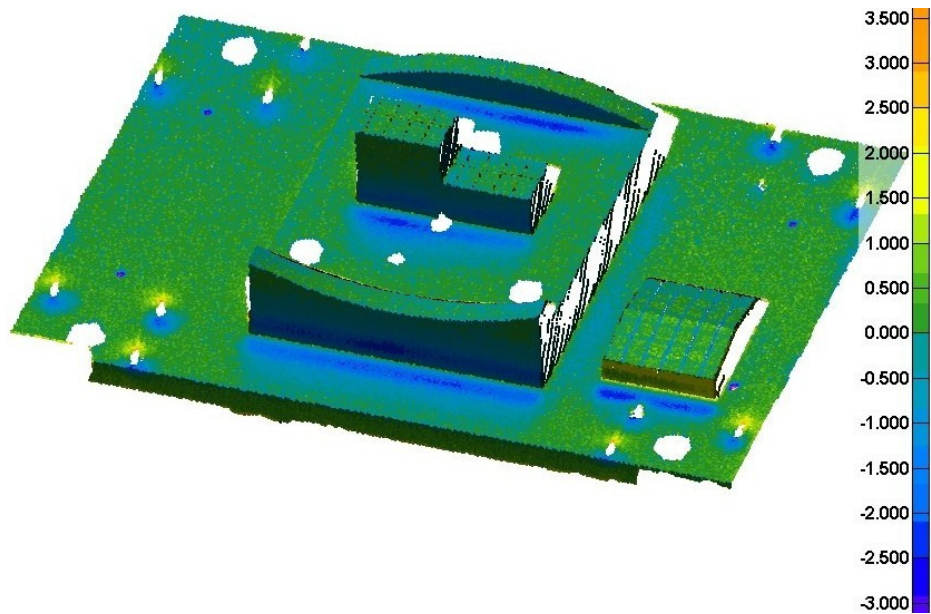


Figure 4.10: Effect of multi-path reflectance on the collected data (error scale in mm).

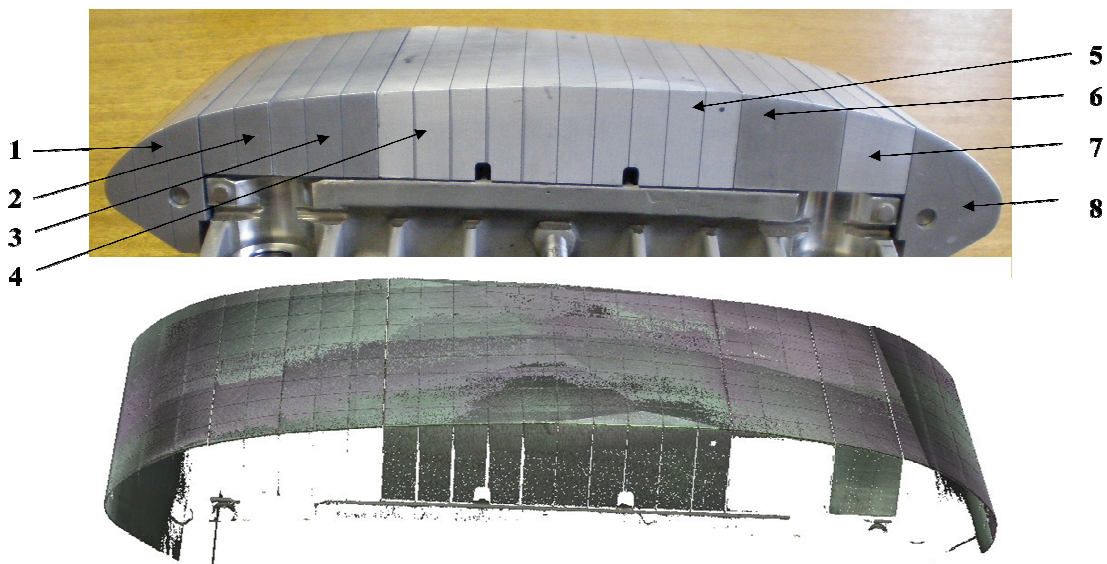
Despite the demonstrated errors, the amplitude modulation technology collected a far greater quantity of data than the other systems on test within a large volume in short time. Figure 4.11 demonstrates the quantity of data collected within one 3 minute scan.



Figure 4.11: Data of inside of IVTF collected by Surphaser scanner, point brightness determined by light intensity returned to scanner. Photograph of same area ~ 2.5m x 3m (inset).

#### 4.4.5. *Effect of Surface Roughness on Measurement Data*

The artefact measured had a consistent surface roughness, with the results collected valid for this surface only. A pre-prototype tile assembly machined from aluminium without final surface treatment became available and to gain familiarity with the Arius3D measurement system at UCL, the pre-prototype tile assembly consisting of a number of tile blocks was measured. The assembly was positioned such that the orientation of the surface with respect to the sensor would be approximately the same. Some of the blocks produced no measurement data, whilst others were captured without problem. All blocks were machined from the same material but differed visually, so a short study was performed to investigate whether a link between surface roughness (affecting surface appearance) and ability of the system to measure the surface existed.



**Figure 4.12: Measurement data of a pre-prototype tile assembly. Photograph (above) and computer visualisation of collected data (below).**

Surface roughness measurements were taken with a Taylor-Hobson Surtronic3 in the metrology laboratory at EFDA-JET. For each of the eight positions on the assembly where visual difference between the surfaces can be seen, six measurements were taken, three in the direction of lay and three across the direction of lay. A mean surface roughness value was calculated for each (Table 4.7).

## Preliminary Experimental Work

Position	Following direction of lay	Across direction of lay
1	0.42	-
2	0.54	-
3	0.47	-
4	3.44	4.34
5	3.69	4.48
6	0.34	0.47
7	0.71	0.75
8	0.53	0.85

**Table 4.7: Surface roughness (Ra) of pre-prototype tile. Data in  $\mu\text{m}$ .**

Comparing the dimensional data (Figure 4.12) with the surface roughness data (Table 4.7) dimensional data were only collected for measurement positions 4, 5 & 7. Although difficult to make any definitive conclusions, the results indicated that an Ra of  $0.71\mu\text{m}$  in the direction of lay and  $0.75\mu\text{m}$  across the direction of lay were required to successfully collect data. This conclusion is only valid for this surface with the given measurement system and surface orientation. A more thorough investigation using a range of surfaces with varying roughness would be required to make wider ranging conclusions.

### 4.5. Summary

Based on the analysis of the data collected, the Arius3D triangulation laser scanner produced data with the most regular sampling and lowest uncertainty. The regular sampling was due to the CMM mounting and although the CMM cannot be used inside the machine, the linear motion should be repeatable using alternative hardware. To increase data collection speed the linear motion could be increased but with a resulting increase in the inter-line point pitch on the measurement surface and a point pitch which differs according to the direction of sensor travel. The portable laser triangulation system was the most flexible system however, point uncertainty on the sphere and plane fitting tests was slightly above the comparable white light system. The use of a state of the art measurement head may have offered uncertainty however, the head, was not the only error source in the test. Figure 4.5 shows one or more lines of measurement data which appear to be above the sphere, likely caused by error in positioning the measurement head in the volume (Figure 3.34). The white light system produced high density, low uncertainty data where individual data were correctly registered however, the white light system's limited working volume and high reliance on registration of multiple data sets will reduce overall accuracy if the measurement volume were to be increased.

## Preliminary Experimental Work

Point projection photogrammetry has limited point density and the point density is closely related to the measurement volume as the further the projector is from the surface, the greater the point pitch becomes. Based on the tests performed, the data point density will be a limiting factor in measurement of small areas e.g. the individual castellations of a tile section (Section 2.3) and measurement close to edges will be determined by the point diameter on the surface and careful positioning. Both may be improved by multiple projector positions however this will result in a large number of additional images being required.

The measurement test artefact was a limiting factor in the evaluation of collected data as the dimensions were not known with sufficient accuracy. Dimensions were determined primarily by the touch-probe CMM survey which could not provide data close to edges and therefore there was limited data on the 'step' and 'roof tile' objects. Although manufacturing tolerances are always likely to be greater than the uncertainty of the measurement equipment in use, tighter manufacturing tolerances and more consideration of the dimensions of the as-built artefact should have occurred in the design phase. As the artefact provided a very limited measurement volume to test measurement systems, an artefact capable of testing a larger volume should be developed for further testing. The development of new test artefacts which build upon the progress and lessons learned in this trial should occur. Using new artefacts, a second equipment trial should be performed using state of the art measurement equipment, in a controlled environment, with a set of tests which can be repeated by each technology under consideration.

## **5. Primary Equipment Trial**

This chapter explains the rationale for a second experimental phase and details the experiments performed and results obtained.

### **5.1.Experiment Rationale**

The preliminary experiential work performed in the first year of research provided information on the performance of measurement systems but was not intended to satisfy the research objectives (Section 1.4). From the preliminary work, two measurement technologies were identified with potential to satisfy the EFDA-JET requirements and as identified in the summary of preliminary work, would require further testing. Given that preliminary testing could not satisfy the research objectives, it was recognised that improved experiments would be required, taking into account further research into the operation of metrology technologies and revisions to the EFDA-JET ITER-Like wall tile design. Due to the material of manufacture, use of the ITER-Like wall tiles was not possible.

A review of measurement system evaluation, tests performed and artefacts used was performed (Section 3.4), which revealed no standard test existed which could satisfy the research objectives. There was work which focussed on specific aspects of measurement however those tests would not satisfy all of the research objectives. The VDI/VDE 2634 Part 3 guidelines (The Association of German Engineers (VDI), 2008) are the most complete set of tests relating to non-contact surface measurement, but these guidelines focus on cooperative surfaces, of which the EFDA-JET tiles are not, and the guidelines were not published until design of tests for this research was complete.

To satisfy the research objectives and create a repeatable workflow for measurement, tests needed to be simple and quick to perform. Data processing was required to be repeatable and free from error, delivering results quickly. To satisfy these needs the research objectives were studied and a number of tests developed which would meet them (Section 5.2.3). These tests required a number of artefacts to be designed, each delivering information to satisfy a specific objective and enabling quick data collection, whilst presenting a surface to meet the requirements of EFDA-JET. Following the preliminary trial it was understood new artefacts would require tighter manufacturing tolerances and improved validation of their as-built dimensions (Section 5.2.1). Additionally, a large volume experiment would be required to assess equipment

## Primary Equipment Trial

performance where total measurement volume exceeds sensor measurement volume (Section 5.2.3.6).

The preliminary experimental work performed in the first year of research highlighted two technologies as most suitable for the measurement of EFDA-JET surfaces: white light fringe projection and laser line triangulation. The particular models of equipment trialled as part of preliminary work were not state of the art and had been superseded by newer models. For the primary experimental work in this research, state of the art measurement systems were used to demonstrate the most advanced incarnation of these technologies. Given that there was no standard method in use to evaluation performance, selection of equipment was based on manufacturer specifications and discussion with operators and researchers within the dimensional metrology community.

In order to test the measurement technology, rather than a particular implementation of that technology, two models of each type of technology were selected. The white light fringe projection technologies are an implementation of 'Light Projection: Bundle of Rays', implementing coded light and phase shift. For a total measurement volume greater than the sensor measurement volume, self-localisation is used e.g. retro-reflective targets, as it was not possible to obtain an implementation of a white light projection system using external tracking e.g. laser or optical tracker. At time of trial, such technologies were not commercially available. The laser line triangulation measurement systems tested both offer dynamic adjustment of laser intensity and use laser or optical tracker for 6DoF positioning (Section 5.2.2).

## **5.2.Experiment Design**

To evaluate measurement equipment performance, all other error sources in the environment were to be minimised (Figure 4.1: Components of a large scale measurement (University College London, National Physical Laboratory, Leica UK, 1999). Environmental factors included: the user performing the measurement (Section 5.3.1), the physical environment e.g. temperature, humidity (Section 5.3.2) and the workpiece measured.

The artefacts produced (Section 5.2.1) served to minimise the workpiece error as all measurement systems measured the same artefacts, with these artefacts having been measured by a system with significantly lower uncertainty (Section 5.2.1.6).

### **5.2.1. Artefacts**

Tests artefacts for measurement by non-contact dimensional metrology equipment have been produced by several organisations (Section 3.4) and for this research (Section 4.1). The artefacts produced by other organisations were intentionally non-specific in form, intended to represent a varied and challenging surface for measurement systems. For this research a very specific surface finish and set of features were required against which a custom set of tests were performed. These tests provided data used to determine whether the measurement systems tested could produce the required information for EFDA-JET (Section 2.4).

Each artefact (Section 5.2.1) was designed and manufactured in such a way that it could be used as a stand-alone artefact or as part of a large volume trial using a measurement test frame (Section 5.2.1.5). Each artefact was mounted to a base (mounting plate) which acted as a local reference system with four  $\varnothing 10\text{mm}$  holes for push-in targets, enabling repeatable positioning on the test frame controlled by a hole and slot machined into the underside of each mounting plate. When used individually each artefact was capable of being mounted to a local reference frame, this having four large spheres for initial registration of data.

Design and specification of all parts for this project was been performed in line with EFDA-JET procedures. The EFDA-JET process included a design review with key interfaces including the remote handling department, design office and inspection department reviewing and commenting on the design and manufacture plan. Successful

completion of the design and review process ensured the artefacts met the design brief and were manufactured with sound engineering basis.

The design of each artefact is described, followed by details of the manufacture and verification which are common to all artefacts.

#### 5.2.1.1. Angle Artefact A

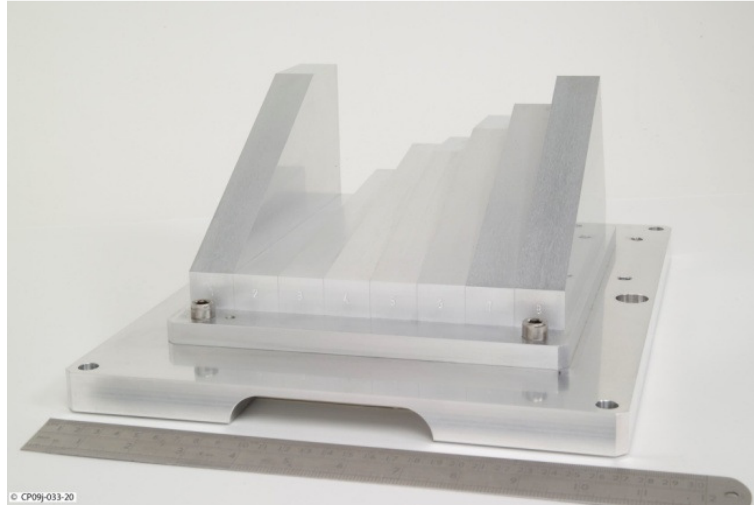


**Figure 5.1: Angle Artefact A**

The artefact was constructed of eight angled blocks, each presented a planar surface with angle to the base of  $0^\circ$  through to  $30^\circ$  in  $5^\circ$  increments,  $55^\circ$  and  $60^\circ$ . The artefact measured 250 x 210mm, with distance of 107mm from base plate to highest point. The artefact was permanently attached to a 350 x 275 x 20mm plate which featured two countersunk holes for retaining bolts and four  $\varnothing 10H7$  holes in the corners for target positioning. The underside of the plate was machined with a blind slot and hole for repeatable positioning and recessed areas for manual handling.

**5.2.1.2. Angle Artefact B**



**Figure 5.2: Angle Artefact B**

The artefact was comprised of 11 individual blocks with planar top faces, the centre block presented a plane at  $0^\circ$  (parallel) to the base and the surrounding blocks angled away at  $5^\circ$  increments to  $50^\circ$ . The  $0^\circ$  block at the centre of the artefact presented a plane with dimensions: 25 x 70mm.

The artefact was permanently attached to a 350 x 275 x 20mm plate which featured two countersunk holes for retaining bolts and four  $\varnothing 10H7$  holes in the corners for target positioning. The underside of the plate was machined with a blind slot and hole for repeatable positioning and recessed areas for manual handling.

**5.2.1.3. Gap & Step**

Two separate artefacts were attached to a single base and measured together. These artefacts provided information about the capabilities of the measurement systems to measure gaps/slots and step/flush.

The step artefact was constructed of nine individual blocks with a nominal height difference between the first and last block of 2.19mm. Within the artefact, adjacent blocks had a nominal step height difference of: 0.02, 0.03, 0.04, 0.10, 0.20, 0.30, 0.50 and 1mm. These dimensions relate to the sizes of step between castellations in a block, step between blocks and inter-tile step (Section 2.3). The manufacturing tolerance for all blocks was: +0.01, -0.00mm. The required accuracy and choice of aluminium as the material (Section 5.2.1.4) made manufacture a challenge, it was suggested by machining companies that for the required accuracy stainless steel would be a more suitable material and could be ground to the required dimensions. Aluminium was not replaced

## Primary Equipment Trial

by stainless steel as no information could be sourced about the similarity of stainless steel to beryllium following surface treatment. Aluminium was retained as the construction material for this piece as it was known the optical properties of the material had impacted the optical measurement systems (Section 4.4.5). Other than material, the artefact manufacturer had to take into account the effect of machine drift and environmental change when manufacturing these parts to stay within tolerance. Each block presented a measurement surface of 20 x 20mm.

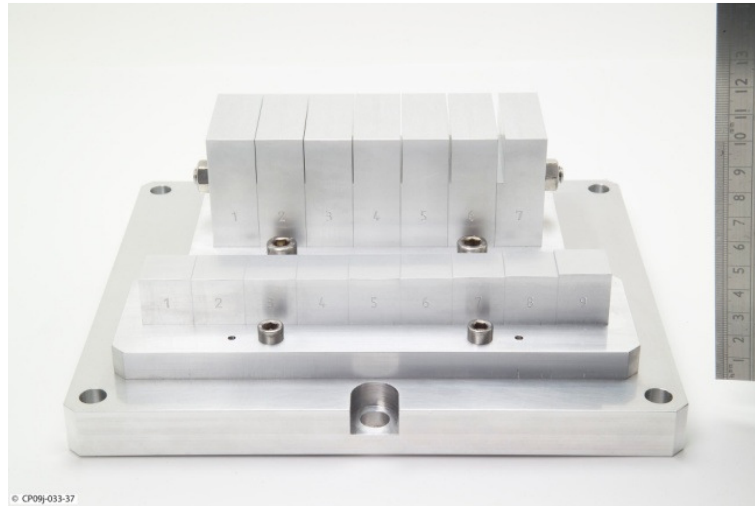


**Figure 5.3: Step artefact (front) & Gap artefact (back) on a single (small) mounting plate.**

The gap artefact was a series of seven blocks which presented six slots with nominal depth of 20mm and widths of: 0.2, 0.3, 0.5, 0.7, 1.0, 3.0mm. The range of slot widths allowed testing of which measurement systems were capable of capturing the surface discontinuity both for intra-tile and inter-tile gaps. The manufacturing process involved six of the seven blocks being machined to remove a depth of material equivalent to the required slot width and depth, treated and then bolted through. Once bolted, the blocks were drilled, reamed, doweled and bolted to a plate before attachment to the small mounting plate.

Both artefacts were permanently attached to a 230 x 196 x 20mm plate which featured two countersunk holes for retaining bolts and four  $\varnothing 10H7$  holes in the corners for target positioning. The underside of the plate was machined with a blind slot and hole for repeatable positioning and recessed areas for manual handling.

### **5.2.1.4. Material Selection & Manufacture**

Beryllium was an unsuitable material for the test artefacts because of handling restrictions (Section 2.3) so alternative materials were investigated. The material

required a surface with similar optical properties to beryllium e.g. surface shade, reflectance. The beryllium manufacturer produced prototype tiles to verify machine setup from aluminium which had similar appearance to the beryllium parts. The material used for the prototype tiles was Alcoa 60601-T651 aluminium alloy and was therefore selected for the manufacture of the test artefacts.

Prior to material choice, consideration was given to the machining method and material form e.g. solid material, plate. Manufacturing each artefact from solid aluminium would have provided greater dimensional stability to the parts however, for the Step and Gap pieces it was advised that for the given design the use of individual parts would minimise machining errors at internal corners caused by the machine tool radius, in addition it was advised manufacturing from solid to be approximately twice the price. Grinding as a method of manufacture was considered because of the improved accuracy over milling however, the technique was discounted as aluminium is typically difficult to grind and not commonly performed because of the softness of the metal. The prototype units were manufactured by Electrical Discharge Machining (EDM) which was researched however was prohibitively expensive. Constructing the artefacts from individual pieces required they be securely positioned and so each part was bolted in place and then drilled, reamed and doweled. Once constructed the artefacts were considered dimensionally stable unless damaged or mishandled.

In order to achieve a surface similar to the beryllium tiles, the aluminium required treatment by submersion in a weak solution of nitric and hydrofluoric acid in order to remove 6-10 $\mu$ m of surface material in line with the design of ITER-Like wall tiles. This acid solution was a variation on the combination used to treat the prototype and beryllium tiles as suppliers were unable to use the original solution. The surface treatment left a less specular surface and removed some of the machining marks however did not remove them completely. The change in machining method and surface treatment left a surface not identical to the prototype tile but one closer to the required surface than available otherwise (Section 5.2.1.6).

### **5.2.1.5. Test Frames**

Two objects were produced to which test artefacts could be attached, a small portable test frame for use away from EFDA-JET (Section 5.2.1.5.2) and a large test frame to which all artefacts could be attached to simulate a portion of the EFDA-JET machine (Section 5.2.1.5.3). Data collected from different viewpoints and orientations required

registration to produce a single data set with common coordinate system (Section 3.3.2). To enable registration, a number of datum clusters (Section 5.2.1.5.1) featuring geometric primitives and EFDA-JET target holders were produced.

#### 5.2.1.5.1. *Datum Clusters*

Each datum cluster featured a large ( $\text{\textcircled{50}}\pm 0.05$  mm) stainless steel sphere with vapour blast surface treatment to produce a diffusely reflecting surface (Figure 5.4). The sphere was mounted on a  $10\pm 0.05$ mm long collar to raise it away from the datum cluster base to enable easier data collection below the equatorial plane of the sphere. The purpose of the sphere was to allow non-contact systems to perform registration of data without using data from the artefact surface itself, also to validate data against the current photogrammetry system. Two target holders surrounded the sphere for push-in targets, the holders accepted photogrammetry targets used at EFDA-JET or other target types using the same fitting. These holders allowed existing photogrammetry procedures and equipment in use at EFDA-JET to be compared against the non-contact systems trialled.

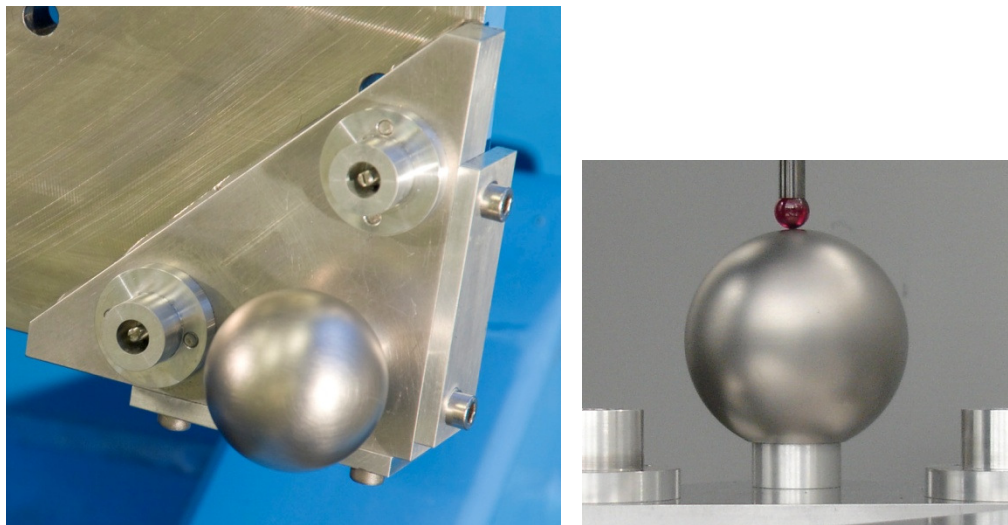


**Figure 5.4: Datum cluster featuring  $\text{\textcircled{50}}\text{mm}$  sphere and EFDA-JET target holders (left), Side view of sphere and collar (right).**

#### 5.2.1.5.2. *Portable Test Frame*

The portable test frame featured two datum clusters and two additional spheres of the same design as those used on the clusters. The positions of the spheres and clusters enabled the orientation of the frame and artefact to be determined without using the complete data set. The frame featured three  $\text{\textcircled{10}}\text{mm}$  dowels, two of which located into a hole and slot on the underside of each artefact mounting plate and provided repeatable

## Primary Equipment Trial

positioning. The underside of the large artefact mounting plate featured a recess so it did not interfere with a dowel used for positioning of the small artefact mounting plate of the gap/step piece. Threaded holes were also present to fix an artefact mounting plate to the frame during measurement. This portable frame has been designed so that it could attach to the centre of the large volume test frame, providing additional registration spheres and datum clusters during the large volume measurement trials.

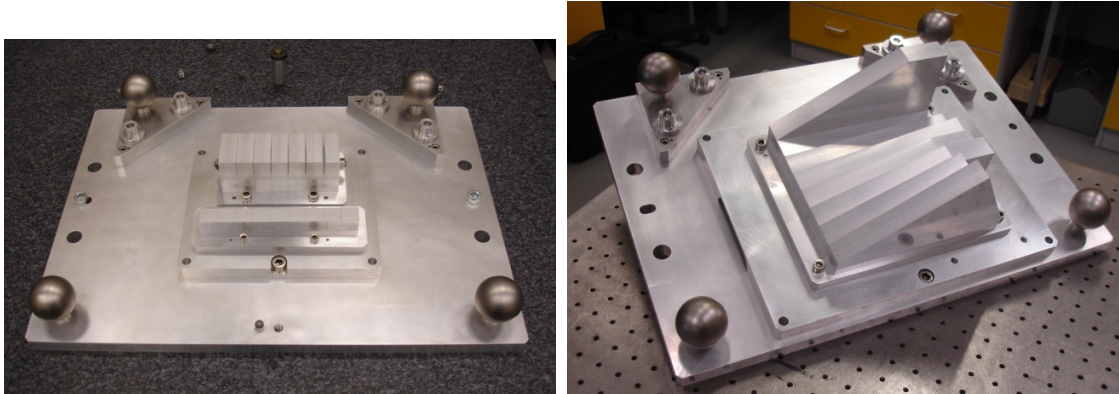


**Figure 5.5: Portable test frame with Gap/Step artefact mounted (left), Angle Artefact A mounted (right)**

### 5.2.1.5.3. *Large Volume Test Frame*

The performance of a large volume test was a requirement for EFDA-JET, to demonstrate that measurement systems could collect data for a volume representative of the real machine. Access to the real machine was not possible and the In-Vessel Test Facility (IVTF) used in preliminary trials (Section 4) was inaccessible because of remote handling trials so an alternative was found. The use of a large volume frame (Figure 5.6) was agreed, the CAD models updated and a number of interface plates designed to enable repeatable attachment of artefacts. Four datum clusters (Section 5.2.1.5.1) were attached and surveyed using photogrammetry.



**Figure 5.6: Large volume measurement test frame with datum clusters at the corners and artefacts attached, metre length included.**

#### **5.2.1.6. Artefact Verification**

Preliminary experimental work demonstrated the need for as-built dimensions of test artefacts to be known with accuracy significantly better than the measurement system to be tested. A value often used is that the system should be between five and ten times (an order of magnitude) better than the data required. The manufacturing tolerances alone would not have provided verification of the as-built dimensions, to obtain such information about the artefacts produced, required a contact measurement system with well understood uncertainty. The most suitable tool was the coordinate measurement machine (CMM) as used in the preliminary experimental work. Use of a ZEISS CMM at NPL was negotiated and measurements made by a trained operator. The CMM could achieve measurement with spatial uncertainty of  $'1.3\mu\text{m}+(L/300)'$  where L is the diagonal of the measurement volume in metres, so  $\pm 0.003\text{mm}$  was achievable for the volume of the artefacts (Evenden, 2009). The four reference holes on each mounting plate were measured and used as a reference system for the artefact. The planar surfaces of the artefacts were measured by moving the measurement probe over the surface following a pre-determined route. This contact scanning method of operation enabled the collection of thousands of points per surface, with  $\sim 1500$  data points collected for the small planes of the step artefact.

## Primary Equipment Trial

Verification of the ‘gap’ artefact dimensions raised a significant challenge as the majority of slots present in the piece are too narrow to allow a suitably sized probe to enter. Several approaches were considered to verify the dimensions of the slots, one approach being the use of a CMM with smaller measurement volume and consequently smaller probe tip diameter. The smaller volume CMM was investigated but no further action was taken due to time limitations. The approach followed was to use the artefact for the non-contact trial, deconstruct the artefact and measure the dimensions of each block individually. Data from this method was dependent on the repeatability of fit of the blocks and to check this, the overall length of the artefact was compared before deconstruction and after the piece has been measured and reconstructed. The use of a vision CMM at NPL was also investigated and some sample measurements were taken. The Vision CMM calculated two- dimensional data in the same manner as a traditional CMM with the depth information obtained from focus of a lens. Vision CMMs were used in conjunction with touch probe CMMs by beryllium manufacturers as a method of verifying the dimensions of prototype tile components (Figure 5.7).

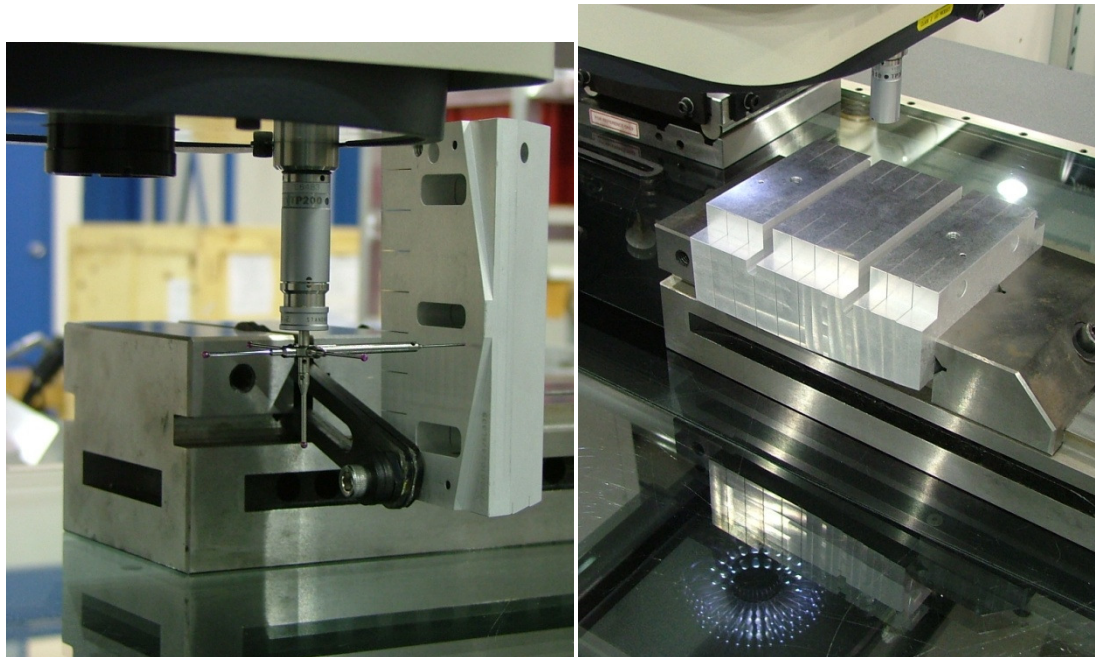


**Figure 5.7: Touch probe & Vision CMMs measuring prototype tile blocks at manufacturer.**

The measurement of the ‘step’ artefact posed a problem as complete measurement of the planar surfaces was impossible. Data could not be collected within a distance equal to the radius of the tip of the touch probe, as the probe would have come into contact with the adjacent block (Figure 5.8). Increasing probe length, reducing probe tip diameter and probe shaft would have all reduced the rigidity of the probe, adversely

## Primary Equipment Trial

affecting the quality of the collected data. The probe used to measure the artefacts was chosen by an experienced CMM operator and used for all artefacts. The dimensions of the step artefact (Table 5.1) showed  $<0.01\text{mm}$  discrepancy between nominal and as-built dimensions, for the material and machining method these discrepancies were acceptable.

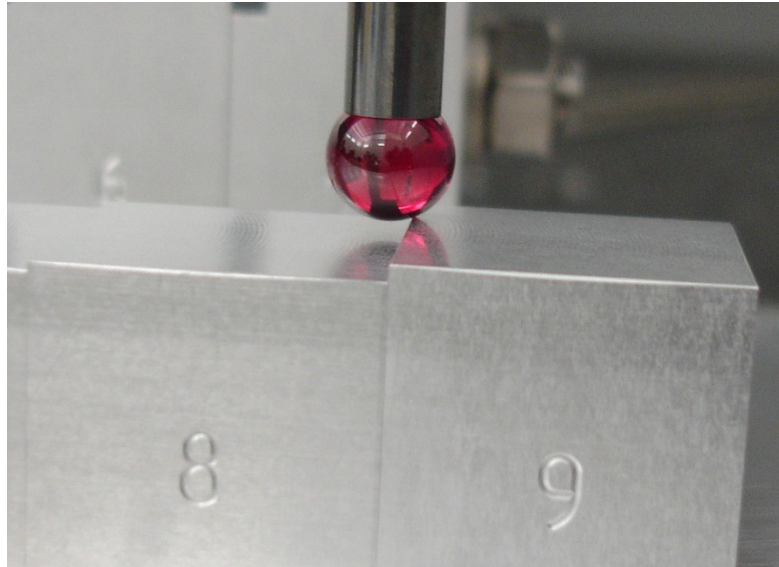


**Figure 5.8: Complete surface of block 8 cannot be measured as probe comes into contact with block 9.**

Step Between Blocks	Nominal	CMM	Discrepancy
1-2	0.02	0.015	-0.005
2-3	0.03	0.023	-0.007
3-4	0.04	0.043	0.003
4-5	0.10	0.102	0.002
5-6	0.20	0.201	0.001
6-7	0.30	0.298	-0.002
7-8	0.50	0.507	0.007
8-9	1.00	0.999	-0.001

**Table 5.1: Nominal and as-built step height between blocks. CMM data  $\pm 0.003\text{mm}$ . All data in MM.**

The surface roughness ( $R_a$ ) of several of the artefacts following surface treatment was measured at EFDA-JET in the same manner as performed for prototype tiles and preliminary experimental work (Section 4.1.1). The measurement results (Table 5.2) indicated the surface was locally smoother than the design specified (nominal value  $1.6\mu\text{m}$ ). The effect of the change in surface roughness on the measurement systems was difficult to quantify however, some preliminary work was performed on the effect of surface roughness on triangulation laser scanner systems (Section 4.4.5), with results indicating the surface was measurable by the systems under test. The smoother surface

## Primary Equipment Trial

resulted in increased specular reflection with an increase in random error within the measurement data, caused by a worsening of the signal to noise ratio. Specular reflection also increased the likelihood of sensor saturation, resulting in the collection of no data in areas of the sensor. To avoid sensor saturation, positioning of the light source and sensor with respect to the surface was critical. Both increased random error and sensor saturation are demonstrated during the Approach Angle test, where the measurement surface was at a critical angle to the light source or sensor (Section 5.4.1).

The measurement artefacts presented a smoother surface than Beryllium tiles and posed a greater challenge to the measurement systems due to increased random error and specular reflection. Data from these tests can be used as an indicator of performance for a non-ideal surface, with improved performance expected for the real Beryllium tiles.

Gap Artefact	$0.78 \pm 0.02\mu\text{m}$
Step Artefact	$0.75 \pm 0.02\mu\text{m}$
Angle B Artefact	$0.82 \pm 0.02\mu\text{m}$

**Table 5.2: Mean surface roughness (Ra) of artefacts following surface treatment.**

### 5.2.2. *Equipment Tested*

Based on previous experimental work (Section 4), the two technologies trialled were white light fringe projection and laser line triangulation. Two implementations of each technology were tested, all being state-of-the art commercially available systems at the time of the trial (2009). As agreed with the suppliers of the equipment, the measurement systems used in this trial will remain anonymous however, representative specifications are provided (Table 5.3, Table 5.4) but it should be noted the lack of a common evaluation method prevents the table being complete.

The white light fringe projection technologies were an implementation of ‘Light Projection: Bundle of Rays’, utilising coded light and phase shift. These systems are referred to as Fringe Projection System/Area Based A & B throughout this work. The systems were both high-end measurement tools designed for engineering metrology with twin sensor units and single projector. Both were calibrated for a measurement volume approximately defined by the area of a large mounting plate (275 x 350mm) simulating the intersection of two tile assemblies. The calibrated volume was selected to maximise data quality and be representative of real use at EFDA-JET.

For these measurement systems, where the total measurement volume was greater than the sensor measurement volume, self-localisation was used e.g. retro-reflective targets,

## Primary Equipment Trial

as it was not possible to obtain an implementation of a white light projection system using external tracking e.g. laser or optical tracker. At time of trial such technologies were not commercially available. .

The two laser line triangulation systems (A & B) were hybrid systems (Section 3.2.5) which featured a hand held measurement head which produced a laser line on the measurement surface capable of dynamic intensity adjustment. The 6DoF positioning/tracking was provided by non-contact optical method (photogrammetric) or laser tracker, the tracking solution defined the measurement volume and positioning accuracy within that volume. Laser line system A was used to measure the artefacts attached to the large volume test frame (Section 5.2.1.5.3) which required the measurement head to move through a greater volume in comparison to the second system which during measurement required movement through a smaller volume.

A phase-based polar measurement system was also used to measure the artefacts although results are not presented in this work as this class of measurement device was found to be unsatisfactory for detailed measurement in preliminary trials (Section 4.4.4). The device tested during this trial demonstrated similar errors to those identified during the preliminary trials.

	Number of Sensors	Sensor Pixel Count (millions)	Measurement Volume (mm <sup>2</sup> )	Depth Resolution
Area Based A	2	6	Max: 950	2μm
Area Based B	2	4	Max: 2000	-

**Table 5.3: Equipment Specifications – Fringe Projection Measurement Systems**

	Measurement Distance	Sensor Depth of Field (mm)	Accuracy (mm)	Sphere Accuracy (Typical) <sup>6</sup>
Laser Line A	~1.5m – 9m Hemi-Spherical Volume	75	-	~50μm
Laser Line B	~1.5 – 6m Pyramidal Volume (~20m <sup>3</sup> )	100	0.023	~60μm

**Table 5.4: Equipment Specifications – Laser Line Measurement Systems**

<sup>6</sup> The value of residuals to a best fit sphere, at 1σ.

### **5.2.3. Tests Performed**

#### **5.2.3.1. Approach Angle**

The approach angle test described in this work utilised Angle Artefact B (Section 5.2.1.2) to satisfy the research objective (Section 1.4), as follows:

- Determine how the angle of measurement system to the measurement surface affects the quality of the collected data. To take into account: random, systematic and angular error.

When measuring a non-planar surface, the angle and direction of surface to a measurement device changes, with likely impact on data quality. By understanding how the angle between measurement system and surface affects data, a measurement strategy which maximised high quality data could be planned. Given that different measurement technologies and devices feature different configurations of light source and sensor, testing was required on a range of devices.

For EFDA-JET, information from this test could be used to optimise the positioning of measurement equipment with respect to the measurement surface. The objective was to collect data over as large an area as possible whilst maintaining a minimum level of data quality in order to minimise the duration of data collection.

Work on the impact of measurement system to surface angle has been performed by Feng et al. (2001) and Van Gestel et al. (2009) for CMM laser line measurement systems, Kühmstedt et al. (2009a) for modelling of phasogrammetry systems, but no experimental work on linear fringe projection systems based on projecting a bundle of rays. Feng et al. (2001) and Van Gestel et al. (2009) used a laser line triangulation device mounted to a CMM to measure a planar surface, with the measurement head at a range of angles. This method was not appropriate for this research as equipment tested were not CMM mounted; instead it was the angle of the surface, rather than the angle of the measurement device which needed to change. This was achieved through the use of Angle Artefact B which provided a series of angled surfaces and enabled data at various angles to be collected in a single session, minimising data collection time. However, the design of Angle Artefact B could have introduced additional challenges for the measurement systems on trial as the angle of the surface with respect to the measurement device could have limited complete measurement of the artefact and the shape of the artefact could have introduce changes in visibility for each facet for optical

systems with multiple components e.g. projection system with one projector and two cameras. The distance of the surface to the measurement device would change with each facet for projection systems set at a fixed distance with possible effect on data quality. The effect of distance to the measurement surface would be affected by the illumination type, causing possible divergence/convergence and increased/decreased definition of the illumination on the measurement surface.

The information required from these tests was as follows:

- Random Error: Determine whether there is an increase in uncertainty in data as the angle between measurement system and surface normal increases by evaluating the RMS of residuals to a least squares best fit plane through data.
- Systematic Error: A qualitative assessment of the distribution of residuals of data for each angled facet.
- Angular Error: An assessment of the angular error of data, as the angle between measurement system and surface normal increases.

The calculation of angular error for EFDA-JET was important as the 6DoF of tile components had to be calculated and could be required if a portion of the tile were to be damaged. In this case, data in the affected area would require exclusion from registration, and orientation of the tile would require estimation from minimal information in the unaffected areas. Any angular error present in the data used for registration could adversely impact the registration. For the measurement systems tested, the angle between the central reference plane and the other angled facets were computed and compared against the as-built values computed from touch-probe CMM data. This form of analysis of the angular error of the surface had not been seen in other published work.

Section 5.2.3.1 details the data collection and processing methods which were used to execute the tests described.

#### **5.2.3.2. Depth of Field**

The depth of field test utilised Angle Artefact A (Section 5.2.1.1) to satisfy the research objective (Section 1.4), as follows:

- Determine how the measurement system to surface distance affects the quality of collected data.

Within the EFDA-JET machine, metrology systems were to be positioned by remote handling equipment and therefore an understanding of the precision with which metrology systems would require positioning with respect to the surface was required. One aspect of the positioning was the distance of the sensor to the measurement surface and whether the distance affected the quality of the collected data. Where data quality varies within the calibrated depth of field, the positioning of equipment would become more important, if data quality remained relatively constant throughout the working volume less precision in positioning the equipment would be required. This information is relevant to any measurement scenario where accuracy and high precision are required, as by understanding the effect of distance, a measurement strategy to optimise collection of high quality data could be designed.

Work has been performed to investigate the impact of range on laser line triangulation systems: Feng et al. (2001), Van Gestel et al. (2009), however results for fringe projection systems were not available. The research presented in this work contributes to existing knowledge by providing a technique to collect and process data for fringe projection technologies (Section 5.3.3.3) and presents results for two state of the art commercial systems (Section 5.4.2).

### **5.2.3.3. Edge Measurement**

Edge measurement testing utilised the Step Artefact (Section 5.2.1.3) to satisfy the research objective (Section 1.4), as follows:

- Assess the impact of ‘edge effects’ (Section 3.2.4) on collected data through the development of a method to identify data between planar regions affected by edge effects. Quantify the extent (from the theoretical ‘sharp edge’) of affected data.

The ability to measure and quantify the dimensions of an edge required the ability to differentiate between the surrounding surfaces and was therefore linked to the level of random and systematic error in the collected data. For measurement of an edge, the errors were supplemented by: the edge profile and radius, material and optical properties of the surface. Where the edge could not be measured, understanding the extent of this region would enable the rejection of un-reliable data, whilst maximising

the region which could be measured. A number of device orientations with respect to the edge were tested to determine the optimal orientation for data collection.

Within EFDA-JET to verify installation of tile assemblies, the radial difference (step height/flush) between surfaces required measurement (Section 2.4.2). Difference in tile position was ~1mm and therefore measurement data with an order of magnitude lower uncertainty (0.1mm) was required. At a smaller level, within the centre section of a tile assembly the smallest radial difference (step height/flush) between castellated parts was nominally 0.040mm, resulting in data of 0.004mm accuracy required. At this level, components were manufactured from a single piece and any change in the flush of the surfaces could have indicated erosion of, or deposition onto the surface. Prior to this research, quantifying such a change was performed using a small touch probe device once the tile had been removed from the machine. The level of accuracy required was in the range of that produced by a touch probe CMM and outside the manufacturer specifications for optical devices trialled. However, the performance of the systems to detect the various step height differences was tested, to understand current state of the art performance.

For the purposes of this test a technique was developed to measure the step (flush) and gap between surfaces from point cloud data, as no standard systems existed for this measurement and it was not covered by the VD/VDE 2634 guidelines or any other work found as part of this research.

The data collection and processing method is defined in Section 5.3.3.4 and results presented in Section 5.4.3.

#### **5.2.3.4. Gap Detection**

Gap detection testing utilised the Gap Artefact (Section 5.2.1.3) to satisfy the research objective (Section 1.4), as follows:

- Gap Detection - For the measurement of sub-millimetre step/gap features, recommend a workflow to minimise errors in the collected data.

As an extension to Edge Measurement, there was an interest in detecting discontinuities in surfaces. Unlike specific gauging tools, the measurement systems under test were not designed for step and gap measurement however, any measurement system could have had the capability to perform measurement of gap dimensions and therefore testing was

performed to determine whether the measurement systems could detect inter-tile gaps of ~3mm and intra-tile gaps of 0.35-0.6mm (Section 2.4) within point cloud data. The dimension of gaps tested was specific to EFDA-JET but the method would be applicable to a gap of any dimension.

The data collection and processing method is defined in Section 5.3.3.5 and results presented in Section 5.4.4.

#### **5.2.3.5. Registration**

Registration tests utilised information and techniques from the Edge measurement tests to quantify the impact of edge data on surface based registration and satisfies the research objective (Section 1.4), as follows:

- Registration – develop a technique that can reliably register data from multiple scans by automatically rejecting data that is predicted to be of indeterminate quality due to physical limitations in the capture process. A key example are edge effects (Section 3.2.4) where data are degraded by increased noise and systematic error and must be removed for accurate and reliable ‘surface based’ registration methods.

Observed edge effects across the different measurement systems demonstrate the presence of unreliable data within 0.5 – 2mm of an edge (Section 6.1.2.3). These ‘unreliable’ data include those impacted by ‘edge effects’, where the recorded data were not a true representation of the measured surface. As a result, data within 2mm of an edge were withheld from the surface-based registration process (Section 3.3.2) performed within a commercial software package<sup>7</sup>.

The method developed for this work combines the rejection technique developed for edge detection, with surface based registration from a commercial software package to assess the validity of the assertion that edge data could affect registration. The presence of an edge was detected by performing an initial registration to the as-built model, or reference model and then utilising the edge detection method detailed in Section 5.3.3.4 to identify data likely to be impacted by edge effects. Comparison of the residuals, normal to the surface of several regions known to be unaffected by edge effects, was performed from a registration using all data and a registration excluding unreliable data.

---

<sup>7</sup> The registration process sought to minimise the distance (residuals) between points and the as-built model, normal to the surface.

A template process is presented, where alternative rejection criteria could be utilised e.g. surface normal angle, to tailor to different applications, but given the form of EFDA-JET tiles, the method developed for edge measurement in this research was implemented.

#### **5.2.3.6. Large Volume**

Large volume testing utilised all of the developed artefacts attached to a large volume frame to satisfy the research objective (Section 1.4), as follows:

- Large Volume – practical artefacts contain highly detailed local surfaces and need to be portable to test equipment on and off site. This work designs and implements a method to support the accurate placement of individual artefacts within a larger volume in order to test system capabilities that require registration, tiling of views and use of 6DoF tracking for example.

A large volume trial was required to simulate measurement in an EFDA-JET representative volume, to determine how increasing the ‘total measuring volume’ as defined by VDI/VDE 2634 Part 3 (The Association of German Engineers (VDI), 2008) would affect data quality. The VDI/VDE 2634 Part 3 guidelines were applicable to this measurement case as it covered multiple view systems where total measuring volume is greater than the ‘sensor measuring volume’ however, they were not compatible with the surface finish required for this project, as the VDI/VDE guideline required a diffusely scattering surface (lambertian reflector) which was not representative of that required for EFDA-JET. The effect of alignment of multiple views through markets/targets or the surface geometry was included within the assessed error.

Additionally, although the VDI/VDE 2634 guidelines (The Association of German Engineers (VDI), 2008) were the most applicable for the measurement systems under test, it was not possible to perform all tests defined in the guidelines. Design of the test frame occurred before the 2634 part 3 guidelines were published in English (December 2008) and so artefacts developed for this research do not include features required for VDI/VDE tests. The probing error (Form and Size) tests were followed however it is noted that in a deviation to the guidelines, the spheres did not have calibration certificates (Section 5.4.6.1). The length measurement quality parameter was followed in spirit by measuring lengths within the volume, but a single ball bar was not used (Section 5.4.6.2). The large volume test frame and datum clusters did not meet the

### Primary Equipment Trial

requirements for full adherence to the part 3 guidelines but the quality parameters provided a starting point to analyse the data.

The data collection and processing method is defined in Section 5.3.3.7, with results presented in Section 5.4.6.

### **5.3.Experiment Execution**

Sections 5.1 and 5.2 described the purpose of the six tests, with this section detailing the test setup and execution. Details of the environment for measurement are provided (Section 5.3.2) followed by common steps applicable to all experiments (Section 5.3.3.1) and detailed information for the setup, execution and processing of data, related to specific tests (Section 5.3.3.2 - 5.3.3.7).

#### **5.3.1. Operator**

User introduced error could have been best minimised through mechanical handling e.g. motion/rotation state, as a mechanical method would have been capable of high repeatability of motion. However, given the measurement technologies considered and the differences in their methods of measurement i.e. area based and line triangulation, no single handling method would have been suitable for all. To reduce complexity of the trial, skilled human operators were used to perform the measurements. No operator was available who was suitably skilled in the use of all measurement systems, therefore it was necessary for each company to operate their own equipment. To minimise the effect of different users, standard data collection techniques were followed by the operators (Section 5.3.3.2 -5.3.3.7). By taking this approach the user introduced uncertainty was reduced as far as possible without complex mechanical handling.

#### **5.3.2. Environment**

To reduce uncertainty introduced by changes in the environment e.g. temperature and humidity, a controlled environment was required. Such an environment was not available at EFDA-JET so measurements were performed in a metrology laboratory at the UK National Physical Laboratory (NPL), with air temperature control of  $20^{\circ}\pm 0.1^{\circ}\text{C}$ .

It was originally planned to locate the large volume test frame with test artefacts attached inside NPL however, the dimensions of the frame prevented this. The frame remained at EFDA-JET with a laser line triangulation system performing measurement of artefacts whilst attached to the frame with temperature monitored during measurement. The second laser line triangulation system measured the test artefacts at the manufacturer headquarters in a controlled environment, necessitated by the availability of equipment. The two white light fringe projection systems measured the test artefacts within the NPL laboratory.

## Primary Equipment Trial

Fringe Projection System A: Measurements performed at NPL.

Fringe Projection System B: Measurements performed at NPL.

Laser Line Triangulation System A: Measurements performed at EFDA-JET with artefacts attached to large volume test frame. Total temperature change from start of measurement to end: 2.5°C. This temperature change is across a time of ~5 hours with measurement of actual artefacts performed towards the end of the trial. It is recognised length measurements between artefacts are susceptible to error because of the temperature change however individual artefacts took minutes to measure and therefore would not be susceptible to significant temperature/dimensional change during that time.

Laser Line Triangulation System B: Measurements performed at system supplier in controlled environment. Test artefacts measured individually within limited volume. Total temperature change during data collection: 0.1°C.

The use of different measurement environments was not optimal however as equipment and operators were provided cost-free, some adjustments had to be made to the planned trial. To minimise the effect of change in environment, artefacts were allowed to acclimatise to the ambient temperature and monitored throughout measurement with a surface probe (Model: RS206-3722). Scaling of data was performed in order that final data from each system was equivalent to measurement at 20°C. Temperature scaling was performed within the software package PolyWorks Inspector prior to any processing.

### **5.3.3. Test Operation**

Sections 5.2.3.1 - 5.2.3.6 describe the tests performed, with each having specific steps for collection and subsequent processing of data (Sections 5.3.3.1 - 5.3.3.7), with a number of steps common to all tests (Section 5.3.3.1).

### 5.3.3.1. Common Setup/Processing Steps

Prior to measurement:

- Artefact attached to the portable mounting plate/large volume frame, using the slot and hole on the underside of the artefact. Secured using the 2 bolts provided.
- Portable mounting plate (and attached artefact) positioned on a flat stable base and clamped to the surface (if possible).
- Artefact and mounting plate allowed to acclimatise to the ambient temperature for 12 hours.
- Using a thermometer with surface probe, the temperature of the artefact prior to and during measurement was recorded.
- The surface was lightly cleaned with alcohol wipe(s) and allowed to dry.
- No surface preparation was permitted e.g. spray to reduce reflection.
- The manufacturer recommended setup procedure for equipment was followed e.g. acclimatise to the measurement environment, position on a stable base.
- Measurement equipment was calibrated/verified prior to measurement (if possible).
- The calibrated measurement area for Area Based measurement systems was set to 275mm x 350mm: this approximated the area of a large mounting plate which simulated the intersection of two tile assemblies. The calibrated volume was selected to maximise data quality and be representative of real use at EFDA-JET.
- Where possible the spheres on the portable test frame were captured using the measurement device.
- Data filtering and interpolation processes were disabled.

Following measurement:

- Data were exported in manufacturer native file format and as American Standard Code for Information Interchange (ASCII) file format text file. The ASCII format presented the data in human readable text as a triplet of floating point numbers to represent the Cartesian coordinate of each recorded position, a second triplet containing surface normal vector information were included if calculated.
- If the artefact was not maintained at 20°C during data measurement, the data were scaled to account for the deviation from the specified temperature (20°C). Scaling was performed in commercial software package PolyWorks Inspector (Innovmetric, 2010).
- The artefact was returned to the transport/storage case.

Visual Basic for Applications (VBA) macro programs were created by the author to automate processing using Microsoft Excel and used in addition to PolyWorks to process data. Scripting and VBA programs automated the processing tasks to avoid human error and ensured all processing was performed the same for each data set.

**5.3.3.2. Approach Angle**

Approach Angle Test Data Collection

The Approach Angle test required two sets of data to be collected for each measurement system tested, the difference between tests being the orientation of the measurement device to the artefact surface. The orientation of the measurement device to the surface simulated approaching a surface from various directions and how this could have affected the quality of the data collected (Figure 5.9).

In Figure 5.9 a measurement system is represented by a red laser line for clarity, although the same angular approach is valid for other measurement technologies e.g. white light fringe projection. In Figure 5.9 ‘a’ and ‘c’ simulate approaching a vertical surface from above and below respectively, referred to as ‘out-of-plane’, with ‘b’ and ‘d’ simulating approaching the same surface from the side at an angle: ‘in-plane’. Figure 5.10 demonstrates the principle of the in-plane and out-of-plane approach tests, where the difference is the orientation of the measurement device to the surface.

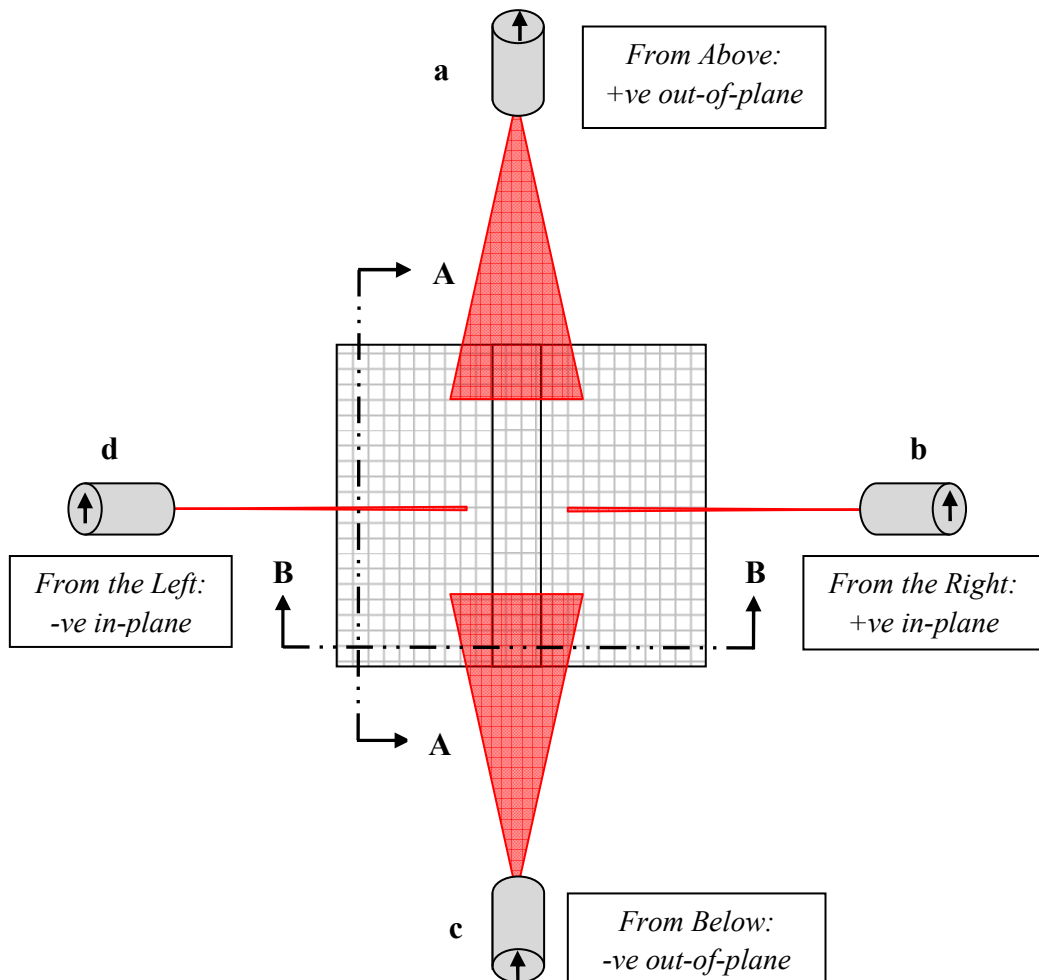


**Figure 5.9: One surface measurement device, collecting dimensional measurement from four positions/directions (a, b, c, d)**

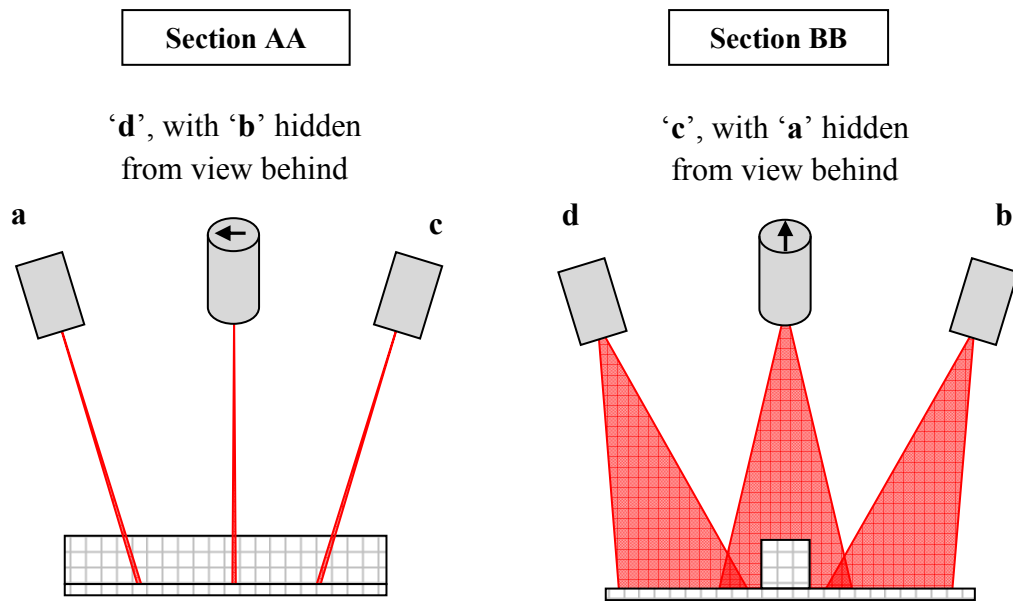


Figure 5.10: With reference to Figure 5.9:

**Section AA - Simulating approaching a surface from above/below (Out-Of-Plane angle).**

**Section BB - Simulating approaching a surface from left/right (In-Plane angle).**

It was necessary to define two data collection techniques, to account for the measurement principles of different equipment. One technique was for area based measurement systems e.g. white light fringe projection (light projection: bundle of rays) and one for laser line triangulation devices. The distinction was necessary as the area based measurement systems were capable of collecting data over the whole artefact surface from a single position, whereas laser line triangulation devices had to traverse the surface, collecting a series of profiles. For each collection technique, two orientations were required to account for the four approach directions (Figure 5.9 & Figure 5.10).

Orientation 1: In-Plane

Orientation 1 (IP) - Area Based Measurement Systems      Figure 5.11      p.167

Orientation 1 (IP) – Laser Line Triangulation Systems      Figure 5.12      p.168

Orientation 2: Out-of-Plane

Orientation 2 (OOP) - Area Based Measurement Systems      Figure 5.13      p.169

Orientation 2 (OOP) - Laser Line Triangulation Systems      Figure 5.14      p.170

5.3.3.2.1. *Approach Angle Test - Orientation 1 (IP) - Area Based Measurement Systems*

Figure 5.11 demonstrates the collection of the first set of data for an area based measurement system. Following completion of the common steps (Section 5.3.3.1), the measurement system was positioned directly above Artefact B, with measurement direction towards the artefact surface (along the surface normal of the artefact base). The orientation of the measurement device was dependent on the orientation of the projected pattern to the measurement surface, with the correct orientation being as shown in Figure 5.11.

The device was positioned at such a distance that the angled faces of the artefact were within the calibrated depth of field of the device. Room lighting was turned off and the intensity of the device illumination adjusted for the measurement surface.

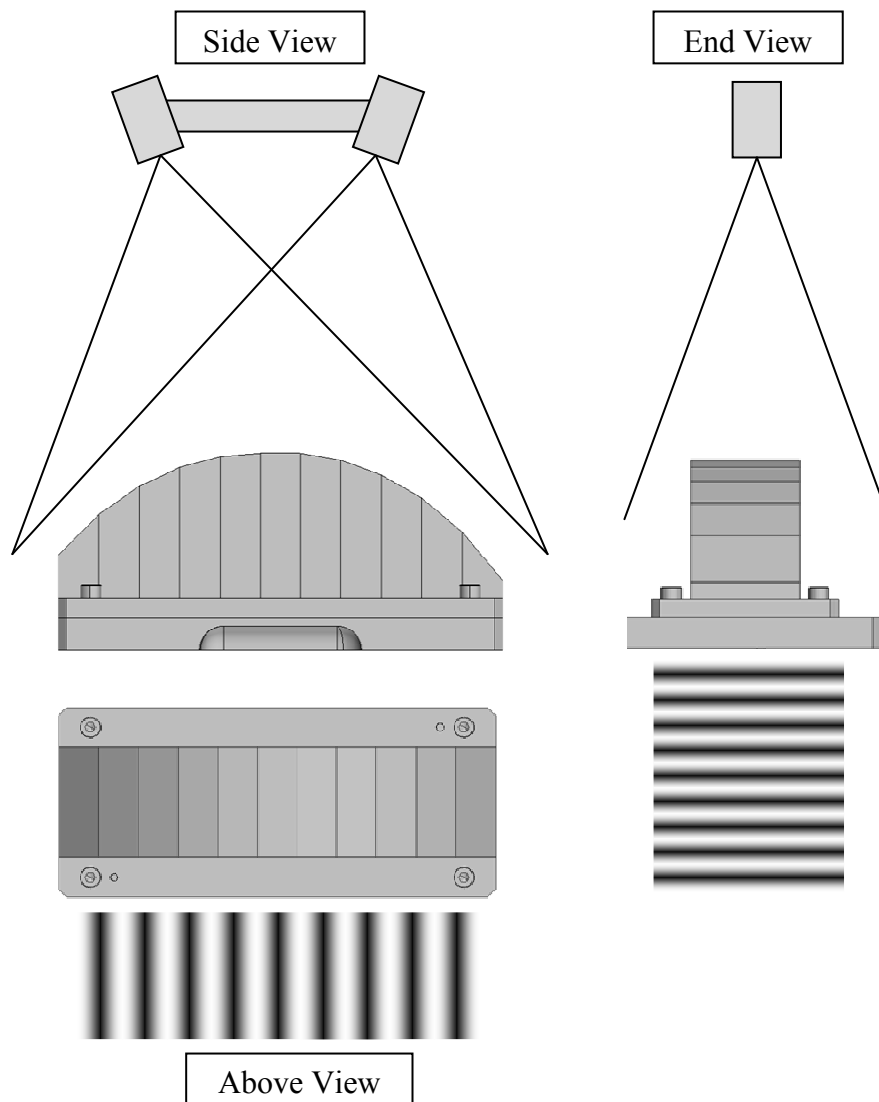


**Figure 5.11: Approach Angle Test - Orientation 1 - For Area Based Measurement Technologies e.g. White Light Fringe Projection.**

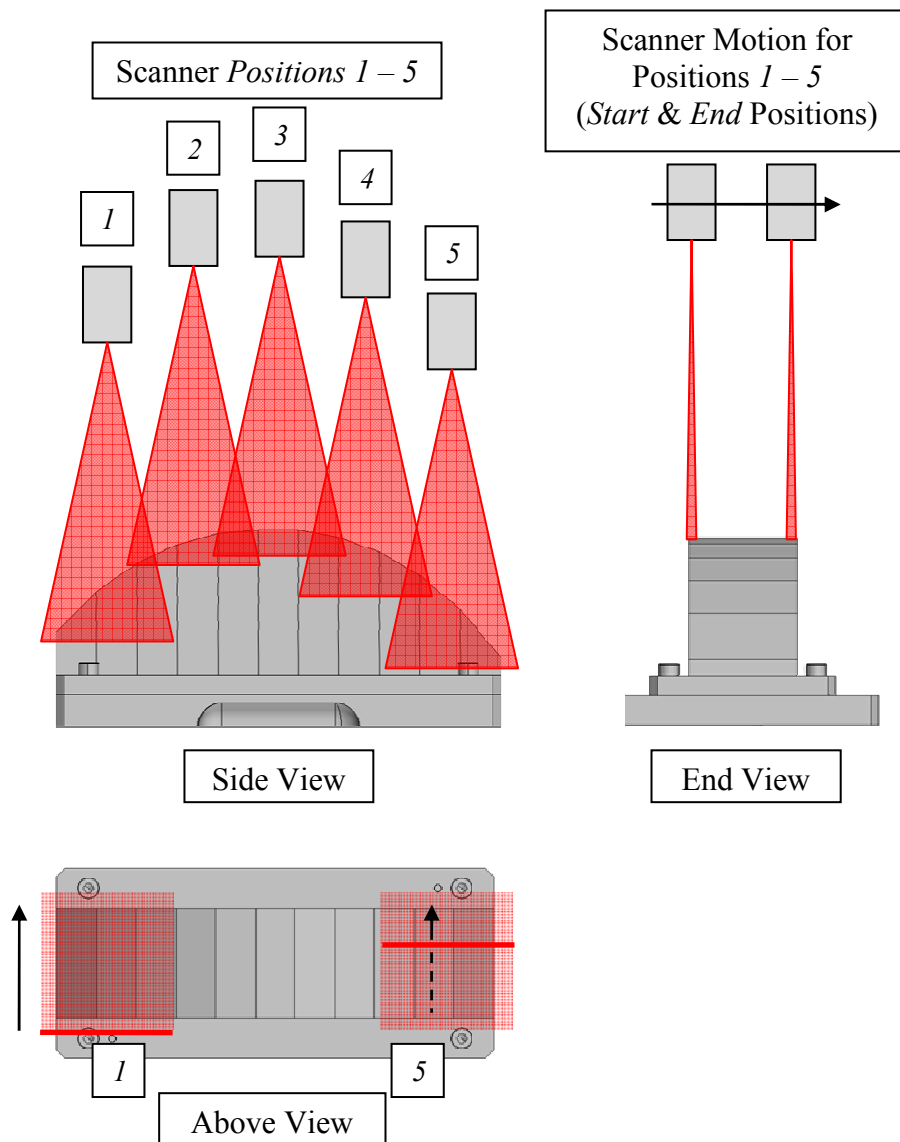
**5.3.3.2.2. Approach Angle Test - Orientation 1 (IP) – Laser Line Triangulation Systems**

Figure 5.12 demonstrates the collection of the first set of data for measurement systems which could not measure the complete surface from a single position e.g. laser line triangulation. Following completion of the common steps (Section 5.3.3.1), the device was positioned above Angle Artefact B, perpendicular to the flat base.

Dynamic adjustment of laser intensity was permitted during measurement but data filtering and interpolation were disabled.

To measure the complete surface, the laser line was required to traverse the surface, with the number of positions defined by the laser line length (in this orientation). The measurement device was positioned in such that any surface measured was within the calibrated measurement volume and this distance maintained throughout measurement.

In *position 1*, the device was moved from the start to end position so the projected line traversed the surface and captured the surface of one or more angled facets. The device was then repositioned in *position 2 start* position, with an overlap of data between *position 1 and position 2*. While capturing data, the device was moved slowly over the surface to the *end* position, at which point the device was repositioned (to *position 3*) and the measurement process repeated. Figure 5.12 shows 5 measurement positions and ‘scans’ of the surface to capture the complete surface.



**Figure 5.12: Approach Angle Test - Orientation 1 - For Laser Line Triangulation Technologies.**

**5.3.3.2.3. Approach Angle Test - Orientation 2 (OOP) - Area Based Measurement Systems**

Figure 5.13 demonstrates the collection of the second set of data for an area based measurement system. Following completion of the common steps (Section 5.3.3.1), the measurement system was positioned directly above Artefact B, with measurement direction towards the artefact surface (along the surface normal of the artefact base). The orientation of the measurement device was dependent on the orientation of the projected pattern to the measurement surface, with the correct orientation being as shown in Figure 5.13. In comparison to Approach Angle Test – Orientation 1 (IP), the orientation of the projected pattern was at 90° to that of the first test. The device was positioned at such a distance that the angled faces of the artefact were within the

calibrated depth of field of the device. Room lighting was turned off and the intensity of the device illumination adjusted for the measurement surface.

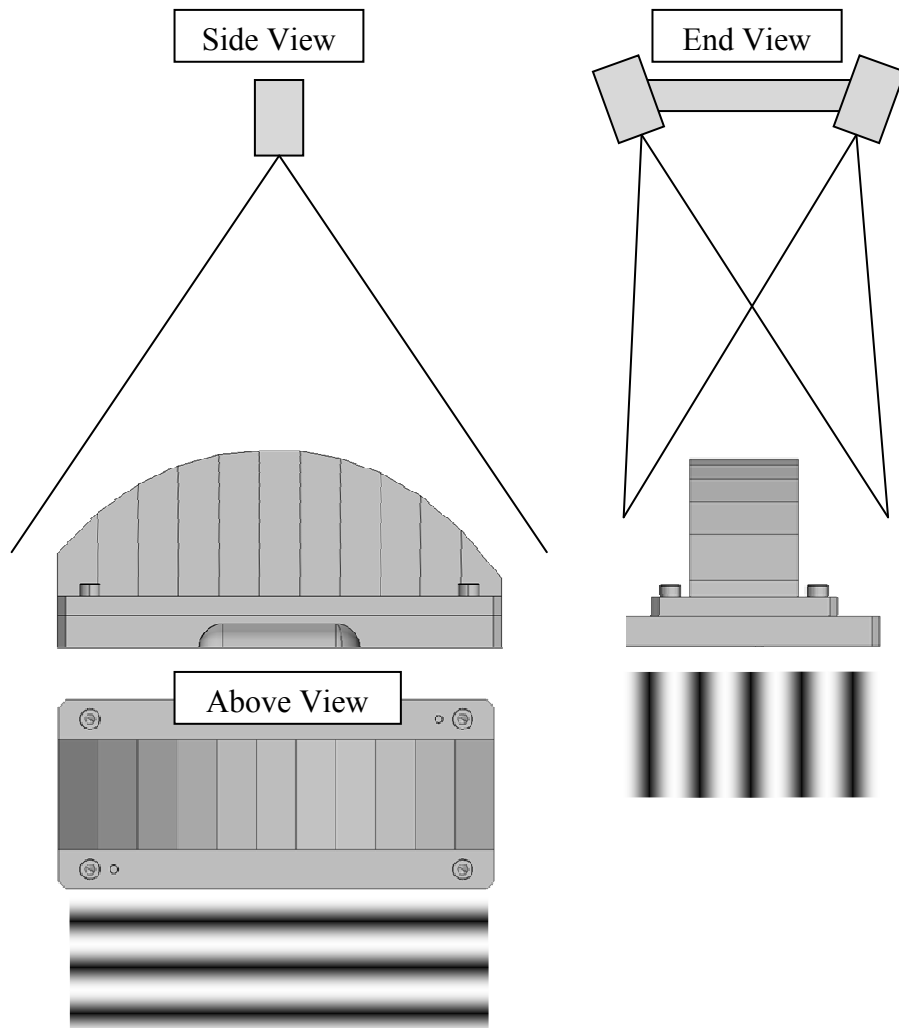


**Figure 5.13: Approach Angle Test - Orientation 2 - For Area Based Measurement Technologies e.g. White Light Fringe Projection.**

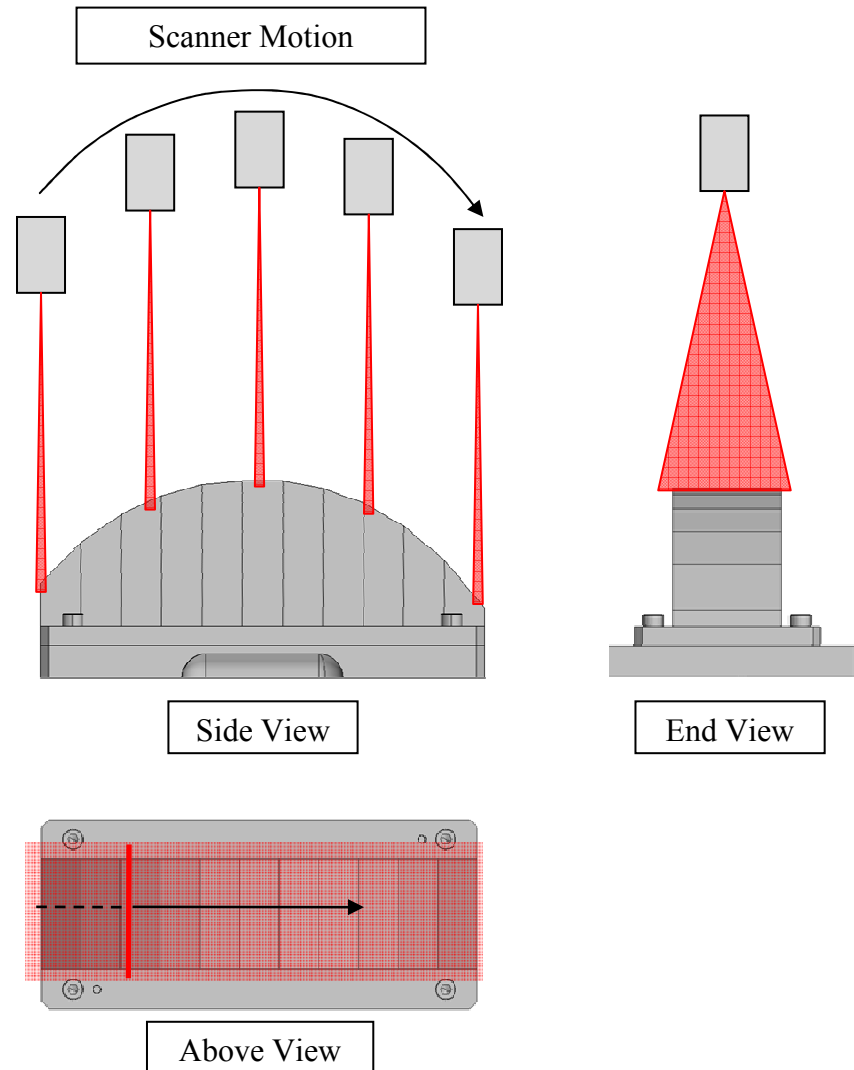
**5.3.3.2.4. Approach Angle Test - Orientation 2 (OOP) - Laser Line Triangulation Systems**

Figure 5.14 demonstrates the collection of the second set of data for measurement systems which cannot measure the complete surface from a single position e.g. laser line triangulation. Following completion of the common steps (Section 5.3.3.1), the device was positioned above Angle Artefact B, perpendicular to the flat base.

Dynamic adjustment of laser intensity was permitted during measurement but data filtering and interpolation were disabled.

## Primary Equipment Trial

To measure the complete surface, the laser line was required to traverse the surface in one continuous movement along the surface. The distance between device and surface remained approximately constant, following the shape of the artefact and within the calibrated depth of field.



**Figure 5.14: Approach Angle Test - Orientation 2 - For Laser Line Triangulation Technologies.**

### Approach Angle Test Data Processing

The Approach Angle test was comprised of a number of sub-tests, where each provided information on a particular aspect of Approach Angle. The sub-tests used the data collected, with two data sets per measurement system. Each data set underwent the same processing, as follows:

i. Data Coverage & Quality

To assess data coverage the collected data were registered to an as-built digital model of the artefact using touch probe data collected by CMM at the National Physical Laboratory (Section 5.2.1). Experimental work performed in the first year of research (Section 4.4.4) demonstrated the existence of ‘edge effects’ and therefore registration to the as-built model was performed using all data, excluding those within 2mm of the edges of the planar surfaces. The registration processed minimised the residual of data points, normal to the CAD surface, seeking to minimise the Root Mean Square (RMS) of all residuals. The RMS of residuals normal to the surface provided an indication of the ‘fit’ of data to the model, a smaller RMS value indicating the data more closely match the CAD model.

Following registration, the residual of data were mapped against the as-built model, creating a colour plot of the residual for each data point collected. This error map indicated where data were present and the residual of that data to the model.

ii. Measurement System Angle to Surface Normal

Data for each of the facets of the Angle Artefact B were extracted and data within 2mm of an edge removed. The remaining data for each facet was used to calculate a least squares best fit plane through the data (one plane per facet per data set). The root mean square (RMS) of the residuals for each plane were calculated and used as an indication of the local error for the given surface angle.

iii. Angular Error

Using a commercial software package, the angle between the central reference plane of the artefact at  $0^\circ$  (parallel to artefact base) and each surrounding facet was calculated. To reduce error, the angle was calculated in a single axis, which passes through each angled facet. To assist the calculation, a plane was fitted along this axis (Figure 5.15). The angle calculation was firstly performed for the as-built CAD model, constructed from the touch probe CMM data and these angles used as the as-built value to compare against.

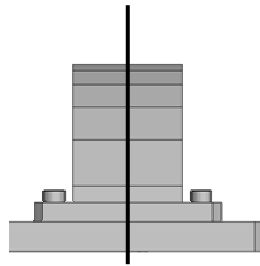


**Figure 5.15: End view of Angle Artefact B, showing a plane intersecting each angled facet to enable calculation of facet angle along a single axis.**

The same angle calculation was performed for each data set collected, measuring the angle between the planes in that data set. Once the angles were calculated, the as-built value was subtracted, leaving the angular discrepancy for each plane in each data set. Due to the calculation method the  $0^\circ$  facet (the central facet) had zero error for each system. Positive error indicated the facet was calculated as steeper than the as-built data, a negative error indicated the facet was recorded with a reduced angle to the reference plane.

### **5.3.3.3. Depth of Field**

#### Depth of Field Test Data Collection

The Depth of Field test used a single data set for each measurement device on test, with the collection technique dependent on the principle of the measurement system e.g. area based measurement systems or laser line triangulation devices.

#### Depth of Field Test - Area Based Measurement Systems

Following completion of the common steps (Section 5.3.3.1), the measurement device was positioned above Angle Artefact A, perpendicular to the flat base. The orientation of the measurement device was dependent on the orientation of the projected pattern to the measurement surface, with the correct orientation being as shown in Figure 5.16. The device was positioned at such a distance that the mid-point of the 30° angled block was at the mid-point of the calibrated depth of field of the device; the distance from measurement system to artefact base was recorded<sup>8</sup>. Room lighting was turned off and the intensity of the device illumination adjusted for the measurement surface.

---

<sup>8</sup> The distance was not recorded during the experiments detailed in this thesis but should be recorded for any future experiments/tests,

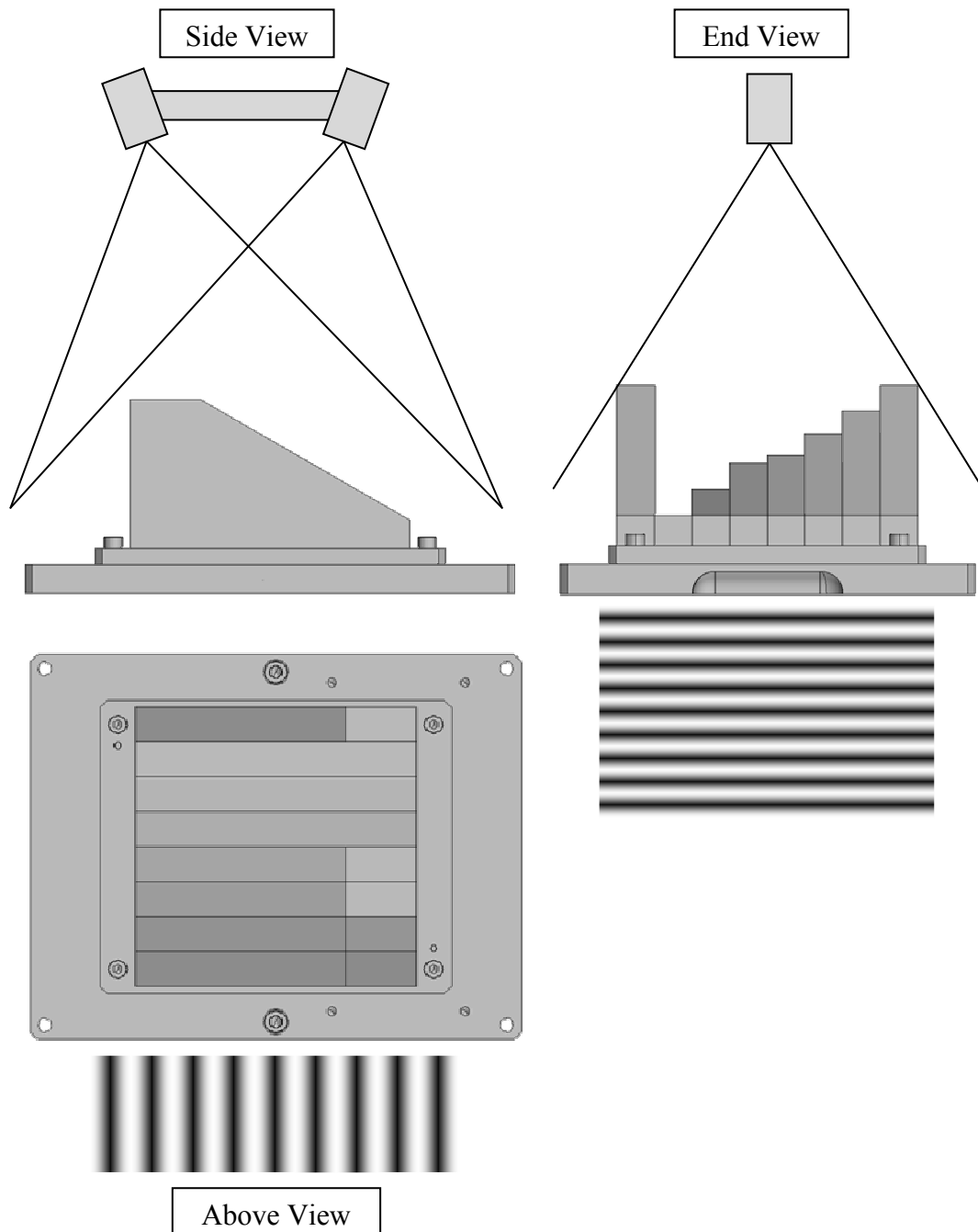


**Figure 5.16: Depth of Field Test - For Area Based Measurement Technologies e.g. White Light Fringe Projection.**

Depth of Field Test - Laser Line Triangulation Systems

Figure 5.17 demonstrates the collection of data from a measurement system which cannot capture the whole object surface from a single position e.g. laser line triangulation. Following completion of the common steps (Section 5.3.3.1), the device was positioned above Angle Artefact A, perpendicular to the flat base. Dynamic adjustment of laser intensity was permitted during measurement but data filtering and interpolation were disabled.

## Primary Equipment Trial

To measure the complete surface, the laser line was required to traverse the surface, taking measurements of each of the angled facets. One continuous scan was collected across the artefact, covering each facet whilst maintaining a constant distance from the artefact base.

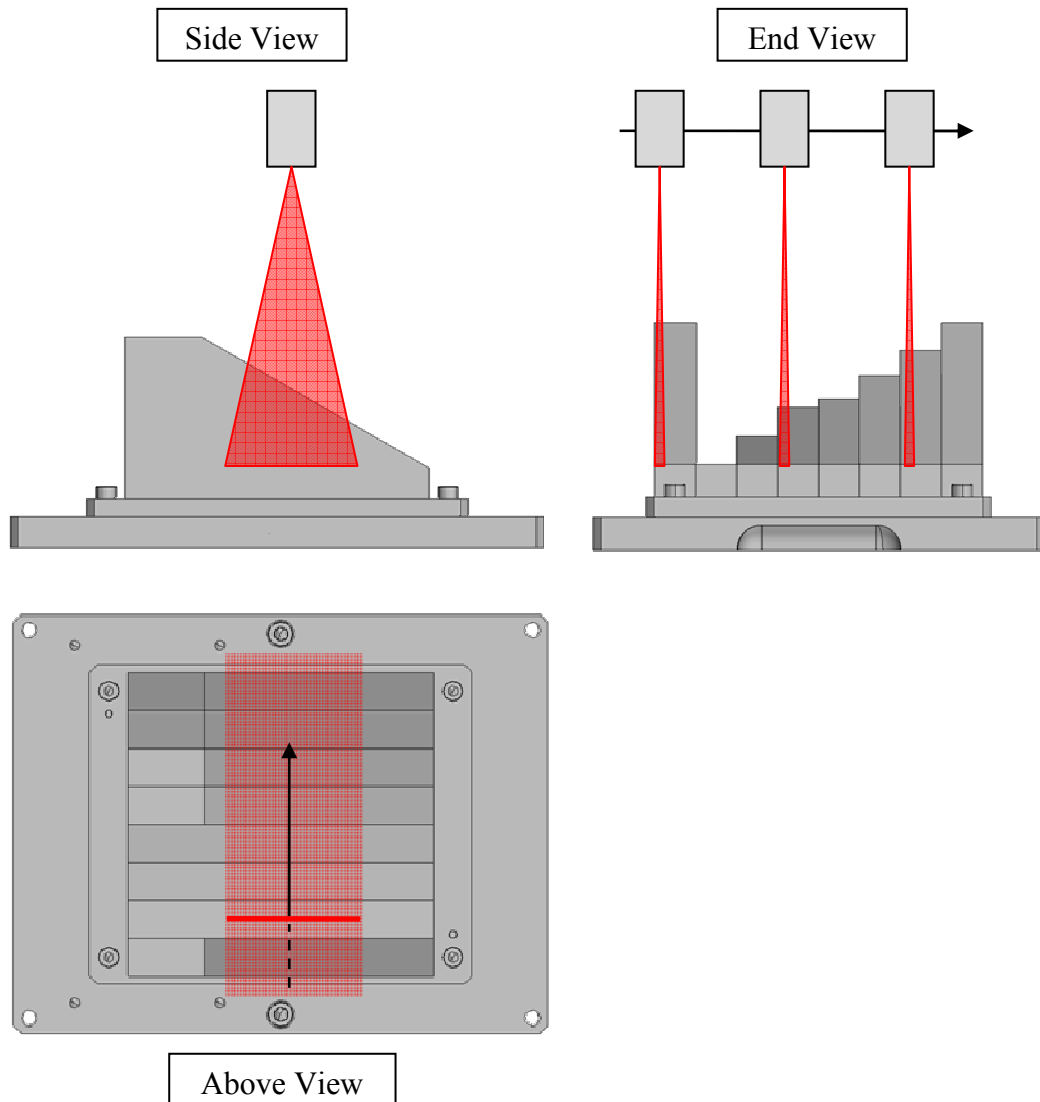


**Figure 5.17: Depth of Field Test - For Laser Line Triangulation Technologies.**

### Depth of Field Test Data Processing

Registration to the as-built CAD model was not required for this test however data were registered to a coordinate system where the large base plane defined an XY plane with a position of 0 on the Z axis. Once the datum system was defined, points within 2mm of an edge on the 30° block were removed (to remove data affected by edge effects.)

## Primary Equipment Trial

The remaining data on the  $30^\circ$  facet were segmented into 6 groups (labelled: A-F) based on their Z coordinate, grouping the data based on their distance to the artefact base and therefore the surface to sensor distance. For the  $30^\circ$  facet and 6 groups, the height (in Z) of each group was 12.5mm (Figure 5.18). Segmentation was performed using Microsoft Excel, evaluating the Z component of the coordinate against a minimum and maximum Z value for each of the 6 groups.

For each group of data created, a least squares best fit plane was created and the residuals of those data to the plane calculated. The root mean square (RMS) of the residuals were reported as an assessment of the random error within the data at the given measurement range.

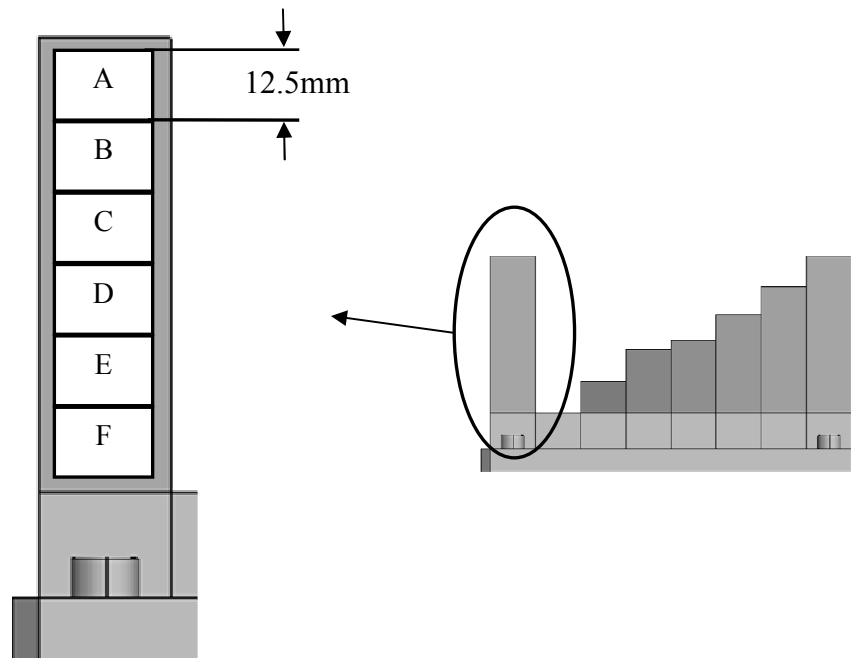


**Figure 5.18: Segmenting data for Depth of Field test**

#### **5.3.3.4. Edge Measurement**

##### Edge Measurement Data Collection

The edge measurement test required the collection of three data sets per measurement device tested, where the orientation of the device to the measurement surface was varied. It was necessary to define two data collection techniques, to account for the measurement principles of different equipment. One technique was for area based measurement systems e.g. white light fringe projection (light projection: bundle of rays) and one for laser line triangulation devices. The distinction is necessary as the area based measurement systems were capable of collecting data over the whole artefact surface from a single position, whereas laser line triangulation devices were required to traverse over the surface, collecting a series of profiles. For each collection technique, three orientations were required which altered the orientation of fringe pattern or laser line on the surface.

##### Edge Measurement Test - Area Based Measurement Systems

Following completion of the common steps (Section 5.3.3.1), the measurement device was positioned above the Step Artefact, perpendicular to the flat base. The device was positioned at such a distance that top faces of the artefact were within the calibrated depth of field of the device. Room lighting was turned off and the intensity of the device illumination adjusted for the measurement surface.

Three sets of data were collected, with a rotation of the measurement device performed between each measurement set (Figure 5.19).

- Position 1: fringes of the projected pattern parallel to the step edges between blocks.
- Position 2: fringes of the projected pattern at 45° to the step edges between blocks.
- Position 3: fringes perpendicular to the step edges between blocks.

A single set of data were collected for each device position, with each being stored in a separate file, labelled according to the test, device name and orientation.

## Primary Equipment Trial

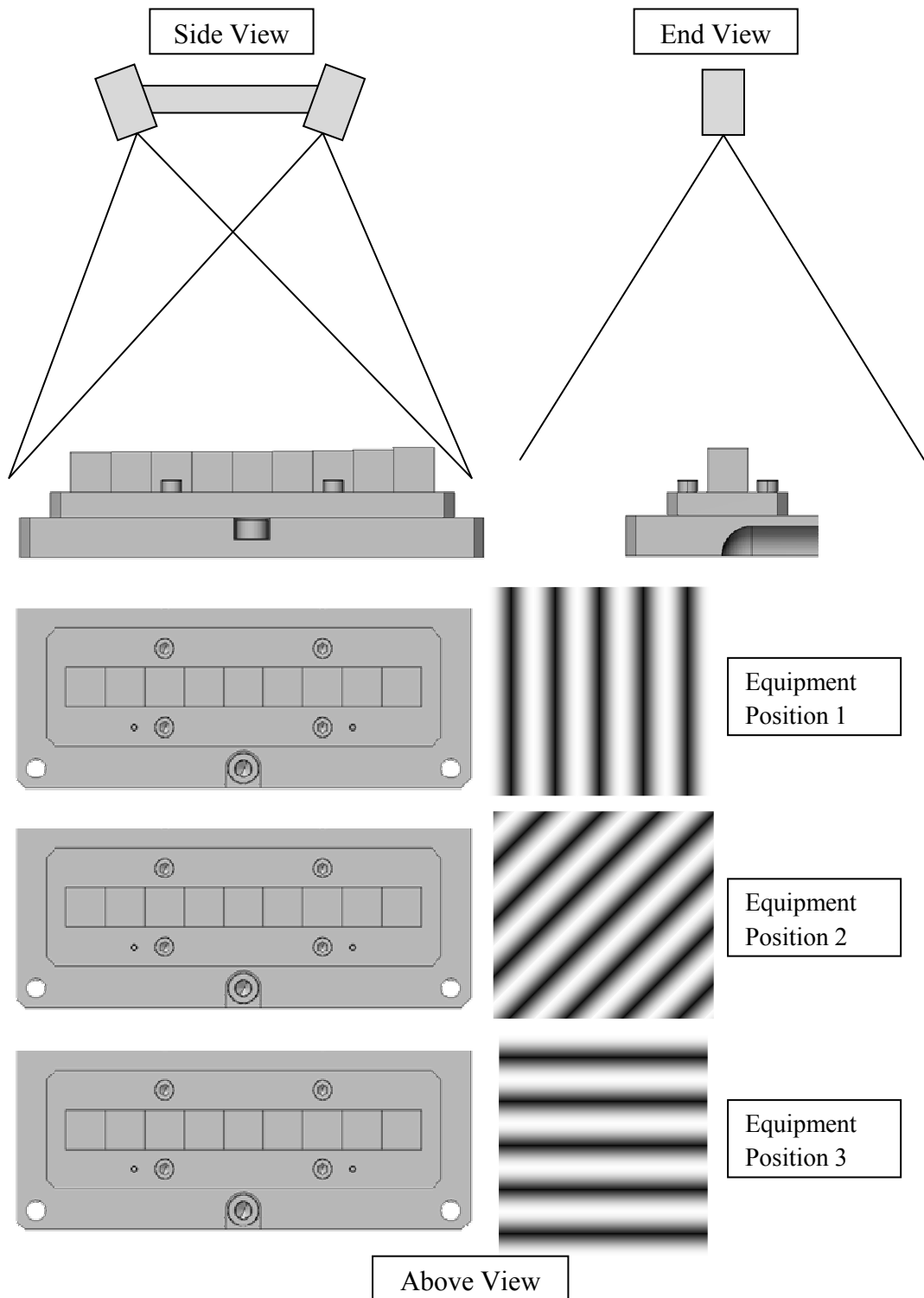


**Figure 5.19: Edge Measurement Test - For Area Based Measurement Technologies e.g. White Light Fringe Projection. One set of data collected per Equipment Position.**

### Edge Measurement Test - Laser Line Triangulation Systems

Figure 5.20 demonstrates the collection of data from a measurement system which cannot capture the whole object surface from a single position e.g. laser line triangulation. Following completion of the common steps (Section 5.3.3.1), the device

### Primary Equipment Trial

was positioned above the Step Artefact, perpendicular to the flat base. Dynamic adjustment of laser intensity was permitted during measurement but data filtering and interpolation were disabled.

Three sets of data were collected, with a rotation of the measurement device performed between each measurement set (Figure 5.20).

- Position 1: projected laser line parallel to the step edges between blocks.
- Position 2: projected laser line at 45° to the step edges between blocks.
- Position 3: projected laser line perpendicular to the step edges between blocks. In this orientation, multiple individual scans were required to capture the complete surface.

A single set of data were collected for each device position, with each being stored in a separate file, labelled according to the test, device name and orientation.

## Primary Equipment Trial

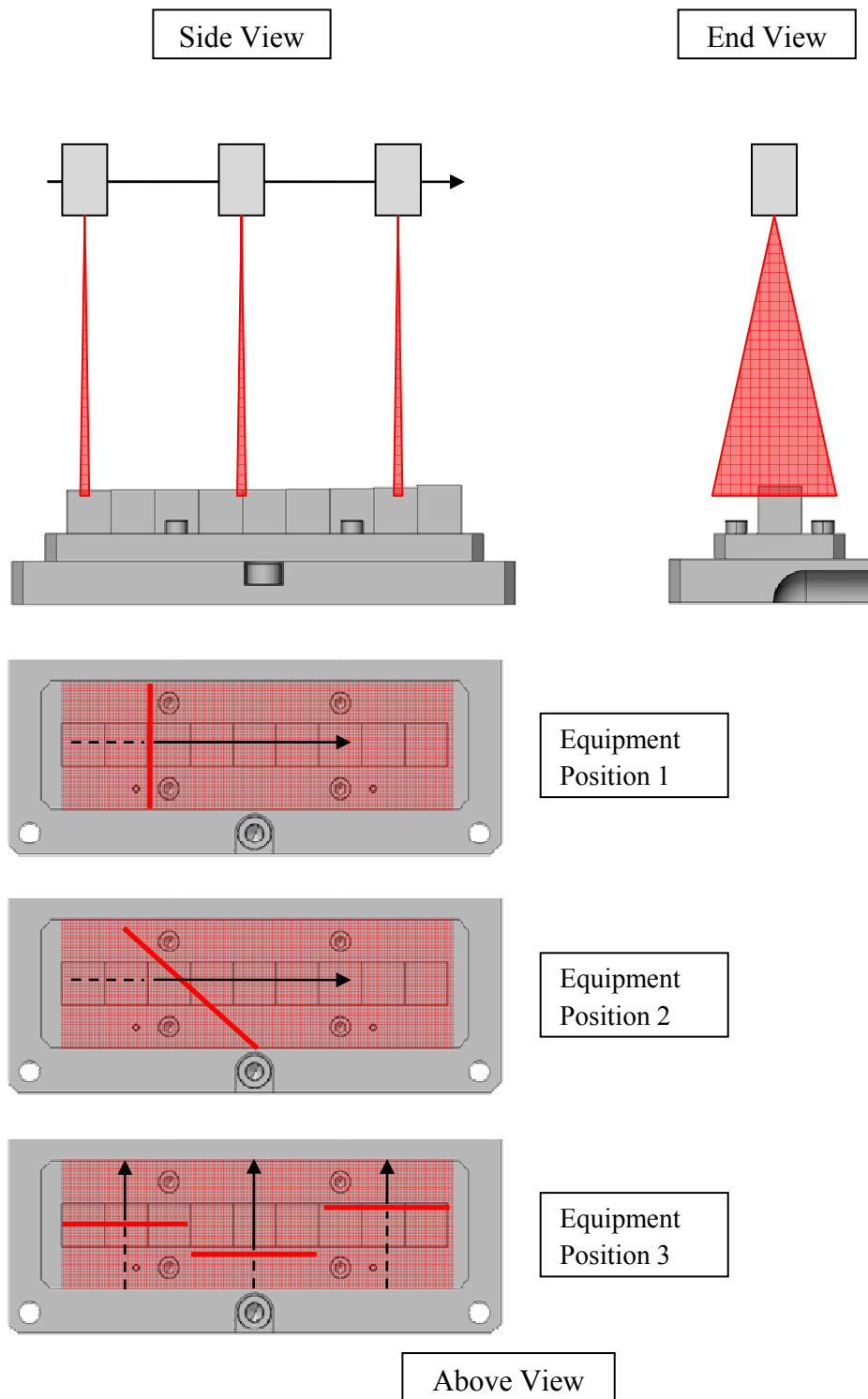


**Figure 5.20: Edge Measurement Test - For Laser Line Triangulation Technologies. One set of data collected per Equipment Position.**

### Edge Measurement Data Processing

Data were registered to the as-built CAD model, using the mounting plate holes for coarse registration and fine registration achieved by least squares best fit of data from

the top faces of the steps, excluding data within 2mm of an edge, minimising the residual of points normal to the surface.

i. Random error

Data within 4mm normal to each surface were isolated (excluding data within 2mm of an edge) and for each area, a least squares best fit plane has been fitted and the RMS and Standard Deviation of the residuals calculated.

ii. Step Height

For each data set, distance measurements were taken from the artefact mounting plate base to the least squares best fit planes created for the facet on each block. Using these distances, the distance between adjacent planes (normal to the base plate) were calculated.

Processing was performed for one data set per measurement system. The Area Based measurement systems (white light fringe projection) used a set collected in a method optimal for that system, selected by the operator. The laser line system results utilised data sets where the projected laser line was parallel to the step edge. For all systems data within 2mm of an edge were excluded from the test.

iii. Quantitative Edge Measurement

All data sets were registered to the as-built CAD model of the Step Artefact using a least-squares surface fitting algorithm within a commercial software package. Accurate registration to CAD was not required, simplified the extraction of relevant data.

For each data set, data on the central areas of the planar facets of the Step Artefact were extracted, excluding data within 2mm of an edge. Extraction was performed using the as-built CAD to identify data points within a boundary on each facet; however extraction could have been performed through manual selection. A least squares best fit plane was fitted through each area of data representing a facet surface, with the RMS residual and standard deviation of the residuals recorded.

For each data set, previously discarded data were re-introduced and the residual (normal to the plane) of each data point to the closest best fit plane calculated. Data were categorised dependent on the magnitude of their residual with respect to the standard deviation of the best fit plane. The determination of where a planar surface ended and a

## Primary Equipment Trial

surface discontinuity began was based on how many standard deviations their residual was from the mean plane. Data were coloured to clearly identify grouping: green data were within  $\pm 1$  standard deviation of the plane; amber/orange points were within  $\pm 3$  and; red points were within  $\pm 4$  standard deviations of the best fit plane mean. Grey data were above  $\pm 4$  standard deviations the fitted planar surface.

### a. Immeasurable Region

Calculation of the distance (perpendicular to the surface normal) between planes utilised the data processing already performed i.e. a strong registration in the z axis, the residual of all points to their closest best fit plane calculated.

In this test, measurement along a single axis to determine distance between planes was not possible as any rotation error on the perpendicular axis would introduce error into the measurement result, increasing the calculated distance.

To overcome imperfect registration a method was developed which relied only on a strong registration of data in the Z axis (horizontal planes on the top of the step blocks). With the edge between surfaces approximately parallel to the Y axis, data within  $\pm 3$  standard deviations of a plane were segmented dependent on their Y coordinate into a number of intervals (Figure 5.21a).

Primary Equipment Trial

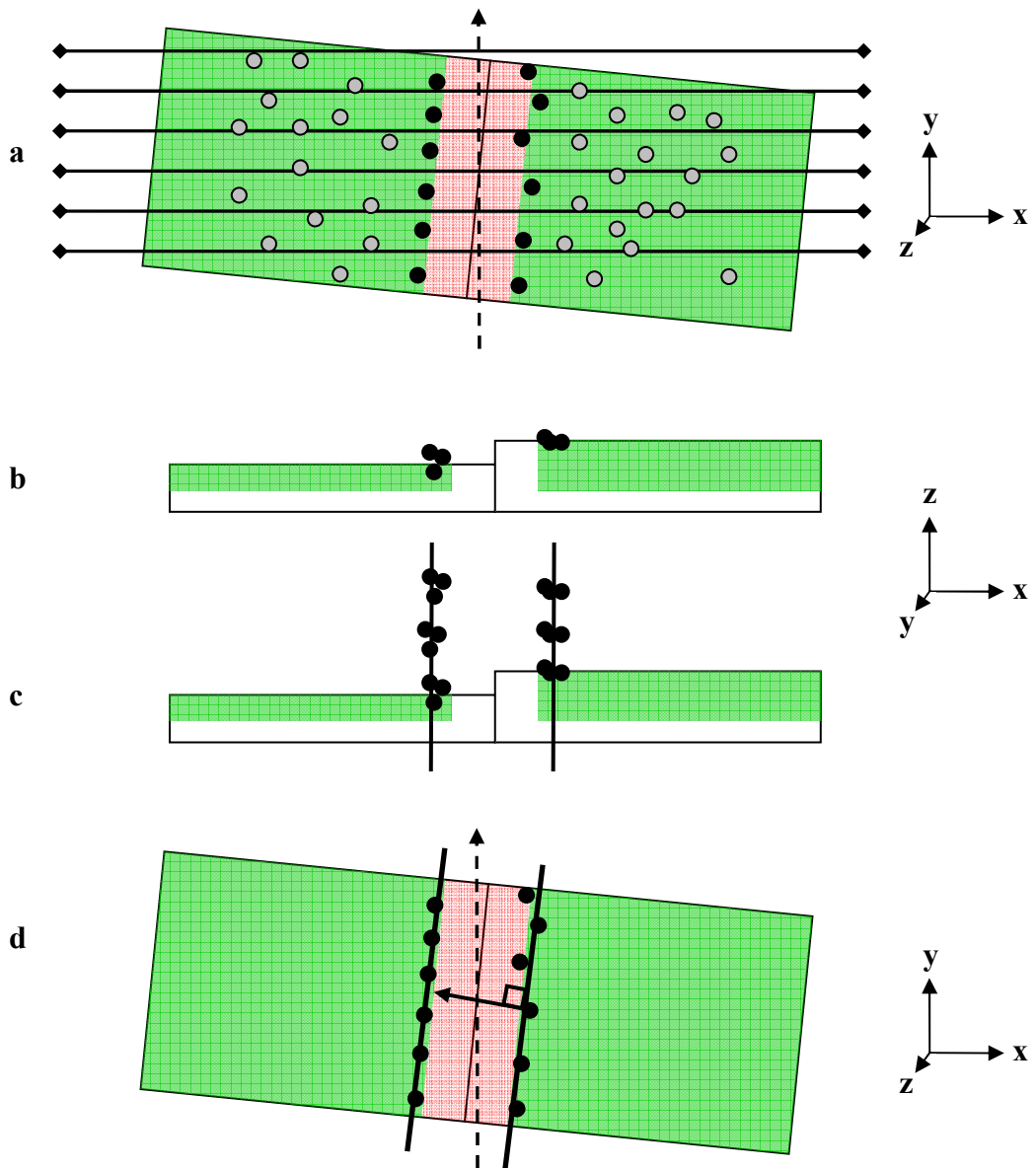


**Figure 5.21: Quantifying the immeasurable region**

For each interval, data with the smallest and largest X coordinates were identified as edge points (Figure 5.21a – solid black points). Because of strong registration along the Z axis, the edge points could be replicated with increased Z coordinate (Figure 5.21b) and used to construct a best fit plane, approximately along the YZ axis (Figure 5.21c).

The distance of edge points from one plane to an adjacent plane were calculated to the best fit plane with distance reported normal to the surface. For two adjacent planes, the horizontal distance could be calculated twice as two sets of edge points and two best fit vertical planes were created.

### **5.3.3.5. Gap Detection**

#### Gap Detection Data Collection

The gap detection test required the collection of three data sets per measurement device tested, where the orientation of the device to the measurement surface was varied. It was necessary to define two data collection techniques, to account for the measurement principles of different equipment: one technique was for area based measurement systems e.g. white light fringe projection (light projection: bundle of rays) and one for laser line triangulation devices. The distinction was necessary as the area based measurement systems were capable of collecting data over the whole artefact surface from a single position, whereas laser line triangulation devices were required to traverse the surface, collecting a series of profiles. For each collection technique, three orientations were utilised and are described below.

The dimensions of the gap artefact manufactured were verified by CMM however, the dimensions of the slots could not be verified by this device (Section 5.2.1.6). A GapGun laser gauge (Section 3.2.4.2) was used to measure the six slots at three locations per slot with sixteen measurements per position, these data were used as the as-built dimensions of the slots against which the measurement systems were assessed. For each measurement the GapGun collected eight JPEG images and performed flush and gap calculation from these (Figure 5.69).

#### Gap Detection Test - Area Based Measurement Systems

Following completion of the common steps (Section 5.3.3.1), the measurement device was positioned above the Gap Artefact, perpendicular to the flat base. The device was positioned at such a distance that top faces of the artefact were within the calibrated depth of field of the device. Room lighting was turned off and the intensity of the device illumination adjusted for the measurement surface.

Three sets of data were collected, with a rotation of the measurement device performed between each measurement set (Figure 5.22).

- Position 1: fringes of the projected pattern parallel to the slots between blocks.
- Position 2: fringes of the projected pattern at 45° to the slots between blocks.
- Position 3: fringes were perpendicular to the slots between blocks.

## Primary Equipment Trial

A single set of data were collected for each device position, with each being stored in a separate file, labelled according to the test, device name and orientation.

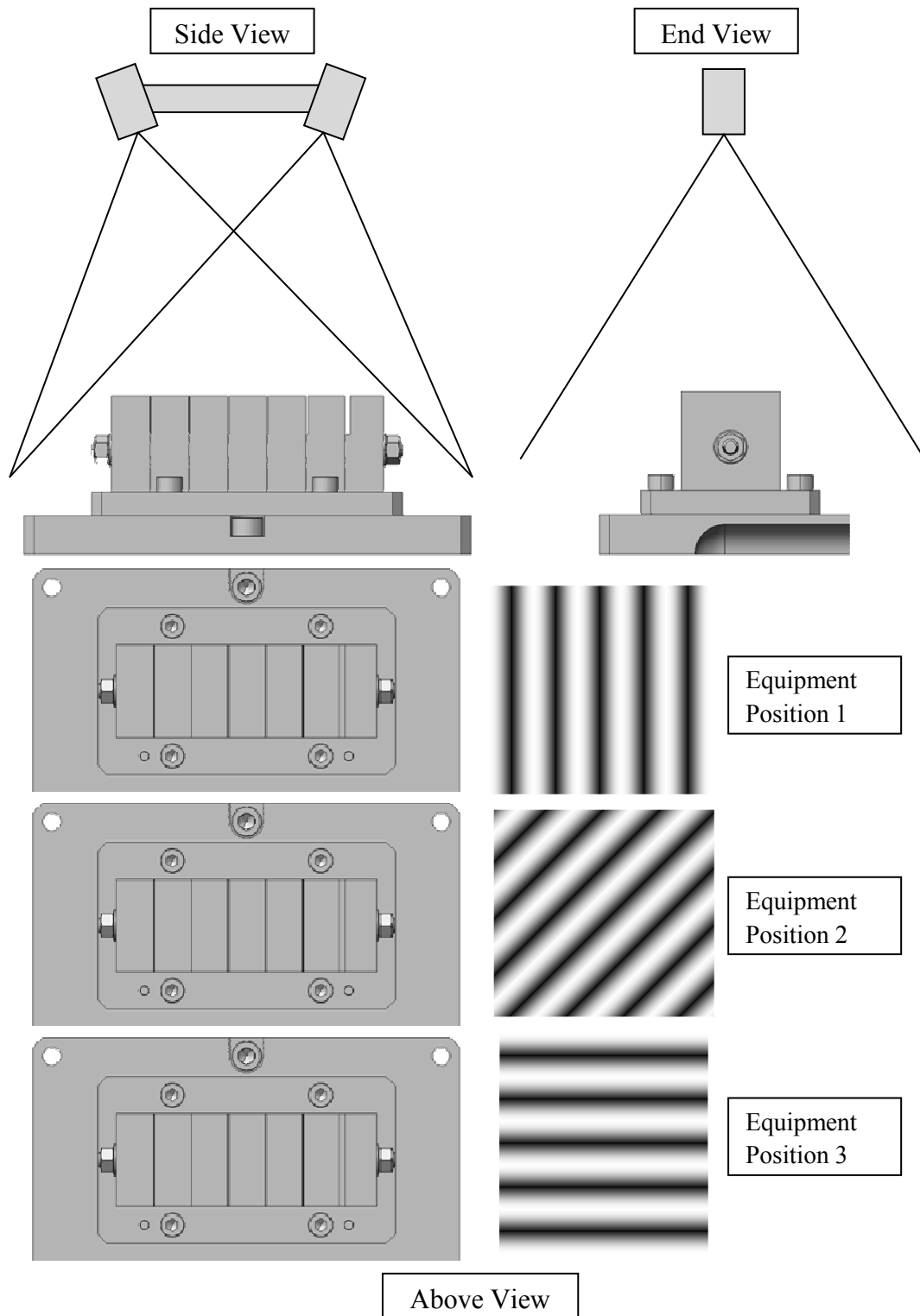


**Figure 5.22: Gap Detection Test - For Area Based Measurement Technologies e.g. White Light Fringe Projection. One set of data collected per Equipment Position.**

Gap Detection Test - Laser Line Triangulation Systems

Figure 5.23 demonstrates the collection of data from a measurement system which cannot capture the whole object surface from a single position e.g. laser line triangulation. Following completion of the common steps (Section 5.3.3.1), the device was positioned above the Step Artefact, perpendicular to the flat base. Dynamic adjustment of laser intensity was permitted during measurement but data filtering and interpolation were disabled.

Three sets of data were collected, with a rotation of the measurement device performed between each measurement set (Figure 5.23).

- Position 1: projected laser line parallel to the slot between blocks.
- Position 2: projected laser line at 45° to the slot between blocks.
- Position 3: projected laser line perpendicular to the slot between blocks. In this orientation, multiple individual scans were required to capture the complete surface.

A single set of data were collected for each device position, with each being stored in a separate file, labelled according to the test, device name and orientation.

Primary Equipment Trial

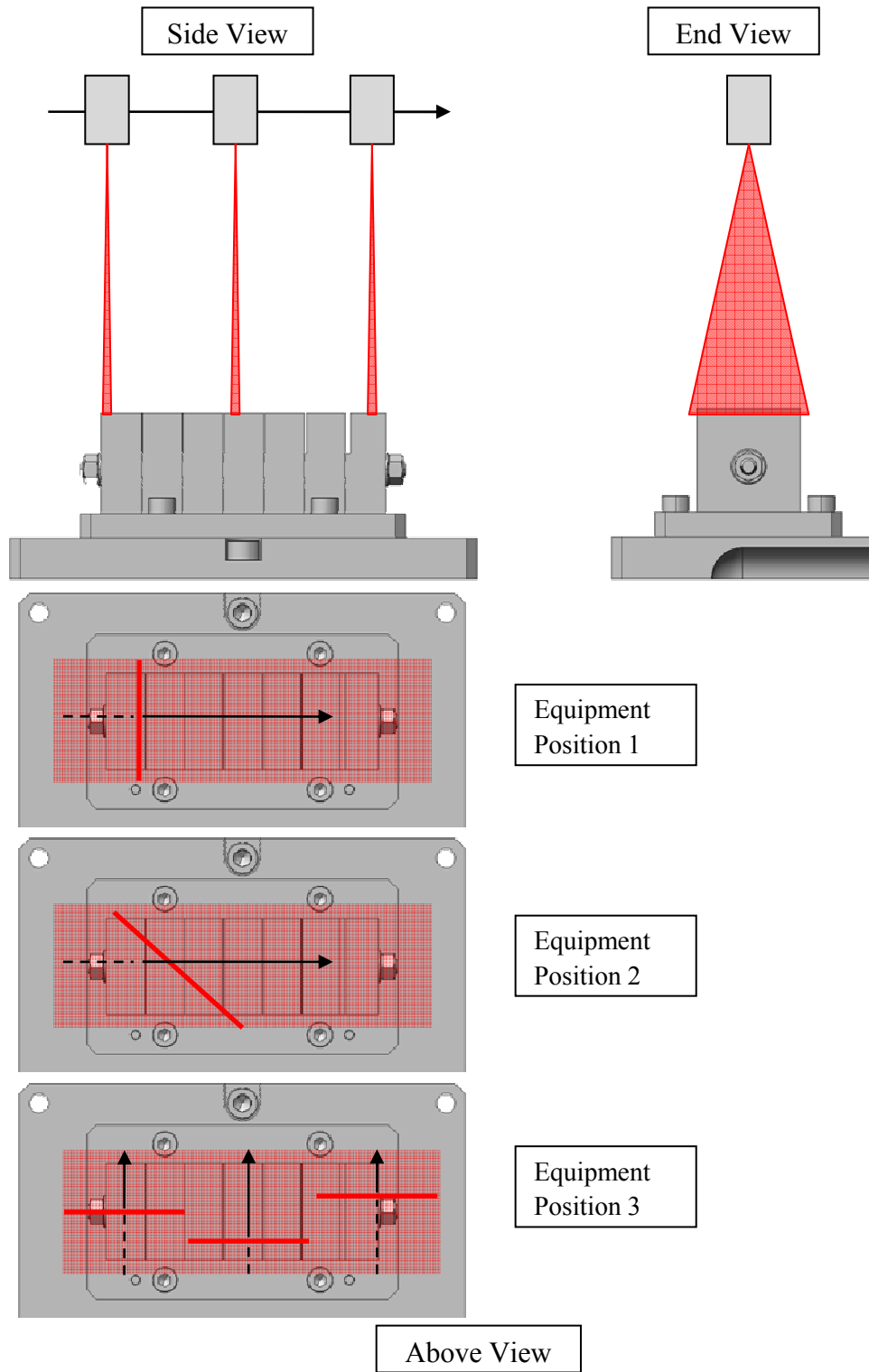


**Figure 5.23: Gap Detection Test - For Laser Line Triangulation Technologies. One set of data collected per Equipment Position.**

Gap Detection Data Processing

i. Qualitative Assessment

Registration of data to the nominal CAD model was based on minimising the root mean square distance of all data, normal to the model surface, using an iterative approach. Data within 2mm of an edge were excluded from the registration process as these data are known to include edge errors however, the effect was a lack of constraint in the data which would result in poor registration. To improve the registration, data on the artefact base and step artefact were included in the registration process. Assessment of measurement data was relative as uncertainty in registration to CAD prevented data being presented in a common coordinate system.

Using the commercial software package PolyWorks Inspector (Innovmetric, 2010), a profile view of the 3mm slot and data were captured and exported for each measurement system to allow qualitative evaluation.

ii. Minimum Resolvable Gap

Using data on the top planar surfaces of the Gap Artefact (excluding data within 2mm of an edge) a best fit least squares plane was constructed. The residuals of all data points normal to this plane were calculated and these points categorised based on the magnitude of their residual in comparison to the standard deviation of the residuals of points used to create the plane.

Data were coloured to clearly identify grouping: green data were within  $\pm 1$  standard deviation of the plane; amber/orange points were within  $\pm 3$  and; red points were within  $\pm 4$  standard deviations of the best fit plane mean. Grey data were above  $\pm 4$  standard deviations the fitted planar surface. Profile images of the slots were collected, using  $< 2$ mm slice through the data. Multiple profile images were produced per slot and data set; as a single profile would not have provided sufficient detail as to whether erroneous data affected the complete slot or only part.

**5.3.3.6. Registration**

The collection of new data was not required for the registration test, instead using data collected for the Edge Measurement test (Section 5.3.3.4) of the Step artefact.

The data were processed according to Section 5.3.3.4, iii. Quantitative Edge Measurement (page 182), where the residual of each data point to the nearest planar area was calculated.

- a. The complete data set was used for an initial registration to the as-built CAD, reporting the residuals of all points with a residual value of  $\leq 2$  standard deviations from a planar region.
- b. Data points identified as  $>2$  standard deviations from a planar region were deleted from the set and a second surface based registration performed.
- c. Residuals of points remaining were reported and a comparison made against those reported in Step a.

### 5.3.3.7. Large Volume

#### Large Volume Data Collection

The Artefacts (Section 5.2.1) were designed to fit on a large volume frame (~3m x 2m) whose dimensions reflected a portion of the real EFDA-JET machine. Each artefact was manufactured with a blind hole and slot on the underside of the mounting plate which interfaced with dowels protruding from known positions (interface plates) on the large volume frame. The artefacts were positioned on the frame in known positions and secured using two bolts, tightened to bring the machined faces of the mounting plate (artefact side) and interface plate (frame side) into contact.



**Figure 5.24: Large volume measurement test frame with datum clusters at the corners and artefacts attached, metre length included**

Once artefacts were positioned on the frame (Figure 5.24), all parts were to be left to acclimatise for a minimum of 12 hours. Ambient temperature of the environment around the frame was monitored for >2 months with large fluctuations in temperature seen within a day and over a longer period (Figure 5.25). For a ~2 month period (July to October 2009) around prior to testing, the minimum and maximum temperature was 9.5° and 26.5°C respectively (excluding peaks related to sensor positioning). Temperature data were collected using a Lascar Electronics EL-USB-2-LCD, accurate to 0.5°C (Lascar Electronics, 2010).

## Primary Equipment Trial

The fluctuations were the result of the building having no environmental control in place other than UV reflective window film. Although not ideal for temperature control, the building was selected as it was located away from the main work of the EFDA-JET site with minimal passing road traffic, no other building users and was large enough to accommodate the frame and area around to perform measurement.

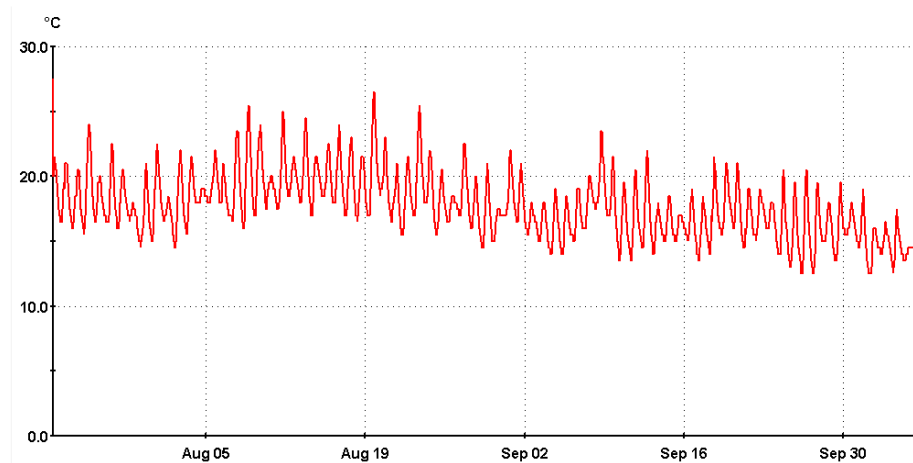


**Figure 5.25: Air temperature around large volume frame in °C for the period July-October 2009.**

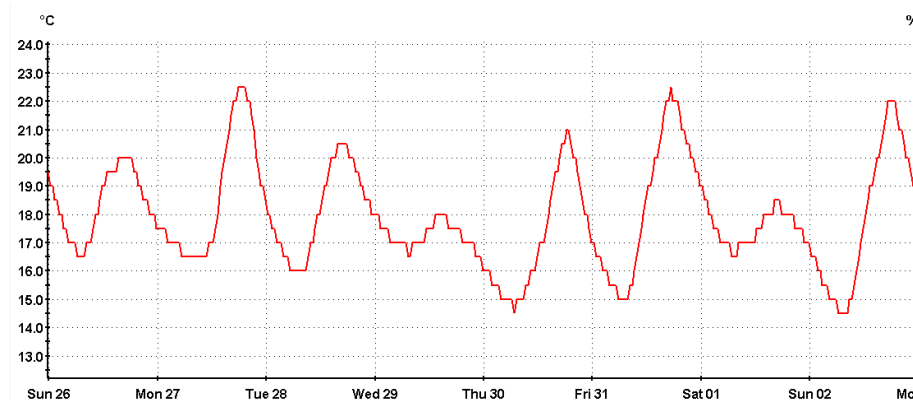


**Figure 5.26: Air temperature change over one week**

Over a day the temperature in the building may have changed by six or seven degrees C with Figure 5.26 indicating the building stored heat throughout the day and reached its coolest point around 9am. The mass of the frame will have slowed the effect of ambient temperature change but will have resulted in slow but constant dimensional change. In line with the common steps defined in Section 5.3.3.1, the temperatures of the artefacts on the frame were recorded, prior to and during surface measurement.

To simulate measurement within the fusion vessel the floor around the frame was marked to indicate where the walls of the machine would have been if the frame were part of the outer wall (Figure 5.27). The stationary tracking part of any hybrid system was positioned with respect to the frame such that within the real machine it would have

be located on the ‘manned access floor’ (Figure 5.27). The access floor was ~800mm wide with an additional ~300mm between the edge of the floor and bottom of the limiter beams on the outer wall (Carman, 2009).

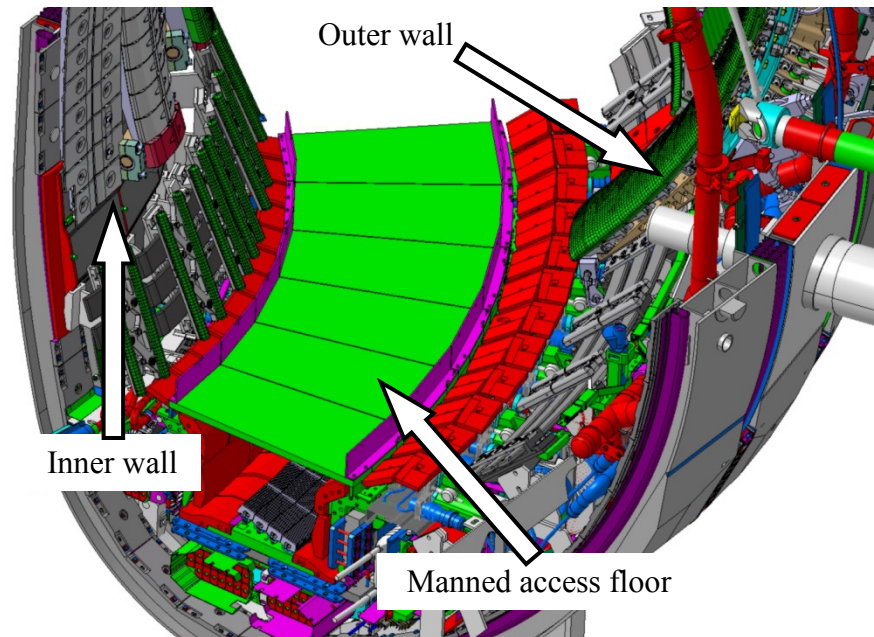


**Figure 5.27: CAD model of a portion of the EFDA-JET machine with manned access floor installed.**

The  $\varnothing 50\text{mm}$  spheres of the datum clusters were measured using scaffolding to access the top spheres, avoiding contact with the frame where possible (Figure 5.24). Spheres were approached from any angle and multiple measurements combined for maximum coverage. The artefacts mounted to the frame were measured following the methods defined (Section 5.3.3).

### Large Volume Data Processing

Where artefacts were measured whilst attached to the large volume test frame, the processing of those data followed the methods detailed within the individual tests (Section 5.3.3.2 - 5.3.3.6). Those data were extracted from the data files using software developed at University College London which used the nominal positions of artefacts from CAD to select data within a given distance from the selected CAD objects. This technique minimised processing time by avoiding the need to load the complete data set into commercial ‘point-cloud’ processing software to extract only the area of interest. The software was limited by the need for data to be registered to the nominal CAD model which required the use of commercial software.

i. Probing Error

The four spheres at the corners of the large volume frame were extracted from data using the extraction software developed at UCL. For each sphere a least squares sphere was fitted to the collected data with maximum 3% of data excluded from the fitting process. The sphere centre position, sphere diameter and RMS of the radial deviations to the constructed sphere were reported.

The range of the radial deviations of data to the fitted sphere (of the points used for fitting) was reported as the form error (*PF*) and the difference between the fitted sphere diameter and calibrated diameter reported as the size error (*PS*).

ii. Length/Sphere Spacing Error

The position and dimensions of spheres on the large volume test frame were measured using photogrammetric methods, and these data served as the reference values. Scale of the photogrammetry data was obtained through the inclusion of calibrated scale bars within the survey. Two physical bars manufactured from glass reinforced plastic (GRP) were present, each with three calibrated lengths, giving a total of six calibrated lengths between 1.4m and 1.7m. The scale bars were: WILD GWCL 182 Invar Code Levelling Rods produced by Leica for use with Theodolites and Auto levels, containing an Invar rod floating inside the GRP frame making the bars physically stable with low coefficient of thermal expansion. 6mm and 10mm diameter retro-reflective photogrammetry targets were fixed to the bars and calibrated by a UKAS approved laboratory, these were also checked against Brunson INVAR scale bars used at EFDA-JET. The calculated RMS scale error for the six scales in the survey was 0.022mm. The photogrammetry survey consisted of 280 images with 720 points.

For each measurement system tested against the large volume frame, the distance between sphere centres (computed from a best fit sphere) were compared against those calculated by target-based photogrammetry.

## **5.4. Results**

### **5.4.1. Approach Angle Test**

The purpose of tests has been outlined in Section 5.2.3.1, with the data collection and processing method described in Section 5.3.3.2.

#### **5.4.1.1. Verification of as-built CAD**

Data collected by the NPL touch probe CMM (Section 5.2.1.6) were used to construct CAD models against which to compare data collected by non-contact optical systems under test. Complete as-built models including edge data could not be created due to limitations of the CMM technology e.g. minimum probe tip diameter and surface normal calculation (Section 5.2.1.6) however planar areas were constructed. Least squares best fit planes without any automated rejection criteria were calculated for each planar area of the artefact from the touch probe data. The plane fitting process minimised the distance of each point, normal to the plane surface, searching for a plane which minimised the root mean square of these distances (residuals). These planes were used as a reference against which to compare data from non-contact optical measurement systems. If the touch probe data had been used without a best fit plane, the area over which comparison could have been performed would have been restricted to those areas where the probe had directly contacted the surface. By comparing optical measurement data against a plane, all data points could be used, however this approach relied on the plane being a good representation of the data points collected by the touch probe. Comparisons were generated by reverse engineering a CAD model from the collected CMM data and comparing the touch probe data to this model. Discrepancies between the registered CMM data and the model demonstrated an agreement for the central portion of the artefact surfaces to within  $\pm 3\mu\text{m}$ , whilst the most steeply angled surfaces at each end showed a maximum discrepancy of  $10\mu\text{m}$ . RMS residuals of  $1-5\mu\text{m}$  were seen for the planes of Artefact B (Figure 5.28). The as-built CAD model was used as the reference against which to compare data from the optical systems.

## Primary Equipment Trial

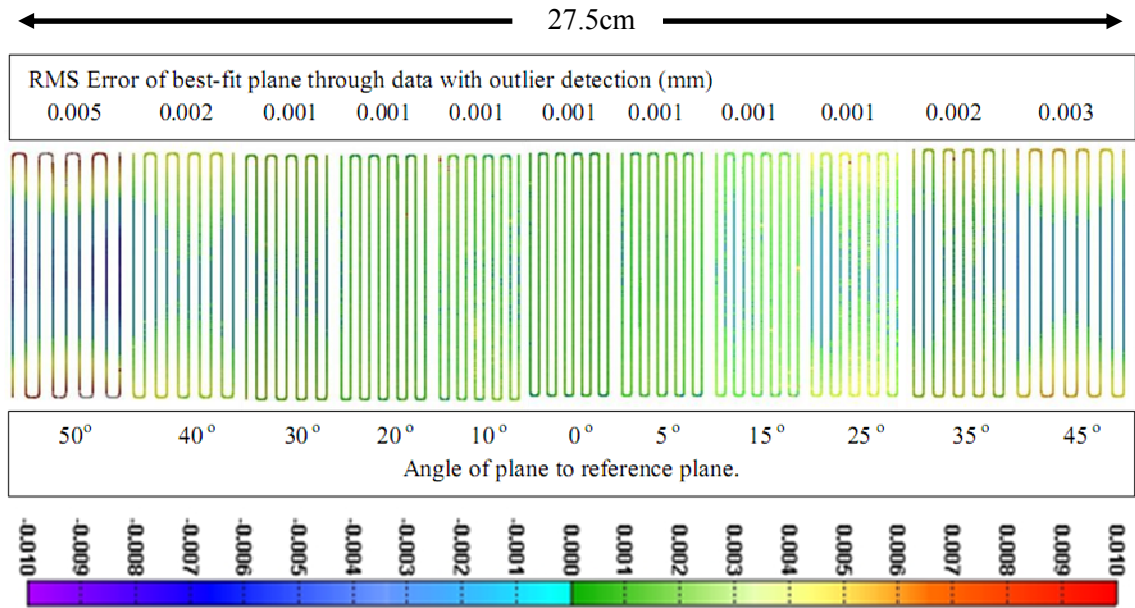


**Figure 5.28: Comparison of CMM data to as-built model of artefact. Error scale in mm.**

The surfaces with greatest angles appeared to have a ‘dip’ in the centre of the block and a ‘rise’ at the edges. It was unclear whether the errors seen were the result of manufacturing difficulties which produced non-planar surfaces or whether the errors were introduced by the CMM measurement. The cause of the error could have been established if the artefact were re-measured by the CMM, with the artefact angled at 50° such that the 50° facet became 0° to the CMM bed and the central reference facet would be at 50°. If the collected data had shown the same error as was seen, the error would have been due to the faces not being planar, if the error had been minimised on the 50° facet (now at 0°) and increased for the reference plane, the error would have lay with the CMM. The error only came to light after CMM data collection had been completed and the data were being processed, therefore the test outlined could not have been completed and the error source remains unknown. It should be noted that the error observed in the CMM measurement was very small compared to the expected performance of the optical measurement systems, therefore these data remained as the reference data for the trial.

EFDA-JET tiles were freeform surfaces because their surface could not be described by a simple mathematical expression (Rodger et al., 2007) however, the artefacts produced were comprised of geometric primitives to simulate the complex tile surface (Figure 3.46b). The analysis method was reliant on these geometric primitives to provide an

indication of measurement system performance allowing controlled comparable measurements.

#### **5.4.1.2. Data Coverage and Quality**

Following the data collection process described in Section 5.3.3.2, the four measurement systems each collected data in two orientations (in-plane and out-of-plane) and were processed as per the method described 'i. Data Coverage & Quality' (page 172).

##### In-Plane Approach Angle

The in-plane angle mappings (Figure 5.29) were collected according to the methods described in Sections 5.3.3.2.1 & 5.3.3.2.2.

The fringe projection systems (Area Based) showed differing levels of data coverage and quality. Projection system A showed areas where incomplete or no data were collected e.g. 5°, 10°, 35°, 40° facets. These areas were believed to be the result of specular reflection causing image saturation (Section 3.2.4.3), occurring where the projection light source and sensing systems were at critical angles either side of a facet surface normal. The specular reflection was increased due to the surface finish of the material being smoother than the design specification, as identified in Section 5.2.1.6.

The effect was most noticeable for the 5° facet of fringe projection system A where no data were recorded. Fringe Projection system B had greater data coverage than system A and data were only missing for a small area of the 30° facet. The coverage differences between area sensing systems A and B were attributable to the differing illumination and detection geometries used. Comparing data to the as-built model and calculating the RMS of the residuals normal to the surfaces showed reduced discrepancy for system A whilst increased noise for system B. The discrepancy in system A showed a tilting of the central 0° facet whilst system B showed what appeared to be angular error on all but the 15°, 25°, 35° and 45° facets. Removal of the errors seen may have been possible by translating the measurement system along the longest length of the artefact.

In this orientation the convex shape of the artefact will have prevented projection systems with two sensors from imaging the complete surface with both sensors, resulting in fewer measurements over that area, increased uncertainty of the data and

with increased uncertainty, decreased accuracy. If the sensors did not capture data with equal quality it is possible an area imaged by a single sensor could have produced data with lower uncertainty than an area imaged by both sensors. This hypothesis could explain the reduced angular error of the 15°, 25°, 35° and 45° facets of area based B in comparison to the rest of the artefact. Both systems trialled utilised the phase-shift principle and therefore the angle between projector and sensor should not have affected the quality of data collected, with both sensors capable of collecting data with equal quality assuming identical sensors. As the surface used was non-lambertian, the angle between light source and sensor could have been increased to avoid specular reflection however, this would have increased the possibility of occlusions. For a lambertian surface, the light source and sensor could be placed concentrically to remove shadows and occlusions between the units, however the use of triangulation with coded light for range determination is no longer possible (Section 3.2.4.3).

The laser line systems tested demonstrate good data coverage although line system A showed limited coverage of the 50° facet and laser system B for the 45° and 50° facets. Although data were missing, the results were not conclusive that the systems could not measure surfaces at ~50°, some data were collected on these facets and therefore lack of data could be the result of any number of reasons including, operator error or scanner to surface distance. A further short trial with scanner in mechanical mounting would have been required to determine the cause. Laser line system A had the greatest discrepancy of all the systems tested, with residuals of  $\pm 100\mu\text{m}$ . It should be noted this system was tested as part of the large volume trial (Section 5.4.6) in comparison to smaller measurement volumes used for other measurement systems. Discrepancies were the combination of angular error on each of the blocks along with ‘waves’ in the collected data and caused the angular error to appear ‘jagged’. The waves were attributable to movement of the tracking system or measurement surface and more clearly seen in the out-of-plane approach mappings (Figure 5.30). Both laser line systems required multiple passes over the artefact to fully image the surface resulting in overlapping data. Within laser line system B data the individual passes of the laser line over the surface were identifiable, caused by differences in the position of the recorded data, also the edges of the line profiles appeared to show positive discrepancy suggesting an upwards curve at the end of a laser line.

Primary Equipment Trial

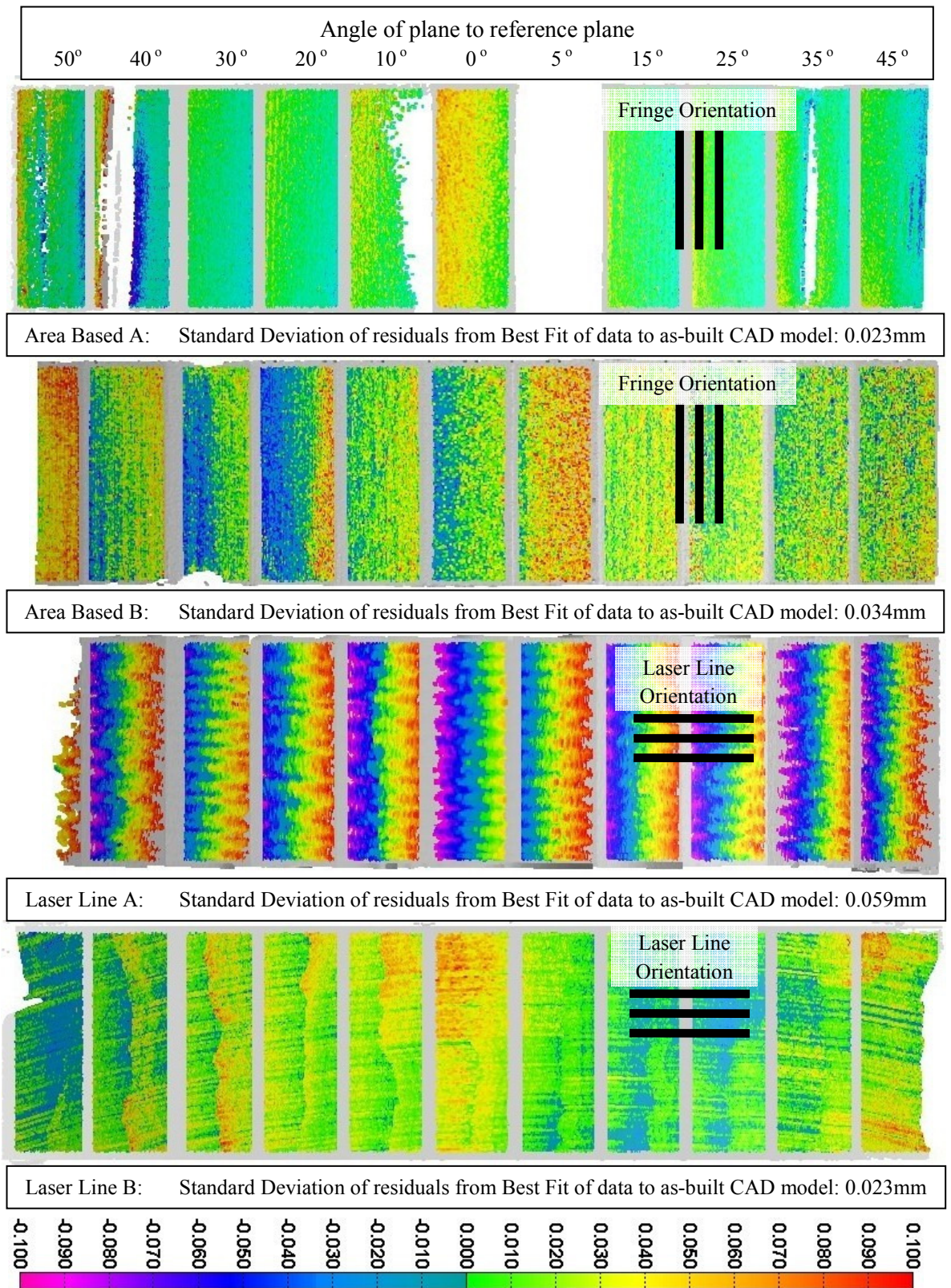
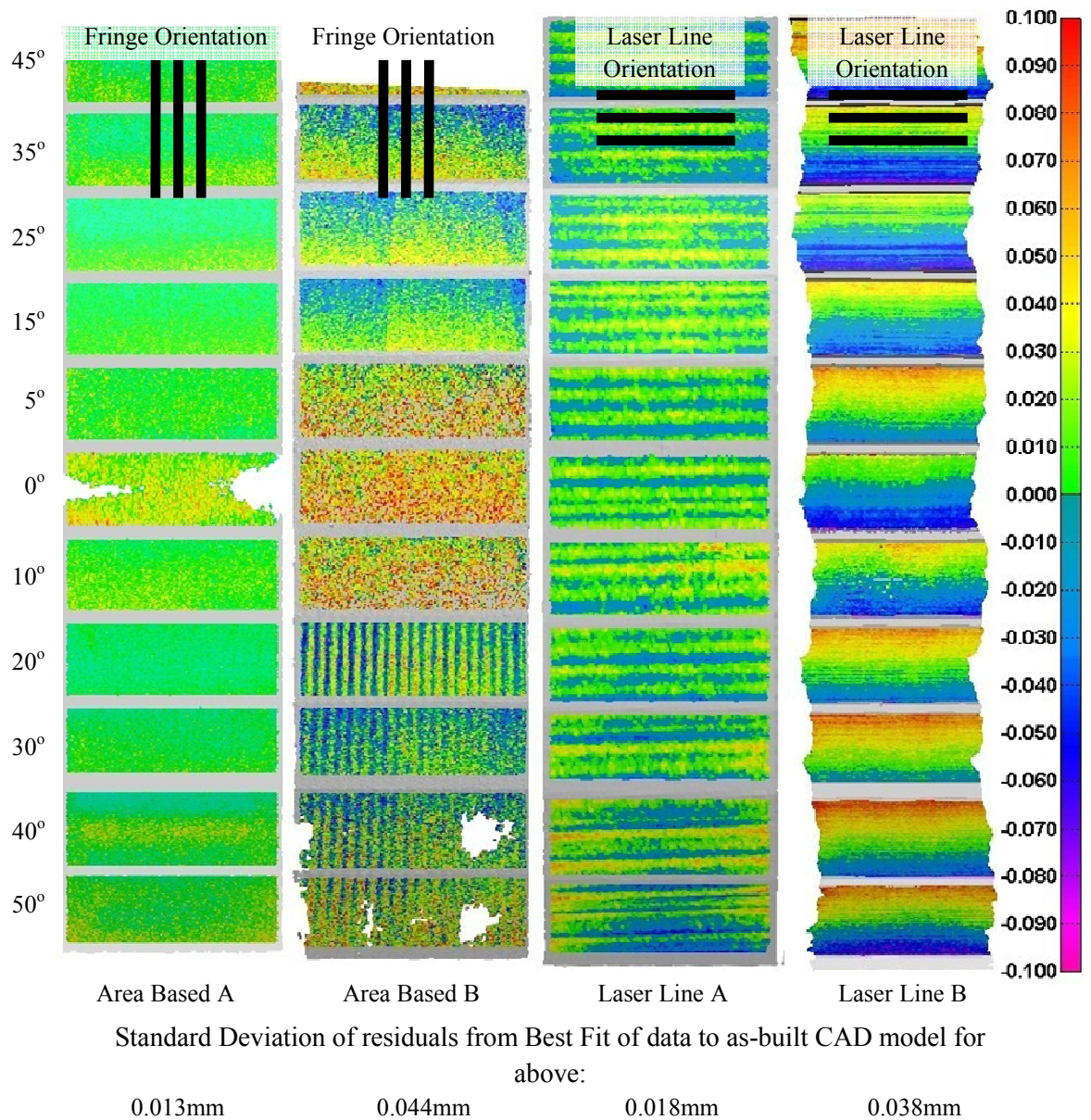


Figure 5.29: Deviation of data from best-fit to model using planar areas. In-Plane Approach Angle.

Out-Of-Plane Approach



**Figure 5.30: Deviation of data from best-fit to model using planar areas. Out-Of-Plane Approach Angle.**

The Out-Of-Plane approach direction (Figure 5.30) resulted in a better level of coverage for both of the fringe projection systems (Area Based A and Area Based B) with specular reflection only limiting coverage for the 0 degree plane with system A. There were increased errors on the 40° and 50° facets which could not be attributed to the inaccuracy of the CAD model as the discrepancy was positive (above the surface by ~30µm) whilst the actual surface was negative. As all data (excluding that near an edge) were used for registration, errors were distributed, making the cause of a particular error more difficult to determine. While fringe system A recorded increased error for the 40° and 50° facets, fringe projection system B failed to record the complete

## Primary Equipment Trial

surface. Data were also missing on the 45° facet, however this appeared to be due to positioning of the measurement system. The central three planes (0°, 5°, 10°) showed a relatively random error whilst clear differences between the planes above the sensor (15°, 25°, 35°) and below the sensor (20°, 30°, 40°) were seen. Above the sensor the planes appeared angled, recorded as steeper than actual. Below the sensor a 'wave' pattern matching the orientation of the fringe pattern was clearly visible within the collected data. The wave pattern could not be attributed to movement of the projection system or part, as is possible for laser systems, as the error would have been expected to occur across the complete artefact - as movement of the projector/sensor would affect all data. .

The hand held laser line scanner was moved over the surface from the 50° facet to the 45° facet maintaining a constant angle to the surface but with change in scanner to surface distance permissible. Laser system A achieved full coverage of all facets and showed discrepancies on the 40° and 50° facets in line with the error present in the as-built CAD model. The wave pattern present in the data was due to movement of the tracking component of the system or the measurement part causing a change in distance (Section 3.2.4.2) (Beraldin, 2004). The data utilised were from a single 'pass' of the laser line over the surface so no overlapping data existed and was collected as one continuous movement which excluded the possibility of significant thermal change. It is possible there was vibration which affected the tracking system and/part during measurement as the trial was held at EFDA-JET however the magnitude of the waves seen was of the order of 90µm. A completely vibration free environment within the vessel could not be guaranteed. Data along a scan line presented lower uncertainty than inter-line data therefore, it is likely the tracking/positioning of the 6 degrees of freedom (6DoF) of the scan head limited the abilities of the measurement system. An implementation of laser line triangulation which utilised Lissajous scanning patterns was developed at National Research Council Canada (NRC) and allowed for motion between the scanner and object, performing imaging, fast object recognition and pose estimation for freely moving objects (Blais et al., 2001b). The Lissajous pattern could be combined with "raster scanning (one line) to acquire high-resolution accurate 3D images." (Blais et al., 2004). An implementation of the technology was developed for measurement of protective tiles on the NASA space shuttle (Blais et al., 2001a).

Laser line system B did not collection data on all facets due to the shorter laser line length of this system compared to system A. In this orientation, a single pass of the

scanner was insufficient to completely capture the part resulting in a need for multiple passes and increased collection time. In addition to limited coverage the data appeared to show systematic angular error on each facet. In the direction of scanning the 'start' of the facet was recorded as lower and the 'end' recorded as higher. This error could have been a registration problem, although a rigid transformation of the surfaces was performed in a commercial software package (where residuals to the surface were minimised) therefore unlikely. The changing distance between surface and sensor could have affected the data, or as with the other laser line system tested, the tracking component of the system could have given rise to this complex angular error.

For the purposes of EFDA-JET the collected data indicated that coverage of a complete tile assembly was possible from a single position and orientation. Fringe projection systems would have required careful positioning to ensure the complete surface could be captured without specular reflection affecting the sensor(s), but could capture the complete assembly from a single viewpoint. Laser line systems could not capture the complete assembly from a single position as they collected a single profile for a given position, but they could have collected data by traversing the measurement head over the tile surface at a constant distance and angle to the surface. What could not be determined from the data presented was whether data on each facet was of the same quality and therefore whether all data could be used, for this, each facet had to be examined individually (Section 5.4.1.3).

#### **5.4.1.3. Measurement system angle to surface normal**

The registration method used for data shown in Figure 5.29 & Figure 5.30 attempted to minimise the sum of the squares of the residuals for all facets simultaneously (ranging from 0.013mm to 0.059mm), which resulted in difficulty determining the random error of an individual facet. It was been established that measurement of all facets of angle artefact B appeared achievable however, it was established whether data present on each facet were of equal quality. Using the eight data sets already collected (two per measurement system, four measurement systems), these data were processed according to 'ii. Measurement System Angle to Surface Normal' (page 172).

Data from each individual facet were used to fit a least squares best fit plane and the residuals to the plane analysed. The root mean square (RMS) of the residuals for each plane were calculated and used as an indication of the local error for the given surface angle (Figure 5.31 - Figure 5.39). This approach removed the impact of systematic

### Primary Equipment Trial

artefact manufacturing error on the data and was applicable because it was known that each facet was planar to better than  $5\mu\text{m}$  from the independent CMM measurement. Registration across a small area should have ignored any larger volume systematic errors present in the data e.g. angular error in the collected data, however some systematic errors are likely to have remained e.g. the wave patterns seen in Area Based B and Laser Line A in Figure 5.30.

### In-Plane Approach Angle

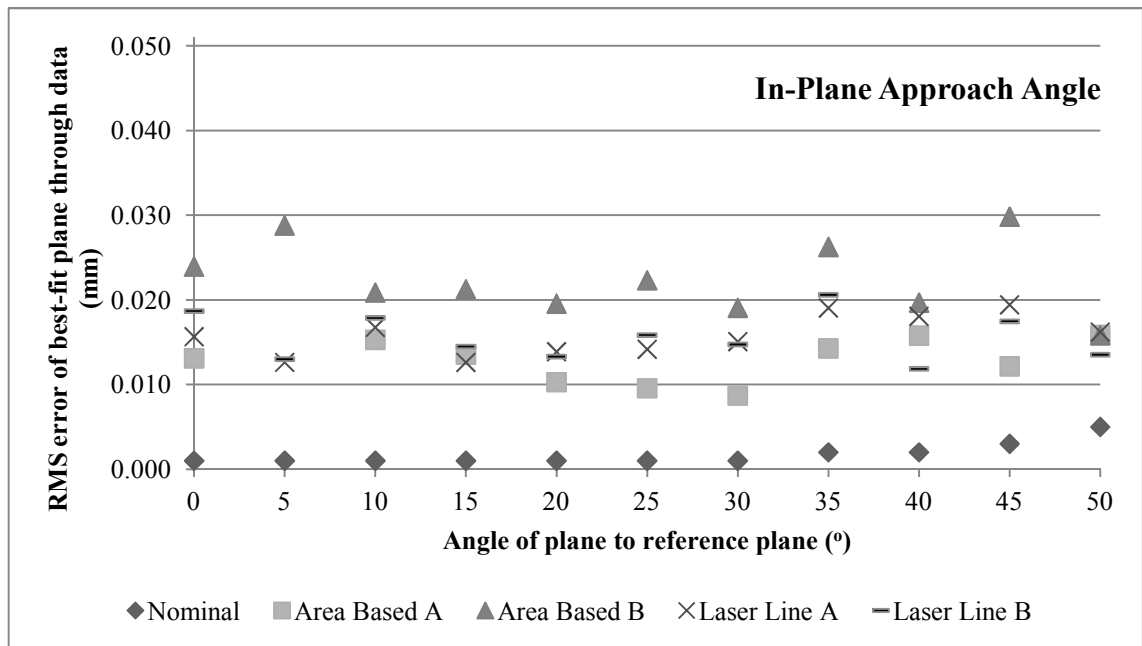


Figure 5.31: RMS error of plane fitting for each facet.

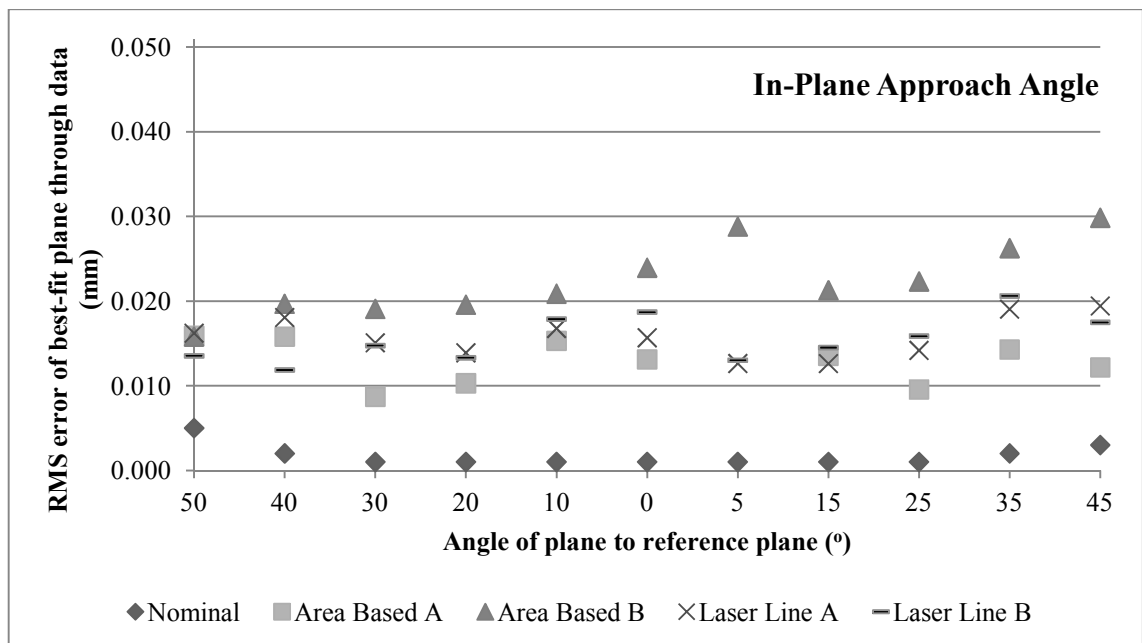


Figure 5.32: RMS error of plane fitting for each facet, plotted according to facet position on artefact.

## Primary Equipment Trial

The In-Plane approach angle is shown in order of increasing facet angle and by position on the artefact (Figure 5.31 & Figure 5.32). The nominal data from the touch probe CMM showed increased error for the 35-50° facets as seen during verification of the as-built CAD model (Section Verification of as-built CAD). Fringe projection system A maintained RMS errors per facet of ~0.008-0.016mm and showed no systematic increase in error as surface angle increased. Fringe projection system B had increased error which did not increase in line with surface angle. When compared with registered data (Figure 5.29), some facets which appeared to have the greatest systematic angular error featured the lowest RMS residuals e.g. 50°, 40°, 30° and 20° facets. In this case the systematic error appeared to be a limiting factor rather than the random error (Section 5.4.1.3.1 & 0). For the laser line systems tested, close agreement was seen between the two systems, with residuals of ~0.012-0.020mm and no apparent systematic increase in error with angle.

Work by Van Gestel et al. (2009) used a laser line scanner from Metris (Nikon Metrology NV, 2010) attached to a CMM so that the CMM provided highly controlled movement within a limited measurement volume. The in-plane angle showed that as the plane angle increases the residuals decrease (Figure 3.54). Data from the trials performed using angle artefact B do not conclusively show the same trend (Figure 5.33) although a possible trend within laser system B could be seen (Figure 5.34).

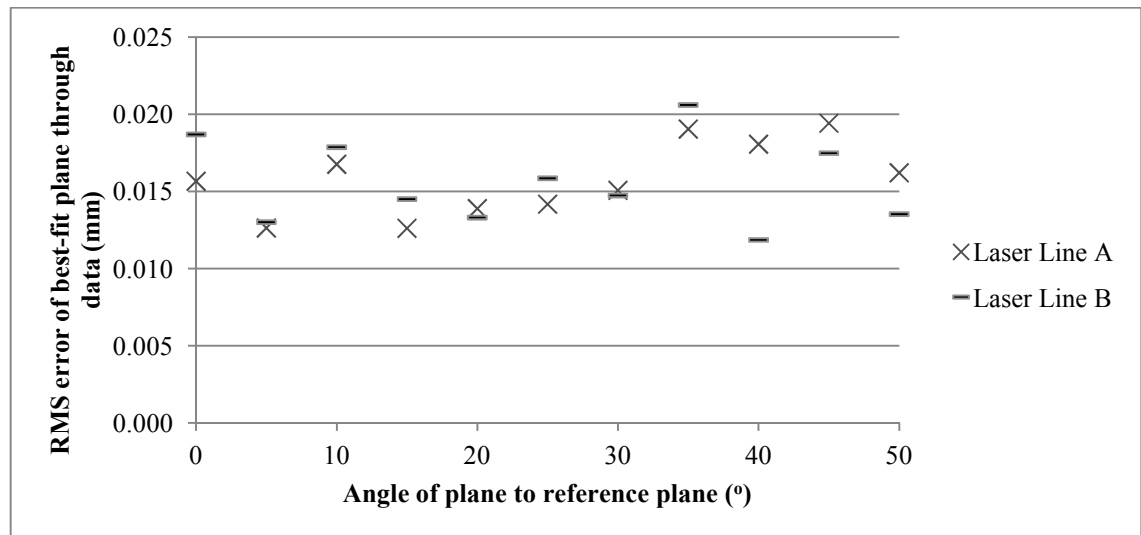
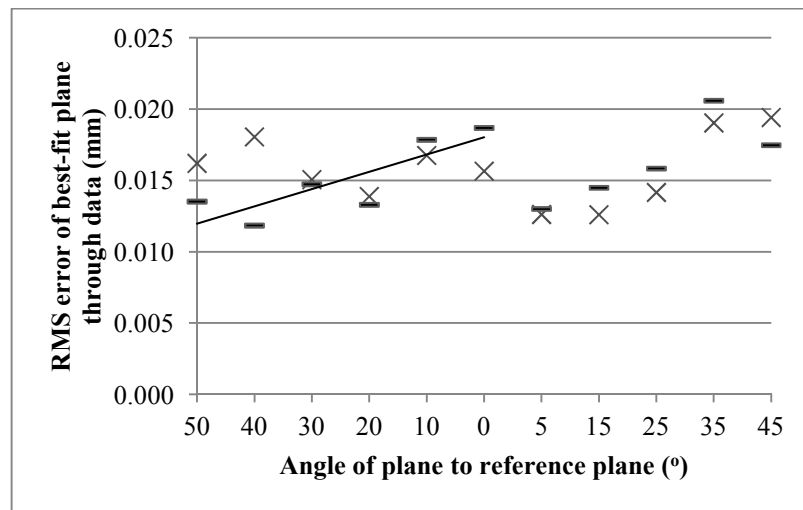


Figure 5.33: Influence of in-plane angle on the standard deviation.

### Primary Equipment Trial



**Figure 5.34: Possible trend in laser line B showing reduced residuals when measuring a ‘rising’ surface.**

Differences in the method by which the scan heads were moved (mechanically versus manually) and tracked (CMM versus optically) will have impacted the results, with the CMM movement and tracking being superior. Additionally, the data presented from this trial utilised  $-50^{\circ}$  to  $+45^{\circ}$  for the in-plane angle whereas it is believed (Figure 3.54) presents data of  $0$  to  $60^{\circ}$ . Where Van Gestel et al. collected data with no overlap between data sets, testing performed for EFDA-JET for the in-plane angle approach case resulted in overlapping data and an averaging caused by the plane fitting process. As data were output as a single data set, analysis of individual scan passes was not possible and the plane fitting process averaged the position and angle of the collected data in a given region to minimise all residuals to the fitted plane. Analysis of data from individual scans would be expected to have revealed finer detail, where that detail was within the random error of the measurement system.

To assess the impact of overlapping data from laser line systems, a planar area was measured with laser line system B, with two passes of the measurement head over the surface and a change in the orientation of the laser line. A least squares best fit plane was fitted through each data set, where the plane position was calculated to minimise the root mean square of the residuals normal to the plane (Figure 5.35). In addition, a plane was fitted through all data for this area, combining data from both passes of the laser line (Figure 5.36).

### Primary Equipment Trial

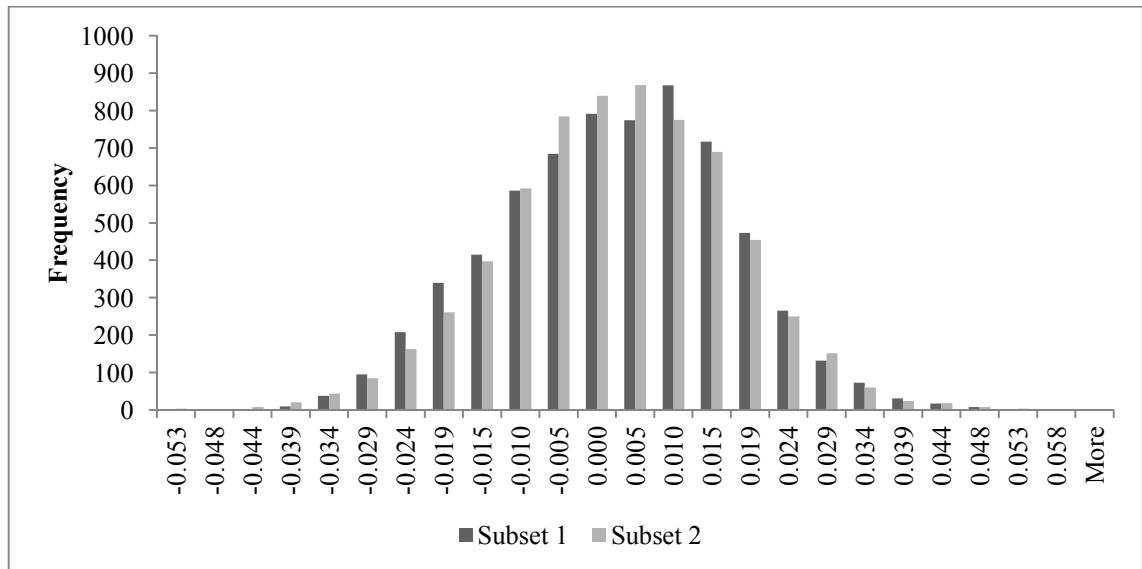


**Figure 5.35: Histogram of residuals for two passes of laser line scanner over a planar surface ( $\pm 4$  standard deviations shown).**

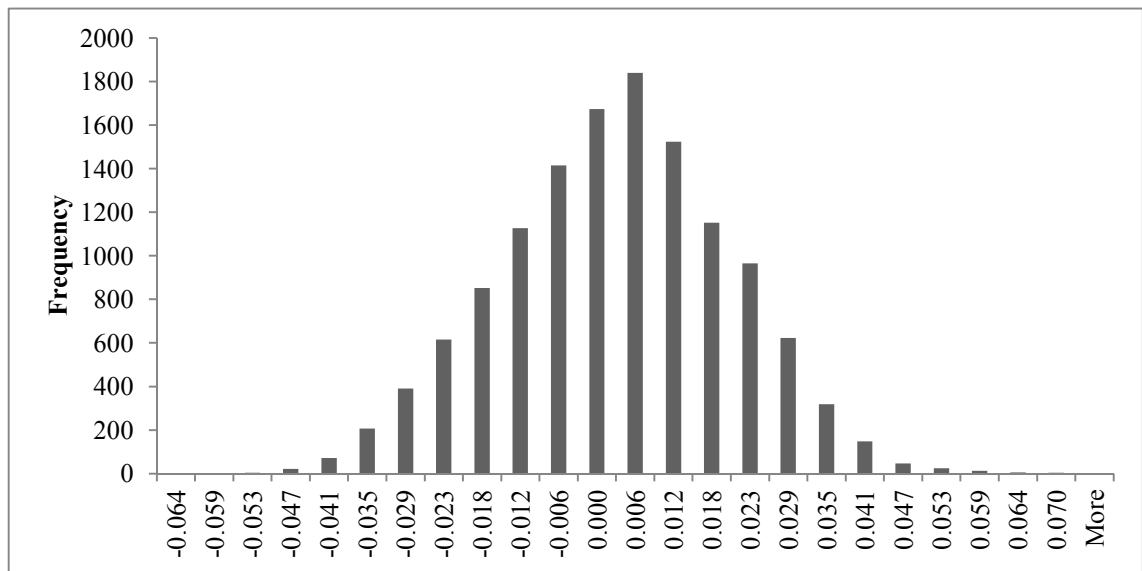


**Figure 5.36: Histogram of residuals for two passes of laser line scanner over a surface - combined data set ( $\pm 4$  standard deviations shown).**

The data and histograms demonstrate that for this data set, an increase of 0.003mm in the standard deviation (RMS error) of the residuals existed where two passes of the laser line over the surface were used. The standard deviation (RMS residuals) of the data for both sets was 0.015mm when processed separately, increasing to 0.018mm where the data sets were combined. The increase in residuals was attributed to errors within the 6DoF of the measurement head. The data sets were suitably close that the systematic error could not be separated from the random error in this case.

Out-Of-Plane Approach Angle

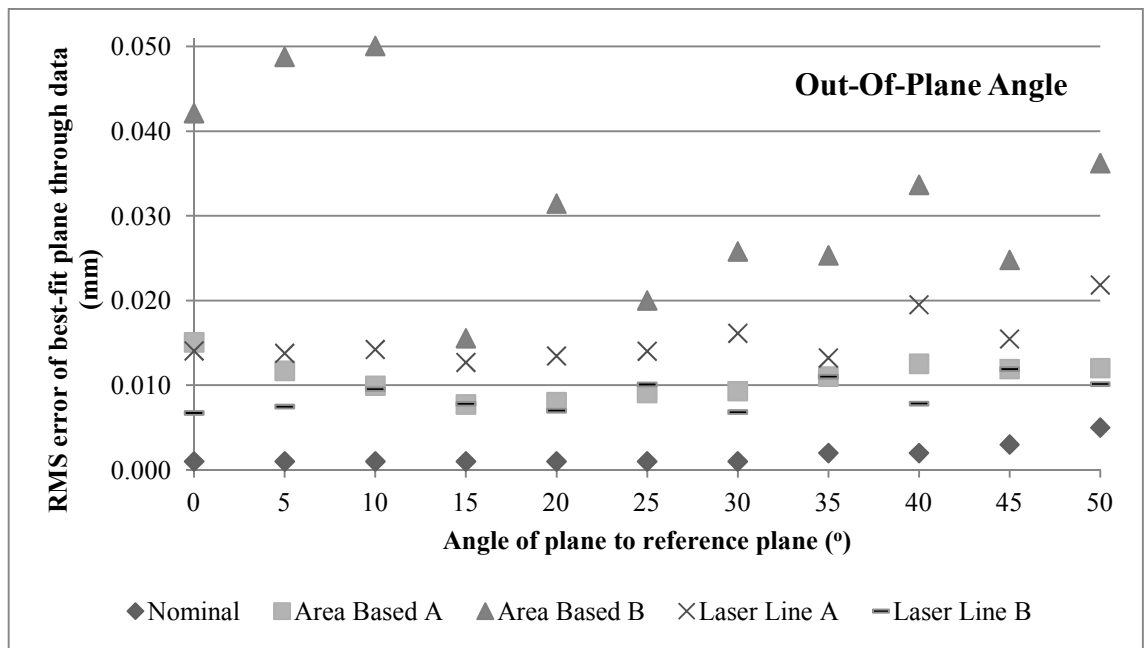


Figure 5.37: RMS error of plane fitting for each facet.

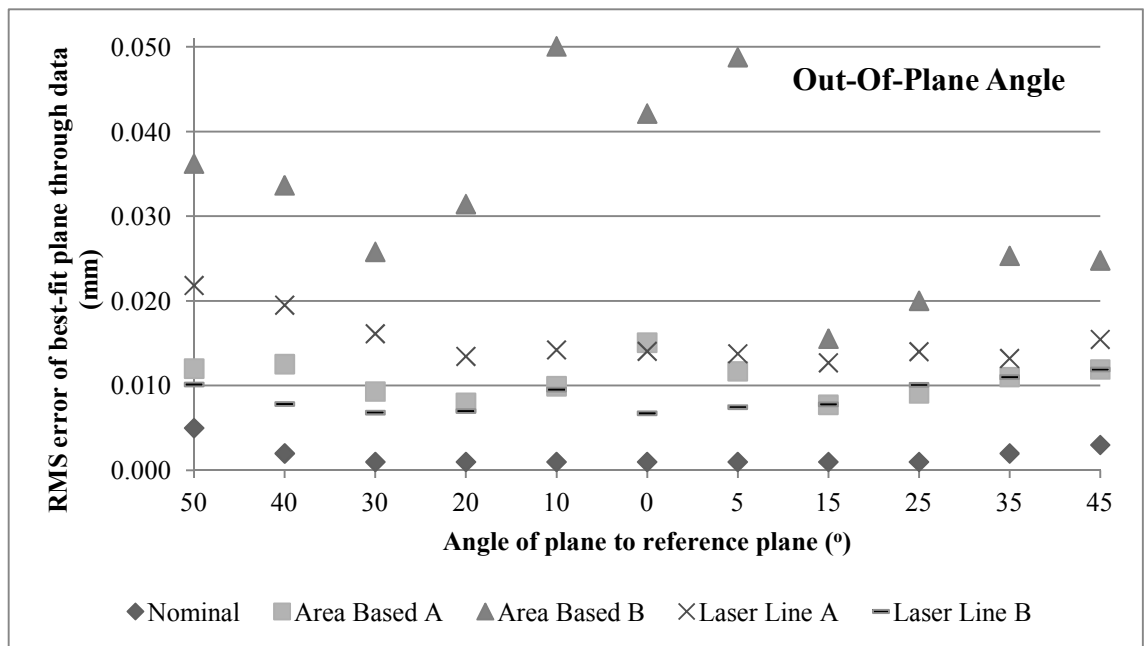


Figure 5.38: RMS error of plane fitting for each facet, plotted according to facet position on artefact.

The out-of-plane angle simulated the angles at which a measurement system could have approached a surface from above/below and the impact on the measured data. The residuals (Figure 5.37 & Figure 5.38) of fringe projection system A were within ~0.015mm for all facets, showing no significant difference to the in-plane approach case. When data were viewed in the order of the facets on the artefact (Figure 5.38) the greatest error occurred at the central 0° facet, reducing on both sides to the 20° and 15°

facets at which point it began to rise. It was not clear whether the 15-20° surface angle presented a ‘sweet’ spot for the measurement system due to the surface angle or position of the imaged data on the sensor. Fringe system B showed greatly increased residuals in comparison to fringe system A with the greatest residuals on the central three facets i.e. 0, 5 and 10°, over 0.050mm. One half of the artefact had increased errors over the other half which could not be attributed to registration or systematic angular error, and indicated a different capability of the two sensors to this particular surface.

For the laser line systems, the RMS of the residuals normal to the surface for laser line system B was consistently better than for line system A, despite the discrepancies noted during comparison to as-built CAD (Figure 5.30). RMS residuals on all facets were >0.015mm, whilst for laser line system A random errors in excess of 0.020mm were recorded. Increased errors on the 30, 40 and 50° facets were noted however, similar errors were not found on the facets in similar location on the other half of the artefact. The increased error may have been the result of the system recording the discrepancy between the as-built CAD and the actual surface however, if this were the explanation a similar increase in residuals would have been expected for the 45° facet. For this implementation of laser line scanning the measurement of a ‘rising’ angled surface appeared to have resulted in an increase in random error (noise). Without knowing the internal configuration of the hand held scanner it was not possible to explain the error other than it was likely due to the scanning head and not the tracking system in use, possibly due to the change in depth of field. Despite careful manufacture, some machining marks were still visible which had not been completely removed by the acid etch surface treatment and would have affected measurement by optical systems (Section 5.2.1.6).

The laser line system used by Van Gestel et al. (2009) had the sensor mounted at a negative angle to the laser line; the zero degree data occurring where the laser line was projected parallel to the surface normal. Data with lowest standard deviation were obtained where the camera was closer to the surface normal than the laser line (Figure 3.54).

Data collected for this work (Figure 5.39) showed that for laser line system A measurement of a ‘rising’ slope produced greater random error, whilst the opposite was true for laser line system B, although with less influence. The difference between

systems may have been caused by a reversal of laser and sensor positions within the measurement head and directional peculiarities of the artefact surface finish.

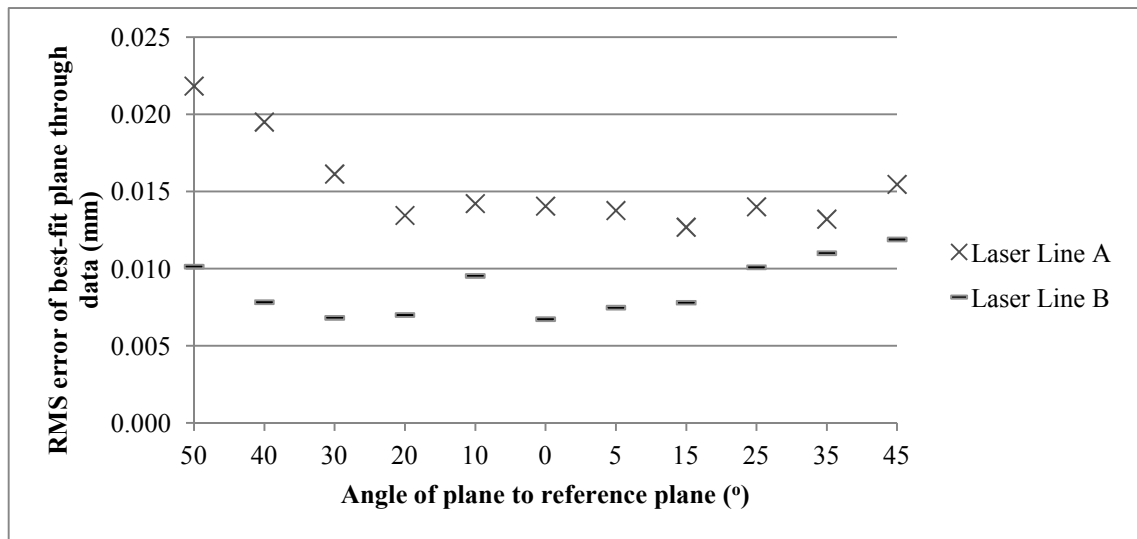


Figure 5.39: Influence of out-of-plane angle on the standard deviation

All systems exhibited significantly greater variation than the measurements made with the CMM probing system. In all tests it was possible to identify the line / fringe direction used by simply viewing the colour coded residuals from the measurement of these planar surfaces.

5.4.1.3.1. Remaining Systematic Error within Data

The RMS of the residuals of data for each facet provided quantitative data regarding the error however did not show the distribution of those errors. Figure 5.40 shows the 40° (Block 2) and 20° (Block 4) facets compared to the as-built CAD model using data from all facets for registration (excluding data within 2mm of an edge) and the second column is the same data compared to a least squares best fit plane created through the facet data.

The presented data, particularly for area based B (in-plane) and laser line B (out-of-plane), demonstrate the removal of an angular trend in the data following the local plane fit. All systems demonstrated clear systematic effects which were not apparent in the sparse CMM data. Such effects confirmed earlier observation that systematic fluctuations attributable to the tracking systems in the case of the laser lines and in the fringe directions for the area based systems were present. Maximum amplitudes of the observed variations amounted to some 90µm for the laser systems and of the order of 120µm for the area based systems. Such variations, particularly for area system B and

### Primary Equipment Trial

laser line system A, represented a fundamental limitation to provide reliable measurement of local changes in tile surfaces. Work to filter the systematic patterns to improve the detection of local changes would be required in combination with an evaluation of the edge measurement capability of the systems. However any filtering method would only be relevant if such patterns could be reliably reproduced to reference surfaces under inspection conditions.

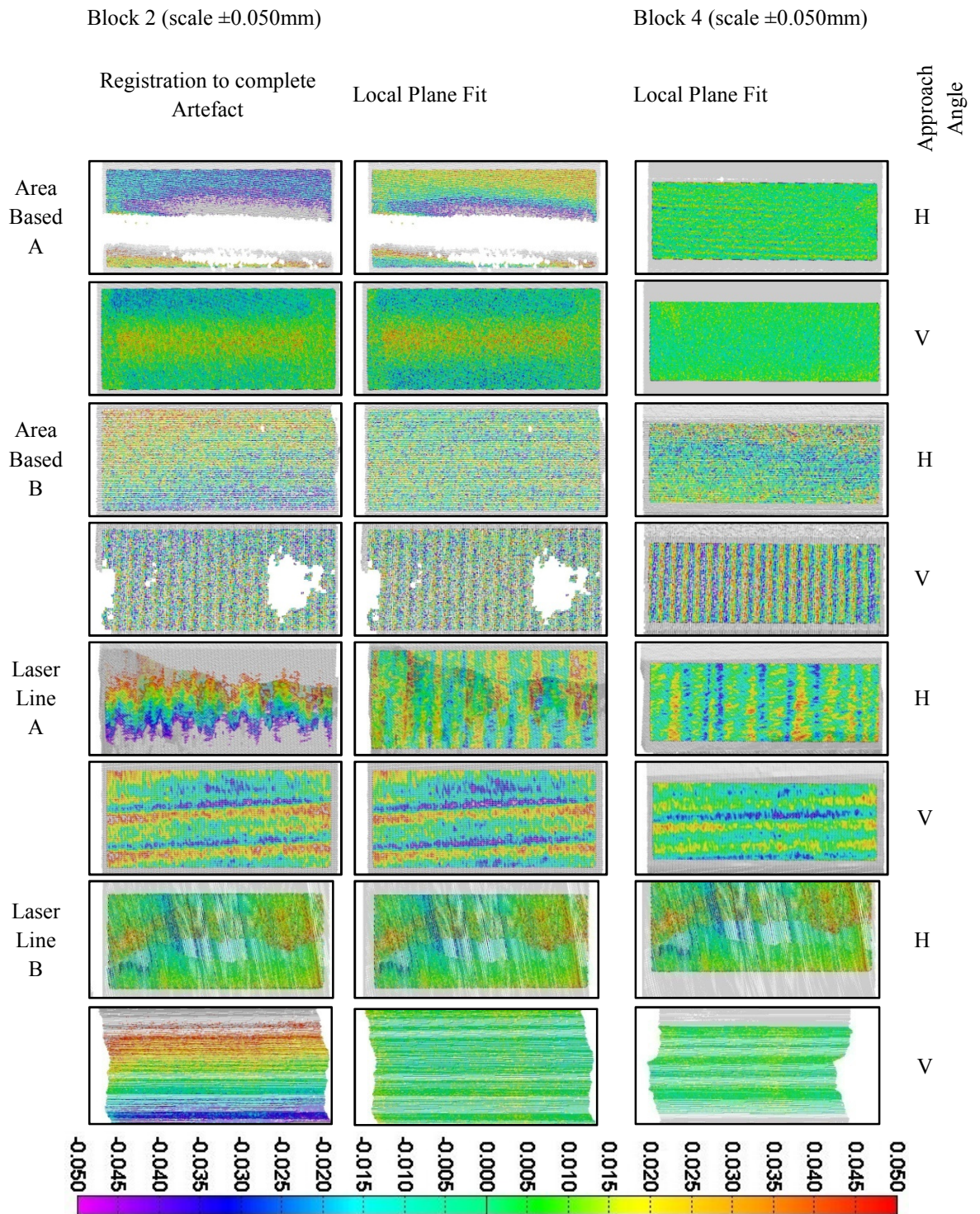
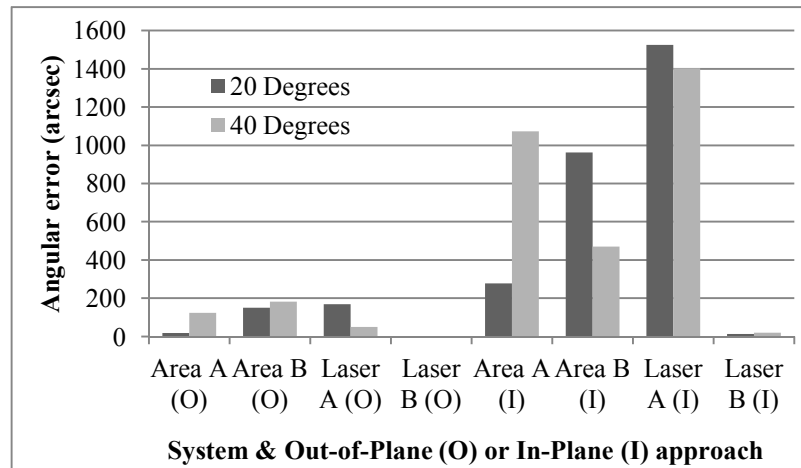


Figure 5.40: Error distribution highlighting systematic errors within the data.

**5.4.1.4. Angular error**

The angle between the 20° and 40° facets (obtained from a registration using all facets) and the least squares best fit planes were calculated (Figure 5.41). No data could be computed for Laser Line system B for the out-of-plane approach angle as the registration process would not complete, for in-plane approach data are present although the error is small.



**Figure 5.41: Discrepancy of computed angle between overall best fit registration and least squares best fit plane.**

The expectation was that the angular error of the 40° facet would be greater than the angular error of the 20° facet however the results showed the orientation of the sensing system had a greater impact. To investigate this further, the angular error of all facets in both out-of-plane and in-plane orientation were calculated.

Out-Of-Plane Approach

To provide further information, processing was expanded to calculate the angle for each plane to the central reference plane for data from each measurement system. The angle between the central reference plane and each facet was calculated from touch probe CMM data and used as the as-built value. The same calculation was performed for each measurement system to their reference plane and the as-built value subtracted, leaving the angular discrepancy. Consequently the 0° facet presented zero error for each system. Figure 5.42 shows the angular error in degrees with data sorted along the horizontal axis by the facet angle with respect to the central reference plane. Positive error indicates the facet was calculated as steeper than the as-built data, a negative error indicates the facet was recorded with a reduced angle to the reference plane. There was no systematic trend of angular error increasing as the facet angle did. As trends within

### Primary Equipment Trial

the data were difficult to understand in this format the data were re-plotted according to the facet position on the artefact (Figure 5.43).

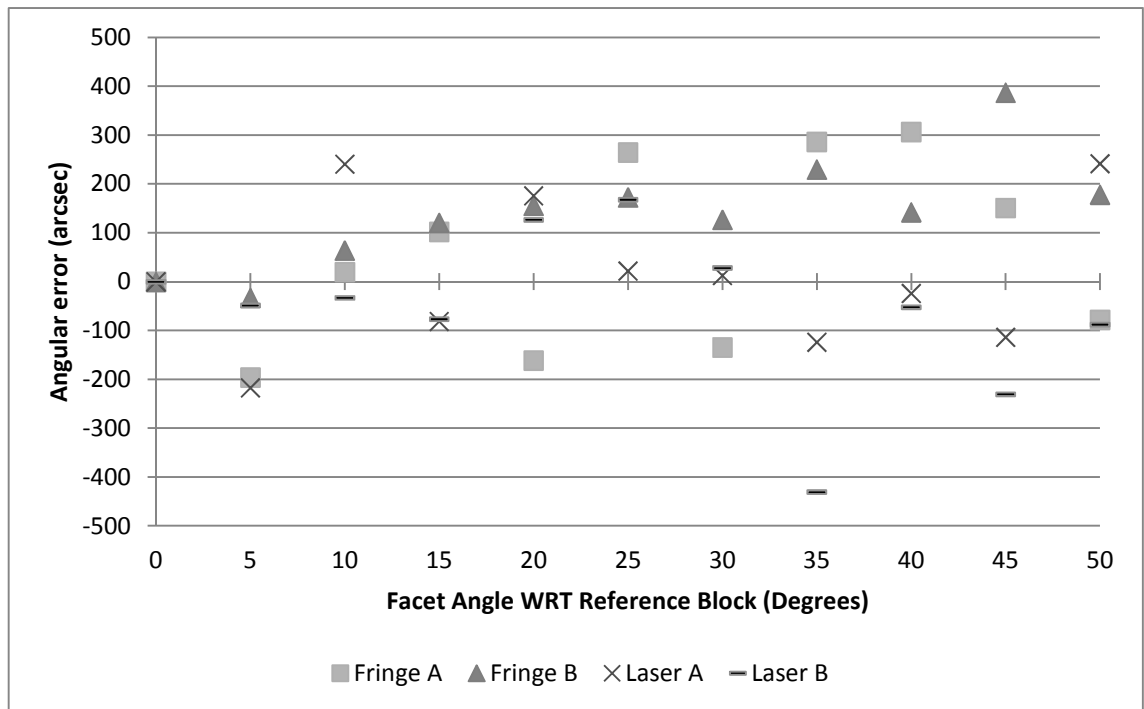


Figure 5.42: Angular error for Out-Of-Plane approach. Data sorted by nominal facet angle.

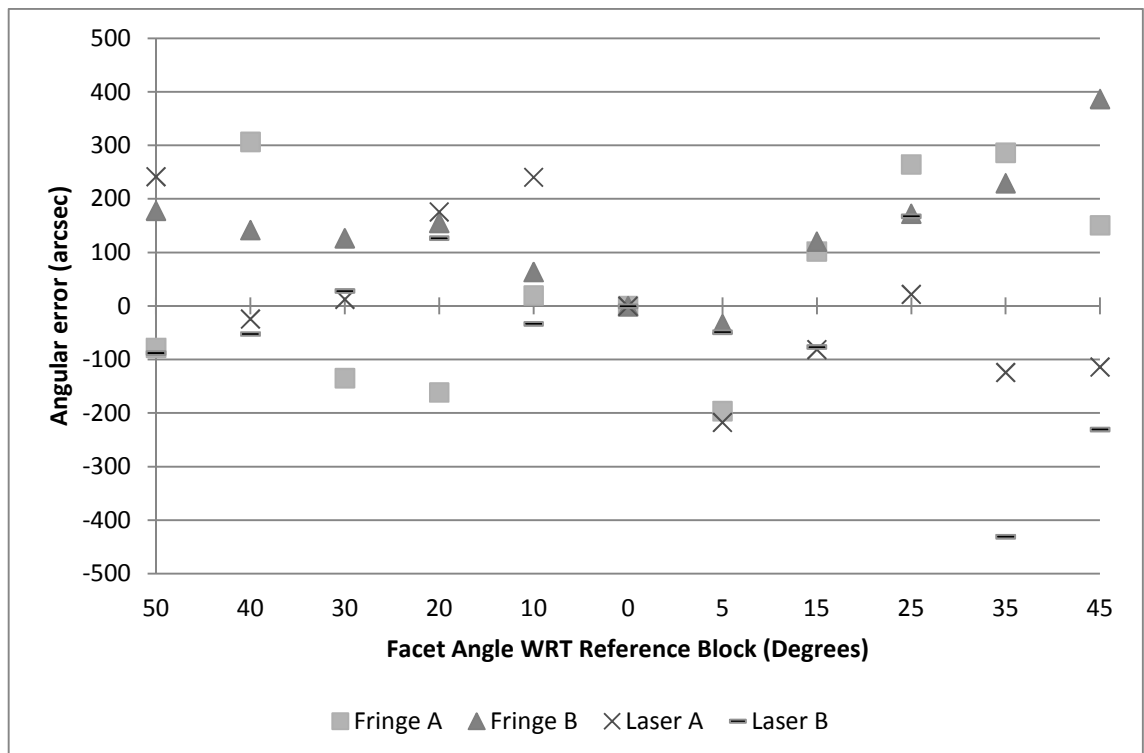


Figure 5.43 : Angular error for Out-Of-Plane approach. Data shown according to position on artefact.

For laser system A, the three closest facets either side of the central reference plane showed a trend for over-estimation of facet angle as the measurement system

## Primary Equipment Trial

approached the central plane and under-estimation of facet angle as the measurement system passed the reference plane. Likely showing the effect of the angle between laser line and camera changing to the surface as the surface ascends and descends from the sensor. For the 40, 30 and 20 degree facets laser line system B showed angular error closely matching line system A but did not show similar discrepancy for the 5, 15 and 25 degree facets. Of the fringe projection systems, area based A presented no systematic bias whilst area based B presented data with a constant overestimation of the surface angle to the reference plane for all but the 5° facet. The magnitude of angular error for all but two measurements were within the tolerance allowed by EFDA-JET of 486 arcsec (Vizvary, 2007) however measurements were close to the permitted limit (Figure 5.47).

To highlight the impact of registration when assessing angular discrepancy between facets a second graph was plotted. Data were 'best-fit' to the as-built CAD model using data on planar areas and for each system and facet, the angle of each to the reference plane of the as-built CAD calculated (Figure 5.44). Angular registration discrepancy between data and the as-built CAD can be seen by the magnitude of angular error on the 0° reference facet. Use of this data which although 'best-fit' using only planar areas, contains registration error would suggest laser line system B will produce significantly different results dependent on the orientation of the measurement head. Data used for assessment of angular error used data where facet angle was computed to the reference plane of that data set and was independent of registration.

### Primary Equipment Trial

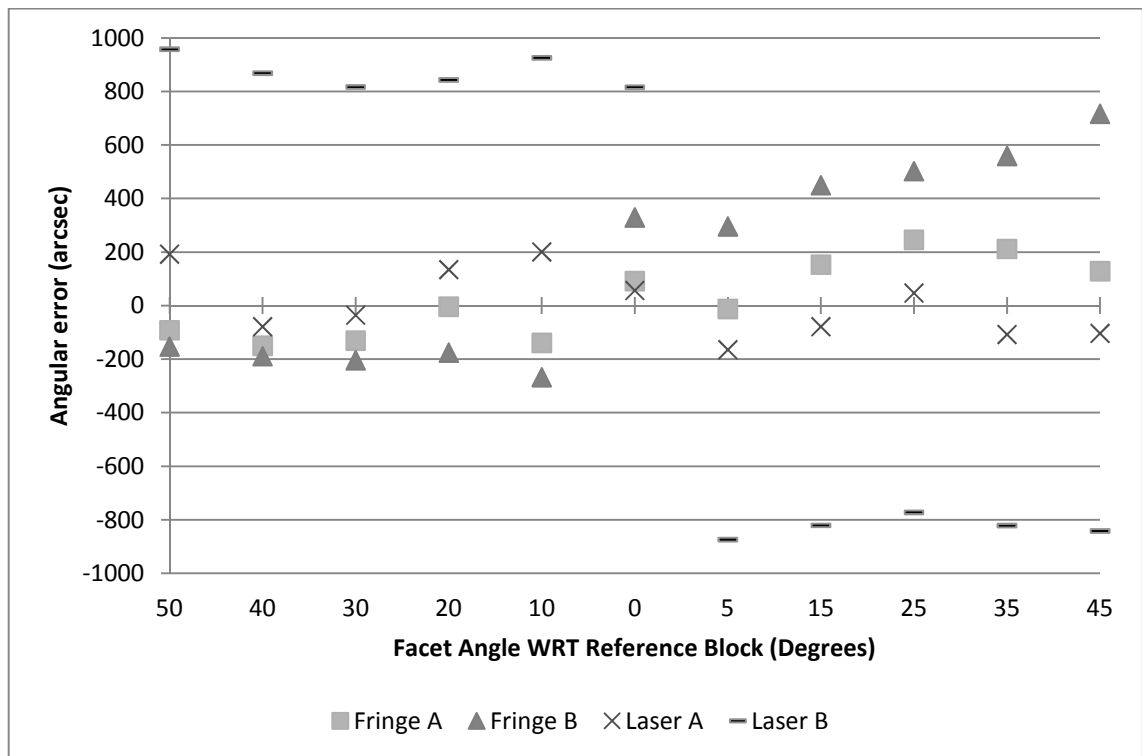


**Figure 5.44: Out-Of-Plane approach angle - facet angle to as-built CAD reference plane, showing the effect of registration error. These data use facet angle computed to the CMM reference plane and are therefore reliant on registration between data and as-built CAD. The angular errors seen on the central 0° reference facet demonstrate the magnitude of mis-registration.**

### In-Plane Approach

Early analysis of angular error using two facets (Figure 5.41) showed great difference between the performance of measurement systems in out-of-plane and in-plane orientations, to verify the results, the angular error for all facets was calculated (Figure 5.46). This graph highlighted that the 20° and 40° facets shown in Figure 5.41 were not representative of the complete artefact. Block two and block four, 40° and 20° facets respectively showed disproportionate error to other facets for at least two of the systems tested.

For fringe projection system A angular error was <50 arc seconds for seven of the facets with increased error on the 40°, 35° and 45° facets. The affected facets had incomplete data coverage (Figure 5.29) however the 10° facet also had incomplete coverage but the angular error was similar to other facets with complete coverage. Fringe projection system B had increased angular error on the 15, 25, 35 and 45° facets of between 280 and 350 arc seconds. Facets in similar positions on the other ‘side’ of the artefact did not present systematic error. Differences between sensors could explain the differences seen. Had the error shown clear increase as the angle increased it could have been

proposed the projected pattern diverged increasing the spacing and width of adjacent fringes on the measurement surface, reducing measurement resolution. Similar work performed using a phasogrammetry projection system (Wakayama & Yoshizawa, 2009; Bräuer-Buchardt et al., 2006)<sup>9</sup>, showed no significant increase in error until the angle of surface exceeded 45° (Kühmstedt et al., 2009a).

The significant error seen in Figure 5.41 for laser line system A was not replicated in Figure 5.46. The difference could be attributed to the data set used to calculate the results which differed between the graphs. Several data sets were collected with the measurement systems, laser line systems collecting patches of data comprised of a number of scan lines per data set. The data used in Figure 5.41 had overlap between individual passes of the laser line removed so each facet had data from a single scan only to remove the effects of overlapping data. The data were re-processed for Figure 5.46 using a set including overlap between different scans as more representative of real world use. During the least squares plane fitting process the difference between the two data sets became clear, where overlapping data existed, the least squares process attempted to fit a plane through the difference scan patches, minimising the effect of outlying data. Where data existed without overlap, angular error in the collected data was more clearly seen and accurately reported in the results. Although multiple passes of the scan head offer the possibility to minimise angular error, a loss of fine detail will also occur due to registration/alignment error between scan passes caused by errors in the tracking system and change in surface to sensor distance (Section 5.4.1.3, Figure 5.35 & Figure 5.36). Laser line system B showed the system to overestimate the facet angle for those to the right of the reference plane whilst large variations were present for those to the left. The variations seen cannot be explained and repeat measurements would be required to ascertain if the variation was a single occurrence or repeatable.

---

<sup>9</sup> where a pattern is projected in two orientations, the second at 90° to the first and captured using two cameras

Primary Equipment Trial

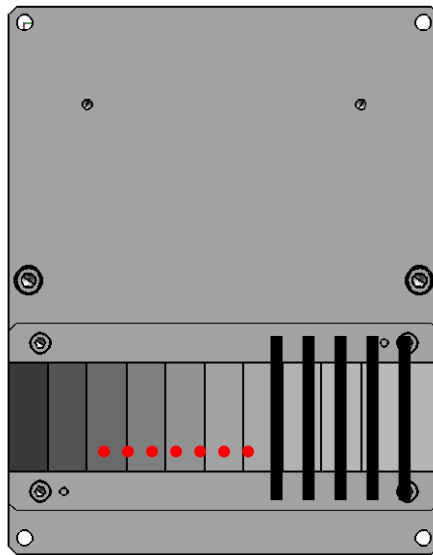


Figure 5.45: Orientation of projected pattern and laser line for in-plane approach test.

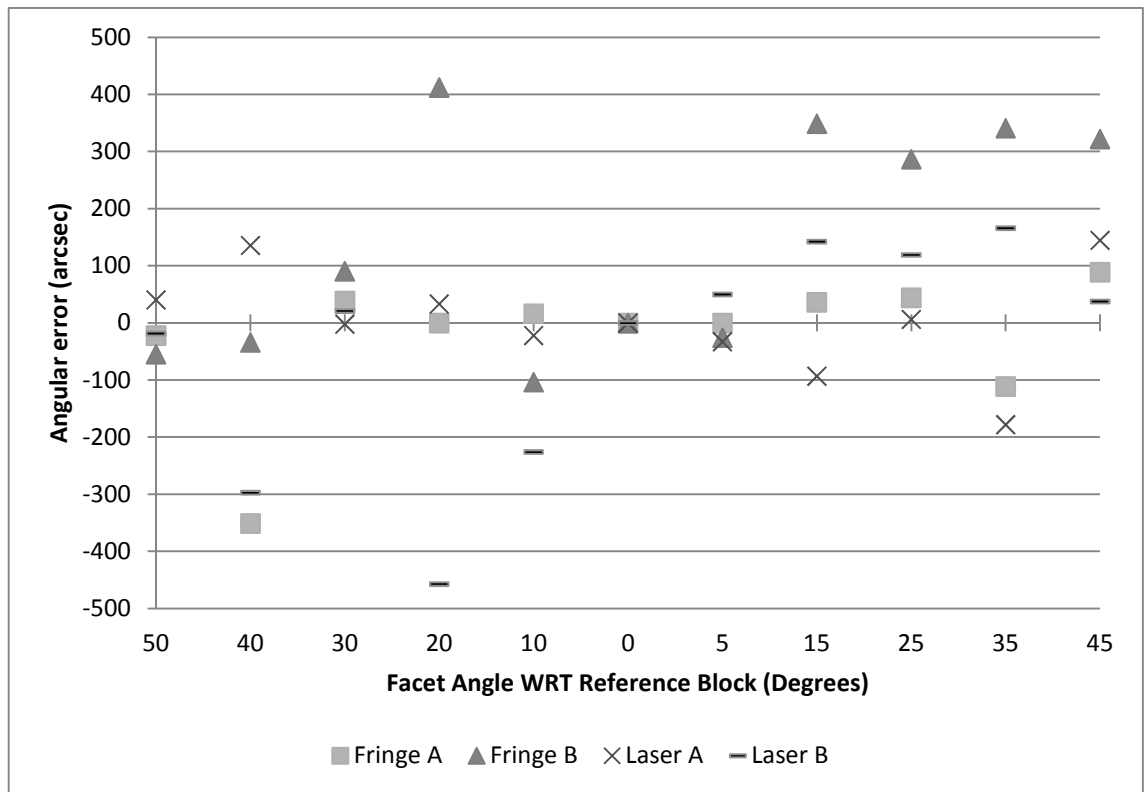
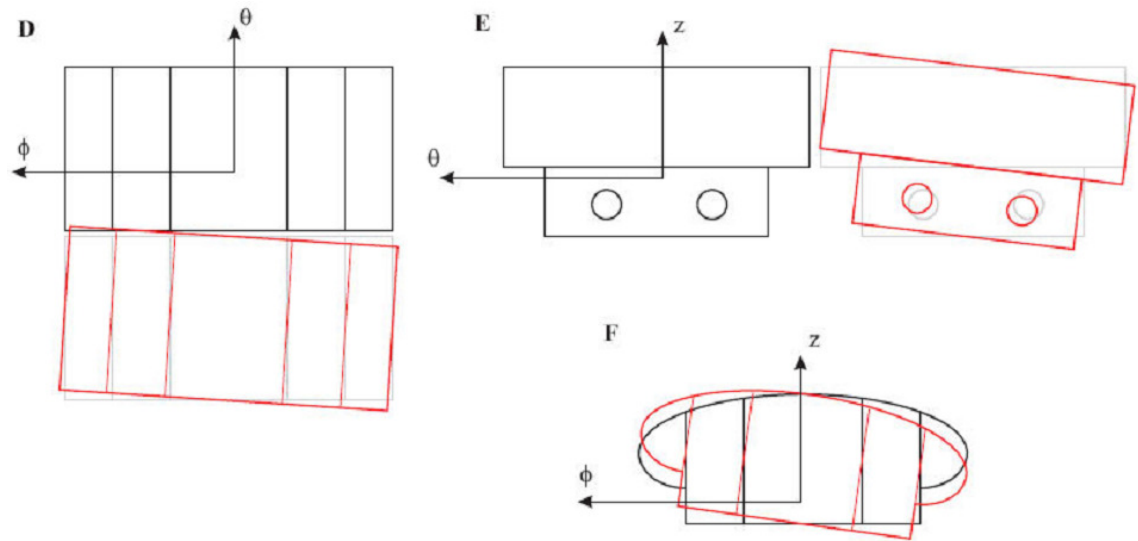


Figure 5.46: Angular error for in-plane approach. Data shown according to position on artefact.

In the case of using a limited area of a tile for registration and determination of 6DoF, any angular error will affect the registration. Several misalignment types exist between two tile assemblies with most relevance for this work being the case where one ‘end’ of a tile assembly is closer to the plasma than the other (Figure 5.47 F). The relative misalignment between adjacent tiles is 486 arc seconds (Vizvary, 2007), which all of the measurement systems tested can achieve. Where angular error near the maximum

## Primary Equipment Trial

permitted tolerance is combined with high uncertainty, the position of the tile assembly with respect to the plasma becomes more uncertain.



**Figure 5.47: Angular error misalignment types (Vizvary, 2007, p.8) courtesy of EFDA-JET**

**5.4.2. Depth of Field Test**

The purpose of this test is outlined in Section 5.2.3.2, with the data collection and processing method described in Section 5.3.3.3.

The impact of depth of field (measurement range) on the quality of the collected data was assessed by analysing planar sections on one of the angled blocks at different distances from the mounting plate. The test had most relevance to white light fringe projection systems as data were collected from a single position where the surface to sensor distance may vary throughout the measurement volume. Laser line systems surface to sensor distance can be adjusted for each collected profile and therefore the surface to sensor distance is less critical although adjustment is dependent on the abilities of the handling system.

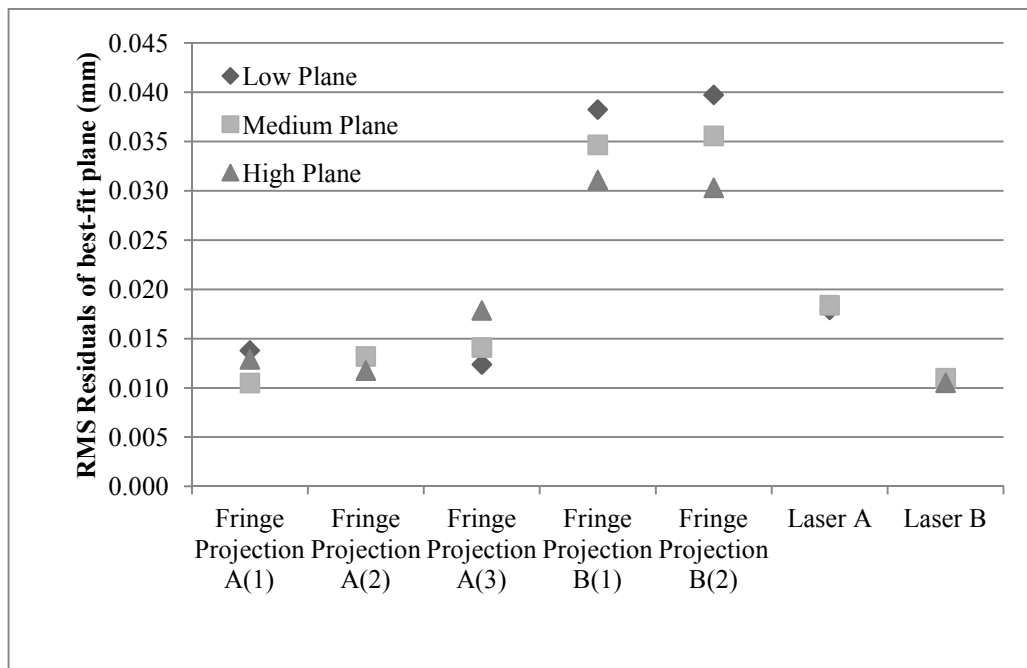


**Figure 5.48: RMS residuals of best fit planes at three depth ranges.**

An initial analysis, sectioned the data into 3 planes per data set (Figure 5.48) and demonstrated a trend within Fringe Projection System B that lower uncertainty occurred where data were closer to the sensing system. To clarify the results data were reprocessed and the test expanded to produce six planes, each covering 12mm in height normal to the mounting plate for each system.

The laser line systems collected data in multiple passes of the scan head over the surface, with the surface to sensor distance changing with each pass due to manual

handling. Because of the inconsistent sensor to surface distance, these data are not processed further.

Figure 5.49 shows two different white light projection measurement systems (A & B) with two or three measurement configurations of the system. Clear difference in the magnitude of the residuals could be seen between the two systems, system B having much greater random error than system A. System B uncertainty decreased as the data became closer to the sensor position, in line with results seen in Figure 5.48, both configurations B(1) and B(2) decreasing  $9\mu\text{m}$  from the ‘lowest’ plane to the ‘highest’.

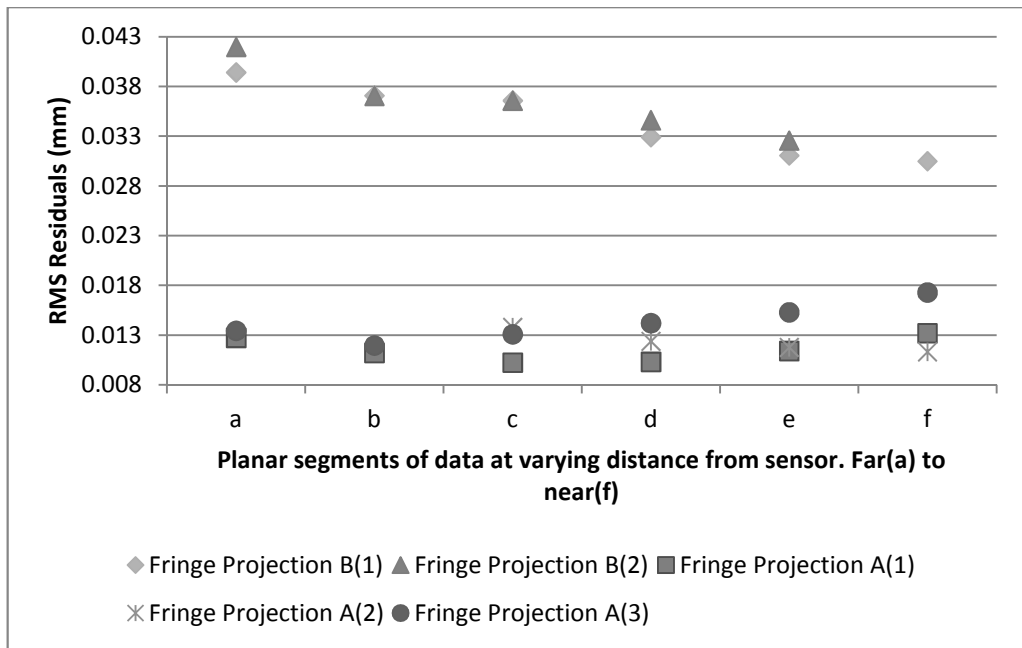


Figure 5.49: White light projection systems - RMS residuals of best fit planes at three depth ranges.

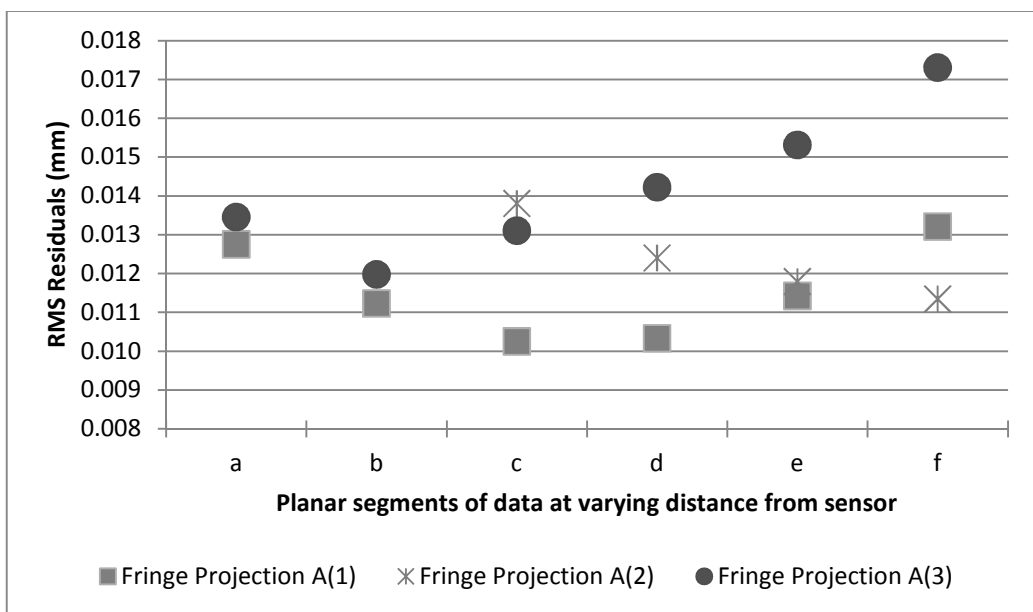


Figure 5.50: White light projection systems B - RMS residuals of best fit planes at three depth ranges - Optimised scale.

System A showed reduced uncertainty in comparison to System B with a maximum range of the residuals of  $5\mu\text{m}$ , to better show the data, they were plotted separately with adjusted scale to highlight the shape of the data (Figure 5.50). For configuration A(1) and A(3) a minima can be seen at plane C and plane B respectively which may have been the same surface to sensor distance, as sensor position may have changed during adjustment of orientation. The data indicate there is an optimal surface to sensor range for measurement System A with  $\sim 0.006\text{mm}$  increase in random error between planar data. Although System B data did not demonstrate a similar curve it did demonstrate a clear trend in the data to reduce random error as the surface approached the sensor. A minimum point would have been reached, although it could not be stated whether error would increase beyond a certain point. As distance of the sensor to the surface was not recorded during testing was not possible to quantify the ‘sweet spot’ of range seen in the collected data, but measurement of the range should be performed with any further work.

The results seen may be the result of optimal fringe spacing on the measurement surface due to perspective projection by the projector lens. As the distance from the projector to the surface increased, the spacing and width of projected fringes increased reducing the ability to record fine detail. This effect is similar to that seen with laser spot and line projection systems where the beam is optimally focused (smallest diameter) at a given range from the measurement system outside of which the beam will diverge. For measurement of fine detail at EFDA-JET, a  $0.006\text{mm}$  reduction in random error as seen for fringe projection A(3) in Figure 5.50 would be significant in increasing confidence in determination of a  $0.040\text{mm}$  step surface detail in the centre of a tile assembly.

Assumptions made for this test are that the sensor has uniform uncertainty with no areas producing data with increased error and that the complete artefact is within the calibrated depth of field of the measurement system.

### **5.4.2.1. Point spacing**

It has been shown that change in surface to sensor distance affected the measurement uncertainty of collected data and therefore it was of interest whether the density of collected data also differed with range. Using the three areas used to construct planes (Figure 5.48) the pitch of data points was calculated from a number of samples. A mean value was calculated by taking 11 random sample points and computing the distance to an adjacent point. Measurement was to the closest point except where data

Primary Equipment Trial

appeared to have an irregular structure e.g. laser line systems and irregular spaced point projection. Where a ‘pattern’ was discernible, approximately half of the measurements were to the closest point, with the remainder to the closest point on an adjacent ‘row’. The mean point to point distance takes into account inter-line spacing and not simply point spacing in a single row (Table 5.5).

<i>Data in mm</i> System & Setup	Low plane		Medium plane		High plane	
	Mean	St Dev	Mean	St Dev	Mean	St Dev
Fringe Projection A(1)	0.175	0.041	0.167	0.036	0.157	0.032
Fringe Projection A(2)	-	-	0.187	0.051	0.168	0.044
Fringe Projection A(3)	0.156	0.024	0.144	0.017	0.139	0.015
Fringe Projection B(1)	0.542	0.167	0.514	0.150	0.470	0.135
Fringe Projection B(2)	0.546	0.202	0.490	0.143	0.530	0.150
Laser Line A	0.220	0.005	0.222	0.007	-	-
Laser Line B	-	-	0.097	0.070	0.100	0.075

**Table 5.5: Point pitch on measurement surface.**

A large standard deviation value suggests some combination of the spacing between lines being different to the point spacing along a single line and data irregularity. To highlight the difference between systems, the standard deviation of Laser A is an order of magnitude less than that of Laser B, suggesting the point spacing on the measured surface was more regular in system A than system B, this conclusion is supported by viewing the measured points (Figure 5.51).

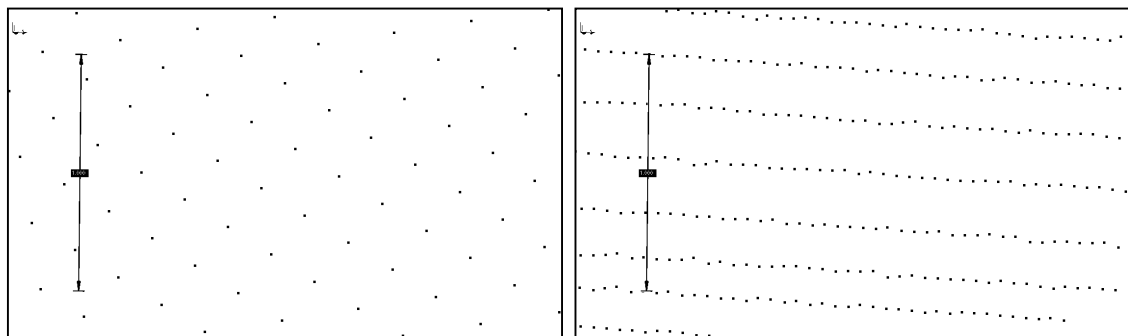


**Figure 5.51: Data point spacing: Laser line A (left), Laser line B (right)**

Calculating the point pitch along a single row of data from a laser line triangulation system (laser line B) and a column of data perpendicular to this profile allowed comparison of inter-line and intra-line spacing and the regularity of data in those orientations. For a ~15mm x 15mm planar area, point pitch along a single profile and perpendicular to that profile were calculated (Table 5.6). The standard deviation of the inter-line and intra-line point to point distances highlighted the difference in regularity

Primary Equipment Trial

of data collection, with distance along a single row/profile showing lower deviation than the motion of the scanner over the surface (Figure 5.52).

	No. Samples	Mean distance	Median distance	Standard Deviation of point pitch
Row/profile	284	0.054	0.053	0.005
Perpendicular to row/profile	174	0.085	0.066	0.069

**Table 5.6: Inter-line and intra-line point pitch for laser line system B (data in mm).**

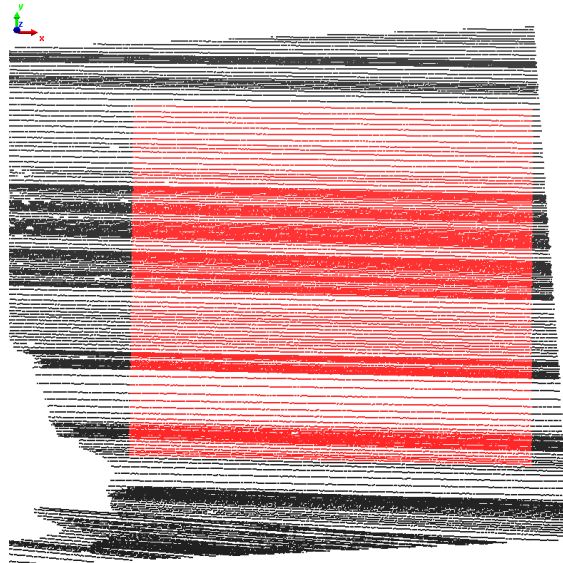


**Figure 5.52: Laser line system B data. 15mm x 15mm area highlighted, used for inter-line and intra-line point pitch calculation. Irregularity of the inter-line spacing is visible.**

For the two laser line systems tested no meaningful conclusions could be produced from the data as the range of the sensor to the measurement surface was not constant throughout the test as it was continuously moved to completely capture the surface. For the two fringe projection systems tested, in four of the five cases the mean point pitch on the measurement surface decreased as the range of the measurement surface to the device reduced. Explanation for this effect is perspective projection resulting in an increasing width of the projected fringes with increasing range. This effect combined with the ‘sweet spot’ for measurement seen in the Depth of Field Test suggested that limiting the measurement area would increase the ability of projection systems to capture data with lower uncertainty and greater ability to capture fine detail. Understanding point pitch was relevant for surface reconstruction where an increased number of sample points would be beneficial to constraint a surface. In the case of laser line systems with very different intra-line and inter-line spacing, correct selection of sensor orientation to surface detail would be required e.g. laser line perpendicular to surface discontinuities. This issue is covered in more detail in Section 5.4.3.2.

### Primary Equipment Trial

The use of resolution targets commonly used for the assessment of photographic recording could have provided details of the resolution of the measurement systems. The resolution of the measurement system at the given ranges would have provided quantitative data of the abilities of the measurement systems to detect and record fine detail. A method of determining resolution of optical 3D measurement systems is being developed by MacDonald (2010) (Section 6.3).

### 5.4.3. Edge Measurement

The purpose of this test is outlined in Section 5.2.3.3, with the data collection and processing method described in Section 5.3.3.4.

#### 5.4.3.1. Random Error & Step Height Measurement

Following data processing method 'i. Random error' (page 182) the results (Table 5.7) showed good agreement with those calculated during the Depth of Field test (Section 5.4.1.3).

System & Orientation	Plane 8	Plane 9
Fringe Projection System A: Parallel	0.012	0.012
Fringe Projection System A: 45°	0.011	0.010
Fringe Projection System A: Perpendicular	0.011	0.009
Fringe Projection System B: Parallel	0.056	0.061
Fringe Projection System B: 45°	0.034	0.032
Fringe Projection System B: Perpendicular	0.034	0.036
Laser Line A: Parallel	0.015	0.016
Laser Line A: 45°	0.014	0.013
Laser Line A: Perpendicular	0.016	0.016
Laser Line B: Parallel	0.014	0.013
Laser Line B: 45°	0.013	0.012
Laser Line B: Perpendicular	0.015	0.011

**Table 5.7: Standard deviation of residuals to least squares best fit planes (mm) at various orientations to the edge feature.**

Measurements were taken from the artefact mounting plate to the least squares best fit planes and the height difference between adjacent planes calculated (Table 5.8). One data set per system was used to measure the step height. Data for the white light systems were from a set collected in a method optimal for that system, selected by the operator. Results for laser line systems were collected with the line parallel to the step edge. For all systems data within 2mm of an edge were not used for the test.

Primary Equipment Trial

Step	Nominal	CMM	GapGun	Fringe A	Fringe B	Laser A	Laser B
1-2	0.02	0.015	0.02	0.016	0.016	-0.023	0.017
2-3	0.03	0.023	0.03	0.016	0.036	0.064	0.033
3-4	0.04	0.043	0.04	0.032	0.043	0.050	0.041
4-5	0.10	0.102	0.11	0.101	0.079	0.066	0.106
5-6	0.20	0.201	0.21	0.205	0.237	0.210	0.196
6-7	0.30	0.298	0.31	0.296	0.282	0.308	0.300
7-8	0.50	0.507	0.52	0.518	0.477	0.490	0.496
8-9	1.00	0.999	1.02	0.976	1.031	1.018	1.015

**Table 5.8: Nominal and as-built step height between blocks. CMM data  $\pm 0.003$ mm. All data in mm.**

To better understand the data, the deviation of the calculated step heights from the touch probe nominal data were calculated (Figure 5.53). Large deviations were seen for area based A and laser A, up to 0.040mm. Investigating some of the errors seen, laser line A calculated step 1-2 as -0.023mm and 2-3 as 0.064mm (Table 5.8). For those deviations to occur block 2 must have been recorded as shorter than actual, causing the negative and positive deviations seen. Similar errors were seen for step 4-5 and 5-6 for system area based B. A single measurement result was dependent on two height measurements therefore an error on one block would have affected two step height measurements.

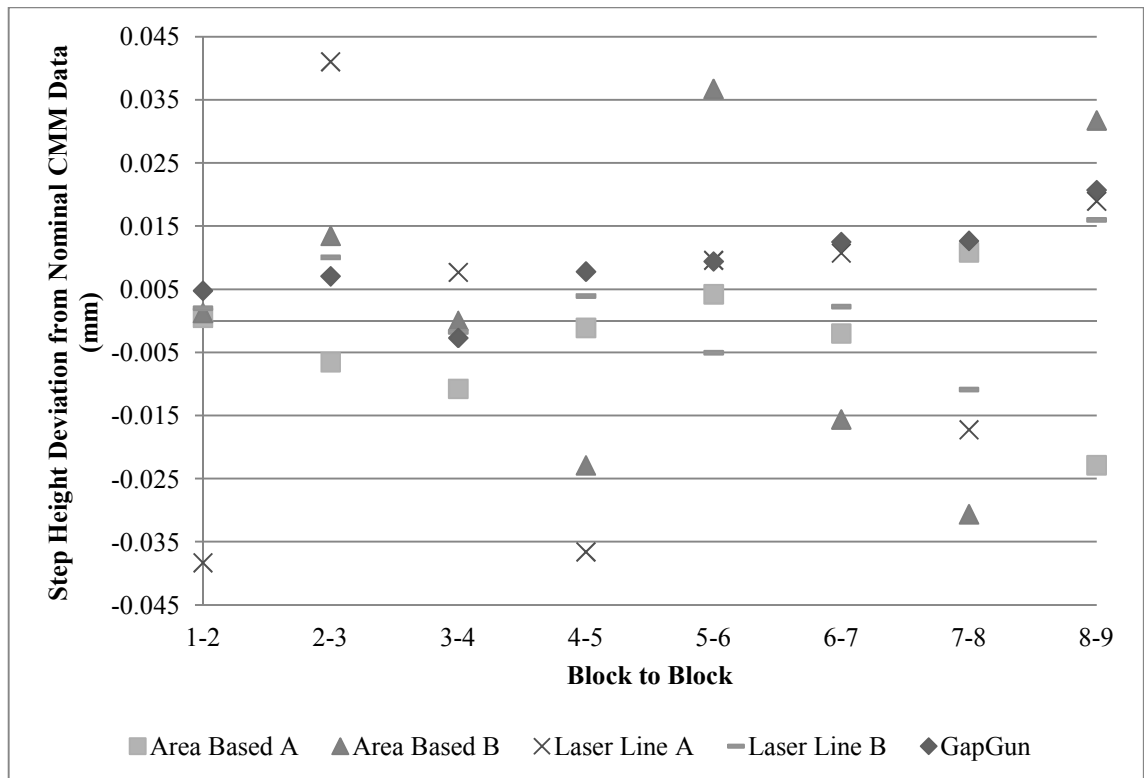


**Figure 5.53: Step height (flush) deviations from touch probe data (mm).**

The significance of deviations seen in Figure 5.53 reduce along the X axis as the as-built step height increases. To better analyse the data they were plotted with the deviation as a percentage of the actual step height from the CMM data (Figure 5.54).

### Primary Equipment Trial

To show the effect more clearly the data were plotted with a limit of 50% of the as-built step height shown (Figure 5.55). Note that some data are not shown as they exceed 50% of the step nominal.

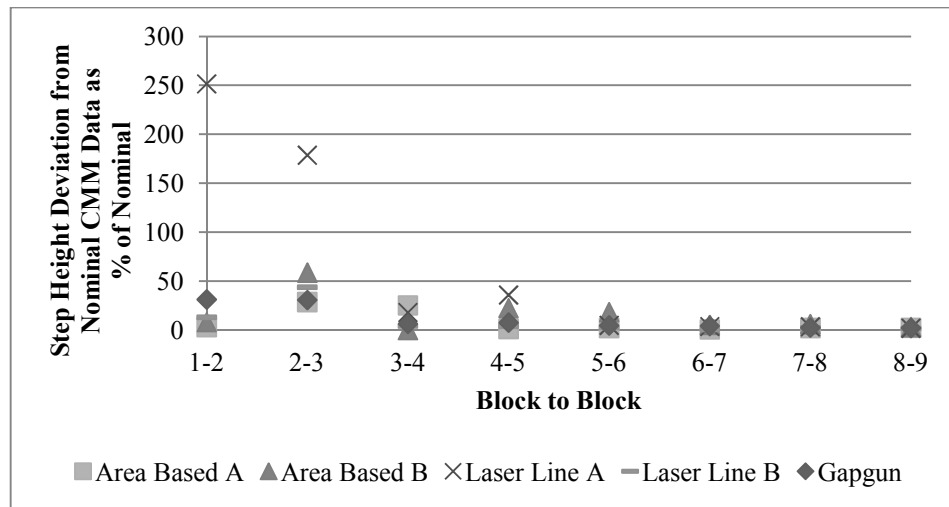


Figure 5.54: Step height deviation as percentage of as-built step height

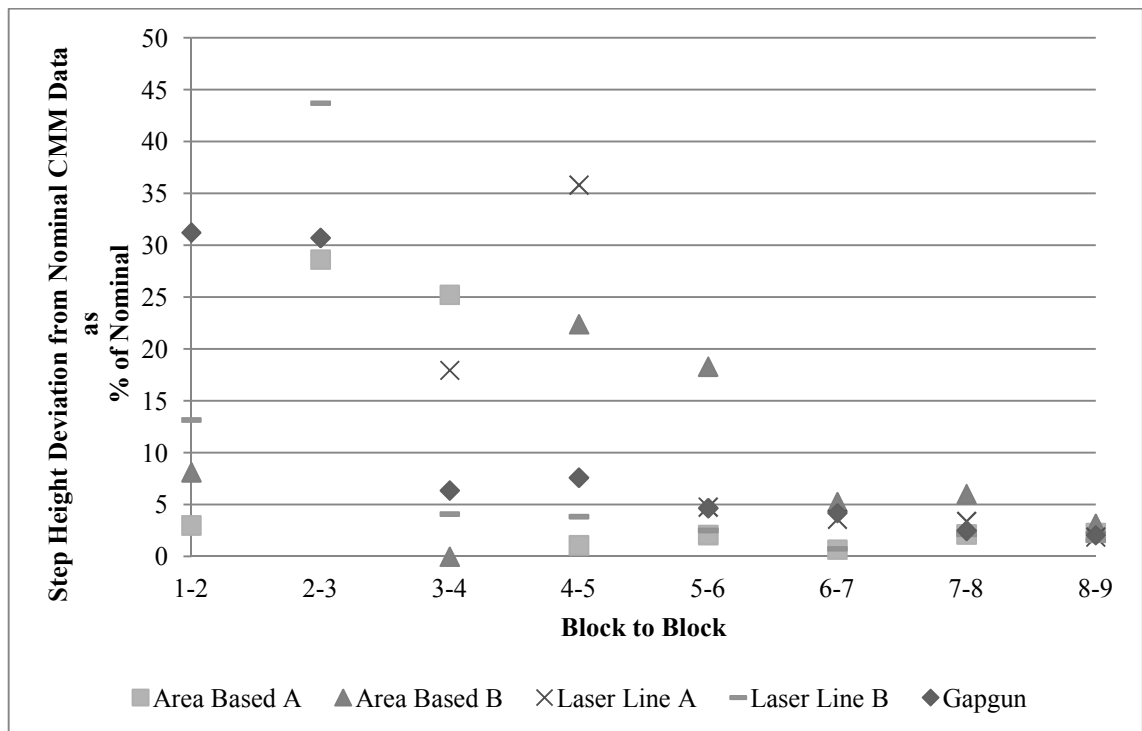


Figure 5.55: Step height deviation as percentage of as-built step height - limited to 50% of actual height.

The structural resolution limit (Robson et al., 2011) for laser line systems defines the response time as the distance taken for the measured height to go from 10% to 90% of the calibrated height along the scanning direction and sets a convenient limit for a measured response of 20% of deviation. Applying a 20% deviation against the systems tested in this work indicates that three of the four systems tested could detect the

## Primary Equipment Trial

0.015mm step. However, highly variable error have been observed whilst measuring edges with these systems making repeatable measurement challenging such that only at step 5-6 (0.201mm) and above did all systems present deviation below 20% of the measured step height. No system presented deviation below 20% for all steps. Area based A presented the 'best' data with all values below 30%, however for step measurement laser line B would have been be most suitable as it was capable of measuring down to the 0.043mm step whilst maintaining measurements within 5% of the nominal

In addition to measuring the distance between surfaces there may have been a necessity to distinguish between data on those surfaces. Table 5.7 shows these non-contact optical measurement systems were capable of producing data with RMS error/standard deviation of  $\sim 0.015\text{mm}$  for the given surface. Using only data within  $\pm 1$  standard deviation of the plane mean ( $\sim 68\%$  of data points assuming normal distribution), the minimum step height between adjacent planes which could be identified would have been 0.030mm. The as-built dimensions of the step artefact showed the smallest three height differences to be: 0.02, 0.03, 0.04mm, therefore it may have been possible to differentiate between the two planes separated by 0.03mm. If data within  $\pm 2$  standard deviation were used ( $\sim 95\%$  of data points), the minimum distance rose to 0.060mm.

Table 5.8 and Figure 5.55 show some systems could measure a 0.015mm step height/flush, however for adjacent surfaces there was a question as to how these areas of data were to be differentiated, when  $\pm 1$  standard deviation of each surface yielded a minimum determinable step height/flush of 0.030mm. Uniquely identifying areas based on standard deviation alone would have required the use of data within  $\pm 1$  standard deviation of each planar area to achieve a useful detection method for this work. For the 0.015mm high step, misclassification of data would be highly likely (Figure 5.56) but was not present for any of the systems for a 0.201mm step height (Figure 5.57). For the 0.015mm step, area based A produced no data within 1 standard deviation of both planes (no red data), because of a low RMS residual/standard deviation of 0.003mm for each plane (Table 5.9). Data for area based A was the amalgamation of multiple images including outlier detection and removal in the manufacturer software and was collected to show the 'best' data the system could collect on the artefact surface.

Primary Equipment Trial

	Plane 1	Plane 2
Area Based A	0.003	0.003
Area Based B	0.026	0.026
Laser Line A	0.017	0.022
Laser Line B	0.013	0.014

Table 5.9: Standard deviation of residuals normal to least squares best fit planes. Plane 1 & 2. MM.

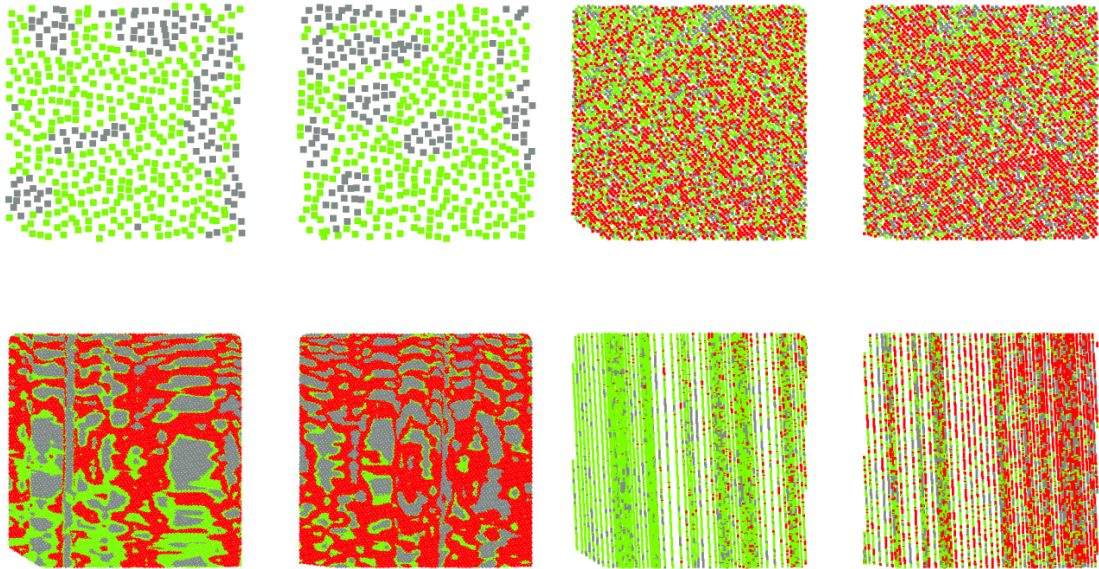


Figure 5.56: Plane 1&2 (0.015mm flush) of step artefact viewed from above. Top left-bottom right: Area Based A, Area Based B, Laser Line A, Laser Line B. Green points are  $\pm 1$  standard deviation of a best fit plane. Red points are  $\pm 1$  standard deviation of both planes. Grey points are greater than  $\pm 1$  standard deviation.

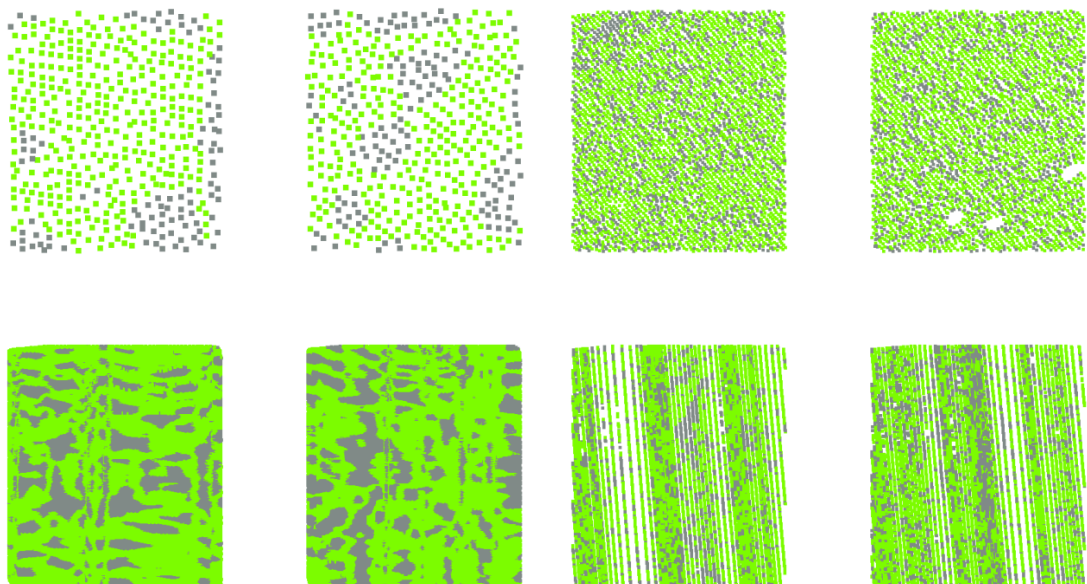


Figure 5.57: Plane 5&6 (0.201mm flush) of step artefact viewed from above. Top left-bottom right: Area Based A, Area Based B, Laser Line A, Laser Line B. Green points are  $\pm 1$  standard deviation of a best fit plane. Red points are  $\pm 1$  standard deviation of both planes. Grey points are greater than  $\pm 1$  standard deviation.

Using the standard deviation of planar areas would be highly sensitive to the parallelism of the planes i.e. if the two planes were not parallel and the step height suitably close to the standard deviation of the measurement system, data may be miscalculated as being within  $\pm 1$  standard deviation of both planes. Where the angle between adjacent planes is small, a large portion of the data may be misclassified. The quantity of data misclassified would be dependent on the standard deviation/RMS error of the best fit planes, the angle between the two planes and the step height between surfaces.

The method developed in this work was unsuitable for the extraction of data relating to individual facets where standard deviation (random error) of the data is greater than or equal to half the step height between adjacent planes. In these cases, data could not be extracted without reliance on good registration to nominal or as-built CAD. Where data were approximately registered to a nominal model and standard deviation of error less than half the smallest step height between adjacent planes, a seed point could be created on each facet of the nominal CAD of an EFDA-JET ITER-Like wall tile. From the seed points, least squares best fit planes could be ‘grown’ using the standard deviation value obtained from these tests to determine where plane growing should end. This technique would allow feature extraction of planar facets from an approximate registration and once complete could be used to improve data registration. Data segmentation algorithms already exist in commercial and open-source software however, any reliance on the surface normal of point data to limit the plane may be unsuccessful as the facets of the EFDA-JET tiles had only small angular change between them and this is where the method developed in this work is of value.

### **5.4.3.2. Assessment of edge measurement**

Given the plane growing technique for feature extraction proposed in Section 5.4.3.1, the edge of the planar areas would cease to be part of that area. As the manufactured edge features a radius (nominal 0.05mm), it was investigated how the edge profile appears and whether a clear definition between planar areas could be identified. Of the four measurement systems tested each demonstrated different abilities to capture a step edge. Data of the step artefact were registered to the as-built CAD model excluding the use of data within 2mm of an edge. Profile images were collected through the data with a 20mm profile width to qualitatively assess the performance of the systems against a 1mm step edge (Figure 5.58). Data from each measurement system are presented by column, four to six profiles are presented for each system, each profile showing a

different configuration of the system e.g. orientation of laser line/projected fringe to the surface discontinuity.

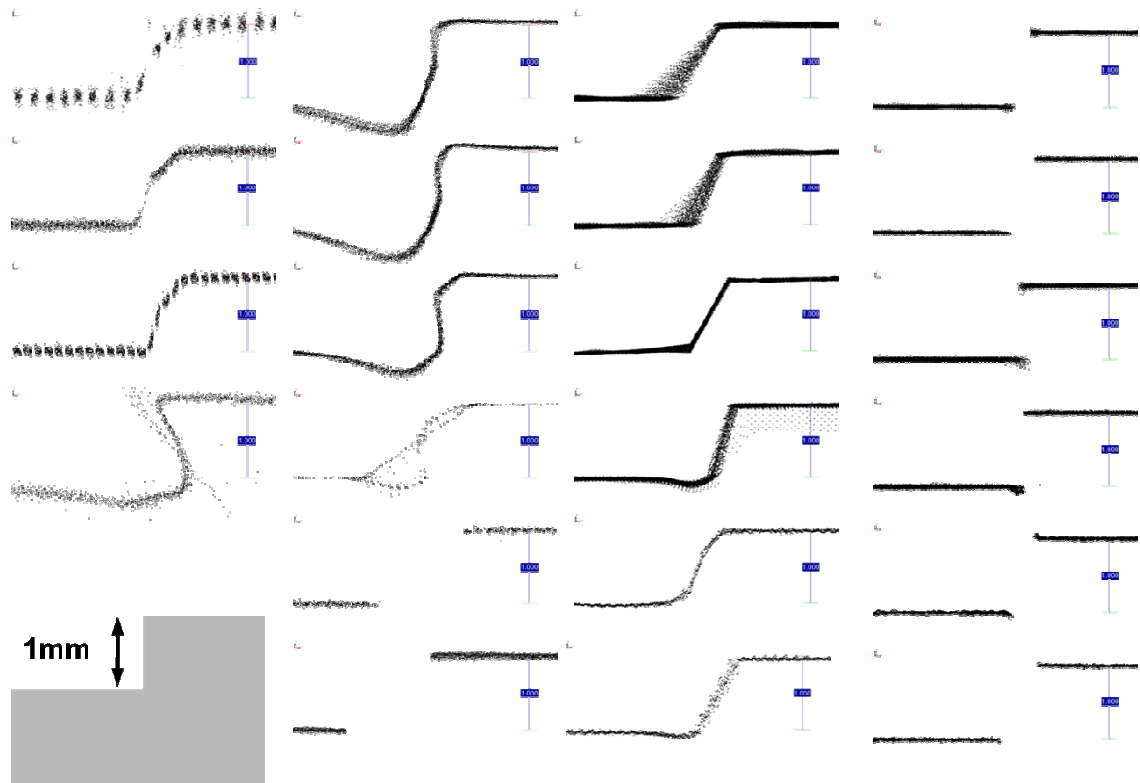


**Figure 5.58: Edge profiles of a 1mm step edge with nominal edge radius of 0.05mm, generated by four measurement systems (Left to right: Fringe Projection B, Fringe Projection A, Laser A, Laser B).**

Clear differences between the two technologies (laser line and white light fringe projection) and between each implementation were seen, with no system producing a profile image matching the nominal profile shown. These differences demonstrate that at least three of the four systems tested introduced errors into the data around edge features, with a high likelihood that all four systems introduced errors. The errors demonstrated could have affected interpretation of the data and in turn, the meaning of the data for EFDA-JET. Additionally, comparison of data collected by different measurement devices would have been impossible as each introduced different error signatures.

## Primary Equipment Trial

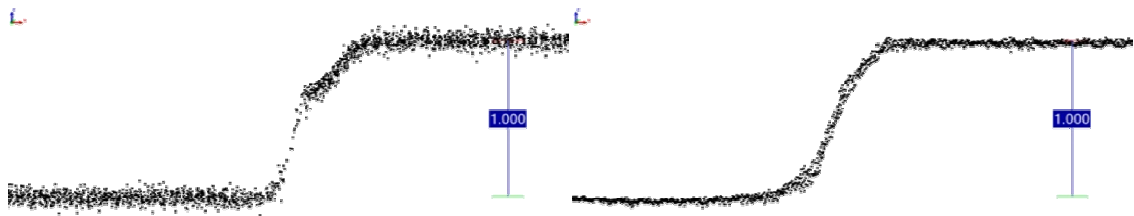


**Figure 5.59(a & b): Edge profiles. Fringe projection B (left), Laser line A (right).**

An example of possible misinterpretation of data is in Figure 5.59a, which is a profile from fringe projection system B. These data show downward curvature of the upper surface which without other evidence would suggest the surface has eroded. For EFDA-JET, investigation of the surface may have resulted in the removal of the tile from the machine to ascertain the cause of the erosion at considerable cost (Section 2.4.4). Compared to other profiles of the same edge from other systems, the same effect was not seen and therefore the measurement system was adversely affecting the data. Figure 5.59b shows downward curvature for the upper plane and upward curvature on the lower plane suggesting that the upper plane had been eroded / melted and material deposited on the lower surface.

These data demonstrated that each of the measurement systems trialled introduced errors into the collected data with significance for a 1mm step edge between surfaces. The initial indications were that the non-contact measurement systems trialled could not perform edge measurement with required accuracy at these dimensions however, quantitative analysis was required to ascertain the magnitude of the discrepancies and if they would affect EFDA-JET. Quantitatively assessing the ability of measurement systems to record data close to an edge would have required traceable measurement data of the artefact. Full surface data could not be obtained from the touch probe CMM because of the small step sizes of the artefact (Section 5.2.1.6). As-built data of the top planar surfaces of the steps existed but the position of the vertical area joining adjacent planes was unknown. The existence of only horizontal data meant that exact registration of data to the as-built CAD model could not be performed because the data did not constrain the motion in all three axes. Because of this, registration to the planar horizontal facets was performed although full constraint in the XY plane was not possible as no edge data were used. The lack of as-built data and insufficient constraint in the collect data presented a challenge for quantitatively assessing the abilities of the measurement systems to record edge data, however an assessment could be made against the assumption of a square edge profile in the physical artefact.

## Primary Equipment Trial

For this test the nominal 1mm step between plane 8 and plane 9 (lower and upper respectively) was used, the standard deviation of each plane for the data sets used can be seen in Table 5.7. The results were calculated using the novel method developed for this research and detailed in Section 5.3.3.4, iii. Quantitative Edge Measurement, (page 182) and presented in Table 5.12.

As a reference, the step was measured with a GapGun laser gauge (Section 3.2.4.2) at three positions, using sixteen measurements per position, the resulting mean step height was 1.02mm and mean gap of 0.07mm. The GapGun was an optical measurement device designed for step (flush) and gap measurements. The GapGun collected a profile of a laser line projected onto the measurement surface perpendicular to the edge to be measured and as such may have been affected by similar problems to the laser line systems under test. Laser Line B with line perpendicular to the edge produced results with smallest deviation to the GapGun result. The mean distance was calculated as the mean absolute distance for 10-12 samples per edge calculated to the best fit plane on adjacent surface, resulting in 20-24 measurements.

		Min	Mean	Max
Fringe System A	Parallel	1.210	<b>1.247</b>	1.310
	~45°	0.062	<b>0.224</b>	0.606
	Perpendicular	0.335	<b>0.382</b>	0.433
	Optimised	1.413	<b>1.467</b>	1.555
Fringe System B	Parallel	0.187	<b>0.379</b>	0.619
	~45°	0.482	<b>0.518</b>	0.607
	Perpendicular	0.346	<b>0.425</b>	0.491
	Optimised	0.166	<b>0.402</b>	0.505
Laser Line A	Parallel Optimised	0.743	<b>0.817</b>	0.923
	Parallel Un-optimised	0.670	<b>0.738</b>	0.829
	~45° (1)	0.527	<b>0.620</b>	0.781
	~45° (2)	0.333	<b>0.384</b>	0.453
	Perpendicular Optimised	0.221	<b>0.259</b>	0.305
	Perpendicular Un-optimised	0.471	<b>0.590</b>	0.805
Laser Line B	Parallel Optimised	0.415	<b>0.520</b>	0.627
	Parallel Un-optimised	0.699	<b>0.863</b>	1.082
	~45° Optimised	0.225	<b>0.261</b>	0.301
	~45° Un-optimised	0.353	<b>0.407</b>	0.549
	Perpendicular Optimised	0.015	<b>0.117</b>	0.275
	Perpendicular Un-optimised	0.041	<b>0.092</b>	0.135

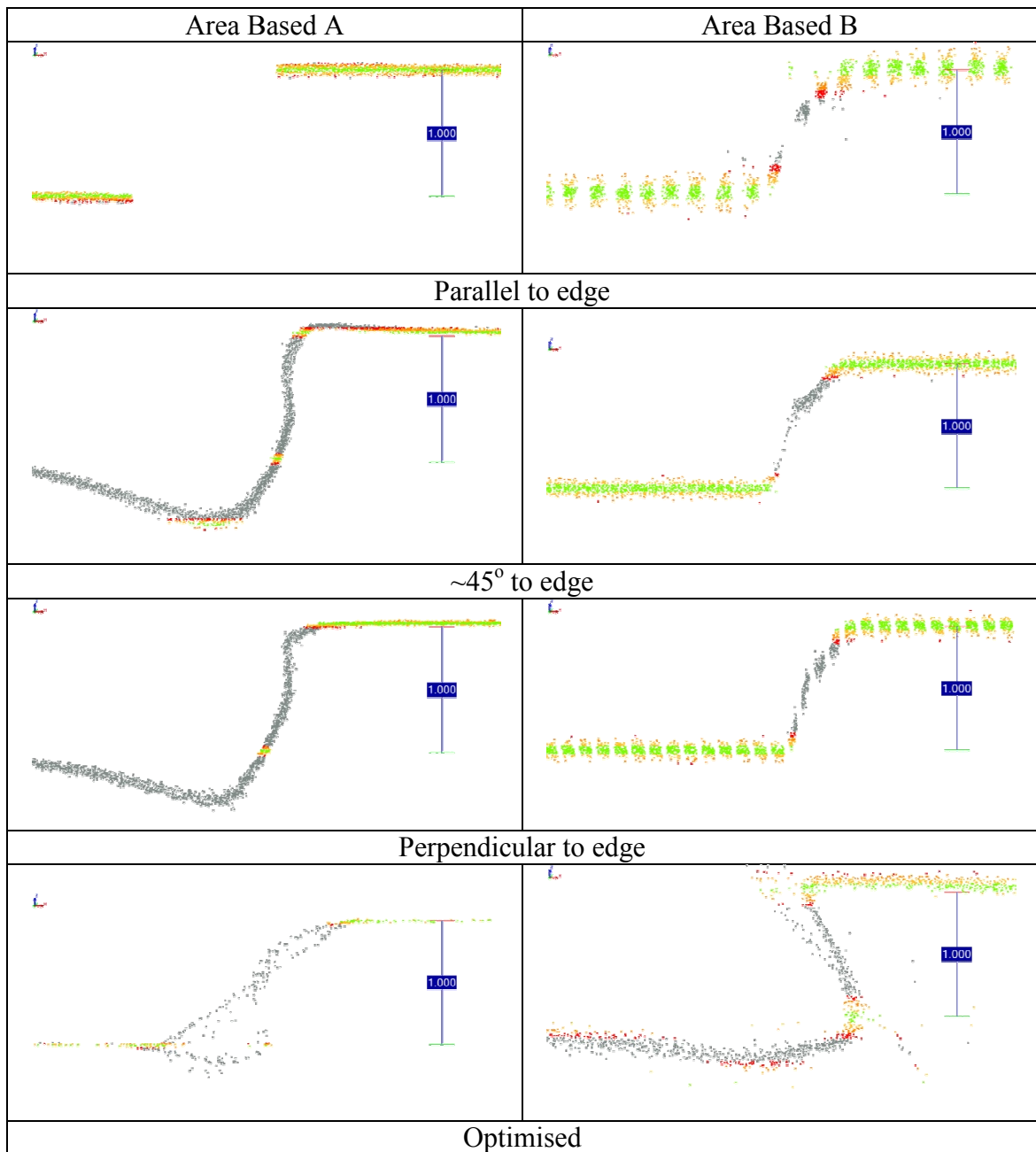
**Table 5.10: Calculated horizontal (gap) distance between Step 8 & 9 (mm).**

Table 5.10 provides quantitative data of the ability of systems tested to measure the gap distance between two adjacent planes. Results were calculated on the basis that data with residual to the plane of greater than 3 standard deviations no longer formed part of that plane. Measurements could be made without perfect registration, requiring strong constraint in a single axis. The method of calculation was imperfect as it did not take into account a situation where there is a negative distance between surfaces e.g. the areas overlap, or where the calculated edge points are not contiguous with the remainder of the surface data. Of the two problems noted, the first appeared only within the fringe projection systems tested (Figure 5.60, Area Based B, Optimised), whilst the second problem occurred for fringe project and laser line technologies (Figure 5.61 & Figure 5.62). Alternative methods to that developed for this work, would have been to use a fixed value equivalent to the nominal edge radius of 0.05mm or to take a profile of the edge and calculate the points of inflection to determine the edge positions. Using the standard deviation of residuals to a plane was selected as it was capable of generating the required information quickly and with minimal processing. Time inside the EFDA-JET vessel during a shutdown period was valued at £15.5k/hour (Section 2.4.4) and so where necessary, decisions from data were to be produced as quickly as possible.

### White Light Fringe Projection Systems

Profiles of a 1mm step imaged by the fringe projection systems tested are shown (Figure 5.60) with the standard deviation of each plane (Table 5.7) affecting the selection of where a planar surface ends and an edge begins. Note each plane has a standard deviation value which affects the colouring of points for each plane, a constant value is not used.

Primary Equipment Trial



**Figure 5.60: Profiles of 1mm step coloured by number of standard deviations from best fit plane.**

Area measurement system A at 45° to the edge highlighted a situation where multiple errors were present in the data which resulted in an incorrect estimation of the distance between ‘usable’ data on the planar surfaces. Usable data were classified as data within  $\pm 3$  standard deviations of the planar surfaces. The upper surface presented a rise towards the edge of the plane, with the identified edge data being non-contiguous with the remainder of the data, this rise was not seen in other configurations of system A, nor is it seen in system B in similar orientation ( $\sim 5^\circ$  difference between systems for this position). For the same data the lower plane (plane 8) curved downward towards the plane edge (Figure 5.61) which affected an area  $\sim 2.2\text{mm}$  from the calculated edge and dropped  $\sim 0.48\text{mm}$  from the calculated plane for block 8. The  $\sim 0.48\text{mm}$  drop coincided

with the 0.5mm nominal step of the next block and resulted in certain points seen in Figure 5.62 being incorrectly identified as part of block 7.

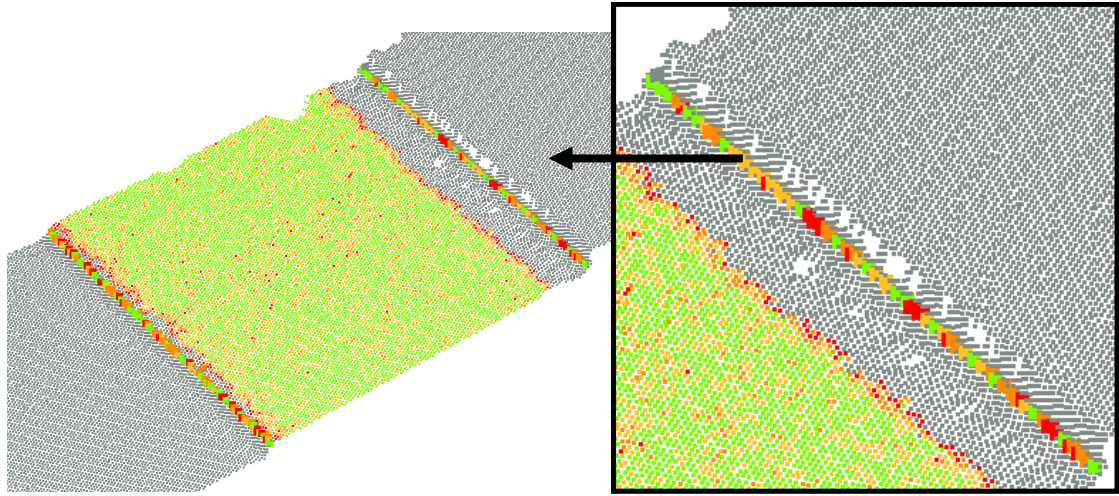


**Figure 5.61: Area A (~45°) angled view showing plane 8 (coloured) between plane 7 and 9. Edge points seen enlarged, separated from main area of plane 8 by 'dip' in the surface.**

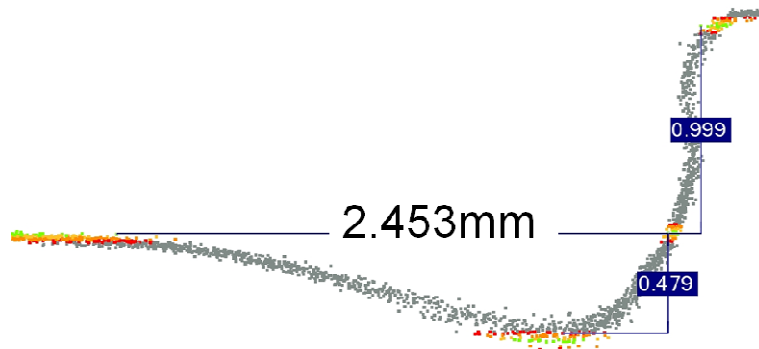


**Figure 5.62: Profile image of Area system A (~45°). Data on the lower plane (plane 8) drops 0.479mm below calculated plane, coinciding with the height of plane 7. This would cause these 'low' points to be wrongly associated with plane 7 instead of plane 8.**

The dip in the lower surface was present for fringe projection system A but not system B and did not appear where the projected pattern was parallel to the edge. A possible explanation is multiple reflections from the vertical area joining plane eight and nine, onto the edge of plane eight (lower horizontal). Multiple reflections between surfaces will affect the fringe pattern and contrast of the image recorded by the sensor(s) and subsequently affect the phase unwrapping process (Section 3.2.4.3). As data were collected on the vertical area, multiple reflections must have occurred or the projection system was not normal to the horizontal surface and was directly illuminating the vertical area. In both situations reflection may occur. The height (flush) between steps was ~1mm and the horizontal affected area was >2mm, therefore reflection alone could

## Primary Equipment Trial

not explain the  $>2\text{mm}$  affected area. A qualitative assessment of the data showed the affected area of the lower plane was reduced as the step height reduced (Figure 5.63), highlighting the association between size of the vertical area joining the two surfaces and the erroneous curved area. The curve joining the lowest area of data and the bulk of data on the plane surface may have been the result of some averaging function in the unwrapping process.

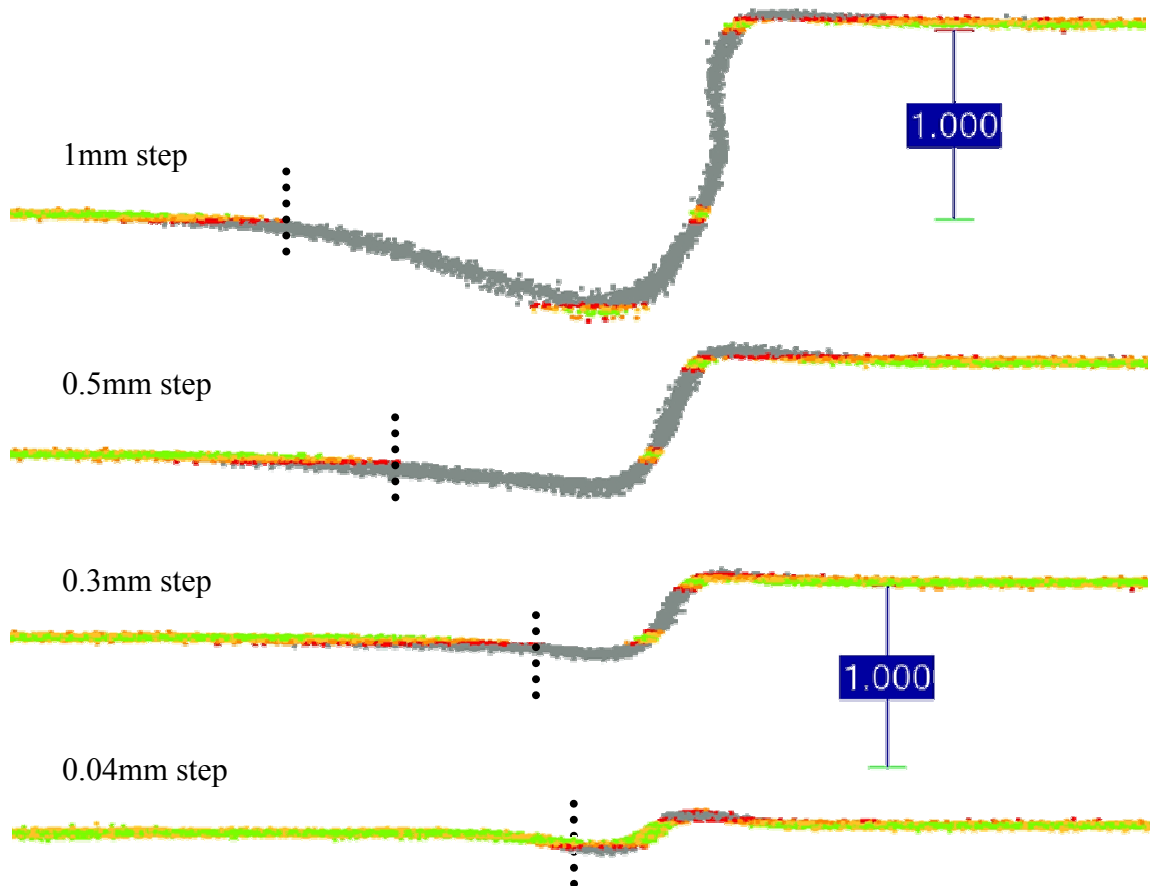


**Figure 5.63: Qualitative assessment of link between step height and affected area of lower plane.**

In the parallel orientation, fringe projection system A recorded  $\sim 1.2\text{mm}$  distance between the horizontal planes where no data were collected. Without accurate registration of data to a model it was not possible to determine whether data were absent on both planes or only one. Any misalignment of the projector with the surface normal could have resulted in an area of the lower plane (plane eight) being shadowed by the plane closer to the projector. However to shadow  $>1\text{mm}$  would have required the projector to be  $\sim 45^\circ$  to the surface normal, which was not the case during data collection. Within the affected region only one of the two sensors would have had

visibility of the affected area however this would only have affected the grey-code part of any measurement process, as the phase-shift process did not require known angle between light source and sensor. It is believed the surface discontinuity created difficulty in uniquely identifying the individual fringe numbers resulting in error in the unwrapping process and no outputted data for this area.

Area based B measurement system presented a downward curve in data on the upper plane (plane 9) with data separated by 0.4-0.5mm (Table 5.10). Taken the ideal case of the Nyquist limit where one pixel is the maximum required to identify a bright fringe; the calibrated measurement area and pixel count of the sensor(s) used, each pixel imaged a surface area of  $\sim 0.34\text{mm}^2$  ( $0.14 \times 0.17\text{mm}$ ) in this particular imaging configuration. Over this area light reflected from the surface will have been averaged and a single intensity value produced. Assuming the projected pattern was sinusoidal, the averaged intensity value will have been correct for the centre of the area imaged. Where the sensor imaged a non-continuous surface, the averaged value will have been incorrect unless the sensor path was coincident with the projector path, which it was not. Dependent on the alignment of the sensor with the surface discontinuity an area of  $\sim 0.34\text{mm}^2$  may have been affected, with incorrect intensity value recorded, affecting calculation of the phase and range. Assuming a square pixel just overlapping a worst case edge at  $45^\circ$ , the  $\sim 0.34\text{mm}^2$  pixel footprint would have hypotenuse 0.22mm, resulting in data within this distance of an edge being subject to systematic error. Applying this to both surfaces would have resulted in data within 0.22mm of the edge centre being affected, this result has good agreement with the 0.4-0.5mm distance calculated and shown in Table 5.10.

Had the number of pixels on the sensor been increased, the pixel footprint would have decreased and improved the ability to measure close to an edge. However, pixel footprint is not the sole factor in determining the minimum measurable distance to a surface discontinuity, with one of the key variables being the principal distance of the projection and sensing systems. Alteration of these and the distance of the system to the surface would have affected the calibrated measurement volume and the angle of light directed to a single pixel e.g. increasing the principal distance would have reduced the measurement area but decreased the angle of light entering the sensor thereby increasing edge measurement ability.

Laser Line Systems

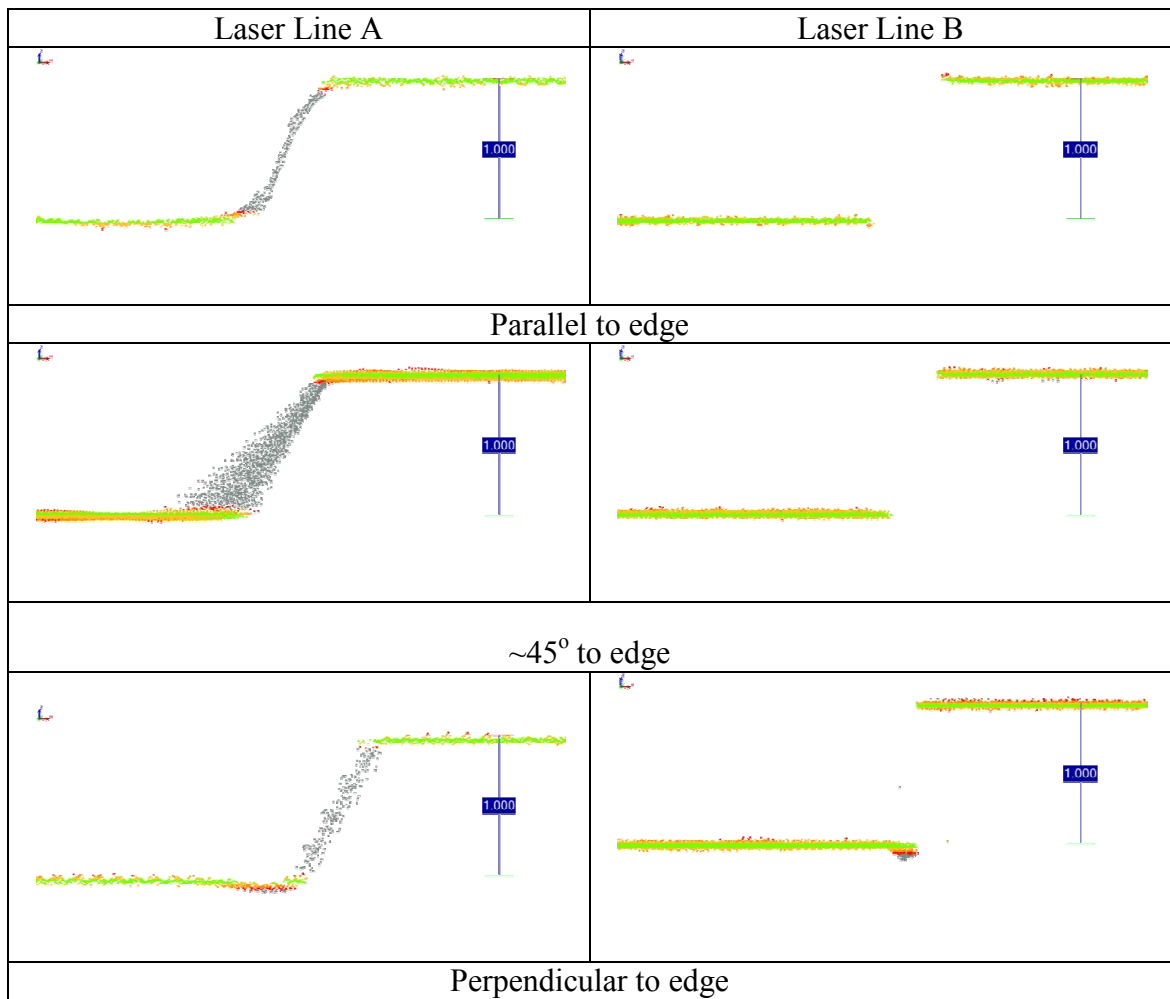


**Figure 5.64: Profiles of 1mm step coloured by number of standard deviations from best fit plane.**

Values in Table 5.10 indicate the two laser line measurement systems have similar ability to measure to an edge, however the profile of the 1mm step showed the two systems produced very different data (Figure 5.64). Laser line system A showed the two planes connected by point data whilst laser line system B had a clear separation between planes with no connecting data. With laser line parallel to the edge, laser line system A produced data where the upper and lower plane fell and rose respectively to meet each other. For the same orientation Laser line system B collected no data. As the laser line was parallel to the edge occlusion is likely to have occurred (Section Figure 3.31) causing the rise of the lower plane as the projected line was not fully visible to the sensor, resulting in a change in the computed centroid of the laser line/spot. The quantity of data on the area between the planes suggested the projected laser line was not parallel to the planes surface normal; in this case the line would have struck the 1mm vertical plane between the steps and have been spread over a large area due to the

glancing angle. With the illumination source not parallel the possibility of reflection onto an adjacent surface was also possible (Figure 5.65).

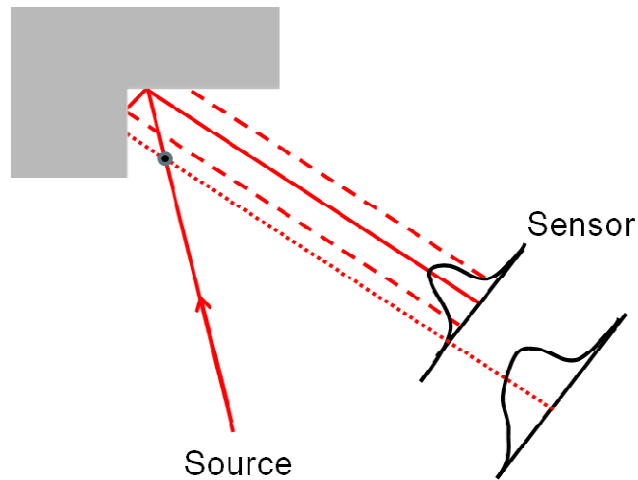


**Figure 5.65: Effect of reflection on laser line/point intersection (After Nitzan (1988))**

The lack of data from laser line system B when compared to system A suggested the internal arrangement of illumination source and sensor were not the same for the two systems. It is proposed that in the direction of motion the illumination source preceded the sensor for system A, whilst for system B the sensor preceded the illumination source. This proposal is not conclusive as the systems featured a variety of internal filtering algorithms which could have altered data acceptance criteria, particularly when non-cooperative surfaces were being measured. Even with a possible difference in internal configuration, laser line A produced a large amount of data which could be considered unreliable whilst system B appears to have taken a more cautious approach and collected/produced no data in the same area. Processing of collected data performed within the measurement device is likely to have affected the output data, with one system having presented regularised data with interpolation which are an integral part of the system.

With the laser line at approximately  $45^\circ$  to the edge, the system A edge profile shows a large amount of data connecting the two planes., when the same data was seen from above the cause could be seen as a 'jagged' edge (Figure 5.66). The jagged profile was caused by aliasing where each projected spot of fringe overlapped the edge to a varying degree dependent on the line/fringe orientation to the edge. The error appeared to be compounded for laser line system A due to interpolation within the measurement system before data were passed to software.

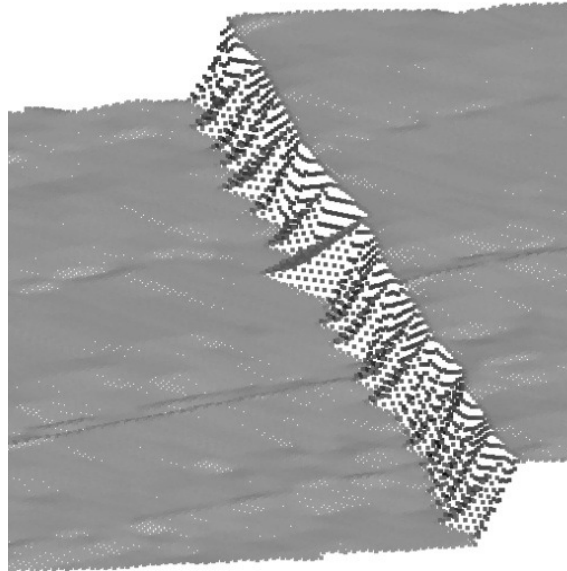


**Figure 5.66: Laser line A, 45° to edge**

With the laser line perpendicular to the edge system B achieved the smallest mean distance of the systems trialled at 0.092mm between planes. This value compared well with the 0.07mm distance calculated by the GapGun laser gauge which was a device designed specifically for the task. A profile of the edge collected by the laser gauge (Figure 5.67) shows good agreement with laser line B in the perpendicular case, including a downward curve of the lower plane. As the GapGun and laser line systems operated using a similar principal, (with system B being the closest of the two laser systems tested to the gauge), it was to be expected that laser B would produce data most similar to the GapGun reference data. The close agreement between GapGun and laser line B measurement data and profile (Figure 5.67) suggested some filtering approach was being used by the GapGun to reject outlying data and calculate its gap measurement. Such an approach may have been the removal of ‘known’ error signatures prior to application of the step/gap calculation method. A similar method could have been applied to laser line B measurement data, assuming individual profiles could be extracted from the data. A more effective method would have been the calculation of gap/step measurement data within the measurement device for each profile collected prior to output.

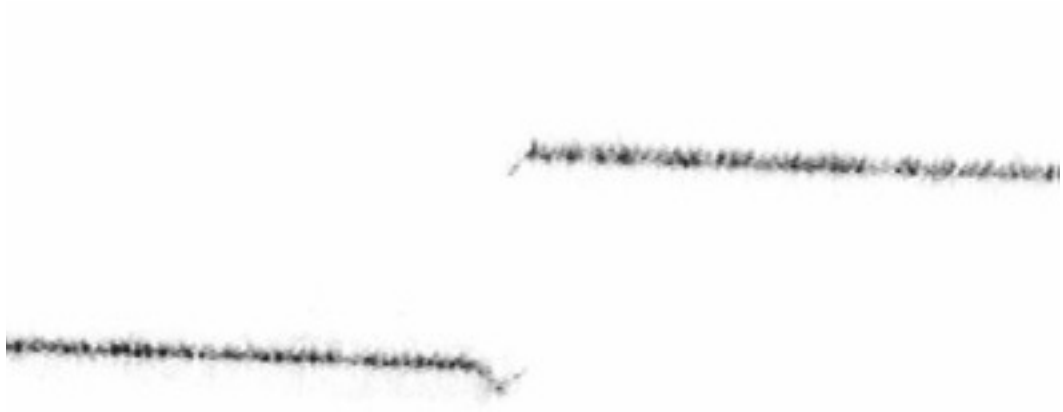


**Figure 5.67: Profile of 1mm step taken by GapGun laser gauge.**

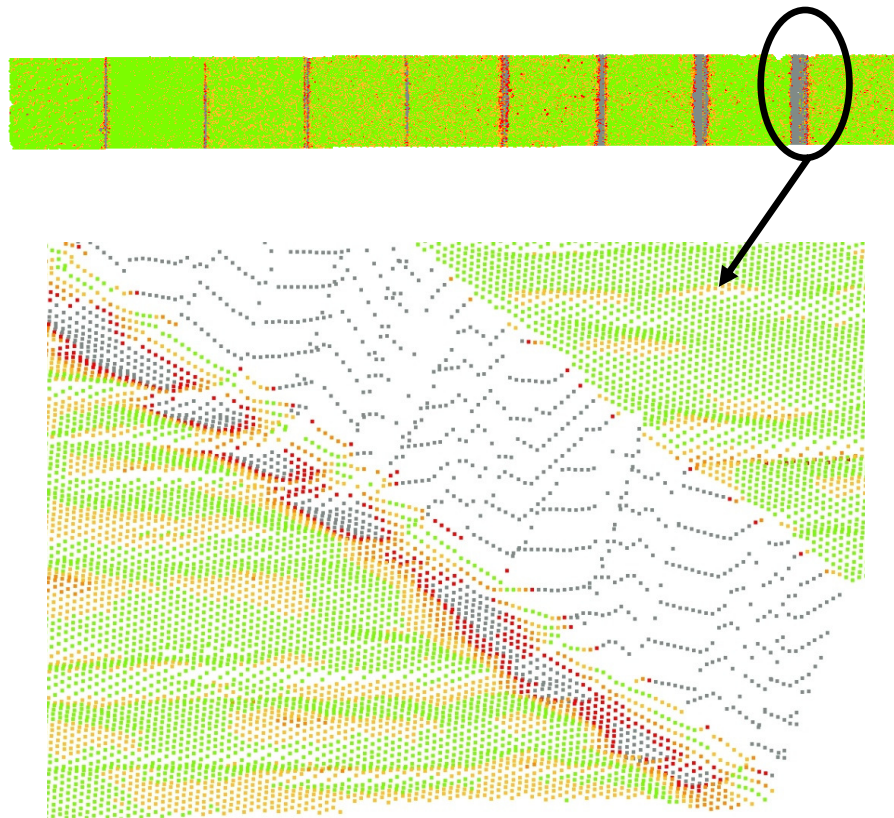


**Figure 5.68: Laser line A perpendicular to edge showing irregular downward curvature of lower surface. Plan view with step size increasing left to right (above), angled view of 1mm step (below).**

Laser line A in the perpendicular case produced data with an irregular downward curvature of the lower planar surface close to the edge (Figure 5.68). A definitive explanation for the ‘pitted’ surface could not be given but may be related to automatic adjustment of the laser intensity as the laser crossed from one plane to the other. Both laser systems dynamically adjusted illumination intensity dependent on received light level at the sensor with an overly bright illumination causing difficulties in the detection of the spot/line centre. However, the problem may be a combination of error sources, one of which being the limitations in the 6DoF tracking of the measurement head

causing 'waves' in the collected data (Section 5.4.1.3). As the lower surface undulated, the worst errors (data greater than  $\pm 4$  standard deviations from the mean residual of the fitted plane shown in grey) existed near the edge where the surface is 'lowest'. The system performed interpolation of the data to output a regularly organised data set, therefore individual profiles could not be distinguished and the data were smoothed.

#### Summary of Edge and Step Measurement

For the measurement of data close to a surface discontinuity, laser line system B produced the most suitable data. Using the chosen system with laser line perpendicular to the edge, assuming error was shared equally between surfaces, data could be collected within  $\sim 0.05\text{mm}$  of the centre of an edge. For laser line system A, measurement within  $0.50\text{mm}$  of an edge should be avoided and data within this region not used. For the fringe projection systems tested, the  $1.2\text{mm}$  distance between planes for fringe projection system A in the parallel orientation produced the most trusted data as no edge data have been produced. For all other orientations data on the lower plane were erroneous for over  $2\text{mm}$  and would have required removal. Fringe projection system B produced similar results regardless of orientation, with smallest distance of  $0.379\text{mm}$  achieved in the parallel orientation. Some of the effects seen for all systems may have been the result of the  $1\text{mm}$  step causing reflection and other effects, such effects may be reduced with a smaller step (flush) distance between planes (Figure 5.63). The results seen are likely to be dependent on the metallic surface finish being measured, with different results expected for highly reflective surfaces e.g. increased errors relating to multi path reflection. For matt surfaces exhibiting more lambertian reflectance than the current artefacts, results may be improved. When information on the surface finish of components removed from the vessel becomes available, additional testing may be required to evaluate measurement system performance against the altered surface and may include study on the effect of ambient lighting on the measurement result.

For inspection tasks a lack of data would be preferable to incorrect data, unless a repeatable signature could be identified in the data and modelled out. However, results from the work carried out in this thesis suggested that such a signature would be highly dependent on the instrument, its orientation to the workpiece, processing software, surface form and finish. In the case of the protective tiles to be measured, it would have been impractical to measure all edges with a laser line system perpendicular to the edge

because of the grid like structure of the tile surface. Regardless of scanner orientation, data seen in the parallel and perpendicular case would be collected. In light of the limitations to scanning systems the use of a fringe projection system such as B where data are predictable and vary little with orientation may be preferable for use at EFDA-JET.

For laser line systems the fundamental limit to performance is speckle produced by the illumination source (Section 3.2.4.2) (Curless & Levoy, 1995). The use of sensors with large pixels can reduce the impact of laser speckle (Beraldin et al., 2003) however with increased pixel size, abilities of systems to collect data close to edges is likely to be reduced.

For the two laser line systems trialled, gap measurement was not significantly improved with ‘optimised’ data collection (Table 5.10). For laser line A, in the three measurement orientations (laser line: parallel, 45° and perpendicular to the edge), for two of the orientations a smaller gap was calculated from the un-optimised data sets (improvement of 0.079 and 0.236mm). For laser line B, optimised data recorded smaller gaps in two orientations out of three, although the smallest gap distance was calculated for a data set collected without optimisation. These data do not provide a conclusive result as to whether the optimisation techniques applied during data collection improve the gap measurement capability of the measurement systems. Repeated measurement of a surface discontinuity would be required to obtain a conclusive result and may be performed in future work (Section 6.3.1).

Further trials using a scan head with dual sensors such as the Perceptron v5 (Perceptron, 2010) could be performed, although as the sensors view the projected line from the same ‘side’, improvement would be expected only in the perpendicular case. A laser line scanner using two sensors, mounted either side of the line could yield improvements in scanning results for the parallel case if data from each sensor were averaged. The effect described by Buzinski et al. (1992) (Figure 3.32) could be minimised. Various effects may be reduced using a synchronised scanner (Rioux, 1984) (Section 3.2.4.2) as the angle between source and sensor is reduced, minimising occlusion. An example of a synchronised laser scanner measuring the gap artefact can be seen (Figure 5.76) with occlusion minimised to such a level that measurement to the bottom of a 20mm deep, 0.2mm wide slot was possible. For the data shown in Figure 5.76 it should be noted that the system was orientated with laser line nominally

## Primary Equipment Trial

perpendicular to the slot, changing this orientation would have resulted in fewer data collected at the slot base due to occlusion.

For fringe projection systems, measurement close to an edge could have been improved by reducing the measurement area. As the measurement area is reduced the need for an external tracking system would arise and registration of multiple individual images would be required with registration error having an increased impact on final data accuracy.

For the measurement systems tested the removal of data within 2mm of an edge was proven to be conservative and the quantity of usable data could be increased for tile inspection. Based on the data processed a suitable distance to exclude data from an edge would be 0.5mm for all systems, however exceptions exist. For fringe projection system A data on the lower plane have severe errors which would require exclusion of data within 2.5mm of an edge where an adjacent plane exists closer to the measurement system with step of 1mm. For the EFDA-JET project the exclusion of data within 0.5mm of an edge on a single tile would be appropriate for all systems as for a step of  $\sim 0.040$ mm no impact on the lower plane was seen.

For inter-tile measurement, 0.5mm was proven to be a suitable distance to exclude data on the tile closest to the measurement system. For the second tile a minimum of 0.5mm of data should be excluded however this value may need to be increased dependent on the step and gap between tiles. Further processing and research would be required to assess if step height between tiles affected the data quality on the lower plane for fringe projection system A. As tiles were not to be connected it is possible that no incorrect data would be seen in EFDA-JET use, as reflection to the side of the first tile would not occur.

Data for all steps could not be processed due to time constraints but could be performed quantitatively to assess the relationship between calculated gap distance between planes and step height. For some of the errors seen conclusive explanations could not be given and it is suggested further work should include simulation of the measurement systems and ray-tracing of the optical paths to better understand the effects seen. Such a study is outside the scope of this project.

#### 5.4.4. Gap detection

The purpose of this test is outlined in Section 5.2.3.4, with the data collection and processing method described in Section 5.3.3.5.

Measured Dimension (mm)	0.22	0.34	0.54	0.74	1.07	3.08
Standard Deviation of data	0.02	0.05	0.02	0.04	0.03	0.02

**Table 5.11: As-built slot width and standard deviation of gap artefact (mm).**



**Figure 5.69: One JPEG image of the 3mm slot on the gap artefact. One of eight images collected and used by GapGun to calculate gap and flush (image cropped top and bottom). Given the calculated gap as 3.08mm (Table 5.11), the line thickness would be ~0.15mm.**

Data were collected with various laser line and projected fringe orientations to determine the optimal orientation to capture the dimensions of the slot. The method of calculating horizontal distance (gap) between surfaces used on the step artefact could not be applied to this artefact as the method relied on a step distance (flush), greater than the standard deviation of data to be present. The planes forming the slot were nominally parallel and level with step distance between them smaller than the standard deviation of the measurement systems. In addition, erroneous data inside the slot were present (Figure 5.72 - Figure 5.75) which if processed by the previous technique would be incorrectly classified, resulting in underestimation of the gap dimensions.

Registration of data to the nominal CAD model was based on minimising the root mean square distance of all data, normal to the model surface, using an iterative approach. Data within 2mm of an edge were excluded from contributing to the registration process but in order to improve constraint in the data, data on the artefact base and step artefact were included in the registration process. Assessment of measurement data was relative rather than on a common coordinate system because of uncertainty relating to the registration of data.

The two fringe projection systems detected the 3mm slot in all orientations and in all cases overestimated the 3mm width due to inability to measure directly to an edge (Figure 5.70). For a single measurement the best performance was achieved with projected fringes perpendicular to the edge however, a more complete profile was created where multiple directions and orientations were used (Figure 5.71). The use of

multiple orientations appeared to have created an incorrect profile on the left side of the gap where distinct data sets were seen, potentially reducing any calculating of the gap dimensions.

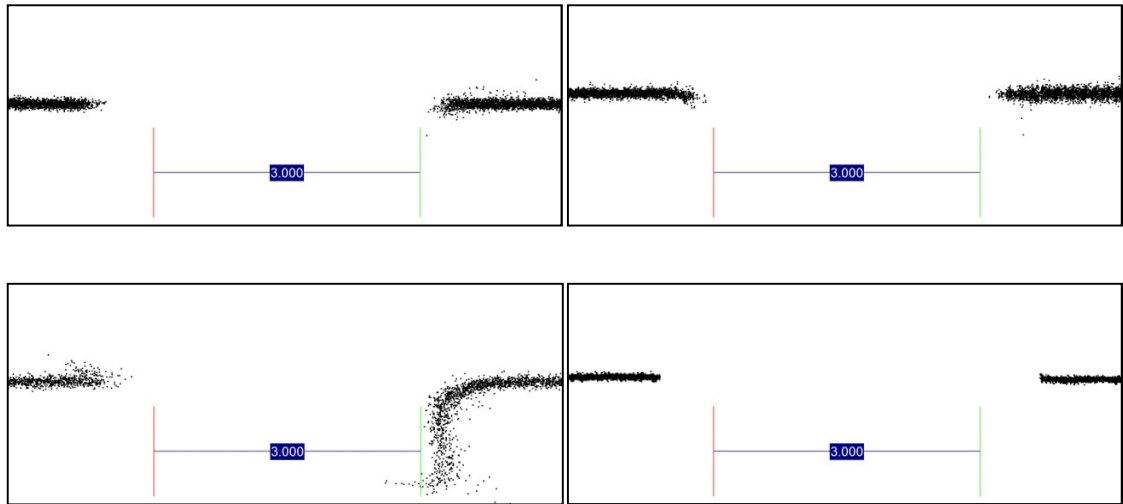


**Figure 5.70: Nominal 3mm slot width imaged by two white light fringe projection systems in various orientations. Top left to bottom right: Fringe System B at  $\sim 45^\circ$  to slots, Fringe System B perpendicular to slots, Fringe System B tilted so as not looking along the surface normal (optimal), Fringe System A parallel to slots.**

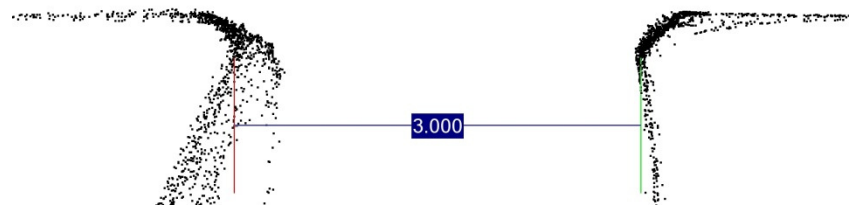


**Figure 5.71: Fringe projection system A: Optimal measurement consisting of multiple orientations aligned using targets.**

Fringe projection systems overestimated the dimensions of the gap whilst in certain orientations the laser line systems produced data inside the slot due to surface reflections. With laser line parallel to the edges, data were produced inside the slot because of multiple reflections (Figure 5.72– Figure 5.75). For the two laser line systems, system B appeared to produce fewer spurious points whilst system A produced two different images dependent on the intensity of the illumination. For the optimised configuration light intensity could be dynamically adjusted so that as the projected line descended into the slot and the quantity of light received by the sensor decreased, the intensity of the illumination was increased to maintain a high signal to noise ratio. In the optimised case several errors were seen, including upward and downward angled data at edges and a strong set of data forming an angled plane inside the slot. As the

## Primary Equipment Trial

scanner moved across the slot internal reflection will have caused all surfaces to be illuminated creating difficulty for the sensor in determining the true line/spot centre. At some point (dependent on slot width and illumination source to sensor angle), the sensor will no longer have had line of sight to the correct intersection with the projected line but part of the slot will still be visible and illuminated due to reflection inside the slot. The sensor will have detected the reflected light and calculated a position based on this return and an incorrect intersection with the projected line, resulting in erroneous data. To determine the exact optical paths, ray-tracing and simulation would be required which, whilst specific to each instrument configuration could be achieved as part of further research. For each effect an angled perspective view of the gap from above is seen along with a profile view of the same data.

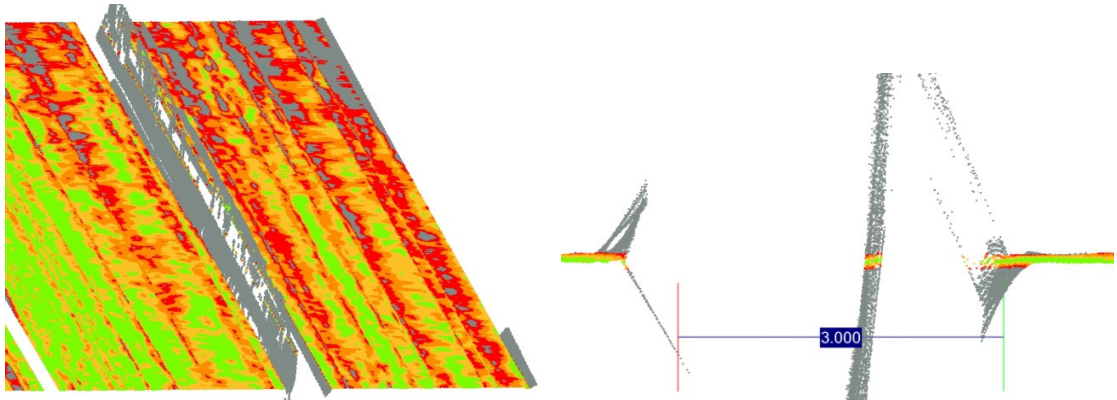


**Figure 5.72: Laser Line System A - Parallel to edge. Optimised incl. dynamic illumination intensity.**

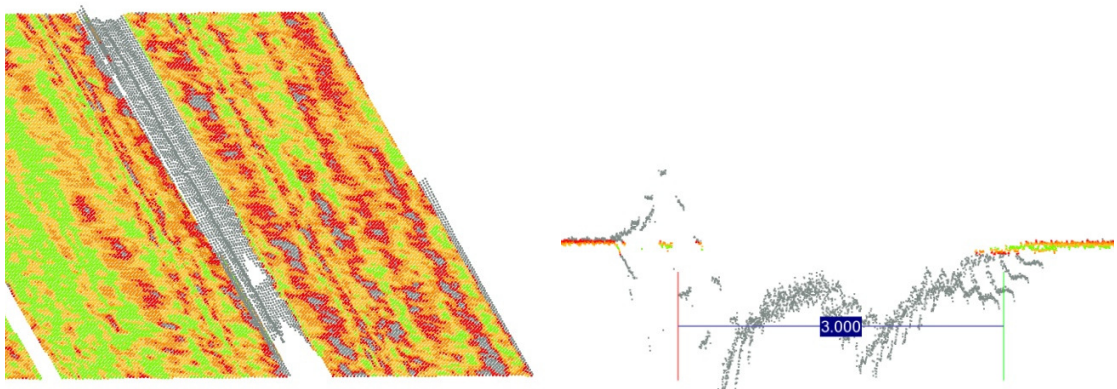


**Figure 5.73: Laser Line System A - Parallel to edge. Without optimisation.**

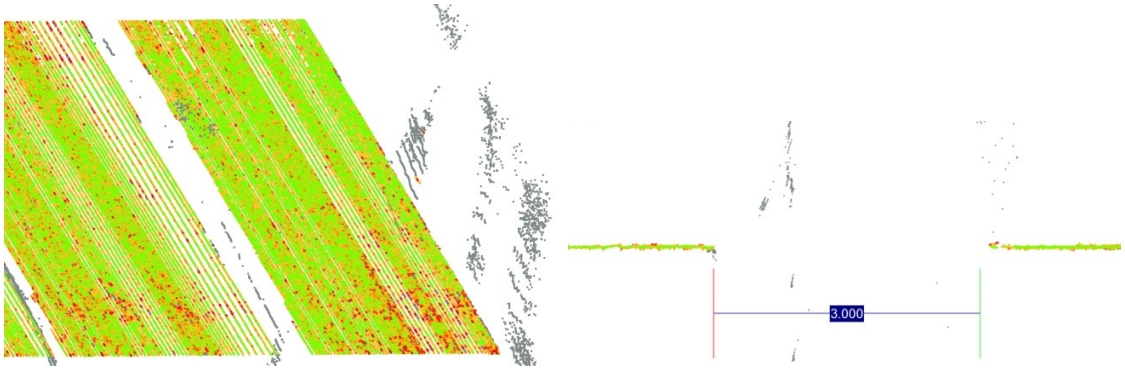


**Figure 5.74: Laser Line System B - Parallel to edge. Optimised incl. dynamic illumination intensity.**

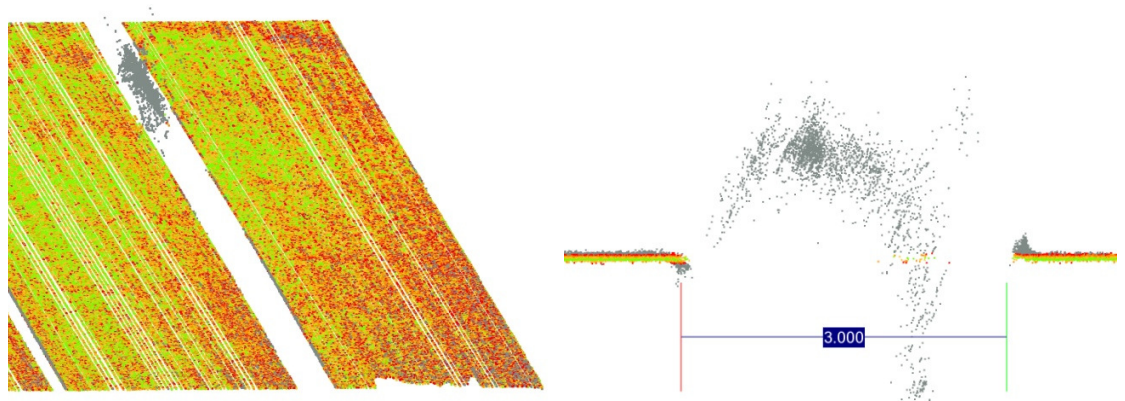


**Figure 5.75: Laser Line System B - Parallel to edge. Without optimisation.**

For the parallel case shown, the use of a synchronised laser scanner would have allowed improved measurement inside the slot and reduced reflection errors. An implementation of the synchronised laser scanner from company Arius3D was fitted to a Helmel CMM at University College London and used to scan the gap artefact (Figure 5.76). The synchronised scanner was positioned with laser line nominally perpendicular to slot edges and collected data on the horizontal plane forming the base of all slots. For the smallest slot(0.2mm), five rows of data points were visible.



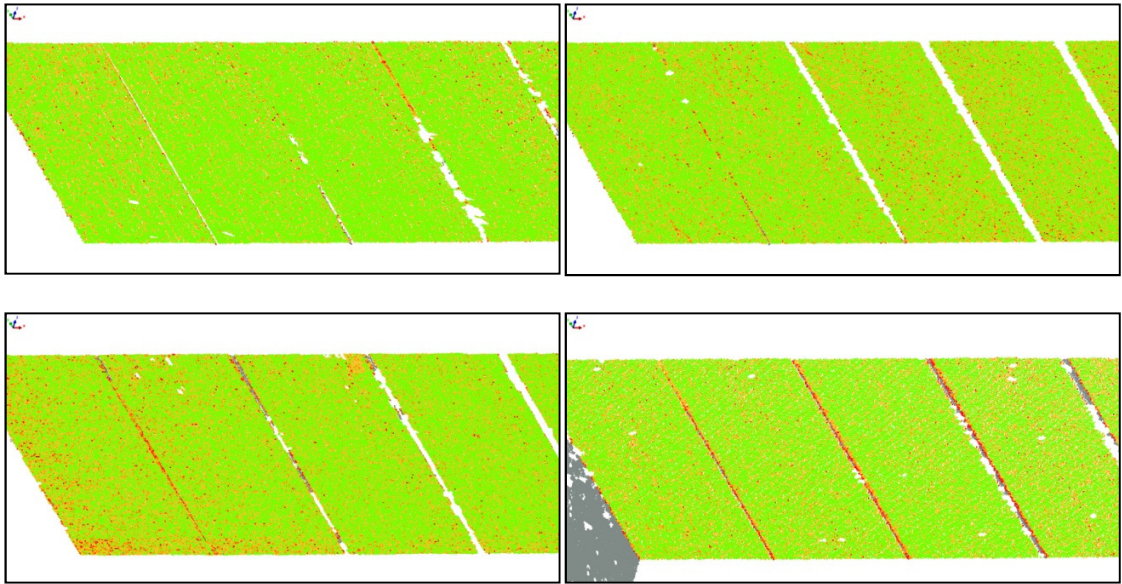
**Figure 5.76: Perspective view of gap artefact side showing left to right, 0.7mm, 1mm and 3mm slots. Data collected by Arius3D laser scanner.**

As with measurement of step edges, it is recommended that the orientation of both laser lines and projected fringes be perpendicular to the edge of any step or slot. Determining the inter-tile gap of 3mm proved achievable for all systems although accurate measurement of the dimensions of the distance between tiles was a challenge. To improve future measurement performance, two measurements could be taken, each with the measurement system directed to a single tile, not normal to the top surface such that measurement of the side of the tile is performed. Using this approach with fringe projection technologies would introduce additional uncertainty as registration error between data sets would affect the calculated distance.

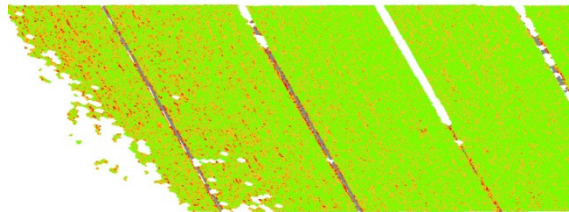
#### **5.4.4.1. Minimum resolvable gap**

Analysing the three smallest slots (0.22, 0.34, 0.54mm) in the same manner as the largest (3mm) slot qualitatively demonstrated those systems capable of detecting the smallest slots and therefore intra-tile gaps.

## Primary Equipment Trial



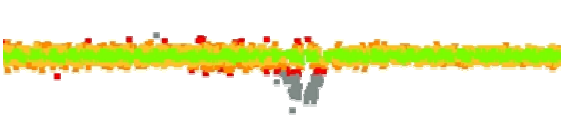
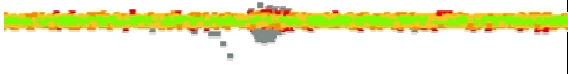
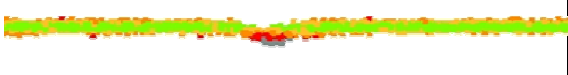
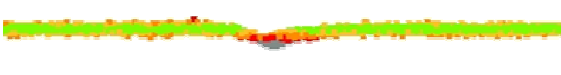
**Figure 5.77: Fringe Projection System B. Top left to bottom right, orientation of projected fringes WRT slots: Parallel, 45°, Perpendicular, Angled away from surface normal.**



**Figure 5.78: Fringe Projection System A.**

Analysing data from the fringe projection systems (Figure 5.77 & Figure 5.78) it was not clear whether the slot had been detected by the measurement system. The same data could be viewed as a profile (Figure 5.79) where several images showed a break in the data within  $\pm 1$  standard deviation and in all images data greater than four standard deviations from the mean are clustered around the slot.

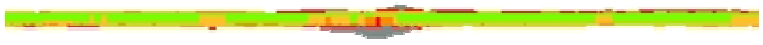
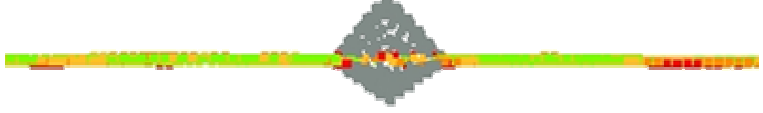
Primary Equipment Trial

<u>Slot 1: 0.22mm</u>	<u>Slot 2: 0.34mm</u>
	
Standard deviation: 0.054mm ∴ Thickness of green line is 0.109mm	
	
Standard deviation: 0.028mm ∴ Thickness of green line is 0.056mm	
	
Standard deviation: 0.036mm ∴ Thickness of green line is 0.072mm	
	
Standard deviation: 0.033mm ∴ Thickness of green line is 0.066mm	

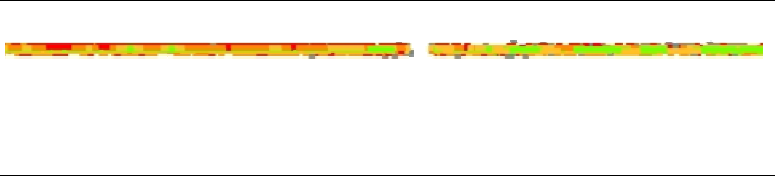
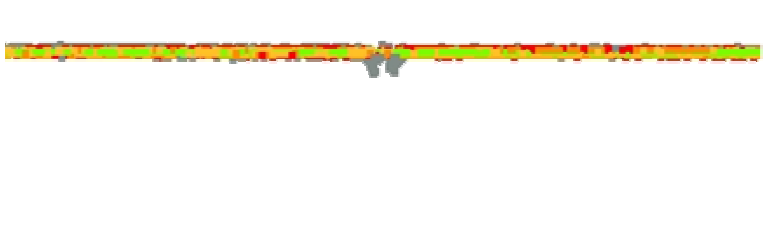
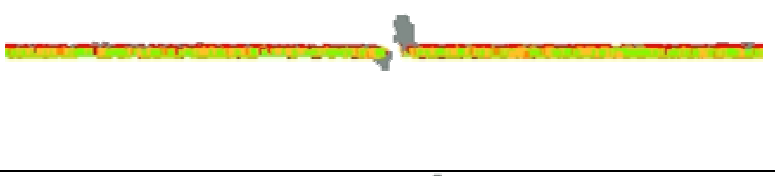
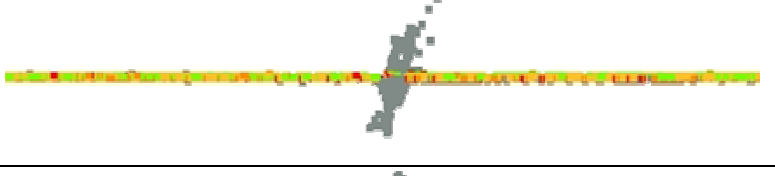
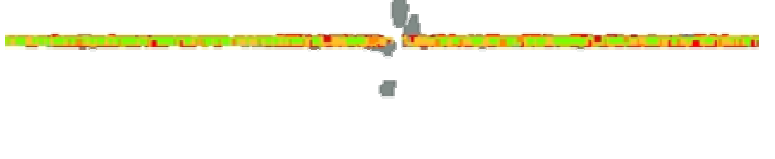
**Figure 5.79: Fringe Projection System B imaging slot 1 & 2 in four configurations/orientations (parallel, 45°, perpendicular, optimised). Green data are within ±1 standard deviation of plane red data is within ±4 standard deviation and grey are greater than 4.**

Using the method for producing profile images in Figure 5.79, the profiles for other measurement systems and orientations tested were generated for slot 2 (0.34mm) to determine if the smallest intra-tile gaps of 0.35mm could be detected (Figure 5.80).

Primary Equipment Trial

<p>Fringe Projection System A</p>	
<p>Laser Line A: Perpendicular Optimised</p>	
<p>Laser Line A: Perpendicular Un- optimised</p>	
<p>Laser Line A: 45°</p>	
<p>Laser Line A: -45°</p>	
<p>Laser Line A: Parallel Optimised</p>	
<p>Laser Line A: Parallel Un- optimised</p>	

Primary Equipment Trial

Laser Line B: Perpendicular Optimised	
Laser Line B: Perpendicular Un- optimised	
Laser Line B: 45° Optimised	
Laser Line B: 45° Un- optimised	
Laser Line B: Parallel Optimised	
Laser Line B: Parallel Un- optimised	

**Figure 5.80: Profiles of Gap artefact slot 2, 0.34mm slot width (Table 5.11).**

For the majority of the measurement systems and orientations data greater than four standard deviation of the best fit plane existed around the slot position. Data within  $\pm 4$  standard deviation appeared to be valid whilst points outside this range appeared to be measurements into the slot/surface discontinuity, or erroneous data. Histograms of residuals normal to a fitted plane supported this assertion (Section 5.4.1.3, Figure 5.35 & Figure 5.36). Without detailed dimensions and accurate registration of data to the as-built model it was not possible to confirm that data with standard deviation of  $\geq 5$  correctly represented the surface. Given that the inspection task in EFDA-JET would be monitoring erosion and deposition it would not be valid to make assumptions about data validity as the surface may alter so as to exhibit some of the shapes seen in Figure 5.80 during operation. It may be possible to use data at  $\geq 5$  standard deviations from the mean fitted plane as part of a technique to detect surface discontinuities. Such a

technique may be particularly suited to the detection of straight line discontinuities such as steps edges and slot edges, with development a possibility for future work.

A relative assessment could be made on each single profile to detect discontinuities. A number of profiles with width of ~1-2mm could be taken across the length of the slot and analysed individually. A single profile using all data should not be used as any data spanning the surfaces would generate a profile showing no break in the data even if that data spanned only a small proportion of the slot. Such a profile would lead to incorrect interpretation that the system cannot detect a discontinuity of that size.

The measurement systems trialled could not measure to the base of the slot although the synchronised laser scanner did have this capability in the tested orientation (Figure 5.76). If data at the base of the slot could have been collected, measurements could have been made on this data to determine slot width, although limitations of measurement close to an edge would have still existed.

With projected fringes perpendicular to the slot fringe system B recorded a clear break in data for slot 2 (0.34mm) whilst neither fringe system recorded a clear break for the smallest (0.22mm) slot. With projected fringes parallel to a slot, the slot will have presented a change in contrast to the illuminated surface. This change in contrast may have had an effect on the calculated phase value for that area and required compensation in the phase unwrapping process (Section 3.2.4.3).

Of the laser line systems, system B recorded clear breaks in the surface data of slot 2 whilst system A created data between the surfaces in all cases. In the parallel case, data outside 5 standard deviations (Figure 5.80 grey data points) could be of use in determining the slot position for laser system A, although could not be used to determine slot width. Detection of a 0.35mm slot was achievable using the measurement technologies tested although determination of that slot width was not possible. Improved results could be seen for the fringe projection systems with a reduction in measurement area, improvement in results for laser line systems may be achievable if the distance to the measurement surface were controlled to minimise the laser line thickness, although a large improvement would not be expected. Multiple measurements performed by a laser line triangulation system, with different orientations to the edge e.g.  $0^\circ$ ,  $45^\circ$ ,  $90^\circ$ , may enable determination of edge position with reduced uncertainty. Assuming error in the 6DoF tracking system is less than the random error of the measurement device, the combination of data from multiple passes would result

### Primary Equipment Trial

in a greater number of samples and improved understanding of edge position. To be effective, removal of data within a multiple of the standard deviation e.g. 3 st.dev., for each set would be required to eliminate outlying data prior to merging.

**5.4.5. Registration**

Using the method described in Section 5.3.3.6, data of the top, planar surfaces of the step artefact have been brought into coarse registration with the nominal model and a ‘best fit’ registration, minimising the distance of data normal to the surface performed. The registration was performed with commercial software package PolyWorks (Innovmetric, 2010). Data within 2mm of an edge were discarded and for the remaining data, the residuals to the model reported. These data (excluding data within 2mm of an edge) were again registered to the model and residuals reported. The exclusion of data within 2mm of an edge resulted in a 0.001mm reduction in the RMS error of the residuals for the planar areas i.e. an improved registration (Table 5.12). Comparison of the point residuals following registration showed a tighter and more balanced grouping around the mean value (Figure 5.81)

<i>Registration Method</i>	<i>Points</i>	<i>Mean</i>	<i>St Dev</i>	<i>RMS Error</i>
All Points	82652	0.0032	0.0111	0.0116
Excluding data with 2mm of edge	82652	-0.0000	0.0106	0.0106

**Table 5.12: Residuals of data to nominal CAD model following removal of 'edge' data.**

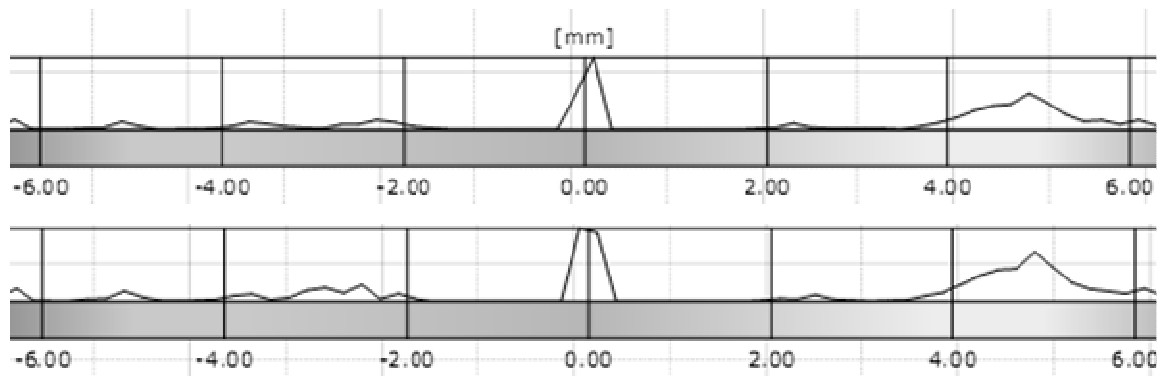


**Figure 5.81: Histogram of residuals of point data unaffected by edge effects, following registration with (top) and without (bottom) edge data**

Based on the experimental work performed, it is advised that for a data set well constrained in all axis and majority of data unaffected by ‘edge effects’, the inclusion of affected edge data would not be expected to significantly impact registration. However, where data lack the features and geometry to fully constrain motion during registration<sup>10</sup> and accuracy is paramount, the removal of affected edge data should be performed.

<sup>10</sup> E.g. data of a flat plane would constrain motion in a single axis only, whereas a plane with a hole would offer constraint in all three axis, but would not prevent rotation. A plane with a circular hole and non-circular slot would constrain data in all axis and rotations.

### Primary Equipment Trial

Such a situation would occur in the EFDA-JET machine with ITER-Like wall tiles consisting of multiple castellations. Once registration was complete, data impacted by edge effects could be reintroduced into the data set for analysis. This approach would enable data from different devices to be more accurately compared by only using the most reliable data for registration.

The workflow for this process would involve: coarse registration to a model, exclusion of data likely impacted by edge effects (using the model to determine the exclusion areas, or through analysis of the data directly using the edge detection method detailed in this work), registration to an as-built model and re-introduction of the excluded data.

It is recognised that the improvement in standard deviation and RMS residual in this case is small and therefore there is an opportunity for further testing to validate this result across a number of measurement technologies and surfaces.

#### **5.4.6. Large Volume**

The purpose of this test is outlined in Section 5.2.3.6, with the data collection and processing method described in Section 5.3.3.7.

One measurement system (Laser Line A) performed measurement in the large volume, with data from that instrument presented alongside the other data (Section 5.4.1 - 5.4.4). The results of testing on individual artefacts with laser line A in the large volume showed no significant difference in data quality to the other systems on test. Although evidence suggested equipment performance for Laser Line System A was in line with other systems used in a smaller measurement volume, the performance of the other systems may not have been equal as the measurement volume increased. This observation would be particularly relevant for white light projection systems within EFDA-JET as data would be an amalgamation of multiple ‘patches’ of data, where local data quality (within a single patch) could exceed the overall data quality affected by registration of multiple patches. Although laser line systems also collect local data in the form of a profile, the data holds very little meaning without the real-time tracking/registration of profiles whereas data from a white light system holds 3D meaning without other patches.

##### **5.4.6.1. Probing Error**

The probing error was defined by two parameters, the Probing Error (form) and Probing Error (size), *PF* and *PS* respectively. Within the VDI/VDE 2634 Part 3 guideline, a sphere was to be positioned arbitrarily at minimum three positions and in each position measured from at least five sensor positions.

The calibrated sphere diameter was not known to an accuracy required for conformance to the VDI/VDE 2634 guidelines. The spheres attached to the large volume test frame were not measured by the touch probe CMM used to calibrate other artefacts due to lack of available time however, four spheres from the same manufacturing process and batch attached to the portable test frame were measured (Table 5.13). Measurement of the four spheres with the portable frame in a single position was not possible, so two sets of measurements were taken. The first measurement set captured sphere 1, 2 & 3, with the second position measuring sphere 1, 2 & 4. The second measurements of sphere 1 & 2 differed from the first by 0.0003mm.

Primary Equipment Trial

Sphere Number	Diameter (mm)
1	50.0103
2	50.0160
3	50.0289
4	50.0347

**Table 5.13: Diameter of portable test frame datum spheres from CMM measurement. ( $\pm 0.0035\text{mm}$ ).**

The range in diameter of the four measured spheres was 0.0244mm (Table 5.13), with the difference attributable to the manually applied vapour blast surface treatment. Given the  $\sim 20\mu\text{m}$  variation these data could not be used for calculation of large volume probing error. Optical measurement data of the individual spheres attached to the large volume test frame were available having been collected by targeted photogrammetry and a tracked touch probe however, both had greater uncertainty than the CMM measurement. For the tracked system the touch probe replaced the hand held laser line scanner as the data collection device and was tracked in the same manner as the line scanner. Data from this probe would have been subject to errors introduced by the tracking system but without effects from the optical line scanner.

Sphere position on frame	Sphere Diameter (mm)		
	Laser Scanning	Touch Probe	Photogrammetry
1 - Top Left	50.128	49.986 (5)	49.876 (14)
2 - Top Right	49.938	49.906 (4)	49.786 (17)
3 - Bottom Left	50.020	50.044 (12)	49.800 (14)
4 - Bottom Right	50.028	50.000 (9)	49.666 (12)

**Table 5.14: Sphere diameter from best fit free radius sphere. Numbers in parenthesis indicate number of points available for sphere fitting.**

For the touch probe data the number of probed points per sphere varied dependent on ease of accessibility, with probed points varying from four to twelve. There appeared to be a relationship between the number of points probed and the computed diameter, the diameter increased with the number of probed points. In light of the close agreement between laser line scanned and probed data for three of the four spheres, the correlation between number of probed points and diameter was inconclusive. Combining the probe data (Table 5.14) and CMM probed spheres of the portable test frame indicated the true diameter of spheres was  $>50\text{mm}$ .

Primary Equipment Trial

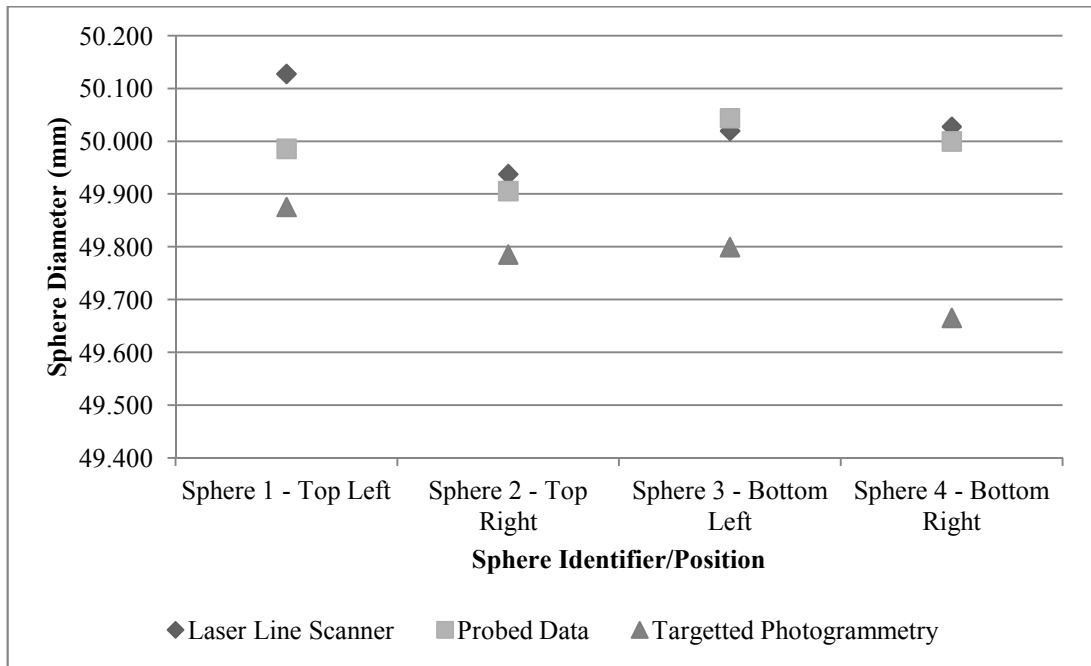


Figure 5.82: Sphere diameter from best fit free radius sphere.

5.4.6.2. Length/Sphere spacing error

To assess the length measurement performance of the laser line system, the length between sphere centres was compared against those calculated by target-based photogrammetry. The laser system produced consistently smaller length measurements than the photogrammetry system, with the discrepancy differing by position and orientation of the measured positions (Table 5.15, Figure 5.83).

Position and orientation of length measurement	Length calculated by photogrammetry (m)	Length discrepancy parts per million: $\mu\text{m per m}$ .
Horizontal High	1.427	-18
Horizontal Low	1.465	-87
Vertical Left	2.340	-2
Vertical Right	2.340	-45
Diagonal 1	2.750	-21
Diagonal 2	2.752	-42

Table 5.15: Length measurement discrepancy of laser line system A compared to target-based photogrammetry.

### Primary Equipment Trial

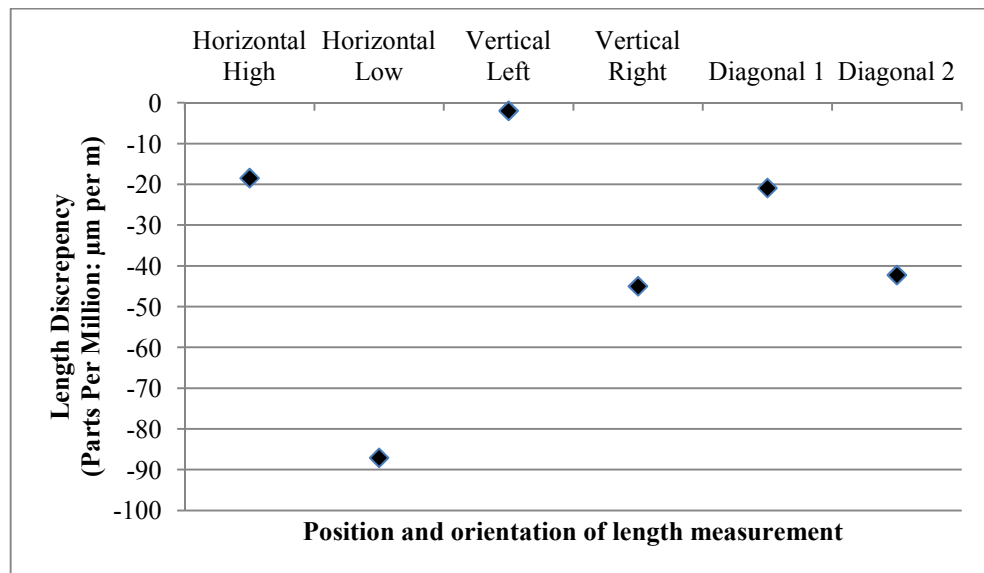


**Figure 5.83: Length measurement discrepancy of laser line scanner compared to target-based photogrammetry.**

The length measurements performed did not take into account the probing error (*PF* & *PS*) present for both the photogrammetry and laser line systems. As demonstrated by Feng et al., (2001) the calculated centre of an unfixed radius, least-squares fit sphere will be affected by data coverage. The impact of incomplete data coverage may be an offset of the calculated sphere centre in the direction away from the collected data, often caused by insufficient access to the surface or line of sight limitations (Figure 5.84).

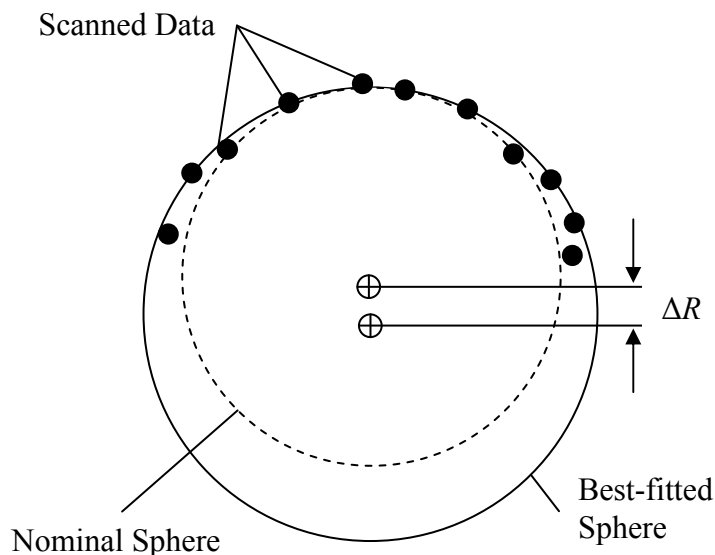


**Figure 5.84: Sphere centre offset away from collected data. After (Feng et al., 2001) with permission from Elsevier.**

This effect would not explain the length discrepancy seen unless the discrepancy existed within the photogrammetry data. The datum clusters were mounted on planes with an

inward tilt (the surface normal converges) so any miscalculation of the sphere centre in the laser scan data caused by the effect described would have increased the length between sphere centres and not decreased it, as was seen in the collected data. Temperature change was compensated for by scaling data accordingly.

Given the length uncertainty of the photogrammetric survey and results calculated (Table 5.15, Figure 5.83), length errors of ~0.025mm were to be expected. The three greatest discrepancies suggested an error in the position of the lower right sphere centre, affecting the 'horizontal low', 'vertical right' and 'diagonal 2' lengths. In the photogrammetric survey this sphere had the lowest number of measured points for the spheres measured, but this number was not significantly less and visibility of the portable measurement head to the tracking system was unobstructed.

From the data seen no simple trend was identifiable within the length discrepancies. Applying the calculated length uncertainty to measurement inside the EFDA-JET vessel would have created a length discrepancy of 0.65mm – this is based on a circle with radius of 4.1m (approximate distance from the centre of the machine to the measurement surface of the outer wall) and a length discrepancy of 0.025mm per metre, over the 25.8m circumference. Measurement will not be performed along a 25.8m length, instead multiple tracking device positions will be used, each introducing additional error as registration of data from that position must be performed.

#### **5.4.6.3. Number of tracking device positions**

For a hybrid measurement system (Section 3.2.5) to operate inside the machine the tracking component could not be positioned in a single stationary position as the central column would have prevented line of sight to all areas. A number of positions would have been required, with that number determined by the minimum and maximum measurement range and the field of view of the tracking device. Using approximate dimensions for the fusion machine, adjusted for the positions of plasma facing components requiring measurement resulted in a measurement volume of: major radius of 4.1m, minor radius of 1.9m and internal vertical height of 3.5m.

For laser tracker systems the horizontal viewing angle was 360° and typical vertical angle 90-140°. Because of the limited vertical angle and minimum range there would be an area around the tracker which could not be measured. For a laser tracker positioned 3.8m from the centre of the machine (0.3m from outer wall) a laser tracker

## Primary Equipment Trial

with  $90^{\circ} (\pm 45^{\circ})$  vertical viewing angle positioned with laser output at half the machine height and minimum measurement distance of 1m, would have been capable of collecting data on all surfaces from four measurement positions equally spaced around the machine. Overlap between data collected in different positions would have been very limited with majority of overlap at the vertical height of the tracker where constraint in the data would have been minimal because of machine shape. Reference objects for registration of device positions would have been required in the central region where maximum overlap between tracker positions occurred. Laser trackers with increased vertical angle would have increased overlap between collected data, although four positions would still have been required to achieve line of sight between tracker positions. Because of limited overlap and possibility for reference objects visible to more than one tracker position, the recommendations would have been for five or six devices positions equidistant within the machine.

The optical trackers investigated were capable of determining the six degrees of freedom of objects such as laser line scanners within a defined measurement volume. The pyramidal measurement volume was defined by the intersection of three linear sensors with typical minimum distance of 1.5m and maximum range of 6m, creating measurement volumes of  $3\text{m}^3$  to  $20\text{m}^3$ . Measurement uncertainty was not constant throughout the volume, varying with volume and range, creating 'zones' of measurement uncertainty. For one commercially available system at maximum range (6m) from the camera bar, a measurement area of 2.7m x 3.7m parallel to the bar would have been created. With the bar mounted horizontally at maximum range, a 'slice' of the machine could have been collected with width up to 0.5m. With tracker positioned centrally within the available volume (central sensor 3.02m from centre of machine) a circle with circumference 19.0m would have been created. Given a circle with 19.0m circumference and ability to collect data in 0.5m sections, it was estimated that 38 positions would have been required to collect data over all surfaces. Fewer positions may have been possible by varying the tracker orientations. The absolute minimum number of positions would vary for each implementation of the technology (i.e. each manufacturer) and calculated performed by computer simulation. No further action was taken as a device was not selected..

It was estimated that for the EFDA-JET machine volume, fewer laser tracker positions than optical tracker positions would have been required. The  $360^{\circ}$  horizontal viewing angle of the laser tracker contributed to the need for fewer positions however

### Primary Equipment Trial

calculations did not take into account movement of the portable laser line scanner by remote handling equipment. Given that the laser tracker would have occupied a portion of the vessel through which remote handling equipment could not move, repositioning the laser line scanner to the 'other side' of the torus may have required more time and resources than using a larger number of tracker positions and moving in a single direction around the torus. In the estimation of optical tracker positions the ability of the technology to be in motion whilst collecting data has not been utilised. With a suitable number of stationary markers in the measurement volume an optical tracker could calculate its position and the position of an object e.g. laser line scanner, with respect to the stationary reference points. Such a system would have enabled the optical tracker and laser line scanner to be in constant motion but would required a large number of stationary, powered LED markers. Any miscalculation of the optical tracker position would have directly impact the uncertainty of all data collected by a laser line scanner or other 'tracked' unit.

## 5.5. Summary

This chapter has presented the primary equipment trial performed for this research, describing new test artefacts developed and a data processing methodology to extract information from those results. Thorough analysis of results has been performed against EFDA-JET specific requirements.

The artefacts produced presented a set of features and a surface finish representative of the replacement ITER-Like wall tiles. Design and manufacture adhered to the EFDA-JET design process, ensuring sound engineering practice was followed. The artefacts and measurement method met the requirements put forward by Van Gestel et al., (2009) with regards to measurement tests, that they be 'easy, fast and representative for the measurement task'. Test artefacts described in literature (Section 3.4) favoured surfaces with diffuse reflectance, in line with recommendations of the VDI/VDE 2634 Part 3 guidelines, published in English in December 2008. By December 2008, artefact design for EFDA-JET was complete and approved by the design review panel. The testing outlined in the VDI/VDE 2634 Part 3 guidelines was applicable for certain aspects of research presented in this thesis e.g. large volume, but would not have provided all the information presented in this work e.g. effect of surface angle on data (Section 5.4.1), effect of change in depth of field (Section 5.4.2), performance of measurement systems for step/gap measurement (Section 5.4.3 - 5.4.4).

Data presented in this work were relevant to EFDA-JET because the surface finish and features of the test artefacts simulated that of the actual tile surface. Considerable effort was placed on the manufacture of the artefacts so that, where 'as-built' dimensions were not available, the nominal CAD model could be used for analysis.

To collect data representative of the intersection between two tile assemblies the measurement volume of fringe projection systems did not collect the datum clusters of the portable test frame. Without measurement of the datum clusters, data were registered to as-built CAD model using a 'best fit' method, minimising the distance of data to a surface rather than the use of spheres as planned. The use of surface data for registration introduced the possibility that errors in the data could have affected registration and subsequent analysis. In light of this, data believed to have increased error at surface discontinuities were excluded from registration. A study using the step

test artefact indicated that where data provided insufficient constraint, edge data may impact registration (Section 5.4.5).

Analysis of edge profiles proved the 2mm of data excluded near a discontinuity to be excessive and could be reduced to 0.5mm for the configurations used. A future improvement would be the addition of spheres attached directly to the artefacts, to be used for registration, allowing easier comparison between data from different measurement systems e.g. comparing positioning of step edge.

Not all processing performed relied on the accurate registration of collected data to the as-built model, but there was a need for accurate alignment between individual parts of a data set. Alignment was provided by the equipment manufacturer e.g. for the laser line systems the alignment was performed by the stationary tracking unit. It has been suggested that individual data within a set could be aligned with greater accuracy than provided by the tracker, and commercial software packages exist with this function. The adjustment of a collection of laser line profiles to other data to improve quality may be appealing, however the effect of possible errors should be considered. The effect erroneous data may have on registration to a CAD model and least squares fitting of data was minimised in this work by excluding data within 2mm of an edge. However it would need to be determined if the same were required when adjusting alignment within a data set. Such an investigation was beyond the scope of this project and so data provided by each manufacturer were transformed uniformly. The ability to process and analyse data without accurate registration to a model was beneficial as it removed error introduced by the registration process and future methods would benefit from the same approach. To generate dimensions and comparisons without accurate registration to a model would be highly beneficial and could be used for edge detection algorithms of surface discontinuities such as the steps and gaps seen in the collected data.

An important outcome of this work has been the provision of a validated data set against which to compare future measurement systems. There was a lack of published data regarding measurement system performance and therefore little opportunity to compare whether data collected was representative of the true system performance. The data and analysis technique developed in this work acts as a baseline against which future dimensional surface metrology equipment at EFDA-JET could be evaluated. The collected data were made available to interested parties so that they may evaluate the data themselves and be aware of some of the various errors and effects seen.

## **6. Conclusions and Further Work**

This research was performed in collaboration with the UK Atomic Energy Authority as industrial partner, focussing on their needs for non-contact inspection of metallic tiles. As operators of the EFDA-JET experimental fusion device, the Authority was interested whether non-contact dimensional metrology equipment could be used inside the EFDA-JET experimental fusion device to verify installation of components, and for periodic monitoring of the surface of protective tiles inside the machine.

This chapter presents a summary of the work performed, an assessment of how the work has met the generic research objectives outlined in Section 1.4 and a critical assessment of the work performed. Evaluation of whether non-contact metrology equipment could meet the requirements of EFDA-JET (Section 6.2) is presented before the chapter concludes with opportunities for future work (Section 6.3).

### **6.1. Summary & Critical Analysis of Work**

To investigate metrology equipment for EFDA-JET and evaluate metrology equipment, physical test artefacts and a processing methodology have been developed and proven through use. Tests have been developed and performed to satisfy the generic research objectives (Section 1.4). By meeting generic objectives, this report can answer the EFDA-JET specific requirements (Section 1.3 & 2) and provide detailed responses to these requirements in Section 6.2.

To generate the required information, the project went through several stages (Section 1.5). The main stages of the project have been the development of a set of tests with which to assess equipment, the creation of test artefacts to be used in testing, measurement of those artefacts using state of the art equipment and the development of a workflow and tools to process the collected data. These activities were performed alongside research into metrology technology (Section 3) and the engineering needs of EFDA-JET (Section 2). In this section the main stages of the research are assessed as to how they contributed to completion of the research objectives, critically analysing the limitations of work and identifying contributions to knowledge.

### **6.1.1. *Development of A New Evaluation Method***

This work presents a new, comprehensive and repeatable process for evaluating the performance of non-contact optical measurement technologies. The process combines state-of-the-art test artefacts, designed and manufactured for this research with a series of experiments and associated data processing activities. These experiments directly address the Research Objectives and in turn the EFDA-JET requirements.

#### **6.1.1.1. Development of New Test Artefacts**

Research into the assessment and validation of dimensional metrology systems highlighted the value to be gained in using known objects to be measured by the systems under test. The object is ‘known’ through prior measurement with a system whose accuracy is significantly greater than the system to be tested, typically an order of magnitude (Beraldin et al., 2007b). The known objects may be referred to as test artefacts and each may take a form that is designed to expose specific features of the interaction between the object and measurement system. None of the artefacts found during research (Section 3.4) presented a suitable form or surface finish and therefore the development of new test artefacts was required.

Early in the work before tile design was finalised, a test artefact was created with surface finish and features to simulate the protective tiles using information from the ITER-Like wall pre-prototype design phase. This exploratory artefact met its goals of providing an initial measurement surface but was designed and constructed before a thorough review of relevant work had been performed (Section 3.4). The artefact was measured using technologies owned and accessible to the project partners to understand more about the data they could produce (Section 4, Section 6.1.1.3). Despite measurement by a touch probe CMM, the artefact dimensions were not understood with sufficient accuracy to provide quantitative assessment of the measurement systems and as tile design became finalised the artefacts did not have suitable features to deliver all information required by EFDA-JET. With finalisation of the EFDA-JET tile design during the second year of this project, it was possible to determine a set of requirements regarding the required accuracy of measurement systems to satisfy the installation tolerances and therefore design artefacts to assess these values (Section 2.4).

To meet the measurement requirements and provide data relevant to EFDA-JET, a number of artefacts were required which would occupy a volume representative of a

portion of the real machine (Section 5.1). Each artefact would have a specific form to satisfy part of the requirements, with all having a surface finish as close as possible to real beryllium protective tiles. Beryllium could not be used for artefact manufacture because it is a carcinogen and aluminium was selected as it could present a surface optically similar following surface treatment. Following manufacture, inspection revealed the final surface to be smoother than the engineered beryllium tiles to be installed in the EFDA-JET machine (Section 5.2.1.6). The difference in surface finish is attributable to change of material and manufacture technique i.e. milling instead of Electrical Discharge Machining (EDM) (Section 5.2.1.4). The smoother surface resulted in a more challenging surface for optical measurement e.g. increased specular reflection saturating the sensor (Section 5.4.1.2).

The artefacts were designed by the author and passed through several iterations before being converted to digital CAD models. The design and procurement process followed the UK Atomic Energy Authority project lifecycle, including a thorough design review where all aspects of the artefact design and manufacture were evaluated with senior members of the Engineering Department and representatives from interface departments including Remote Handling. On completion of the design review process the artefacts can be said to have met the design brief and were manufactured using sound engineering principles with the author as project manager. To validate the dimensions of the constructed artefacts, measurement was performed with a Zeiss touch probe CMM at the UK National Physical Laboratory providing traceable dimensional measurement.

The artefacts produced were limited by their lack of features with which to perform feature based registration, necessitating the need for surface based registration. Artefacts were designed with features for registration however these were not of use, as:

- Holes of incorrect diameter were specified, preventing the use of retro-reflective targets and small spheres (both with the same registration centre) for registration.
- To obtain data relevant to EFDA-JET the measurement systems were calibrated for an area approximately equal to the dimensions of two tile assemblies. This area was smaller than the dimensions of the portable mounting plate and excluded the datum spheres from the collection area.

## Conclusions and Further Work

- Touch probe data on the artefact surfaces were present and used for registration as accuracy of this data was known however, for the step and gap artefact the data had insufficient constraint for accurate registration and limited the processing possible e.g. direct comparison of computed edge position between measurement systems, quantitative analysis of areas of erroneous data on each surface.

For the purposes of evaluating equipment for EFDA-JET it is acknowledged that the surface finish of the developed artefacts differed from the surface of the beryllium tiles. This change in surface finish produced a more challenging surface for measurement, although did not affect the generic research objectives (Section 1.4).

If further artefacts were to be developed, the following improvements could be made:

- A number of diffusely reflecting spheres should be permanently attached directly to the artefacts to be used for feature based registration.
- Angle Artefact A and B could be amalgamated into a single artefact. This artefact would present a series of angled facets as per Artefact B but either side of the artefact a planar surface at  $30^{\circ}$  to the base, as per Artefact A. This new piece would enable the Approach Angle and Depth of Field tests to be collected in a single measurement, reducing collection time.

Despite the limitations identified, the artefacts developed were the most complete set of artefacts currently available at the time for evaluating non-contact optical metrology equipment of the type described in this work. They were designed and manufactured to ensure dimensional stability and were verified to the National Length Standard. The artefacts enabled repeatable measurement, quick data collection, minimum equipment repositioning and simple processing.

### **6.1.1.2. Development of Experiments and Data processing techniques**

In conjunction with artefact design a method of processing and extracting information from the collected data was developed. Where possible methods were based on national and international guidelines and published academic work (Section 3.4). The approach was based on simplifying processing to extract relevant information for EFDA-JET whilst maintaining transparency at all stages by avoiding the use of closed-source software and proprietary file formats. Some use of commercial software was necessary,

but in these cases, the software selected was shown to be suitable for the given task by certification by an external body (Albarran et al., 2008, p.232). The developed processing technique allowed the evaluation of equipment performance on the developed test artefacts whilst minimising the possibility of human operator error and reducing processing time.

In addition to developing the method to determine whether the tested systems could produce the required information, research into the integration and use of the collected data at EFDA-JET was performed. Data collected as a 'point cloud' could be imported into the CAD environment although early tests showed large numbers of data to be difficult to handle, this appeared to be changing, with similar software packages able to handle two billion point objects (Autodesk, 2010). The point objects were commonly without any information other than position, making use limited without calculating additional information such as connectivity between data. Conversion of the point data to CAD objects through reverse engineering was possible but would have involved significant manual effort as discovered during a month secondment to the W7X experimental fusion device in Greifswald, Germany. During the secondment the full data collection and processing lifecycle was experienced, including converting point data to polygonal mesh and through to watertight NURBS surfaces (Section 3.3.1). Experience and suggestions for EFDA-JET were presented to engineers and management with the guidance that a similar number of people were employed to reverse engineer models at W7X as were employed producing and maintaining the main configuration model. The use of software developed at University College London (Section 1.6) to segment a point cloud using only a registered polygon mesh would have allowed individual parts of the data to be imported and used in the CAD environment without manual selection. Using this approach in future work would reduce processing time and repeatability of data extraction.

A new technique for detecting edge points of adjacent planes has been developed with the purpose of determining the position of an edge without the need for accurate registration to a CAD model. The technique requires strong registration in one plane, and the processing can be simplified where the edge can be transformed to be approximately parallel to one axis of the coordinate system. Two planar surfaces with height difference between them of twice the standard deviation of the residuals to each plane are required in order to extract points. The method does not use a fixed value to detect edge points, but a multiple of the standard deviation of the fit and so varies with

the magnitude of random error in the measurement system. The technique is simple to implement and allows data points at the extent of the planar surface to be extracted with minimal processing and manipulation of the data, and is suited for combination with a least squares plane growing algorithm for segmentation of a large cloud, filtering data close to the edge of a planar surface.

Repeatability of the experiments performed is limited by the need to use test artefacts developed, or a verified copy. As analysis used the as-built dimensions of the artefacts rather than the nominal dimensions, reproducing the artefacts would be acceptable as long as they were correctly verified using a measurement system traceable to the national length standard.

The data processing methods developed in this work utilised a number of scripts and commercial software packages but does not present a 'one step' process. Scripts reduce the possibility of user error during processing but there is a need for a user to launch the correct script and provide correct input data. For the process to be quicker and simpler, full automation of the processing could be implemented although this is entering the field of Computer Science. The use of commercial software for certain tasks, including screen capture and creation of images would require researchers following the method to use alternative software if they did not have access to the commercial package.

Execution of the tests relied on manual operation of equipment which resulted in certain results not being available e.g. Depth of Field test results for Laser Line systems and the ability to quantify distance of measurement system to surface. The use of a motion stage for controlled motion would have been a valuable addition to the data collection process and provided greater repeatability.

A complete set of tests has been developed (Section 5.2.3.1 - 5.2.3.6) which satisfy the Research Objectives (Section 1.4). These tests evaluated the performance of non-contact optical measurement systems and could be utilised to assess the performance of future measurement systems in a repeatable manner. The rationale for design of tests (Section 5.1, 5.2) and detailed instructions are provided (Section 5.3). The tests have been proven through use and have provided a contribution to knowledge in this field (Section 6.1.1.3).

Using the research tools and software developed during this project, EFDA-JET now has the tools to extract point data from large data sets based on the nominal model,

without manual selection. Inspection of the limiter tile assemblies with point pitch on the measurement surface of 0.5mm would generate >200 million point objects (Section 2.4.5) for only the limiter tile units, with this number increasing where additional data are required. At the start of this research, to inspect a tile assembly against nominal would require the manual selection and extraction of data relating to the measured part before insertion into the CAD software, to maintain software performance. This technique was necessary as the complete data set exceeded the capabilities of the software, but resulted in additional work for the inspection department and possibility of human error during the selection process. Using the research tools developed, collected data registered to the nominal CAD model could be segmented based on simplified polygon models of the required parts, with significant manpower and time saving possible.

### **6.1.1.3. Equipment Trials**

Using the exploratory test artefact developed in the first year of research, surface measurement technologies owned by EFDA-JET and University College London were used to measure the surface and perform processing in line with newly emerging VDI/VDE 2634 guidelines (Section 4). Although the equipment was not state of the art, it provided information about the quantity of data which would be collected and experience of how such data could be processed. Technologies tested included white light projection, laser line triangulation, point projection photogrammetry and target-based photogrammetry. A large volume trial was performed inside the in-vessel test facility (IVTF) at EFDA-JET, a mock-up of the inside of the real machine used for training. This trial included the test artefact and used a polar measurement system based on phase-shift of light in flight to calculate distance (Section 4.4.4). The device tested was a state of the art commercially available system and data were processed in the same manner as earlier testing.

With the development of new test artefacts, a new series of trials were performed using technologies which offered the most potential for measuring inside the EFDA-JET machine, based on the exploratory trials and a review of metrology technologies (Section 3.2). Two of the technologies were selected for further testing, those being white light fringe projection (Section 3.2.4.3) and laser line triangulation (Section 3.2.4.2). Both technologies were incapable of measuring the complete machine from a single position because of limited sensor measurement volume and therefore some form

of method to register individual data would have been required. The white light projection systems demonstrated their abilities to collect data over an area of two tile assemblies but did not demonstrate their ability for collecting data with a total measuring volume greater than their single sensor measurement volume. Laser line systems tested had a fixed tracking unit which calculated the six degrees of freedom of a hand held unit collecting surface profiles. To minimise environment influences, particularly temperature and humidity, trials were conducted in a controlled environment at the UK National Physical Laboratory where possible. To perform a large volume measurement, one of the systems collected data at the EFDA-JET site in a volume approximately equal to that of half an octant of the real fusion machine.

The experimental phase (Section 5) validated the tests and data processing methodology developed in this research by collecting data from four state-of-the-art metrology tools using the tests developed. These data were processed according to the developed methodology, demonstrating the complete collection and processing workflow. The tests demonstrated applicability of the method to area based measurement systems e.g. white light fringe projection, and laser line triangulation systems. The equipment trial also provided the data to address the EFDA-JET specific research requirements, detailed in Section 1.3 and addressed in Section 6.2, without which this research would not address the needs of EFDA-JET.

A limitation to the equipment trial was that a single environment for data collection was not used, necessitating the need to scale data according to the artefact temperature during measurement. For the large volume trial the impact of attachment to a large stainless steel frame using stainless steel bolts was not modelled and could have introduced a temperature gradient. Although performed in a leading commercial software package, scaling introduced an additional potential error source into the measurement chain, but one which was necessary to secure use of the measurement equipment.

As only one measurement system was tested against the large volume test frame, the performance of the other measurement systems over a large volume cannot be estimated. For the white light fringe projection technologies some form of self-localisation or external tracking would be required (Section 3.2.5) which has not been tested because: an implementation of the externally tracked solution was not available at

the time of testing, installation of a suitable number of targets/markers for self-localisation was not applicable to EFDA-JET.

The repeatability of testing would have benefited from controlled motion of the laser line triangulation measurement devices during data collection and although not a limitation of the work performed, would be a valuable improvement to further testing. A motion stage was considered for this data collection phase however, with the locations and time available it could not be included.

### **6.1.2. Results**

In addition to the development of an evaluation methodology and addressing the EFDA-JET requirements, a number of contributions to knowledge in the field of surface metrology have been identified from the following tests:

#### **6.1.2.1. Approach angle**

The impact of angle between measurement system and surface normal has been presented for two laser line triangulation and two white light fringe projection technologies. These results contribute to current knowledge as results for these classes of measurement system had not previously been published. Evaluation of a laser line triangulation system mounted to CMM (Van Gestel et al., 2009) and phasogrammetry white light projection system (Kühmstedt et al., 2009a) have been presented by other researchers and highlights the timeliness and relevance of the research presented in this thesis, with publications by the author being published in 2007 and 2009 (Brownhill et al., 2007; 2009a; 2009b). The published papers report aspects of work performed and presented in this thesis, relating to the exploratory artefact (Section 4) and preliminary results of the primary equipment trial (Section 5).

It has been demonstrated that for laser line system A, the tracking system recording the 6 degrees of freedom of the hand held laser line scanner is the limiting factor for data collected with this system. The laser line profiles collected by the system showed low error however, in the direction of movement a 'wave' motion with magnitude  $\sim 90\mu\text{m}$  was identified and is constant across the piece. Such an error had been identified by Beraldin (2004) as resulting from movement between workpiece and stationary tracker. Without a second set of data confirmed to be free of vibration, the explanation put forward by Beraldin (2004) must stand

#### **6.1.2.2. Depth of Field**

The Depth of field test performed in this research contributes to knowledge through demonstrating the existence of an optimal working range for fringe projection systems. The optimal range could not be quantified as the distance between measurement system and surface was not recorded during the trials but over a 75mm range a 0.006mm improvement in random error was observed as the surface approached the sensor for one measurement system. The optimal range would be dependent on the design of the projection system and the measurement volume to which it is calibrated.

The second fringe projection system exhibited similar results although highlighted a limitation with the testing, in that the artefact surface did not extend the complete depth of field so quantitative results could not be provided for that system. Additionally, a limitation of the results for practical application is that the absolute distance of the measurement system to the surface was not recorded and therefore the absolute position of the 'sweet spot' from the measurement device is unknown; this has been addressed for future testing by including this instruction within the experiment guidance.

#### **6.1.2.3. Edge Measurement**

Work by Buzinski et al. (1992), Curless & Levoy (1995) and Blais (2005) describe the errors likely to occur at surface discontinuities but do not provide examples from real data, this work has demonstrated the errors in real data sets for state of the art equipment.

This work has demonstrated the existence of a new error not described in other works, relating to the downward curve of a surface next to a step edge when measured with a fringe projection system. The error was only apparent for one of the tested systems and related to reflection from one surface affecting the light intensity recorded on another surface and a resultant error in the phase calculation. The effect had a significant impact on the data collected, making a large area of data unusable. The errors shown in this work demonstrate that measurement of a step edge/surface discontinuity will be subject to systematic error dependent on the orientation and configuration of the measurement system. Testing has also shown that significant differences in data may be seen from equipment that utilise the same technical principle.

For the calibrated measurement volume and systems tested, results demonstrated that data within 0.5mm of an edge should be ignored for registration purposes as these are

likely to be impacted by ‘edge effects’. The 2mm used during testing was proven to be overly cautious and could be revised to enable greater data to be used as part of the registration process. Results indicated 0.5mm was sufficient for the majority of systems tested although this distance should be increased where there is an adjacent surface closer to the measurement device. This value will alter for projection systems dependent on the calibrated measurement area and focussing. Development of a model to calculate the optimal distance is worthy of further work but beyond the scope of this project.

### **6.1.2.4. Registration**

As part of developing a repeatable means of registering surface data, tests were performed on the impact of edge data on surface-based registration. For the gap artefact a reduction in RMS Error of 0.001mm was demonstrated when data impacted by edge effects (identified by the method developed) were not utilised for surface-based registration. Although a small improvement, for applications requiring high precision, such an improvement may prove beneficial e.g. measuring 0.040mm features on EFDA-JET tiles.

### **6.1.3. Summary of Contribution**

This work has developed a new, repeatable process for evaluating non-contact surface measurement equipment, including: design and manufacture of a new set of test artefacts, a data collection and processing methodology and scripts to automate processing. This method is available for users of non-contact surface metrology technologies to assess the performance of their equipment, re-evaluate in the future and compare the performance of other measurement systems.

By utilising the evaluation method developed against four state of the art measurement systems it has been possible to demonstrate that ‘edge data’ can adversely affect surface based registration; that for white light fringe projection systems there is an optimal range within the calibrated volume which can reduce random error of data by  $\sim 6\mu\text{m}$ ; identified a new edge effect error not previously identified; provided data on the impact of measurement system to surface normal angle including for white light fringe projection systems not previously published and provided recommendations and examples of orientations to collect optimal edge measurement data including examples from validated data sets.

## Conclusions and Further Work

Results have been presented and published at international conferences for metrology and Fusion Engineering and elements of the processing methodology used within another metrology research project.

## 6.2. Conclusions for EFDA-JET

This section addresses the requirements laid out in Section 6.1 with conclusions directly related to the EFDA-JET requirements (Section 1.3), derived from the work performed during this research.

### 6.2.1. *Can optical, non-contact surface measurement tools verify installation of plasma facing components to sub-millimetre accuracy?*

- Can the measurement systems measure the complete volume?

All of the measurement systems tested can be deployed as hybrid systems (Section 3.2.5) utilising a moving measurement head and static tracking position. A hybrid system would be the optimal choice to minimise the need for surface markers for registration as the limiter tile surface lacks the form or texture for self localisation and tiles are not unique in their design. Given that the commercially available options for hybrid systems use optical or laser ‘trackers’, one example of each technology was selected and the number of stationary tracker positions required calculated. The minimum number of positions required, from preliminary calculations, is for a laser tracker which could collect data on all surfaces with absolute minimum of four positions. Surface measurement with four positions should be achievable but five or even six positions would be recommended to provide improved registration between tracker positions and ensure all areas can be accessed (Section 5.4.6.3).

- Estimated time for complete measurement of limiter tile surfaces?<sup>11</sup>

A polar measurement device e.g. ToF or phase-shift (Section 3.2.4.1), would require a number of instrument locations similar to that calculated for a laser tracker. The measurement system would be delivered by remote handling equipment and located on a stable surface e.g. the in-vessel manned access floor or custom mounts, measurement could be remotely started once the remote handling equipment was outside the measurement area. For this setup, the movement and correct positioning of the measurement system by remote handling would require greater time than the measurement itself. Large quantities of data could be collected in a matter of hours, with a polar surface measurement system, less than 1 hour per measurement position is estimated based on the work performed. However the data have shown to have a number of errors caused by multiple reflection and laser spot diameter (Section 4.4.4)

---

<sup>11</sup> See: Figure 2.3: Inside the EFDA-JET machine (June 2005) with two of the limiter beams highlighted Figure courtesy of EFDA-JET, pp.36.

which make the system unsuitable for measurement other than the overall form of the machine.

In order to estimate the time required to measure the inside surface of the EFDA-JET machine using a hybrid measurement system (Section 3.2.5), several components must be calculated: 1) the number of stationary tracking positions required and time for remote handling to reposition and setup the tracker in a new location, 2) time taken to record the surface of a single tile assembly, 3) movement time between assemblies including any time required for equipment to become stable before measurement can occur (for white light projection systems). These factors will determine the time required for data collected, but no data processing. During the trial, measurement with a white light projection system took ~2 minutes and with the calibrated measurement area could measure 2 tile assemblies per measurement. Estimating 1800 limiter tile assemblies within the machine (Section 2.3.1), the data collection time for these tiles would be ~30hrs. Given the recommendation for a tripling of data collection advised in the following Section (“Can 2.5mm gap (inter-tile) be detected”), the total collection time would increase to ~90hrs. For a laser line triangulation system a realistic estimate of measurement time for a single assembly is two minutes which would result in a measurement time of ~60hrs. An increased collection speed for a laser line system could be achieved but, inter-line (profile) distance would increase and an increased chance of interpolation, both reducing point pitch on the measurement surface and reducing edge detection capabilities. Mechanical handling would offset some effects of increased speed over the surface, producing regular inter-line spacing and data density

The estimates provided do not account for repositioning of the tracking or measurement device, nor do they include other tile types of regions of the vessel e.g. diverter region. Estimating complete collection time i.e. for all surfaces, is beyond the scope of this project but could be achieved by the EFDA-JET design office by applying information provided by this project (Section 6.2.3).

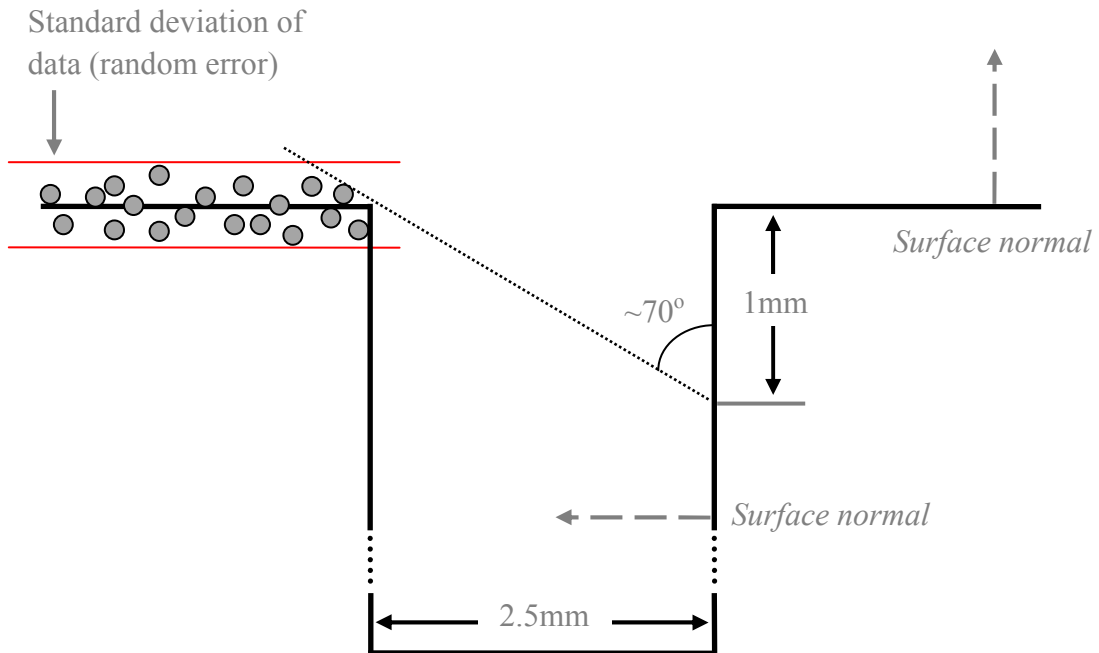
- Can 2.5mm gap (inter-tile) be detected?

A 2.5mm nominal gap exists between limiter tile assemblies in the poloidal direction of a limiter beam (Section 2.4.2). Measurement systems must be able to detect this gap to identify individual assemblies. All systems tested could detect the gap, with white light fringe projection systems overestimating the dimensions of the gap each time. Laser line systems were found to create spurious data inside the slot attributable to internal

## Conclusions and Further Work

reflection in the test artefact. For a slot with greater depth internal reflection may be reduced and spurious data may not be created although this cannot be proven from data collected. For detection and measurement of a gap feature of this dimension, a laser line system perpendicular to the slot edge would be advised.

A fringe projection system angled so as not normal to the surface could be used to capture the inside edge of the slot (Figure 5.71). To achieve lowest data uncertainty, the measurement system should be horizontal so that there is overlap between the areas measured by each sensor in the system. In this orientation the tile assembly would be approached from above or below, with approach to the surface of up to  $50^\circ$  from the surface normal acceptable (Figure 5.30). With this orientation of device, the projected fringe pattern would be perpendicular to the slot edge and in testing produced data with smallest relative slot dimensions (Figure 5.70). Measurement data inside the slot should reach a depth exceeding the standard deviation of the measurement system data (random error), or a multiple thereof (Figure 6.1). For the systems tested, standard deviation of residuals to a fitted plane through data were  $<20\mu\text{m}$  for three of the four systems (Figure 5.38) and a measurement depth of 1mm is advised. To achieve 1mm measurement depth inside the 2.5mm wide slot, a measurement system could be up to approximately  $70^\circ$  to the normal of the top surface. To collect data inside the slot and the main tile surface, a two stage measurement process would be suggested, measuring the main (plasma facing) area of the tile at optimal angle to reduce random error,  $15\text{-}30^\circ$  for fringe projection system A (Section 5.4.1.3), and then measurement of the slot at  $\sim 50^\circ$  to the slot surface normal (Figure 5.42) which will be  $\sim 40^\circ$  to the surface normal of the primary plasma facing surface. The two stage process is an attempt to minimise random error on the primary plasma facing surface and reduce the angular error of data collected within the slot.



Suggested measurement depth required for 2.5mm width slot, based on random error of  $\leq 20\mu\text{m}$  is 1mm.

**Figure 6.1: Side view of 2.5mm slot between tile assemblies – it is suggested that measurement into the slot to a depth of 1mm is required in order to exceed the random error of data on primary plasma facing surface.**

Using the method described, three measurements per tile assembly would be required, increasing data collection time and cost in comparison to a single measurement, but would provide more information. Additionally, 6DoF tracking errors would impact the registration between slot and tile surface data. Where 6DoF errors exceed those of the measurement device (as seen for laser line system A, Section 5.4.1.2), re-registration of slot data to that of the primary plasma facing surface could be performed, minimising the point to point distance on the measurement surface between the data sets to improve alignment between the data sets (Section 3.3.2). Such an alignment would be affected by the angular error present in the data and is the reason for selecting the approach angle for the slot as that which has the lowest angular error.

### ***6.2.2. Can optical, non-contact surface measurement tools quantify dimensions and surface change of protective tiles?***

- Can 0.6mm intra-tile gap be reliably detected?

A tile assembly would consist of 5-7 tile blocks with nominal gap between blocks of 0.6mm (Section 2.3). Only the central block within an assembly was fixed, with the other blocks held in place by pins with nominal gap of 0.6mm between them. From the

Gap Artefact a series of profiles from the 0.22, 0.34 and 3mm slots were extracted and processed as they provided data with good overall match to EFDA-JET needs. A reasonable assumption could be made that if a measurement system could detect a 0.35mm gap, which several systems were capable of (discussed below), then a 0.6mm would also be achievable.

- Can 0.35mm gap between castellations be reliably detected?

Each tile block was machined from solid with gap between castellations of 0.35mm, the dimensions of the slots would change with expansion and contraction but major change would only occur through damage to the surface. At this measurement level the purpose would be to monitor and quantify any change to the tile surface. With the fringe projection systems tested the gap could be reliably detected by one system when the projected pattern was perpendicular to the slot edges. The capability of this system could be increased, at the expense of working volume, by reducing the measurement volume to provide greater resolution. For the laser line systems, one system could detect the gap when laser line was perpendicular and at 45° to the edges of the slot, where clear breaks in the data were evident (Section 5.4.4). At this level of detail where small features are of interest, one must be sure that no interpolation is occurring within the data as this introduces “additional error influences” (The Association of German Engineers (VDI), 2008).

The smallest slot width on the gap artefact was 0.22mm which was detected by the measurement systems with differing abilities. One of the fringe projection systems showed a clear break in data within 3 standard deviations of the plane but also showed data outside of this range, because of this the slot is only visible in profile view. Measurement of feature this size of was beyond the capabilities of the fringe projection systems at the selected working volume. Moving these instruments closer and reducing the measurement volume would increase the ability of these systems to detect such features and when combined with the low random error (~0.01mm) that these technologies have shown themselves capable of, measurement of the surface could be achieved (Section 5.4.3.1).

For the laser line systems tested, clear breaks in the data around the slot were seen, specifically for measurement where the line was perpendicular to the slot edges. Erroneous data were produced inside the slot, forming a ‘v’ or ‘u’ shape between the surfaces and in the 45° case a ‘wall’ of points rising up from one surface and a similar

sized group of points descending from the opposite side of the slot. The geometry of the sensing head would suggest working at the minimum stand-off from the surface and measuring slots with laser line perpendicular would produce data with greatest likelihood of detecting slots. Further cannot be said as the gap test artefact had no smaller slots as these were not required for EFDA-JET.

- Can 0.2mm intra-tile step be reliably detected?

Between tile blocks in an assembly the nominal step height was 0.2mm, this step being required for a block to shadow the adjacent block and protect it from damage (Section 2.3.1). All of the tested systems detected the 0.2mm step on the artefact, with deviation to the reference <20% of the reference height (Section 5.4.3.1). The 0.2mm step present on the step artefact was the last step at which all systems offered data with deviation under 20% of the reference height.

- Can 0.04mm step between castellations be reliably detected?

In the central block of a tile assembly the step between castellations was nominally 0.04mm and change in this height could indicate erosion or deposition of the tile surface and damage. Given the random error present in the measurement systems the detection of a 0.04mm step would be a challenge as the random error on each surface may be half the step height. The measurement of a 0.04mm step would be possible but would require data to be registered to a model in order to extract the relevant data and identify individual planar areas. Without registered data, detecting a change between surfaces would present a significant challenge as the magnitude of the random error approaches the actual step height. Where the random error is half the step height, detection would not be possible using the methods employed in this work as the random error equates to the standard deviation of the data sets such that a clear distinction between the two sets would not be possible. This approach is also very reliant on the parallelism of the two surfaces.

### ***6.2.3. What is the optimal approach to a surface to perform surface measurement in the EFDA-JET tokamak?***

- Can a complete tile assembly be captured from single position/orientation?

From a single position normal to the centre of a tile assembly, a fringe projection system was capable of collecting data on all facets, up to and including 50° (Section 5.4.1.2, Figure 5.29 & Figure 5.30). Because of the shiny reflective surface finish

required by the EFDA-JET project, careful positioning of the projection system to the surface and control of the intensity were required to avoid sensor saturation (Section 5.4.1.2).

Laser line systems were required to traverse the surface to collect data and therefore could not collect the complete surface from a single position, but were tested to check whether they could measure the surface with the sensor at a fixed orientation to the surface. For the two systems tested, 100% coverage was achieved by one system however laser line length must be considered as in the vertical orientation one system had insufficient length to complete measurement in a single pass resulting in increased measurement time and cost for EFDA-JET use.

- How does angle of approach to a surface affect data quality?

For the systems tested, all could collect data up to and including  $50^\circ$  to the surface normal (Section 5.4.1.2), which was the limit imposed by the artefacts produced based on EFDA-JET requirements (Section 1.3). Two approach angles were considered, simulating approaching a surface from above/below and left/right (vertical and horizontal approach respectively).

In the horizontal approach case (Section 5.4.1.3, Figure 5.31 & Figure 5.32) fringe projection system A maintained an RMS error per facet of  $\sim 0.008\text{-}0.016\text{mm}$  showing no systematic increase in error with increasing surface angle. Fringe projection system B had increased error in comparison to system A, but again uncertainty did not increase in line with surface angle. For the laser line systems, overlapping data appears to have had an averaging effect which was seen in the clustered residuals following least squares best fit plane fitting, maintaining error of between  $0.01\text{-}0.02\text{mm}$  for both measurement systems (Figure 5.33).

For the vertical approach case (Section 5.4.1.3, Figure 5.37 & Figure 5.38) the RMS errors for fringe projection system A were less than  $\sim 0.015\text{mm}$  for all facets, which showing no significant difference to the horizontal approach case. Fringe system B showed greatly increased residuals of the order of  $10\text{-}40\mu\text{m}$  in comparison to fringe system A, and increased errors for one half of the artefact to the other half, suggesting different capability of the two sensors. Over the  $0^\circ\text{-}50^\circ$  range of angles, Laser line A had increased error up to  $0.02\text{mm}$  for the steepest rising facets and laser line B a similar increase in error but total range of the error being  $\sim 5$  microns (Figure 5.39). Where

increased error existed for the vertical approach, this could be minimised by starting measurement in the centre of the assembly and working outwards, although this would increase measurement time as a single movement over the surface could not be performed. For all systems and orientations there was no clear evidence that the angle of the surface being measured had an impact on the random error in the data.

Although random error within the data was not greatly affected by increase in angle between measurement system and surface, systematic angular errors did occur. In the horizontal approach case increased angular errors existed for fringe projection system B, where one of the two sensors deployed by the system was occluded by the artefact, however this was not seen in the second system tested (Section 5.4.1.3, Figure 5.38). Such a case could only occur where the measurement system used multiple sensors. For a single sensor system, occlusion would always result in the collection of no data whilst occlusion occurred. For the laser line system the averaging effect seen with calculation of random error again appears to have aided the systems, with data largely free of angular error.

In the vertical approach case one fringe projection system showed no angular error whilst the other had constant overestimation of the surface angle for all but one facet of the artefact used for the test. For laser line system A, overestimation of surface angle was seen on rising surfaces and underestimation of downward angled surfaces, the same effect was not seen for the other laser line system tested.

- How precisely do measurement systems need to be positioned relative to the surface to be measured?

Testing the effect of altering the distance between measurement system and surface revealed for both fringe projection systems the existence of a ‘sweet spot’ where random error reached a minimum. The sweet spot was the result of optimal fringe spacing on the measurement surface caused by the perspective projection of the projector lens. As the distance from the projector to the surface increased, the spacing and width of projected fringes increased reducing the ability to record fine detail. Over the 75mm range tested, a 0.006mm reduction in random error was seen for one of the systems which could greatly assist in measurement of fine detail relating to the monitoring of surface damage. The position and shape of the sweet spot cannot be quantified as the range of the measurement systems from the surface was not constant for all measurement systems or configurations. It is recommended that when selecting a

system, a set of tests imaging an artefact at a range of distances are carried out to characterise optimal working volume.

**6.2.4. *What method can be used by EFDA-JET to assess the performance of measurement systems, now and in the future?***

A method has been developed using test artefacts presenting features and surface finish close to the real EFDA-JET protective tile surface. Real tiles were not tested as the material used required a controlled environment and handling and offered no opportunity to quantify ‘how good’ the measurement systems actually were on the final surface finish. Measurement of the artefacts in the directed manner (Section 5.3) would allow future equipment and data to be directly compared against the data and results from this trial. The use of artefacts and a controlled collection method reduced the effect of the measurement environment for the purpose of leaving the measurement system as the only significant error source for a given surface form and finish (Figure 4.1).

Data processing and automation software has been developed in VBA which can operate within the Microsoft Excel spreadsheet package installed on desktop computers at EFDA-JET. A user familiar with the Excel package would require no additional training to use the developed packages, only needing to be told how to execute the required packages. Automation tools developed within the PolyWorks software package utilised functions already within the software, but removed the need for the user to remember a complex series of instructions, instead only needing to click an icon. The method and research tools developed have been proven through use in this work and parts have been used on a research project between University College London and aerospace manufacturer Airbus.

**6.2.5. *Summary for EFDA-JET***

Based on the described requirements (Section 6.2.1-6.2.4), non-contact optical surface measurement technologies could be used to verify the installation of components within the EFDA-JET vessel to sub-millimetre accuracy. The monitoring of the plasma facing surface could be performed by the measurement systems with the recommendation to use a white light projection system and capture the complete tile assembly from a single position, removing uncertainty associated with registration of data. This method would require knowledge of which assembly is being measured and an off-line analysis of

## Conclusions and Further Work

results. It would be assumed that an area of the surface is unchanged against which to register newly collected data to a previous survey.

Measurement time has been estimated at a minimum of 30hrs to collect data on all limiter tile assemblies within the machine, excluding time for positioning of tracking equipment within the vessel. At a cost of £15.5k per hour spent inside the vessel (Section 2.4.4), a complete survey of the limiter tiles using the equipment and setup in this trial would cost ~£500k excluding equipment costs and staffing. Using the information provided in Section 6.2.4, the optimal data collection method can be determined to obtain data with minimum uncertainty, whilst minimising data collection time and therefore financial cost.

### **6.3. Further Work**

Future work to build on the results of this project could be divided into two areas, the first deals with improvements to the testing phase and data collection. The second area of future work would be the development of processing techniques to simplify and speed up data processing whilst extracting more information from the collected data.

#### **6.3.1. Testing**

For future testing and data collection the inclusion of a photographic spatial resolution target within the measurement volume is suggested to determine the resolution of the measurement device which in turn will allow a rapid assessment to be made of the measurement capability to small features which characterise localised inspection. Registration of data should be performed without use of the surface data; to achieve this, spheres should be directly attached to the test artefacts to guarantee they are included in any measurement and can be used for registration. Such a method would ensure data sets could be analysed independent of 'edge effects' introduced by the measurement system and that the position of edge features within the data could be directly compared between measurement systems. Spheres were present on the portable test frame however the calibrated measurement volume of tested fringe projection systems was insufficient and therefore the spheres were not present for each data set. For laser line systems where measurement volume was dictated by the 6DoF tracking unit, data were processed in line with that performed for data from the fringe project systems in order to maintain a consistent processing methodology. For future data collection the use of mechanical handling would be advised in order to achieve greater repeatability in testing and greater resolution when determining optimal angle of measurement system to a surface discontinuity.

The effect of measurement system angle to a surface has been tested for angles up to 50° within the design specification of angle artefact B. 50° was selected as the maximum angle to create on the artefact as approach to a surface within the EFDA-JET vessel at greater than 50° was considered an unlikely event, a decision validated by the successful completion of the EFDA-JET design review process. The approach taken by Van Gestel et al. (2009) to use a planar surface capable of being positioned at 0° (parallel to the sensing system) and a series of different angles would provide simpler data to process and would be without any effect of change in range, but would require greater time for collection and an accurate rotation stage. Measurement systems have provided

## Conclusions and Further Work

data on a range of artefacts and orientations with the artefacts designed to collect maximum data in a reasonable time (<1 day). Change of measurement practice to use a single plane requiring repositioning would increase data collection time greatly.

The existence of optimal range for fringe projection systems has been identified but cannot be quantified from the data collected. Further trials should record the range of the measurement system to the surface, with a series of measurements performed at varying range to characterise individual system capability. The same tests should be performed with altered calibrated measurement volume to assess whether optimal range can be calculated from the known calibrated measurement area. Such a trial should be performed in conjunction with generation of a mathematical model to include the geometry and optical properties of the measurement system.

In order to minimise environmental influence and collect data which demonstrates the true performance of the measurement system, only one system (laser line system A) measured the artefact attached to the large volume test frame. The absolute performance of a white light measurement system for the EFDA-JET volume cannot be inferred but relative assessment has been performed revealing important information about measurement performance to surface features. A further trial should be performed with a hybrid white light measurement system, measuring all artefacts attached to the large volume frame.

It must be noted that the measurements made within this work are a single example of measurement system performance. Although great care has been taken to provide an environment, test artefacts and testing methodology to minimise errors other than those from the measurement system, some additional errors are likely to exist. As part of further trials, repetitive testing should be performed to ensure results are representative of the system performance. It is recognised that with additional measurements, time required would increase greatly and require even greater cooperation of measurement system providers, but the reassurance gained from these tests is justified by the savings made during the EFDA-JET time critical shutdown process (Section 2.4.4). In order to collect data with a statistically significant number of samples the loan of equipment may be necessary, but collection would also require operator training to avoid the introduction of an operator as an additional error source.

To better understand the capabilities of the measurement systems the resolution of those systems would require calculation. A suitable approach would be the inclusion of an ISO 16067-1 test target within the measurement area for any future testing.

Since re-submission of this work, further work on methods to evaluate non-contact optical measurement systems has been performed, with a notable contribution being Carrier et al., (2011). Carrier et al. present a new artefact and number of tests based around the Geometric dimensioning and tolerancing to characterise measurement systems.

### **6.3.2. Processing**

The edge detection technique developed in this work could be combined with a region growing method to segment data into planar regions and allow automatic calculation of gap/slot widths. Regions could be limited with the known capability of each measurement system to limit the extent of a least squares best fit plane and the lateral distance of each point to the plane. Existing segmentation algorithms based on the analysis of surface normal may not be appropriate for the tile surface where only small angular change exists between facets. Additionally, the processing techniques used in this work could be fully automated to generate all required outputs based only on the input of a data set registered to the as-built CAD model.

The developing work of L. MacDonald a research student at University College London and his use of a slanted edge function to measure edges and determine resolution of measurement systems should be investigated within the context of 3D data capture with optical systems. The work is developing techniques to evaluate the resolution required to record objects and can applied to evaluate the resolution of 2D and 3D measurement systems.

## 7. References and Bibliography

AEESF, 1998a. *Laser Imaging System Studies and Experimental Tests: Introductory Stage Report*. Unpublished.

AEESF, 1998b. *Minutes of LIVVS Programme, First Stage Meeting*. Frascati: Unpublished Associazione EURATOM ENEA sulla Fusione.

AEESF, 1999. *Laser Imaging System Studies and Experimental Tests: Second Stage Report*. Unpublished.

Ahola, H., Heikkinen, V., Keranen, K. & Suomela, J., 2001. Modified ITER In-Vessel Viewing System. *Fusion Engineering and Design*, 58-59, pp.513-16.

Ahola, H. et al., 1998. ITER In-Vessel Viewing System Prototype Campaign. In Beaumont, B., Libeyre, P., de Gentile, B. & Tonon, G., eds. *Proc. 20th Symposium on Fusion Technology*, 1998.

Akca, D. et al., 2007. Performance Evaluation of a Coded Light System for Cultural Heritage Applications. In *Videometrics IX*. San Jose, USA, 2007. SPIE The International Society for Optical Engineering.

Albarran, T. et al., 2008. Preliminary Budget Methodology for Reverse Engineering Applications Using Laser Scanning. In J. Bártolo, ed. *Virtual and Rapid Manufacturing*. London: Taylor & Francis. p.232.

Alcoa, 2007a. *Cast Aluminium*. [Online] Available at: [http://www.alcoa.com/mill\\_products/catalog/mic-6.pdf](http://www.alcoa.com/mill_products/catalog/mic-6.pdf) [Accessed 30 January 2007].

Alcoa, 2007b. *Wrought Aluminium*. [Online] Available at: [http://www.alcoa.com/mill\\_products/catalog/pdf/6061-T651.pdf](http://www.alcoa.com/mill_products/catalog/pdf/6061-T651.pdf) [Accessed 30 January 2007].

ASTM, 2010. *ASTM International Technical Committee E57*. [Online] Available at: <http://www.astm.org/COMMIT/COMMITTEE/E57.htm> [Accessed 09 March 2010].

Autodesk, 2010. *AutoCAD 2011*. [Online] Available at: [http://www.randsoftware.com/imaginit/1/pdfs/technology/software/2011\\_autocad\\_2011\\_top\\_10\\_reasons.pdf](http://www.randsoftware.com/imaginit/1/pdfs/technology/software/2011_autocad_2011_top_10_reasons.pdf) [Accessed 16 June 2010].

Baribeau, R. & Rioux, M., 1991. Influence of Speckle on Laser Range Finders. *Applied Optics*, 30(20), pp.2873-78.

Bartolini, L. et al., 2001. Experimental Results of Laser in Vessel Viewing System (LIVVS for JET). *Fusion Engineering and Design*, 58-59, pp.507-11.

Bartolini, L. et al., n.d. *In-Vessel Viewing System For Nuclear Fusion Machines Based On A Laser Radar Vision System*. Unpublished.

Basis software Inc., 2009. *Surphaser 3D Scanners*. [Online] Available at: <http://www.surphaser.com/> [Accessed 11 February 2010].

Bell, S., 1999. *Measurement Good Practice Guide: A Beginner's Guide to Uncertainty of Measurement*. London: UK: National Physical Laboratory.

## References and Bibliography

- Beraldin, J.-A., 2004. Integration of Laser Scanning and Close-range Photogrammetry - The Last Decade and Beyond. *International Archives of Photogrammetry Remote Sensing and Spatial Information Sciences*, 35(7), pp.972-83.
- Beraldin, J.-A., 2008. Digital 3D Imaging and Modeling: A Metrological Approach. *Time Compression Magazine*, January/February. pp.33-35.
- Beraldin, J.-A. et al., 2000. Active 3D Sensing. In *Modelli E Metodi per lo studio e la conservazione dell'architettura storica*. Pisa, 2000. University: Scola Normale Superiore.
- Beraldin, J. et al., 2007a. Traceable 3D Imaging Metrology: Evaluation Of 3D Digitizing Techniques In A Dedicated Metrology Laboratory. In Gruen, A. & Kahmen, H., eds. *In Proc. Eighth Conference on Optical 3-D Measurement Techniques*. Zurich, Switzerland.
- Beraldin, J.-A. et al., 2003. Optimized Position Sensors for Flying-Spot Active Triangulation Systems. In *Proc. Fourth International Conference on 3-D Digital Imaging and Modeling (3DIM)*. Banff, Canada, 2003.
- Beraldin, J.-A. & Gaiani, M., 2005. Evaluating the Performance of Close Range 3D Active Vision Systems for Industrial Design Applications. In Beraldin, J.-A., El-Hakim, S., Gruen, A. & Walton, J., eds. *Videometrics VIII.*, 2005. SPIE.
- Beraldin, J.-A. et al., 2007b. Traceable 3D imaging Metrology. In *Proceedings- SPIE The International Society for Optical engineering*. San Jose International Society for Optical Engineering.
- Bergevin, R., Soucy, M. & Gagnon, H., 1996. Towards a General Multi-View Registration Technique. *IEEE Transactions on Pattern Recognition and Machine Intelligence*, 18(5), pp.540-47.
- Besl, P. & McKay, N., 1992. A Method for Registration of 3-D Shapes. *IEEE Transactions on Pattern Recognition and Machine Intelligence*, 14(2), pp.239-56.
- Blais, F., 2004. Review of 20 Years of Range Sensor Development. *Journal of Electronic Imaging*, 13(1), pp.231-4.
- Blais, F. et al., 2001a. Target Tracking, Object Pose Estimation, and Effects of the Sun on the NRC 3-D Laser Tracker. In *Proc. 6th International Symposium on Artificial Intelligence, Robotics and Automation in Space (i-SAIRAS 2001)*. Québec, Canada.
- Blais, F., Beraldin, J.A. & El-Hakim, S., 2001b. Real-time 3D Pose Estimation Using Photogrammetry and Laser Based Geometrical Target Tracking for Autonomous Operation in Space. In *Proc. 5th Conference on Optical 3-D Measurement Techniques*. Vienna, Austria.
- Blais, G. & Levine, M., 1995. Registering Multiview Range Data to Create 3D Computer Objects. *IEEE Transactions on Pattern Analysis and Machine Intelligence*, 17(8), pp.820-24.
- Blais, F., Picard, M. & Godin, G., 2004. Accurate 3D Acquisition of Freely Moving Objects. In *Proc. 2nd International Symposium of 3D Data Processing, Visualization, and Transmission (3DPVT'04)*. Thessaloniki, Greece, 2004. IEEE Computer Society.
- Blais, F. et al., 2005. High Resolution Imaging at 50µm Using A Portable XYZ-RGB Color Laser Scanner. In *International Workshop on Recording, Modeling and Visualization of Cultural Heritage*. Ascona, Switzerland, 2005.

## References and Bibliography

- Boehler, W., Bordas Vicent, M. & Marbs, A., 2003. Investigating Laser Scanner Accuracy. In *Proc. XIXth CIPA Symposium*. Antalya, Turkey, 2003.
- Boehler, W., Heinz, G. & Marbs, A., 2002. The Potential of Non-Contact Close Range Laser Scanners for Cultural Heritage Recording. *International Archives of Photogrammetry Remote Sensing and Spatial Information Science*, 34(5/C7), pp.430-36.
- Borgeat, L. et al., 2007. Visualizing and analyzing the Mona Lisa. *IEEE computer graphics and applications* [0272-1716], 27(6), pp.60-68. Ref:404.
- Brade, R., 1992. *Torus Hall In Vessel Datum Ring Survey To Inner Wall Datum Balls*. Site Inspection Report. No. 4435. Unpublished.
- Brade, R., 2007. *Personal Communication*. Unpublished.
- Bräuer-Buchardt, C. et al., 2006. Distance Dependent Lens Distortion Variation in 3D Measuring Systems Using Fringe Projection. In *BMVC06*. Edinburgh, UK, 2006. <http://www.macs.hw.ac.uk/bmvc2006/papers/150.pdf>.
- Breuckmann GmbH, 2010. *Breuckmann GmbH - optical 3D Scanner*. [Online] Available at: <http://www.breuckmann.com/index.php?id=breuckmanngmbh&L=2> [Accessed 08 February 2010].
- Breuckmann, 2009. *stereoSCAN 3D*. [Online] Available at: <http://www.breuckmann.com/index.php?id=stereoscan&L=2> [Accessed 09 February 2010].
- Brooks, R. & Heflinger, L., 1969. Moiré Gauging Using Optical Interference Patterns. *Applied Optics*, 8(5), pp.935-39.
- Brownhill, A., Brade, R. & Robson, S., 2007. Non-Contact Surface Measurement in a Hazardous Environment. In *8th Conference on Optical 3-D Measurement Techniques*. Zurich, Switzerland, 2007.
- Brownhill, A., Brade, R. & Robson, S., 2009a. Performance Study of Non-Contact Surface Measurement Technology for use in an Experimental Fusion Device. In Remondino, F., Shortis, M. & El-Hakim, S., eds. *Proc. of SPIE*. San Diego, USA Optical Society of America. Note: This paper has different content to the similarly titled paper presented at SOFE conference 2009.
- Brownhill, A., Brade, R. & Robson, S., 2009b. Performance Study of Non-Contact Surface Measurement Technology for Use in an Experimental Fusion Device. In *Proc. 36th International Conference on Plasma Science and 23rd Symposium on Fusion Engineering Conference, ICOPS-SOFE 2009*. San Diego, USA IEEE. Note: This paper has different content to the similarly titled paper presented at SPIE Optics & Photonics conference 2009.
- Brunson, 2010. *SMRs*. [Online] Available at: <http://www.brunson.us/Products/SMR.asp> [Accessed 19 March 2010].
- BSI, 1995. *Part 1: Basic and general terms (VIM) & Part 3: Guide to the expression of uncertainty in measurement BSI PD6461*. Milton Keynes: British Standards Institution.
- Bureau International des Poids et Mesures, 1984. *Resolution 1 of the 17th meeting of the CGPM (1983)*. [Online] Available at: <http://www.bipm.org/en/CGPM/db/17/1/> [Accessed 10 January 2010].

## References and Bibliography

- Burnside, C.D., 1976. *Electronic Distance Measurement*. London, England: Crosby Lockwood Staples.
- Buzinski, M., Levine, A. & Stevenson, W., 1992. Performance Characteristics of Range Sensors Utilizing Optical Triangulation. In *Proc. IEEE National Aerospace and Electronics Conference (NAECON)*. Dayton, USA, 1992. IEEE.
- Carman, P., 2009. *Personal Communications*. Unpublished. Unpublished.
- Carrier, B., MacKinnon, D., Cournoyer, L. & Beraldin, J.-A., 2011. Proposed NRC Portable Target Case for Short-Range Triangulation-Based 3-D Imaging Systems Characterization. In *IS&T/SPIE Electronic Imaging Conference 7864A, 3D Imaging Technology*. San Francisco, California, 2011.
- Chen, F., Brown, G. & Song, M., 2000. Overview of Three-Dimensional Shape Measurement Using Optical methods. *Optical Engineering*, 39(1), pp.10-22.
- Chen, Y. & Medioni, G., 1992. Object Modelling by Registration of Multiple Range Images. *Image and Vision Computing*, 10(3), pp.145-55.
- Cheok, G., Lytle, A. & Saidi, K., 2006. Status of the NIST 3D Imaging System Performance Evaluation Facility. *Laser Radar Technology and Applications XI*, 6214, pp.62140F-1 - 62140F-12.
- Cheok, G., Saidi, K. & Franaszek, M., 2009. Target Penetration of Laser-Based 3D Imaging Systems. In *Proceedings SPIE 21st Annual Symposium on Electronic Imaging 2009 - 3D Imaging Metrology Conference*. San Jose, USA, 2009. SPIE.
- Cheok, G., Saidi, K. & Lytle, A., 2007. Evaluating a Ranging Protocol for 3D Imaging Systems. In *Proceedings of ISARC 2007*. Kochi, India., 2007.
- Chetverikov, D., Stepanov, D. & Kresk, P., 2005. Robust Euclidean Alignment of 3D Point Sets: the Trimmed Iterative Closest Point Algorithm. *Image and Vision Computing*, 23, pp.299-309.
- Clarke, T., 1998. Non-Contact Measurement Provides Six of the Best. *Quality Today*, 46-48 July.
- Clarke, T. & Fryer, J., 1998. The Development of Camera Calibration Methods and Models. *The Photogrammetric Record*, 16(91), pp.51-66.
- Colleti, A., 2001. *Fault Analysis Report on Tilt & Pan Gears Systems of the JET Laser in Vessel Viewing System (LIVVS)*. Unpublished.
- Creaform, 2010. *Handyscan 3D Scanners | REVscan, VIUscan, EXAscan, MAXscan, ERGOscan*. [Online] Available at: <http://www.creaform3d.com/en/handyscan3d/products/default.aspx> [Accessed 18 February 2010].
- Curless, B. & Levoy, M., 1995. Better Optical Triangulation through Spacetime Analysis. In *Proc. Fifth International Conference on Computer Vision (ICCV'95)*. Boston, MA, USA, 1995. IEEE Computer Society.

## References and Bibliography

- Cyberware, 1999. *Cyberware*. [Online] Available at: <http://www.cyberware.com/> [Accessed 09 March 2010].
- Dal Bello, S. et al., 1998. An Autonomous Mobile Tracked Vehicle for RFX First Wall Inspection. *Fusion Technology*, 34(3), pp.1155-59.
- Davies, E.R., 1997. *Machine Vision: Theory Algorithms Practicalities*. 2nd ed. San Diego: Academic Press Inc.
- Deksnis, E. et al., 1997. Beryllium Plasma Facing Components: JET Experience. *Fusion Engineering & Design*.
- Dobers, T., Jones, M. & Muttoni, Y., 2004. Using A Laser Scanner For The Control Of Accelerator Infrastructure During The Machine Integration. In *International Workshop on Accelerator Alignment*. Geneva, 2004.
- Dold, J., 1998. The Role of a Digital Intelligent Camera in Automating Industrial Photogrammetry. *Photogrammetric Record*, 19(92), pp.199-212.
- Dorsch, R., Häusler, G. & Herrmann, J., 1994. Laser Triangulation: Fundamental Uncertainty in Distance Measurement. *Applied Optics*, 33(7), pp.1306-14.
- Eeten, P. et al., 2009. Component Design in Tight Areas in the Cryostat of Wendelstein 7-X - Configuration Management and Control. In *Fusion Engineering, 2009. SOFE 2009. 23rd IEEE/NPSS Symposium on.*, 2009.
- EFDA-JET, 2007. *EFDA-JET*. [Online] Available at: <http://www.jet.efda.org/pages/content/organisation/projects.html> [Accessed 07 Augustus 2007].
- EFDA-JET, 2010. *Remote Handling | EFDA JET*. [Online] Available at: <http://www.jet.efda.org/remote-handling/> [Accessed 22 February 2010].
- Eggert, D., Fitzgibbon, A. & Fisher, R., 1998. Simultaneous Registration of Multiple Range Views for Use In Reverse Engineering of CAD Models. *Computer Vision & Image Understanding*, 69(3), pp.253-72.
- El-Hakim, S. & Beraldin, J.-A., 1994. On the integration of range and intensity data to improve vision-based three-dimensional measurements. *SPIE Videometrics*, III, pp.306-21.
- El-Hakim, S. et al., 1997. Two 3-D Sensors for Environment Modeling and Virtual Reality: Calibration and Multi-View Registration. *ISPRS Highlights*, 2(1), pp.13-21.
- El-Hakim, S., Beraldin, J.-A. & Blais, F., 1995. A Comparative Evaluation of the Performance of Passive and Active 3-D Vision Systems. *Proc. SPIE*, 2646(14).
- Eos Systems Inc., 2009. *PhotoModeler Scanner - 3D Scanner for dense surface 3d scanning*. [Online] Available at: <http://www.photomodeler.com/products/pm-scanner.htm> [Accessed 10 January 2010].
- Evenden, A., 2009. *Personal Communication*. Unpublished.
- FARO, 2006. *Laser Tracker X & Xi*. [Online] Available at: [http://www.faro.com/FaroIP/Files/File/Techsheets%20Download/UK\\_Laser%20Tracker%20Brochure%20-%2004REF203-062.PDF](http://www.faro.com/FaroIP/Files/File/Techsheets%20Download/UK_Laser%20Tracker%20Brochure%20-%2004REF203-062.PDF) [Accessed 26 March 2010].

## References and Bibliography

- FARO, n.d.a. *FARO Laser Tracker*. [Online] Available at: <http://www.faro.com/lasertracker/> [Accessed 11 February 2010].
- FARO, n.d.b. *FARO UK - Measuring arms*. [Online] Available at: <http://measuring-arms.faro.com/> [Accessed 12 February 2010].
- Feng, H.-Y., Liu, Y. & Xi, F., 2001. Analysis of Digitizing Error of a Laser Scanner System. *Precision Engineering*, 25, pp.185-91.
- Forest, J., Salvi, J., Cabruja, E. & Pous, C., 2004. Laser Stripe Peak Detector for 3D Scanners. A FIR Filter Approach. In *17th International Conference on Pattern Recognition (ICPR'04)*. Cambridge, UK, 2004. IEEE Computer Society.
- Fraser, C., 1997. Digital Camera Self-Calibration. *ISPRS Journal of Photogrammetry and Remote Sensing*, 52(5), pp.149-59.
- Gagnon, H., Soucy, M., Bergevin, R. & Laurendeau, D., 1994. Registration of Multiple Range Views for Automatic 3-D Model Building. In *In IEEE Conf. on Vision and Pattern Recognition*. New York, USA, 1994.
- Gelfand, N., Ikemoto, L., Rusinkiewicz, S. & Levoy, M., 2003. Geometrically Stable Sampling for the ICP Algorithm. In *Proc. International Conference on 3D Digital Imaging and Modeling.*, 2003.
- Geodetic Services Inc., 2006. *Basics of Photogrammetry*. [Online] Available at: <http://www.geodetic.com/Whatis.htm> [Accessed 10 January 2010].
- Geodetic Systems Inc., 2010a. *Geodetic Systems Inc.* [Online] Available at: <http://www.geodetic.com/> [Accessed 10 January 2010].
- Geodetic Systems Inc., 2010b. *PRO-SPOT*. [Online] Available at: <http://www.geodetic.com/products/products.asp?pro-spot.htm> [Accessed 10 January 2010].
- Godin, G., Rioux, M. & Baribeau, R., 1994. Three-Dimensional Registration Using Range and Intensity Information. In El-Hakim, S., ed. *Proc. SPIE*. Boston, Massachusetts, 1994. SPIE.
- Godin, G. et al., 2001. An Assessment of Laser Range Measurement on Marble Surfaces. In *Proc. 5th Conference on Optical 3D Measurement Techniques*. Vienna, Austria, 2001.
- GOM, 2010. *GOM - Measuring Systems - ATOS*. [Online] Available at: <http://www.gom.com/EN/measuring.systems/atos/system/system.html> [Accessed 10 January 2010].
- Goodman, J., 1976. Some Fundamental Properties of Speckle. *Journal of Optical Society of America*, 66(11), pp.1145-50.
- Gruen, A. & Akca, D., 2005. Least Squares 3D Surface and Curve Matching. *ISPRS Journal of Photogrammetry and Remote Sensing*, 59(3), pp.151-74.
- Harding, K. & Qian, X., 2004. *Phase Shifting Based 3D Systems*. [Online] Available at: [http://www.machinevisiononline.org/public/articles/Phase\\_Shifting\\_3D\\_Systems.pdf](http://www.machinevisiononline.org/public/articles/Phase_Shifting_3D_Systems.pdf) [Accessed 14 May 2009].

## References and Bibliography

- Hebert, M. & Krotkov, E., 1992. 3-D Measurements from Imaging Laser Radars: How Good Are They? *Intl. Journal of Image and Vision Computing*, 10(3), pp.170-78.
- Heikkinen, V., Aikio, M., Keranen, K. & Wang, M., 2002. Fiberoptic in-Vessel Viewing System for the International Thermonuclear Experimental Reactor. *Review of Scientific Instruments*, 73(7), pp.2616-23.
- Herd, F., 2005. Assembly Technology for the W7-X Stellarator. In *Fusion Engineering 2005, Twenty-First IEEE/NPS Symposium on.*, 2005.
- Hexagon Metrology, 2010. *Hexagon Metrology - Portable Measuring Arms*. [Online] Available at: [http://www.hexagonmetrology.com/portable-measuring-arms\\_234.htm](http://www.hexagonmetrology.com/portable-measuring-arms_234.htm) [Accessed 12 February 2010].
- Hoppe, H. et al., 1992. Surface Reconstruction from Unorganized Points. In *19TH ANNUAL CONF OF THE ASSOC-FOR-COMPUTING-MACHINERY : COMPUTER GRAPHICS AND INTERACTIVE TECHNIQUES ( SIGGRAPH 92 )*., 1992.
- IBM, 2005. *Evernham Motorsports Engineers a Winning Program with CATIA V5 and SMARTEAM*. [Online] Dassault Systemes Available at: <http://a1.media.3ds.com/fileadmin/COMPANY/CUSTOMER-STORIES/PDF/Evernham-Motorsport-flyer-En.pdf> [Accessed 10 January 2010].
- Innovmetric, 2010. *PolyWorks: 3d scanner software*. [Online] Available at: <http://www.innovmetric.com/polyworks/3D-scanners/home.aspx?lang=en> [Accessed 21 April 2010].
- Inokuchi, S., Sato, K. & Matsuda, F., 1984. Range Imaging for 3D Object Recognition. In *Proceedings of the International Conference on Pattern Recognition*. Montreal, 1984.
- Inspection & Metrology Team, 2006. *JET Site Inspection Report JET6931*. Inspection Report. Oxford: Unpublished EFDA-JET.
- ITER, 2010. *The international ITER project for fusion: Why?* [Online] Available at: <http://www.iter.org/PROJ/Pages/ITERMission.aspx> [Accessed 07 January 2010].
- Jacobs, G., 2006. Understanding Spot Size for Laser Scanning. *Professional Surveyor Magazine*, September.
- Jazayeri, I. & Fraser, C., 2008. Interest Operators In Close-Range Object Reconstruction. In *Proceedings of: International Society of Photogrammetry and Remote Sensing*. Beijing, 2008.
- Jutzi, B. & Stilla, U., 2006. Characteristic of The Measurement Unit of A Full-Waveform Laser System. In *ISPRS Commission I Symposium*. Paris, France, 2006. International Society for Photogrammetry and Remote Sensing.
- Khali, H. et al., 2003. Improvement of Sensor Accuracy in the Case of a Variable Surface Reflectance Gradient for Active Laser Range Finders. *IEEE Transactions on Instrumentation and Measurement*, 52(6), pp.1799-808.
- Kilpelä, A., 2004. *Pulsed Time of Flight Laser Range Finder Techniques for Fast, High Precision Measurement Applications*. Academic Dissertation. Oulu, Finland: University of Oulu Department of Electrical and Information Engineering, University of Oulu.

## References and Bibliography

- Kühmstedt, P., Bräuer-Burchardt, C. & Notni, G., 2009a. Measurement Accuracy of Fringe Projection Depending on Surface Normal Direction. *Optical Inspection and Metrology for Non-Optics Industries. Proc. of SPIE*, 7432.
- Kyle, S., 2005. *Large Scale Metrology: Overview of Systems and Applications*. Lecture Notes. Unpublished.
- Kyle, S., 2008. *Accessing The LVM Knowledge Database: What's Needed, What's Available?* [Online] Available at: [http://www.lvmc.org.uk/2008/10.20\\_S.Kyle.pdf](http://www.lvmc.org.uk/2008/10.20_S.Kyle.pdf) [Accessed 08 March 2010].
- Kyle, S. & Bevan, K., 2009. *Developments in LVM Training*. [Online] Available at: [http://www.lvmc.org.uk/2009/npl\\_presentation\\_on\\_lvm\\_training\\_-\\_npl\\_v2.3.pdf](http://www.lvmc.org.uk/2009/npl_presentation_on_lvm_training_-_npl_v2.3.pdf) [Accessed 2010 March 08].
- Labsphere, 2006. *Labsphere : Materials and Coatings : Spectralon®*. [Online] Available at: <http://www.labsphere.com/productdetail.aspx?id=226> [Accessed 25 February 2010].
- Lartigue, C., Contri, A. & Bourdet, P., 2002. Digitised Point Quality in Relation with Point Exploitation. *Measurement*, 32, pp.193-202.
- Lascar Electronics, 2010. *Lascar Electonics*. [Online] Available at: <http://www.lascarelectronics.com/temperaturedatalogger.php?datalogger=375> [Accessed 06 June 2010].
- Leica Geosystems, 2008. *The Leica Absolute Interferometer: A New Approach to Laser Tracker Absolute Dsitance Meters*. Promotional Material. Switzerland.
- Levoy, M., 2002. *Why is 3D Scanning Hard?* [Online] Available at: <http://www-graphics.stanford.edu/talks/> [Accessed 10 November 2008].
- Levoy, M., 2009. *The Digital Michelangelo Project*. [Online] Available at: <http://graphics.stanford.edu/projects/mich> [Accessed 09 March 2010].
- Lichti, D., Brüstle, S. & Franke, J., 2007. Self Calibration and Analysis of the Surphaser 25HS 3D Scanner. Hong Kong, 2007. Proceedings of FIG.
- Litwiller, D., 2001. CCD vs. CMOS: Facts and Fiction. *Photonics Spectra*, January.
- Liu, B., Adams, M., Ibáñez-Guzmán, J. & Wijesoma, W., 2004. Range Errors Due To Occlusion in Non-Coaxial LADARs. In *Proc. 2004 IEEE/RSJ International Conference on Intelligent Robots and Systems*. Sendai, Japan, 2004. IEEE.
- Luhmann, T., Bethmann, F., Herd, B. & Ohm, J., 2008. Comparison and Verification of Optical 3-D Surface Measurement Systems. In *In Proc. International Society of Photogrammetry and Remote Sensing XXXVII*. Beijing, China, 2008.
- Luhmann, T., Robson, S., Kyle, S. & Harley, I., 2006. *Close Range Photogrammetry: Principles, Methods and Applications*. Caithness: Whittles Publishing.
- MacDonald, L., 2010. *Detail Matters: Spatial Resolution in Digital Representation of Cultural Heritage Objects*. Presentation. London: Unpublished University College London.

## References and Bibliography

- Macklin, B. et al., 1994. Alignment Systems for Pumped Divertor Installation at JET. In Herschbach, K., Maurer, W. & Vetter, J., eds. *Proceedings of 18th Symposium on Fusion Technology.*, 1994.
- Macklin, B. et al., 1995. Application of 'Best-Fit' Survey Techniques Throughout Design, Manufacturing and Installation of the MKII Divertor at JET. In *SOFE '95. 'Seeking a New Energy Era'. 16th IEEE/NPSS Symposium.*, 1995.
- Macklin, B. et al., 1998. Engineering a Remote Survey of JET's Divertor Structure Under Condition of Restricted Access Using Digital Photogrammetry. *Photogrammetric Record*, 16(92), pp.213-23.
- Marbs, A. & Boochs, F., 2006. Investigating the influence of ionizing radiation on standard CCD cameras and a possible impact on photogrammetric measurements. *International Archives of Photogrammetry and Remote Sensing*, pp.184-89.
- Meadows, D., Johnson, W. & Allen, J., 1970. Generation of Surface Contours by Moiré Patterns. *Applied Optics*, 9(4), pp.942-47.
- Menon, M. et al., 2001. Remote Metrology, Mapping, and Motion Sensing of Plasma Facing Components Using FM Coherent Laser Radar. *Fusion Engineering and Design*, 58-59, pp.495-98.
- Metronor, 2009. *Metnonor CMM - PRODUCTS/Portable CMM/DUO/DETAILS*. [Online] Available at: <http://www.metnonorcmm.com/default.asp?page=24> [Accessed 16 February 2010].
- Morey, B., 2009. Shop-Floor Metrology. *Manufacturing Engineering*, November. <http://www.sme.org/cgi-bin/find-articles.pl?&ME09ART49&ME&20091101&&SME&>.
- NASA, 2000. *NASA Space Shuttle Orbiter Protection Systems From NSTS Shuttle Reference Manual (1988)*. [Online] Available at: [http://science.ksc.nasa.gov/shuttle/technology/sts-newsref/sts\\_sys.html](http://science.ksc.nasa.gov/shuttle/technology/sts-newsref/sts_sys.html) [Accessed 10 Augustus 2007].
- NASA, 2006. *NASA Facts: Orbiter Thermal Protection System*. [Online] Available at: <http://www-pao.ksc.nasa.gov/kscpao/nasafact/pdf/TPS-06rev.pdf> [Accessed 10 Augustus 2007].
- NASA, 2007. *NASA Press Release*. [Online] Available at: [http://www.nasa.gov/centers/ames/news/releases/2007/07\\_52AR.html](http://www.nasa.gov/centers/ames/news/releases/2007/07_52AR.html) [Accessed 10 Augustus 2007].
- National Physical Laboratory, 2009. *Freeform Surfaces*. [Online] Available at: <http://www.npl.co.uk/dimensional/freeform> [Accessed 2010 March 08].
- National Research Council Canada, 2009. *A Real-Time 3D Laser Tracking and Imagine System Developed Jointly with Neptec*. [Online] Available at: <http://www.nrc-cnrc.gc.ca/eng/ibp/iit/about/laser-tracking.html> [Accessed 09 March 2010].
- Neptec, 2007a. *Neptec*. [Online] Available at: [http://www.neptec.com/Neptec\\_LCS.html](http://www.neptec.com/Neptec_LCS.html) [Accessed 10 Augustus 2007].
- Neptec, 2007b. *Neptec Group, a NASA Prime Contractor*. [Online] Available at: <http://www.neptec.com/> [Accessed 09 March 2010].

## References and Bibliography

- Neri, C. et al., 2005a. Parallel Hardware Implementation of RADAR Electronics Equipment for a Laser Inspection System. *IEEE Transaction on Nuclear Science*, 52(6), pp.2741-48.
- Neri, C. et al., 2005b. Experimental Result of the Laser in Vessel Viewing and Ranging System (IVVS) for ITER. *Fusion Engineering and Design*, 75-79, pp.613-18.
- Neri, C. et al., 2007. The laser in vessel viewing system (IVVS) for iter: Test results on first wall and divertor samples and new developments. *Fusion Engineering and Design*, 82(15-24), pp.2021-28. doi:10.1016/j.fusengdes.2006.12.006.
- Neri, C. et al., 2009. The upgraded laser in vessel viewing system (IVVS) for ITER. *Fusion Engineering and Design*, 84(2-6), pp.224-28. Proceeding of the 25th Symposium on Fusion Technology - (SOFT-25).
- NextEngine Inc., 2010. *NextEngine*. [Online] Available at: <https://www.nextengine.com> [Accessed 10 January 2010].
- NextEngine Inc, 2010. *NextEngine Desktop 3D Scanner*. [Online] Available at: <https://www.nextengine.com/indexSecure.htm> [Accessed 10 January 2010].
- Nikon Metrology NV, 2010. *Nikon Metrology*. [Online] Available at: <http://www.nikonmetrology.com/home.php> [Accessed 12 February 2010].
- NIST, 2006. *BRTL: Construction Metrology and Automation Group*. [Online] Available at: [http://www.bfml.nist.gov/861/CMAG/publications/NISTIR\\_7357.pdf](http://www.bfml.nist.gov/861/CMAG/publications/NISTIR_7357.pdf) [Accessed 09 Augustus 2008].
- Nitzan, D., 1988. Three-Dimensional Vision Structure for Robot Applications. *IEEE Transactions on Pattern Analysis and Machine Intelligence*, 10(3), pp.291-309.
- Northern Digital Inc., 2008. *NDI: Optical Trackers - High Accuracy Portable CMM, Laser Scanner, and Dynamic Motion Measurement*. [Online] Available at: <http://www.ndigital.com/industrial/products-opticaltracker.php> [Accessed 16 February 2010].
- Notni, G., 2010. *Fraunhofer IFO*. [Online] Available at: [http://www.iof.fraunhofer.de/departments/optical-systems/\\_media/kolibri\\_multi\\_02\\_2007\\_e.pdf](http://www.iof.fraunhofer.de/departments/optical-systems/_media/kolibri_multi_02_2007_e.pdf) [Accessed 09 December 2009].
- Oliveira, J. & Buxton, B., 2005. *Tech Report - RN/05/13 - An Efficient Octree For Interactive Large Model Visualization*. Technical Report. London: University College London Department of Computer Science, University College London.
- Oliver, B., 1963. Sparking spots and Random Diffraction. *Proceedings of the IEEE [0018-9219]*, 51(1), pp.220-21.
- Pace, N., 2010. *Personal Communication*. Email dated 07/07/2010. Unpublished.
- Pamela, J., 2006. The JET programme in support of ITER. In *24th Symposium on Fusion Engineering Technology*. Warsaw, 2006.
- Patel, B. & Parsons, W., 2002. Operational Beryllium Handling Experience at JET. In *Proceedings of SOFT*. Helsinki Finland, 2002. EFDA-JET-CP(02)05/20.

## References and Bibliography

- Payne, J., 1973. An Optical Distance Measuring Instrument. *The Review of Scientific Instruments*, 44(3), pp.304-06.
- Peggs, G. et al., 2009. Recent Developments In Large-Scale Dimensional Metrology. *Proceedings of IMechE*, 223, pp.571-95.
- Perceptron, 2010. *Perceptron*. [Online] Available at: <http://www.perceptron.com/index.php/en/-industrial/scanning-solutions/manual-scanning.html> [Accessed 31 May 2010].
- Pfeifer, N. & Briese, C., 2007. Laser Scanning - Principles and Applications. In *Proc. Geo-Sibir'2007*. Nowosibirsk, Russia, 2007.
- Phase Vision Ltd, 2008. *Inspection on the Production Line*. [Online] Available at: <http://www.phasevision.com/> [Accessed 08 February 2010].
- Philips, J., Liu, R. & Tomasi, C., 2007. Outlier Robust ICP for Minimizing Fractional RMSD. In Godin, G., Hébert, P., Masuda, T. & Taubin, G., eds. *In Proc. Sixth International Conference on 3-D Digital Imaging and Modeling*. Montréal, Québec, Canada, 2007.
- Physikalisch-Technische Bundesanstalt (PTB), 2010. *Physikalisch-Technische Bundesanstalt*. [Online] Available at: [http://www.ptb.de/index\\_en.html](http://www.ptb.de/index_en.html) [Accessed 21 April 2010].
- Pilkington, 2010. *Specular and Diffuse Reflection*. [Online] Available at: <http://www.pilkington.com/europe/uk+and+ireland/english/building+products/pilkington4architects/reference/about+glass/appearanceofglass/reflection.htm> [Accessed 24 March 2010].
- Potsdamer, J. & Altschuler, M., 1982. Surface Measurement by Space-Encoded Projected Beam Systems. *Computer Graphics Image Processing*, 18, pp.1-17.
- Pulli, K., 1999. Multiview Registration for Large Data Sets. In *Second International Conference on 3D Digital Imaging and Modeling*. Ottawa, 1999.
- Rabbani, T., Dijkman, S., van den Heuvel, F. & Vosselman, G., 2007. An Integrated Approach for Modelling and Global Registration of Point Clouds. *ISPRS Journal of Photogrammetry and Remote Sensing*, 61(6), pp.355-70.
- Remondino, F. & El-Hakim, S., 2006. Image-Based 3D Modelling: A Review. *The Photogrammetric Record*, 21(115), pp.269-91.
- Ridgen, J. & Gordon, E., 1962. Granularity of Scattered Optical MASER Light. *Proceedings of the IRE [0096-8390]*, 50(11), pp.2367-68.
- Rieger, P., Ullrich, A. & Reichert, R., 2006. Laser Scanners With Echo Digitization for Full Waveform Analysis. In *Proc. Workshop on 3D Remote Sensing in Forestry*. Vienna, 2006.
- Rioux, M., 1984. Laser Range Finder Based on Synchronized Scanners. *Applied Optics*, 23(21), pp.3837-44.
- Robson, S., Beraldin, A., Brownhill, A. & MacDonald, L., 2011. *Artefacts for Optical Surface Measurement*, 2011. SPIE.
- Robson, S. & Shortis, M., 2007. 1. Engineering and Manufacturing. In J. Fryer, H. Mitchell & J. Chandler, eds. *Applications of 3D Measurement from Images*. Cauthness: Whittles Publishing.

## References and Bibliography

- Rodger, G., Flack, D. & McCarthy, M., 2007. *A Review of Industrial Capabilities to Measure Free-Form Surfaces*. HMSO.
- Rüeger, J.M., 1990. *Electronic Distance Measurement*. 3rd ed. Berlin, Germany: Springer-Verlag.
- Rusinkiewicz, S., 2005. *ICCV 2005 Short Course: 3D Scan Matching and Registration*. [Online] Available at: [http://www.cs.princeton.edu/~bjbrown/iccv05\\_course/iccv05\\_icp\\_gr.pdf](http://www.cs.princeton.edu/~bjbrown/iccv05_course/iccv05_icp_gr.pdf) [Accessed 26 February 2009].
- Rusinkiewicz, S. & Levoy, M., 2000. QSplat: A Multiresolution Point Rendering System for Large Meshes. In *SIGGRAPH*. New Orleans, USA, 2000.
- Rusinkiewicz, S. & Levoy, M., 2001. Efficient Variants of the ICP Algorithm. In *In Proceedings of the Third Intl. Conf. on 3D Digital Imaging and Modeling*, 2001.
- Ryer, A., 1997. *Light Measurement Handbook*. [Online] Available at: <http://www.intl-light/handbook> [Accessed 25 July 2007].
- Salavy, J.-F., 2002. *Final report on the tile chamfering and power handling of the MKII divertor*. France: CEA Direction De L'Energie Nucléaire Département Modelélisation De Systèmes et Structures. Rapport DM2S.
- Salvi, J., Pagès, J. & Batlle, J., 2004. Pattern Codification Strategies in Structured Light Systems. *Pattern Recognition*, 37(4), pp.827-49.
- Sansoni, G. et al., 1997. Three-Dimensional Imaging Based On Gray-Code Light Projection: Characterization of a Measuring System for Industrial Applications. *Applied Optics*, 46(19), pp.4463-72.
- Savio, E., De Chiffre, L. & Schmitt, R., 2007. Metrology of Freeform Shaped Parts. *CIRP Annals - Manufacturing Technology*, 56(2), pp.810-35.
- Shortis, M., Clarke, T. & Short, T., 1994. Comparison of Some Techniques for the Subpixel Location of Discrete Target Images. *Proceedings of SPIE - Videometrics III*, 2350, pp.239-50.
- Smith, W., 1966. *Modern Optical Engineering: The Design of Optical Systems*. New York: McGraw-Hill.
- Spampinato, P. et al., 1998a. A Laser Metrology/Viewing System for ITER In-Vessel Inspection. *Fusion Engineering and Design*, 42, pp.493-299.
- Spampinato, P., Barry, R., Herndon, J. & Menon, M., 1999. A Remotely Deployed Laser System for Viewing/Metrology. In *In Proc. ANS 8th Topical Meeting on Robotics and Remote Systems*. Pittsburgh, PA, 1999.
- Spampinato, P. et al., 1996. A Laser Scanning System for Metrology and Viewing in ITER. In *Sixth International Symposium on Robotics and Manufacturing (ISRAM'96)*, 1996.
- Spampinato, P. et al., 1998b. A Remotely Deployed System for In-Vessel Metrology and Viewing. *Fusion Technology*, 34(4, part 3), pp.1151-54.

## References and Bibliography

- Steinbichler Optotechnik, n.d. *Competence in Optical Measuring and Sensor Technology*. [Online] Available at: [http://www.steinbichler.de/en/main/comet\\_5.htm](http://www.steinbichler.de/en/main/comet_5.htm) [Accessed 08 February 2010].
- Stoddart, A. & Hilton, A., 1996. Registration of Multiple Point Sets. In *In Proc. International Conference on Pattern Recognition*. Banff, Alberta, Canada, 1996.
- Takasaki, H., 1970. Moiré Topography. *Applied Optics*, 6(6), pp.1467-72.
- Talarico, C. et al., 2001. Laser In Vessel Viewing System for Activated Areas: Mechanical Design, Manufacturing and Tests., 2001.
- Taylor-Hobson, n.d. *Surtronic 3 User Guide*.
- TEKES FFUSION, 2003. ISBN: 952-457-095-5 *Final Report 1/2003*. TEKES FFUSION – Finnish Fusion Energy Research Programme.
- Teutsch, C. et al., 2005. Evaluation and Correction of Laser-Scanned Point Clouds. *Proc. of Videometrics VIII, SPIE*, 5665.
- The Association of German Engineers (VDI), 2008. *VDI/VDE 2634 Part 3: Optical 3D-Measuring Systems Multiple View Systems Based on Area scanning*. Guideline. The Association of German Engineers (VDI).
- Thiel, K. & Wehr, A., 2004. Performance Capabilities of Laser Scanners - An Overview and Measurement Principle Analysis. In Thies, M., Koch, B., Spiecker, H. & Weinacker, H., eds. *Laser-Scanners for Forest and Landscape Assessment*. Freiberg, Germany, 2004. International Society for Photogrammetry and Remote Sensing.
- Third Dimension, 2010. *Third Dimension: Non contact metrology*. [Online] Available at: <http://www.third.com/index.shtml> [Accessed 10 January 2010].
- Trobina, M., 1995. *Error Model of a Coded-Light Range Sensor*. Technique Report. Zurich, Switzerland: Communication Tehnology Laboratory, Image Science Group, ETH-Zentrum.
- Trucco, E. & Verri, A., 1998. *Introductory Techniques for 3-D Computer Vision*. New Jersey, USA: Prentice Hall.
- Tuominen, V. & Niini, I., 2008. Verification of the Accuracy of a Real-Time Optical 3D-Measuring System on Production Line. In *The International Archives of the Photogrammetry, Remote Sensing and Spatial Information Sciences*. Beijing, China, 2008. International Society for Photogrammetry and Remote Sensing.
- UCL Department of Geomatic Engineering, 2007. *CAD Reps of 3D Spatial Data*. Lecture Notes. London, UK: Unpublished University College London.
- United Kingdom Health and Safety Executive, 1995. *Beryllium and You*. [Online] Available at: <http://www.hse.gov.uk/pubns/indg311.pdf> [Accessed 10 April 2007].
- University College London, National Physical Laboratory, Leica UK, 1999. *Best Practice for Non-Contacting CMMs: Project 2.3.1/2/3 - Large Scale Metrology: Ref.MPU 8/61/1 - 09 12 1999*. London, England: University College London, National Physical Laboratory, Leica UK.

## References and Bibliography

- Urban, R., Stroner, M. & Kremen, T., 2009. The Test of Distance Accuracy Dependence on Angle of Incidence. In *Proc. 9th Conference on Optical 3-D Measurement Techniques*. Vienna, Austria, 2009.
- Van Gestel, N., Cuypers, s., Bleys, P. & Kruth, J.-P., 2009. A Performance Evaluation Test for Laser Line Scanners on CMMs. *Optics and Lasers in Engineering*, 47, pp.336-42.
- van Lente, E., 1995. *Investigation of Measurement Systems in Remote Handling Operations at JET*. Oxford: Unpublished JET.
- Vizvary, Z., 2007. *Tile Shaping Tolerance Assessment*. Oxford: Unpublished EFDA-JET.
- Wahl, F., 1984. *A Coded-Light Approach for 3-Dimensional (3D) Vision*. Research Report. Zurich, Switzerland: IBM Zurich Research Laboratory, 8803 Rüschlikon, Switzerland IBM Zurich Research Laboratory.
- Wahl, F., 1986. A Coded Light Approach for Depth Map Acquisition. In *Mustererkennung 1986. 8. DAGM Symposium*. Paderborn, Germany, 1986. Springer-Verlag.
- Wakayama, T. & Yoshizawa, T., 2009. Surface Profilometry. In T. Yoshizawa, ed. *Handbook of Optical Metrology: Principles and Applications*. CRC Press. pp.465-66.
- Wehr, A. & Lohr, U., 1999. Airborne Laser Scanning - an Introduction and Overview. *ISPRS Journal of Photogrammetry & Remote Sensing*, 54, pp.62-82.
- Wesson, J., 2000. *The Science of JET*. Oxford: JET Joint Undertaking.
- Wilson, D. et al., 1999. *Latest Developments in the Use of Industrial Digital Photogrammetry at JET*. Oxford: Unpublished JET Joint Undertaking.
- WMMMC, 2007. *West Midlands Manufacturing Measurement Centre*. [Online] Available at: <http://www.wmmmc.co.uk/> [Accessed 2007].
- Woodley, N., 1992. *In Vessel Datum Ring*. Site Inspection Report. No. 4444. Unpublished.
- Woodley, N., 2010. *Personal Communication*. email.
- Young, M. et al., 2007. Viewpoint-Coded Structured Light. In *Proc. IEEE Computer Society Conference on Computer Vision and Pattern Recognition (CVPR)*. Minneapolis, Minnesota, USA, 2007. IEEE Computer Society.
- Zhang, Z., 1994. Iterative Point Matching for Registration of Free-Form Curves and Surfaces. *International Journal of Computer Vision*, 13, pp.119-52.

## 7.1. Publications & Presentations

- Brownhill. A., Brade. R., Robson. S., 2007. Non-Contact Surface Measurement in a Hazardous Environment. In Proc. 8th International Conference on Optical 3-D Measurement Techniques. Zurich, Switzerland.
- Brownhill. A., Brade. R., Robson. S., 2009. Performance study of non-contact surface measurement technology for use in an experimental fusion device. Fusion Engineering, 2009. SOFE 2009. 23rd IEEE/NPSS Symposium on , pp. 1-4.
- Brownhill. A., Brade. R., Robson. S., 2009. Performance study of non-contact surface measurement technology for use in an experimental fusion device. Proc. SPIE 7447, 744708.
- Invited speaker at the opening of the UK National Physical Laboratory Freeform Measurement Centre, Teddington, UK (October, 2009): Evaluating non-contact metrology equipment for remote measurement of metallic surfaces.
- Brownhill. A., Brade. R., Robson. S., 2009. Performance evaluation of fringe and laser triangulation systems for the measurement of metallic surfaces. Large Volume Metrology Conference (LVMC), Chester, UK.
- Robson. S., Beraldin. A., Brownhill. A., MacDonald. L., 2011. Artefacts for surface measurement. SPIE Optical Metrology: Videometrics, Range Imaging and Applications (Munich, Germany).